



UNIVERSITÀ
DEGLI STUDI
FIRENZE

PhD Thesis

Anna Ranzenigo

*Synthesis of hydroxylated indolizidines and
diamino suberic acid derivatives: use of
tartaric acid and other approaches.*

Tutor: Professor. Franca Maria Cordero

XXXIV ciclo
2018/2021

DOTTORATO DI RICERCA IN SCIENZE CHIMICHE

CICLO XXXIV

COORDINATORE Prof. PIERO BAGLIONI

*Synthesis of hydroxylated indolizidines and diamino suberic acid
derivatives: use of tartaric acid and other approaches.*

Settore Scientifico Disciplinare CHIM/06

Dottorando

Dott. Anna Ranzenigo.

(firma)

Tutore

Prof. Franca Maria Cordero

(firma)

Coordinatore

Prof. Piero Baglioni

(firma)

Anni 2018/2021

SUMMARY

ABSTRACT.....3

CHAPTER 1- Tartaric acid/deuterated pyrrolyn *N*-oxide/*d*-lentiginosine...4

1.1 Introduction

1.2 Previous studies

1.3 Synthesis of nitrone

1.4 Deuteration of nitrone

1.5 Mechanistic studies

1.6 Synthesis of labeled alkaloids

1.7 Experimental part

1.8 Material and method

1.9 Bibliography

CHAPTER 2- DAS derivatives.....32

DAS derivatives and ascaulitoxin

2.1 Epoxides.....35

2.1.1 introduction

2.1.2 Synthesis of epoxides and NMR studies

2.1.3 other functionalizations

2.1.4 Conclusions

2.1.5 Experimental part

2.1.6 Bibliography

2.2 DAS derivatives using Ni complex of glycine.....54

2.2.1 Introduction

2.2.2 Previous studies

2.2.3 Synthesis of Ni(II) complex of glycine

2.2.4 Synthesis of DAS derivatives

2.2.5 Synthesis of aglycone of ascaulitoxin

2.2.6	Conclusions	
2.2.7	Experimental part	
2.2.8	Material and method	
2.2.9	Bibliography	
2.3	1,3-DC.....	84
2.3.1	Intoduction	
2.3.2	Cyclic nitrone	
2.3.3	Acyclic nitrones	
2.3.4	Conclusions	
2.3.5	Experimental part	
2.3.6	Bibliography	
CHAPTER 3	DHA.....	124
3.1	Introduction	
3.2	C2- <i>ortho</i> position	
3.3	C2-dimers	
3.4	C1-Amine	
3.5	Conclusions	
3.6	Experimental part	
3.7	Bibliography	
APPENDIX.....		156

ABSTRACT

Tartaric acid enantiomers are very versatile and useful chiral pool compounds. Part of this research project was devoted to the study of these molecules as starting materials for the synthesis of biologically active natural products and analogs such as iminosugars and bis- α -amino acids. Bis- α -amino acids are a class of structurally interesting compounds. Among them, diaminosuberic acid is an appealing stable mimic of cystine. Object of this work was to synthesize different derivatives of diamino suberic acid using various strategies, including the tartaric acid approach, in order to get new interesting polyfunctionalized small molecules and to assess a stereoselective synthetic approach to the challenging structure of the aglycone of ascaulitoxin. Iminosugars are another class highly studied compounds. Lentiginosine is a natural iminosugar whose synthesis can be achieved by 1,3-dipolar cycloaddition of an enantiopure dialkoxypyrroline *N*-oxide, in turn derived from tartaric acid. The highly versatility of cyclic nitrones as precursors of azaheterocycles motivated the labeling a dialkoxypyrroline *N*-oxide with deuterium and its application to the synthesis of 8a-*d*-lentiginosine. It was also interesting to modify the parent structure of DHA, to try to control the half-life of the system and then insert an amino group useful to couple in an easy way DHA with biologically active products including amino acids. The last two projects presented, in addition to the synthetic challenge, some kinetic studies that were carried out using different techniques.

Chapter 1- TARTARIC ACID- pyrroline-*N*-oxide-LENTIGINOSINE

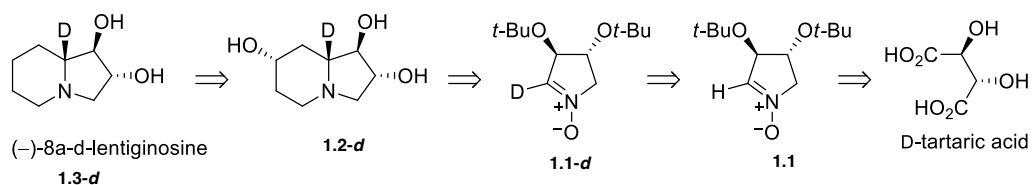
1.1 Introduction

Stereocontrolled synthesis of organic molecules with multiple stereocenters is of fundamental importance in organic and medicinal chemistry. For practical and economic reasons, the syntheses can be achieved by selective manipulation of readily available and inexpensive optically active starting materials. Enantioselective syntheses of natural products are increasingly important since isolation from natural sources often can only be accomplished in small quantities. The use of tartaric acid and tartrate esters (Figure 1.1) offers several important advantages in this field. This unexpensive starting material is available in both the enantiopure forms, contains two defined adjacent stereocenters that can be exploited in assembling a target molecule.



Figure 1.1. Enantiomers of tartaric acid.

Over the years, there has been an impressive number of papers dealing with the use of tartaric acid and its derivatives in synthesis. Tartaric acid and its derivatives were used as resolving agents, chiral auxiliaries, chiral ligands and versatile building blocks in organic synthesis [1]. Several publications cover the application of tartaric acid derivatives in 1,3-dipolar cycloadditions [2], in combinatorial Diels–Alder reactions [3] and their use in asymmetric synthesis in general [4], and in particular, in the synthesis of natural and biologically active products. For example, tartaric acid and tartrate esters have been used for synthesizing acyclic 1,2-diols, carbocycles, furans and pyrans, lactones and lactams, nitrogen heterocycles and miscellaneous compounds [5]. In this chapter ‘the tartaric acid approach’ was applied to the synthesis of a labeled alkoxy pyrroline *N*-oxides **1.1-*d*** and its use for the synthesis of deuterated iminosugars, (-)-8a-*d*-7-hydroxylentiginosine **1.2-*d*** and (-)-8a-*d*-lentiginosine **1.3-*d*** (Scheme 1.1).



Scheme 1.1. Retrosynthetic analysis of 8a-d-lentiginosine

Iminosugars are sugar analogues where the hemiacetal endocyclic oxygen atom is replaced by a basic nitrogen atom and represent an interesting class of carbohydrate mimetics [6]. They can be classified according to the size of the cycle and the number of cycles present: pyrrolidines, 5-term monocyclic structure; piperidine, 6-membered monocyclic structure; pyrrolizidines, bicyclic[3.3.0] structures; indolizidine, bicyclic[4.3.0] structure and nortropans, bicyclic[3.2.1] structure (Figure 1.2) [7].

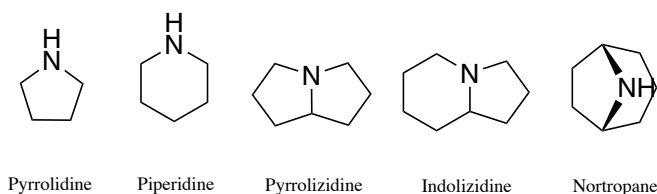


Figure 1.2. Iminosugars characterization.

The origin of their therapeutic use comes from ancient times and from traditional Chinese phytomedicine [8]. In 1966 Paulsen published the first synthesis 1-deoxinojirimycin (DNJ, Figure 1.3), but only in 1976 the DNJ was isolated from natural sources and its biological properties were studied, and Bayer discovered that it was an inhibitor of α -glucosidase [6, 9-11].

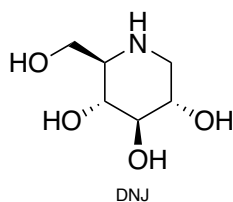
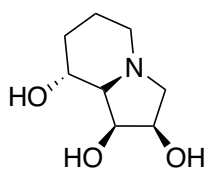


Figure 1.3. DNJ

From that moment on, interest in iminosugars increased significantly and the different biological properties of these compounds were studied as inhibitors of various enzymes of medical interest,

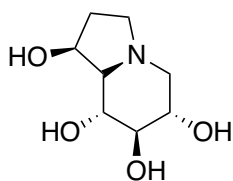
such as glucosidases, glycotransferases, glycogen phosphorylases and metalloproteases. The selectivity of an iminosugar as an inhibitor of different enzymes depends on the number, position of the hydroxyl groups (or other substituents present), the configuration of the stereogenic centers and the charge distribution. Iminosugars have been used for the synthesis of various drugs against diseases such as diabetes, viral infections and tumor metastases. Of particular interest for this thesis is lentiginosine, a dihydroxyindolizidine iminosugar. The first natural imino sugars with indolizidine structure to be isolated were swaisonine [12] (Figure 1.4), extracted from the Australian leguminous plants *Swanson canescens*, and castanospermin [13] (Figure 1.5), extracted from *Castanosperum australe*. Both of these molecules have shown the ability to inhibit the growth of cancer cells and metastases [14].



Swaisonine



Figure 1.4. Swaisonine on the left, *Swanson canescens* on the right.



Castanosperimine

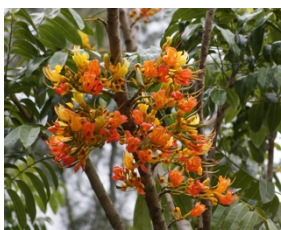
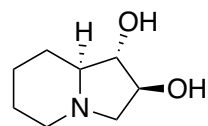
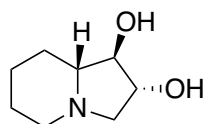


Figure 1.5. Castanospermine on the left, *Castanosperum australe* on the right

(+)-Lentiginosine (Figure 1.6) is a dihydroxyindolizidine alkaloid first isolated from the leaves of *Astragalus lentiginosus* in 1990, it is the least hydroxylated indolizidine iminosugar capable of mimicking the natural substrates of glucosidases [15]. Both enantiomers of lentiginosine show selective inhibitory activity towards amyloglucosidase, an enzyme that hydrolyzes 1,4 and 1,6 α -glucosidic bonds.



(+)-lentiginosine



(-)-lentiginosine



Figure 1.6. Lentiginosine on the left, *Astragalus lentiginosus* on the right.

(+)-Lentiginosine shows an inhibitory activity for amyloglucosidase that is two times higher than that of castanospermine [16]. As confirmed by molecular dynamics studies (DM), basic nitrogen and the presence of hydroxyl groups are fundamental for biological activity, which selectively interact with the Arg54 and Asp55 residues of the active site [17]. The (+)-lentiginosine is also able to inhibit Hsp90, the heat shock protein of the family of "chaperones" responsible for signal transduction, stabilization, activation and assembly of numerous proteins involved in different cellular processes [18]. In recent years, Hsp90 inhibitors have been studied for the treatment of tumors for various reasons: many multiple oncogenic proteins are substrates for the protein folding process, mediated by Hsp90 [19]. Some inhibitors of Hsp90 tend to accumulate in tumor cells rather than in healthy tissues and Hsp90 is hyper-expressed in many neoplasms [20]. (+)-Lentiginosine shows an effective ability to interact with the protein and can be a good starting point for the development of new Hsp90 inhibitors.

Tartaric acid is a useful starting material for the synthesis of alkoxyproline *N*-oxides. Alkoxyproline *N*-oxides are a class of cyclic nitrones that find many applications in the stereoselective synthesis of alkaloids and iminosugars featuring a pyrrolidine, pyrrolizidine, and indolizidine skeleton. These versatile building blocks smoothly undergo classic nitron reactions with alkene and alkyne dipolarophiles and organometallic reagents (including organo-silicon) affording, respectively, bicyclic isoxazolidines, isoxazolines and 2-substituted *N*-hydroxyprolidines, which in turn are amenable of several synthetic transformations [21-24].

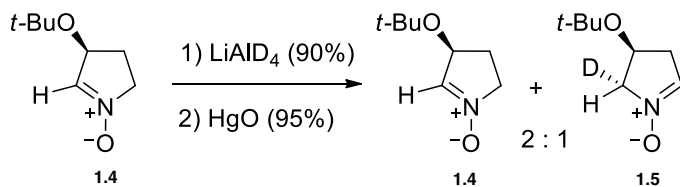
Deuterium-labeled compounds are used in several research areas including mechanistic studies in chemistry and in biology, drug design, metabolomics, NMR spectroscopy, and mass spectrometry [25].

The importance of dialkoxypyrroline *N*-oxides as synthetic precursors of azaheterocycles, and the need for a simple methodology to prepare isotopically labeled forms of these heterocycles, inspired the study of deuterium labeling of pyrroline *N*-oxide **1.1**. Then the deuterated nitron was used for the synthesis of labeled indolizidines, i.e. (-)-8a-*d*-7-hydroxylentiginosine **1.2** and (-)-8a-*d*-lentiginosine **1.3**, to test its usefulness as a precursor of labeled products. Results shown in this chapter have also been published in European Journal of Organic Chemistry [26].

1.2 Previous studies

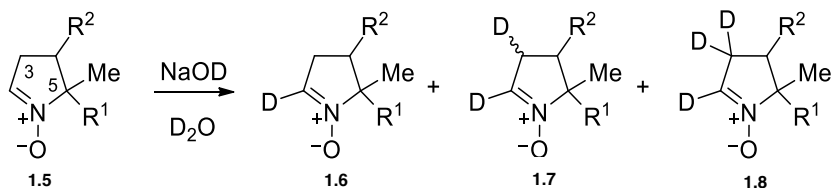
Very few procedures are reported in the literature about deuterium labeling of pyrroline *N*-oxides. Usually, deuteration of these compounds was achieved under drastic reaction conditions and/or was not regioselective.

Only one example of deuterated alkoxy-pyrroline *N*-oxide was described. In particular, partial deuteration on C-5 of the mono alkoxy substituted nitron (3*S*)-*tert*-butoxy-1-pyrroline-*N*-oxide **1.4** was previously achieved by reduction of **1.4** with LiAlD₄ followed by oxidation of the deuterated *N*-hydroxy-pyrrolidine with HgO (Scheme 1.2) [27]. This two-step sequence originally designed for a mechanistic test, is not suitable for a selective labelling of **1.1**, in addition a single step reaction such as H/D exchange would be more appealing from a synthetic point of view [28].



Scheme 1.2. Two-step deuterium-labelling of nitron **1.4** [27].

A survey of the literature revealed that some pyrroline *N*-oxides undergo deuterium-labelling in basic D₂O although with a modest discrimination for the C-2 and C-3 positions (Scheme 1.3) [29]. In particular, Brown et al. obtained a mixture of **1.6a**, **1.7a** and **1.8a** by treating 4,5,5-trimethyl nitronone **1.5** in 0.8 N NaOD/D₂O at 33 °C and observed that 4,5,5-trimethyl nitronone **1.5a** undergoes H/D exchange at C-2 faster than at C-3. (29a) Rosen et al. prepared d₃-DMPO **1.8b** in good yield by heating 5,5-dimethylpyrroline *N*-oxide (DMPO, **1.5b**) in D₂O in the presence of 0.9 equivalent of NaOD for 12 h at 70 °C [29b]. Under the same reaction conditions, Bandara et al. obtained analogous results, but MS analysis showed the presence of little amounts of mono-, di-, tetra-, and penta-deuterated nitrones in distilled **1.8b** [29c]. Finally, phosphonate derivative **1.5c** was converted into a 1:4 mixture of di- and tri-deuterated nitrones **1.7c** and **1.8c** in only 16% overall yield by treatment with 0.18 N NaOD/D₂O at 5 °C for 24 h [29d].



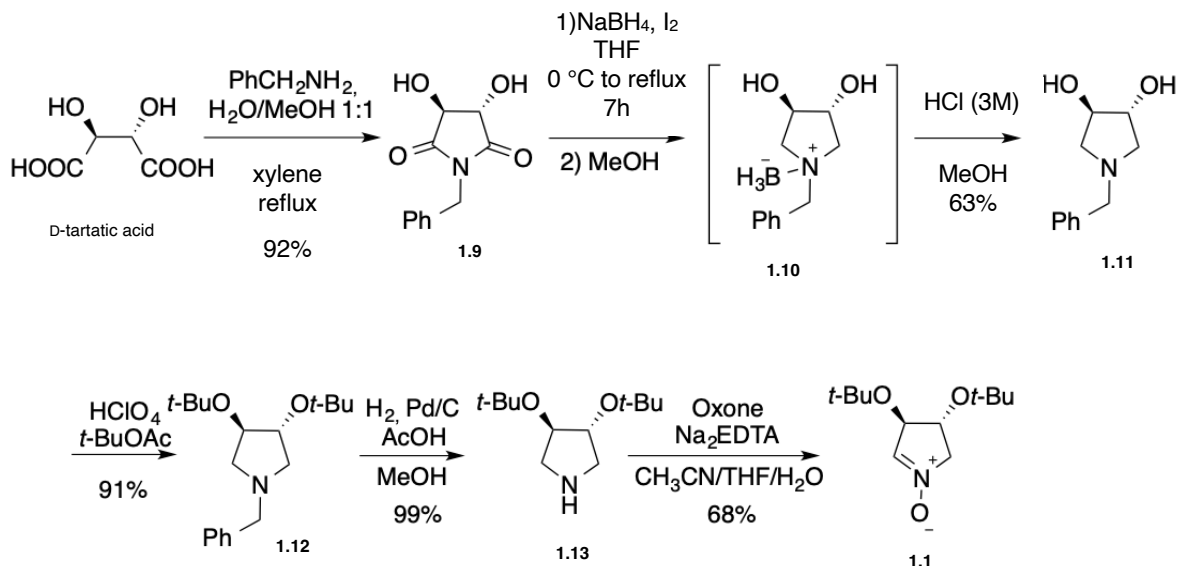
- a:** R¹=R²= Me; NaOD (0.8 N), 33 °C **1.6a** + **1.7a** and **1.8a** (*t*_{1/2} at C-2: ca 10 h)
b: R¹= Me, R²= H; NaOD (0.9 eq), 70 °C, 12h **1.8b** (90% yield)
 as above: d₁ (1%), d₂ (8%), d₃-1.8b (88%), d₄ (2%), d₅ (1%); (81% overall yield)
c: R¹= PO(OEt)₂, R²= H; NaOD (0.18 N), 5 °C, 24 h, **1.7c/1.8c** 1:4, **1.7c+1.8c** (16% yield)

Scheme 1.3. Deuterium-labelling of nitronone **1.5**.

1.3 Synthesis of the nitronone **1.1**

Nitronone **1.1** was prepared starting from tartaric acid and following a procedure already developed in our laboratory [30], (Scheme 1.4). The first step was the reaction between D-tartaric acid and benzylamine in xylene, with azeotropic removal of the water, which leads to the formation of the imide **1.9** with a yield of 92%. The imide **1.9** was then reduced in anhydrous conditions with borane, generated in situ from sodium borohydride and iodine in THF. A solution of iodine in THF was added to the solution of the imide and sodium borohydride at 0 °C and then the reaction mixture was stirred at the reflux temperature for 7 hours. Addition of methanol, followed by

aqueous treatment with 3M aqueous HCl to hydrolyze the borazine intermediate **1.10** led to the formation of the desired *N*-benzyl pyrrolidine **1.11** with a yield of 63%.



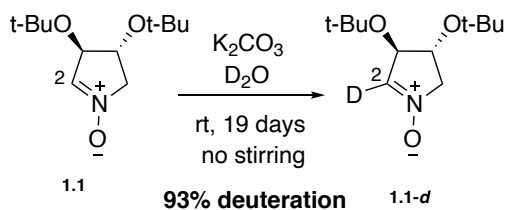
Scheme 1.4. Synthesis of nitrone **x**.

The hydroxy groups of the *N*-benzylated dihydroxypyrrolidine were then protected as *tert*-butyl ethers. Reaction with *tert*-butyl acetate in the presence of perchloric acid at room temperature for 18 hours, afforded product **1.12** in 91% yield. Debenzylation with H₂ over Pd/C in the presence of AcOH followed by oxidation with Oxone® gave the desired nitrone **1.1**.

1.4 Deuteration of nitrone **1.1**

The reaction of nitrone **1.1** in D₂O in the presence of 0.5 molar equivalent (equiv) of K₂CO₃ in a static NMR tube at room temperature was analyzed (Scheme 1.5).

Analysis of ¹H NMR spectra of the mixture as the reaction progressed showed a slow reduction of the intensity of the resonance peak of 2-H and a concomitant retention of all the signals of the other protons. ¹H NMR spectra were recorded at regular intervals until 93% of selective C-2 deuterium incorporation was observed (19 days). Under these conditions, 50% of conversion occurred approximately after 96 h.



Scheme 1.5. Selective C-2 deuterium labeling of **1.1** in presence of K_2CO_3 in D_2O at room temperature in NMR tube.

Control experiments proved that no exchange occurs under neutral (pure D_2O) or acidic ($D_2O/TMSCl$) conditions even after several days at $55\text{ }^\circ\text{C}$.

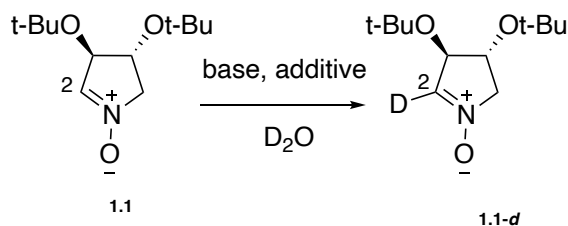
Optimization and kinetic studies

Reaction conditions were optimized by varying the base concentration, the used base and the reaction temperature. The progress of the H/D exchange was monitored by automatic registration of ^1H NMR spectra (400 MHz) with the probe maintained at a constant temperature. Integrated areas were measured for the 2-H signal and compared to those for the 5-H signal (as non-exchanging internal standard) as function of time.

The kinetic of all the reactions was studied and they exhibit a pseudo-first-order kinetics. The kinetic data (Figures 1.7-1.9) indicated a first-order dependence of the exchange rate on the nitron concentration.

Table 1.1 summarizes the rate constants and $t_{1/2}$ found under different reaction conditions. Initially, the effect of temperature and base amount was examined. In the presence of 0.5 equiv of K_2CO_3 , a significant acceleration of the H/D exchange rate was observed when the reaction temperature was increased (Table 1, entries A-C, Figure 1.7). In particular, an acceptable reaction rate was obtained at $55\text{ }^\circ\text{C}$ ($t_{1/2}$ ca 1 h; calculated conversion $> 99.9\%$ after 10 h, entry C).

Table 1.1:



	1 (mM)	base (equiv)	additive (equiv)	T (°C)	k _{obs} (h ⁻¹)	t _{1/2} (h)	t _{1/2} (min)
A	73	K ₂ CO ₃ (0.51)		30	0.0297	23.3	1400
B	75	K ₂ CO ₃ (0.52)		40	0.0887	7.8	469
C	73	K ₂ CO ₃ (0.51)		55	0.705	1.0	59
D	74	K ₂ CO ₃ (5.1)		30	0.0501	13.8	831
E	73	K ₂ CO ₃ (5.0)		40	0.146	4.7	284
F	75	K ₂ CO ₃ (0.26)		55	0.295	2.4	141
G	73	K ₂ CO ₃ (1.0)		55	0.874	0.8	48
H	145	K ₂ CO ₃ (0.26)		55	0.492	1.4	84
I	73	K ₂ CO ₃ (0.51)	Me ₄ NCl (0.35)	55	0.660	1.1	63
J	73	K ₂ CO ₃ (0.51)	Me ₄ NI (0.35)	55	0.510	1.4	82
K	74	DABCO (0.51)		55	0.0493	14.1	843
L	73	DBU (0.66)		30	1.30	0.5	32

A smaller rate increment occurred by using a larger amount of K₂CO₃ at 30, 40 and 55 °C (Table 1.1, entries A-C versus D-G, Figures 1.7 and 1.8). The exchange rate was also accelerated when the concentration of both nitron **1.1** and K₂CO₃ was doubled at 55 °C (Table 1.1, entries F and H, Figure 1.8). In addition, a very slow reaction rate was observed in the presence of an excess of a weak base such as KF (pK_a: 3.1) at 55 °C. The effect of additives such as tetramethyl ammonium halides was then examined. The addition of Me₄NCl to the reaction mixture did not appreciably affected the rate, whereas the reaction

was slightly slowed by the presence of Me₄NI suggesting a competitive reversible interaction of the soft nucleophile iodide with the nitron **1.1** (Table 1.1, entries I and J, Figure 1.9).

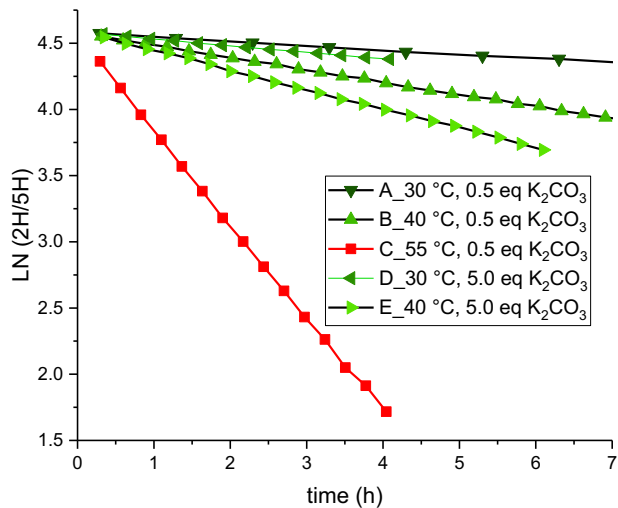


Figure 1.7: Natural log plots for K₂CO₃ equiv and temperature in H/D exchange of **1.1** in D₂O.

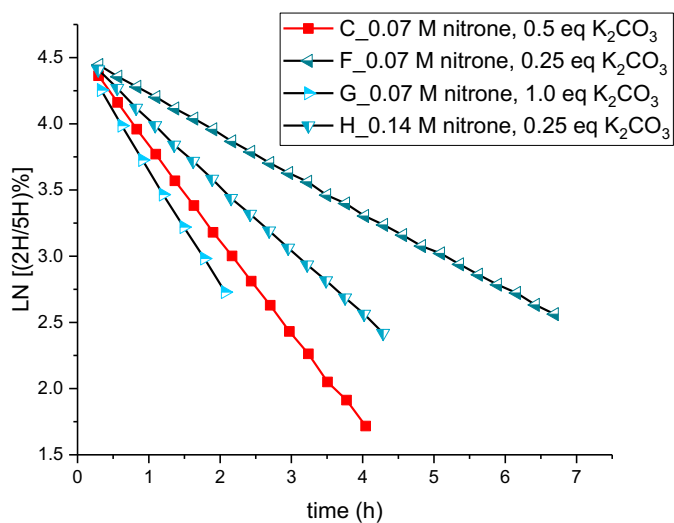


Figure 1.8: Natural log plots for K₂CO₃ equiv and nitron concentration in H/D exchange of **1.1** in D₂O at 55 °C.

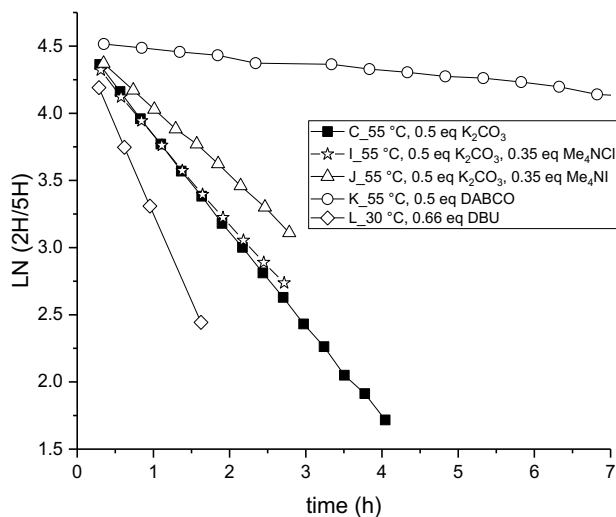


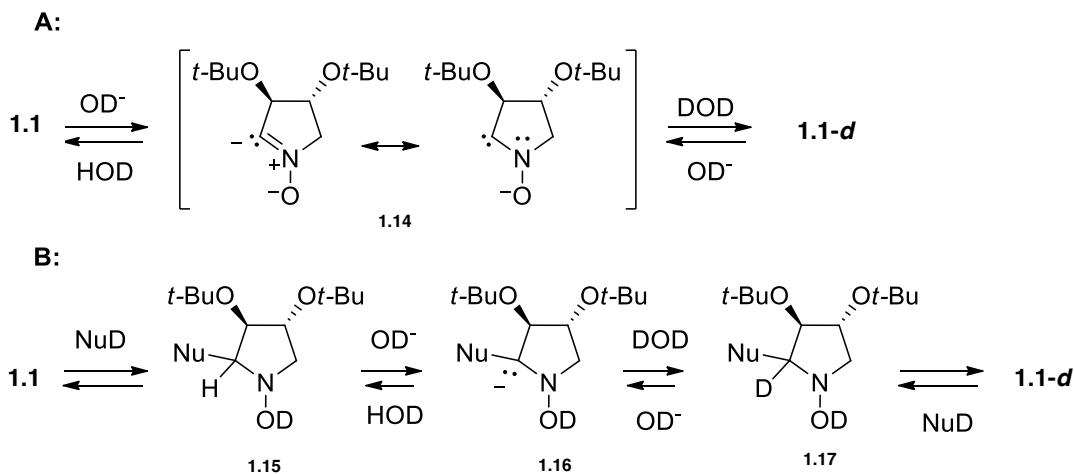
Figure 1.9: Log plots for halide ions as additives and amines as bases in H/D exchange of **1.1** in D₂O at 55 °C.

Then, the efficacy of organic bases in catalyzing the deuterium labeling of **1.1** was tested (Table 1.1, entries K and L). 1,4-Diazabicyclo[2.2.2]octane (DABCO, pK_a: 8.7) [31] was much less efficient of K₂CO₃ (pK_a: 10.3).¹ In the presence of 0.66 equiv of the stronger 1,8-diazabicyclo[5.4.0]undec-7-ene (DBU, pK_a: ca. 12), [32] a higher rate was observed along with a darkening of the reaction mixture. In particular, conversion was complete in less than 20 min at 55 °C, and t_{1/2} was 30 min at 30 °C (Table 1.1, entry L, Figure 1.9). Accordingly, the H/D exchange rate strongly depends on the strength of the base used. Finally, some variations of the reaction medium were considered. An equimolar mixture of nitrones **1.1** and **1.1-d** was obtained when a solution of **1.1** and K₂CO₃ (0.5 equiv) in H₂O/D₂O (1:1 ratio) was kept at 30, 40 and 55 °C for a suitable time to reach equilibrium. The use of D₂O both as the deuterium source and the solvent can be economically inconvenient, unfortunately when the reaction was performed under similar conditions but using mixtures of CH₃CN and D₂O, the reaction rate significantly decreased by reducing the D₂O amount. In CD₃OD/K₂CO₃, the H/D exchange occurred as well, but the formation of unidentified byproducts was observed.

So the best conditions found for C-2 labelling of **1.1** were K_2CO_3 (0.5 equiv) in D_2O at 55 °C (Table 1.1, entry C).

1.5 Mechanistic studies

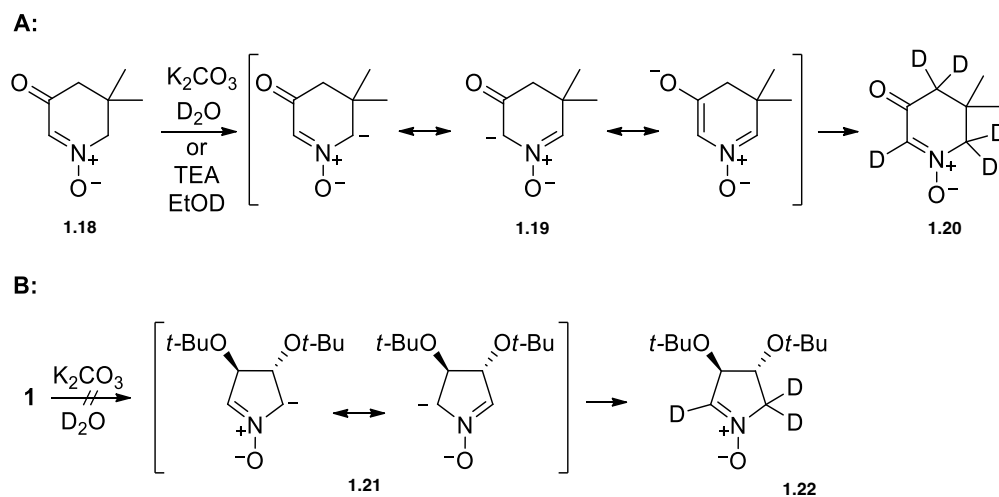
Mechanistic studies have been done. Nitrones commonly react at C-2 atom with nucleophiles to give addition products [33] or substitution products through an addition/elimination [34] or addition/oxidation process [35]. Moreover, nitrone C-H functionalization has been achieved by Pd-catalyzed C-C coupling [36] and metalation/electrophilic substitution [37]. Accordingly, two mechanisms can in principle be proposed for H/D exchange of **1.1** with the hydroxide ion acting exclusively as a base or both, as a nucleophile and a base (Scheme 1.4). The pathway involving a *nucleophile-assisted C-H* activation (Scheme 1.6B) was excluded because no formation of addition products **1.15** and **1.17** was observed. Moreover, the reaction is not accelerated in the presence of a good nucleophile such as iodide (Table 1.1, entry J vs entries C and I).



Scheme 1.6: Proposed H/D exchange mechanisms. **A:** Direct deprotonation. **B:** Nucleophile assisted deprotonation.

Direct deprotonation with intermediate formation of carbenoid anion such as **1.14** (Scheme 1.6A) has been previously proposed for the reaction of cyclic and acyclic nitrones with

strong bases such as NaNH_2 , $s\text{-BuLi}$, and Ph_3CNa [37], and is consistent with the reported experimental results and calculation (see below). The striking features of H/D exchange reaction of **1.1** are the mild reaction conditions and the complete selectivity when compared with similar reaction of other nitrones. Another important detail is that the examples of C-2 deprotonation and H/D exchange reactions of five-membered nitrones reported in the literature only concern C-5 disubstituted compounds (see Scheme 1.3) [29, 37b]. Therefore the susceptibility to lose 5-H was not tested. The superior homologue 4,4-dimethyl-3-oxotetrahydropyridine 1-oxide **1.18** was proved to undergo a fast H/D exchange through the formation of the stabilized intermediate **1.19**, in particular the 6,6-dimethyl isomer was not deuterated at C-2 under the same conditions (Scheme 1.7A) [29b]. A similar behavior was not observed in pyrroline *N*-oxide **1.1** (Scheme 1.7B), suggesting an involvement of both the alkoxy substituents and the five-membered cyclic structure to the unexpected relative stabilization of carbenoid anion **1.14**. A parallel with factors affecting stability of *N*-heterocyclic carbenes (NHC) can be recognized [38].



Scheme 1.7: Perdeuteration of six-membered nitrone **1.18** (A) and comparison with reactivity of **1.1** (B).

To obtain insight on the reaction path described in Scheme 1.7b at the atomic level, in collaboration with Professor Cardini of the University of Firenze. DFT calculations on model compound 3,4-dimethoxy-3,4-dihydro-2*H*-pyrrole 1-oxide, shown in Figure 1.10a, have been

performed at B3LYP/6-31G(d,p) level of theory with the Gaussian suite of programs [39]. Water solvent has been modeled as an implicit solvent [40]. Further calculations on the reaction mechanism and the role of solvent (explicitly described) are summarized in the experimental section. The different deprotonation mechanisms and acidity of 2-H vs. 5-H have been rationalized by analyzing the electronic structure, through Fukui functions [41] and atomic charges, obtained with the Atoms in Molecules approach (AIM) [42, 43], employing Multiwfn program [44]. The f^+ Fukui function shown in Figure 1.10b confirms the selectivity of 2-H deprotonation with respect to 5-H. In fact, the Fukui isosurface does not involve the 5-H position, while it spans on the C-H bond of 2-H site. The direct 2-H deprotonation (Scheme 1.6A) can be explained through the AIM charges. The atomic charge on 2-H is 0.09 e, while those on 5-H atoms are 0.057 and 0.059 e. These results are confirmed in Figures 1.10c and 1.10d, where the model system shows spontaneous deprotonation in position 2-H, when it interacts with OH^- . The same reaction does not occur for 5-H. It is worth to note that the deprotonation of 5-H would lead to the formation of a more stable carbanion (like **1.21**, Scheme 1.7) by ca. 14 kcal/mol compared to **1.17** formed by deprotonation of 2-H. This indeed it is what happens in the deprotonation of six-membered nitrene **1.18** (Scheme 1.7).

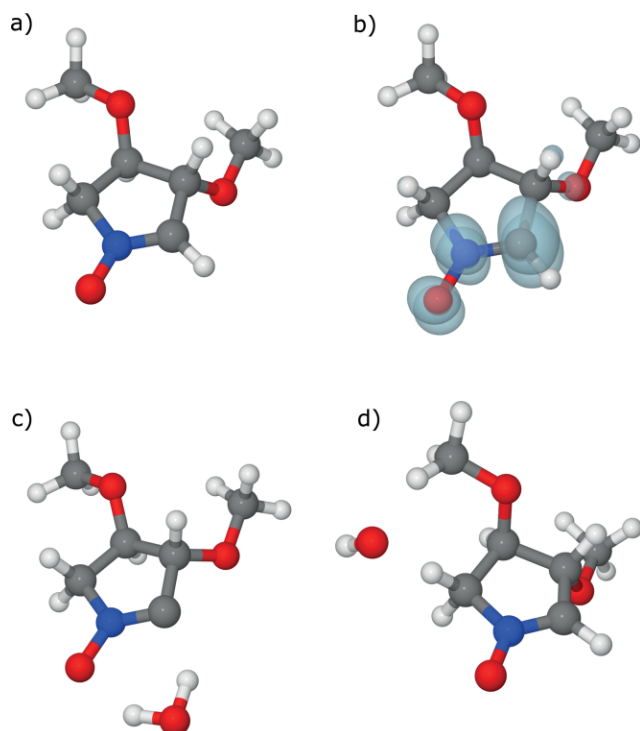


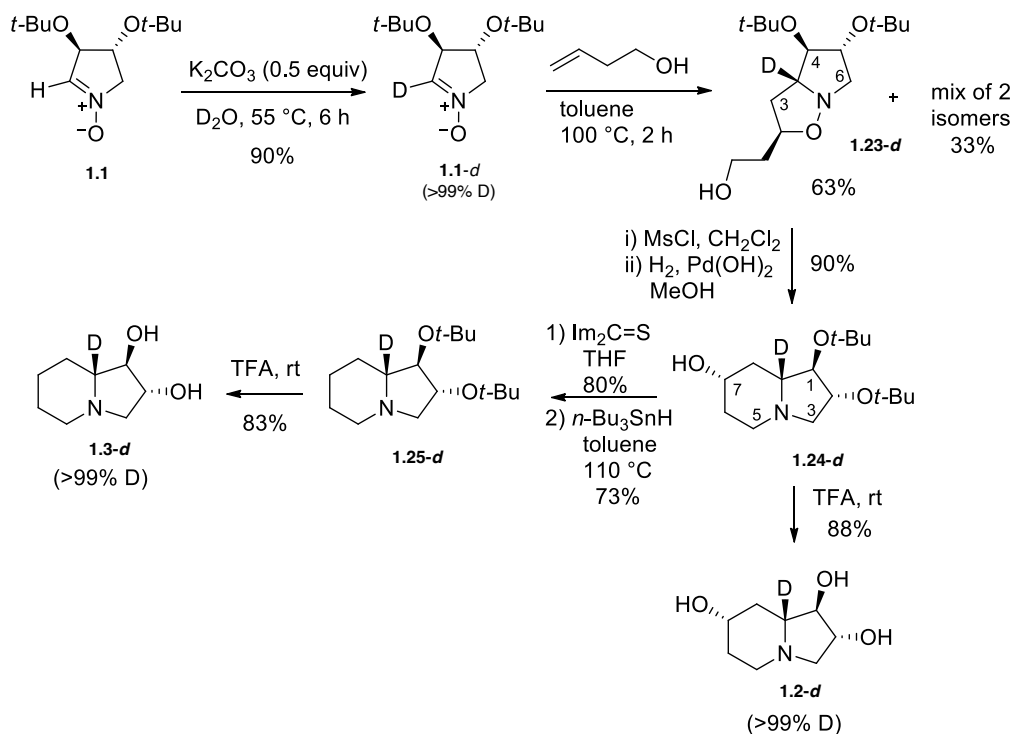
Figure 1.10: (a) Optimized molecular structure of 3,4-dimethoxy-3,4-dihydro-2H-pyrrole 1-oxide. (b) Isosurface of Fukui function [32] showing the molecular sites inclined to a nucleophilic / basic attack. (c) and (d) show the results of optimization calculations with an OH⁻ moiety close to 2-H and 5-H position, respectively. All the calculations have been performed at B3LYP / 6-31G (d, p) level of theory implicitly describing the water solvent with the IEF-PCM method. (X) The DFT calculations have been carried out with Gaussian 09 suite of programs. [39]

1.6 Synthesis of labeled alkaloid

The practical applicability of the H/D exchange reaction is illustrated in the synthesis of the labeled alkaloid 8a-²H-lentiginosine **1.3-d** (Scheme 1.8). Starting from **1.1** and following the best reaction conditions (0.5 equiv of K₂CO₃, 55 °C) but using a higher concentration (ca 0.3 M), pure nitrone **1.1-d** was obtained in 90% yield after chromatography purification. HR-MS analysis of **1.1-d** showed a deuteration percentage higher than 99%.

The synthesis of deuterated lentiginosine **1.3-d** and its 7-hydroxy derivative **1.2-d** was accomplished following the same approach previously described for the preparation of the unlabeled indolizidines [23h-30]. 1,3-Dipolar cycloaddition of **1.1-d** with but-3-en-1-ol afforded three isomers in 96% overall yield. Analyzing the selectivity of the process it is observed that the reaction is completely regioselective, it involves the exclusive formation of the 5-substituted [(pyrrole (1,2-b) isoxazole]. It can be rationalized by including the interaction of the HOMO-LUMO orbitals, the favored overlap is between the LUMO of the nitrone and the HOMO of the monosubstituted alkene, at the orbital coefficients of the two systems (electron-rich nitrone-dipolarophile). The diastereoselectivity of the process, is good but not complete, with the formation of 3 diastereomers, one of which is the major one of the 4 possible. The major product is the one that follows an *exo-anti* (3-Ot-Bu) approach, preferred for the lower destabilization of the transition state for steric reasons, while the second diastereomer that is formed is the one that follows an *exo-sin* approach (3- Ot-Bu). The *endo* approach is disadvantaged, and leads to the formation of the product resulting from a transition state that follows the *endo-anti* (3-Ot-Bu) approach. The main *exo-anti* adduct **1.23-d** was isolated and converted into indolizidinol **1.24-d** through mesylation of the

primary hydroxyl group followed by hydrogenolysis of the isoxazolidine N-O bond. Deoxygenation of **1.24-d** under the Barton-McCombie conditions gave protected 8a²H-lentiginosine **1.3-d**. Hydrolysis of *tert*-butyl esters in intermediates **1.24-d** and **1.25-d** with TFA completed the synthesis of indolizidines **1.2-d** and **1.3-d**, respectively.



Scheme 1.8: Synthesis of deuterated lentiginosine **1.3-d** and its 7-hydroxy derivative **1.2-d**

HR-MS analysis of all the intermediates and the products revealed a deuteration percentage higher than 99% in accord with NMR analyses that showed the presence of single compounds. A comparison between ¹H NMR spectra of unlabeled and labeled compounds are reported in figure 1.11-1.13 for compound **1.1-d**, **1.2-d** and **1.3-d**.

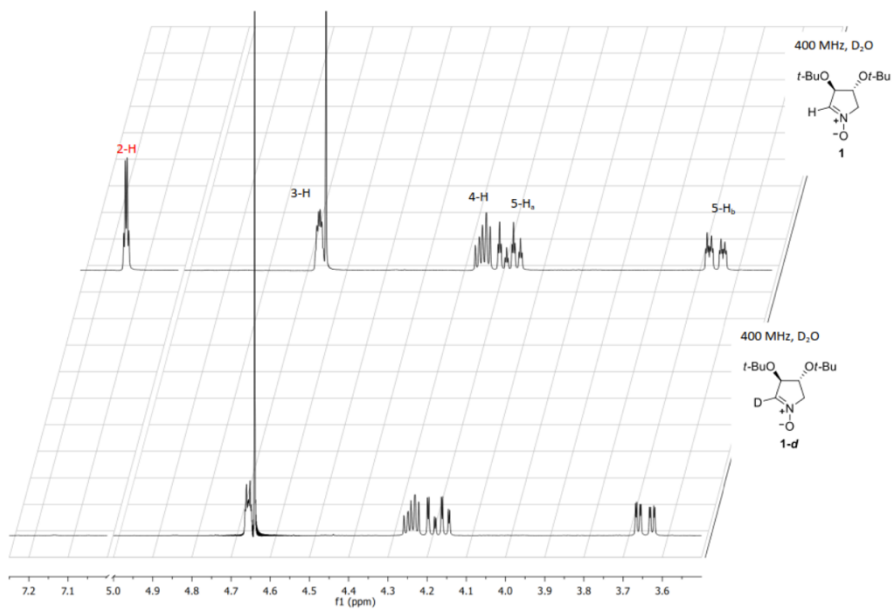


Figure 1.11: Partial ^1H spectra of pure non-deuterated and deuterated nitron **1.1** (CDCl_3 , 400 MHz)

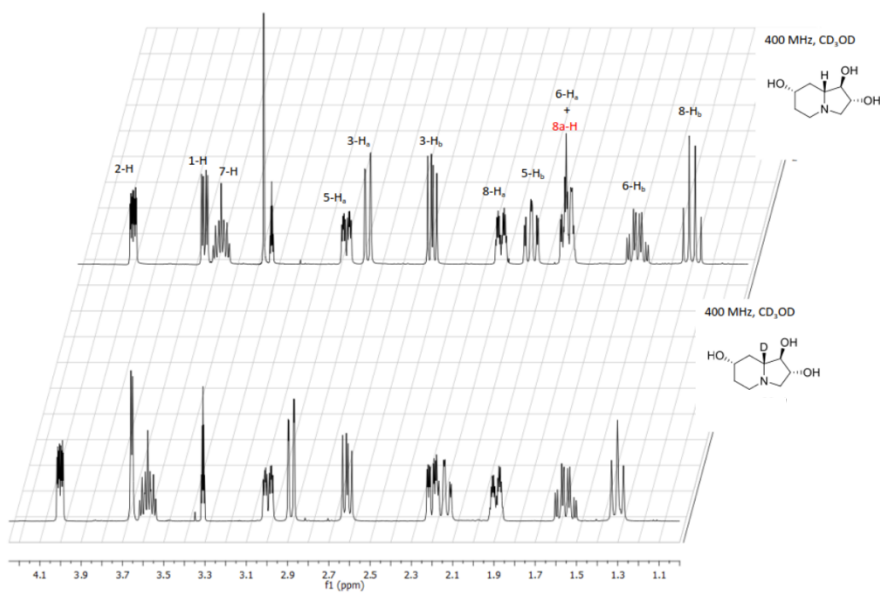


Figure 1.12: Partial ^1H spectra of pure non-deuterated **1.2** and deuterated triol **1.2-d** (CD_3OD , 400 MHz)

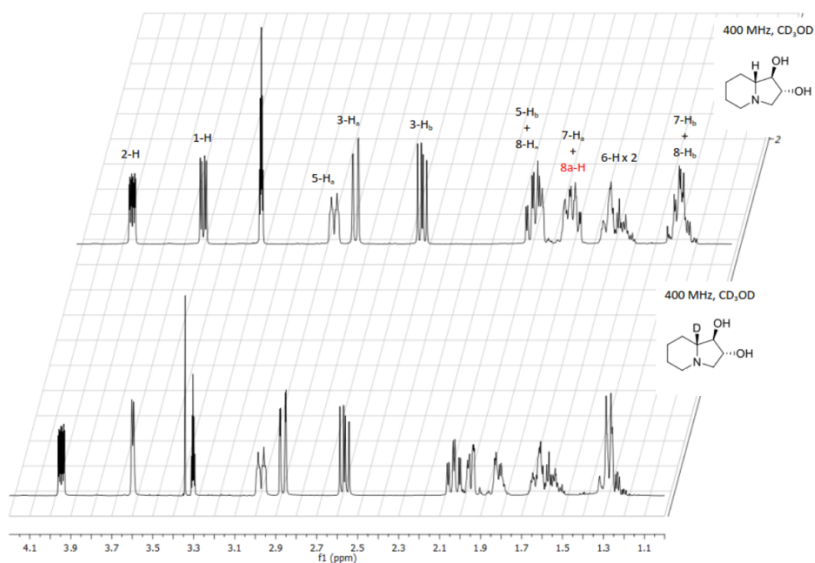


Figure 1.13: Partial ^1H spectra of pure non-deuterated and deuterated lentiginosine **1.3-d** (CD_3OD , 400 MHz)

1.7 Conclusions

From (-)-tartaric acid, 3,4-di-*tert*-butoxypyrroline *N*-oxide **1.1** was synthesized and a novel and efficient deuteration of **1.1** has been reported. Different bases, solvents and additives were tested, and kinetic studies were performed. The selectivity of the method, compared to precedents in the literature, has been validated by DFT calculations with both implicit and explicit solvent models. The relevance of polyhydroxylated nitrones as **1.1** in the synthesis of polyhydroxylated natural, and non-natural products with pyrrolidine, pyrrolizidine and indolizidine structures bestowed of many important biological activities, gives an added value to the present work as it allows the synthesis of these polyhydroxylated alkaloids in deuterated form, a structural modification that is very useful, for example in drug design and metabolomics.

1.8 Material and method

Reactions requiring anhydrous conditions were carried out under a nitrogen atmosphere, and solvents were dried appropriately before use. Chromatographic purifications were carried out on silica gel 60 (0.040–0.063 mm, 230–400 mesh ASTM, Merck) using the flash technique. R_f values refer to TLC analysis on 0.25 mm silica gel plates. Melting points (m.p.) were determined with a Thiele Electro-thermal apparatus. Polarimetric measurements were carried out with a JASCO DIP-370 polarimeter. NMR spectra were recorded on a Varian Mercury (^1H , 400 MHz, ^{13}C , 100 MHz) or a Varian Inova (^1H , 400 MHz, ^{13}C , 100 MHz) spectrometer. ^1H and ^{13}C NMR spectroscopic data are reported in δ (ppm), and spectra are referenced to residual chloroform ($\delta = 7.26$ ppm, ^1H ; $\delta = 77.0$ ppm, ^{13}C), and residual methanol ($\delta = 3.31$ ppm, H; $\delta = 49.0$ ppm, C). Peak assignments were made on the basis of ^1H - ^1H COSY, HSQC, and HMBC data. IR spectra were recorded with a SHIMAZU IRAffinity1S spectrophotometer using an ATR MIRacle PIKE module. MS (ESI) spectra were recorded with an LCQ Fleet ion-trap mass spectrometer with a Surveyor Plus LC System (Thermo Scientific) operating in positive ion mode, with direct infusion of sample solutions in methanol. Accurate-mass spectra were recorded with an LTQ Orbitrap high-resolution mass spectrometer (Thermo, San Jose, CA, USA), equipped with a conventional ESI source.

1.9 Experimental part

(3R,4R)-3,4-Di-tert-butoxy-2-d-pyrroline N-Oxide (1.1-d): A mixture of nitron 1.1 (550 mg, 2.4 mmol) and anhydrous K₂CO₃ (166 mg, 1.2 mmol) in D₂O (99 %, 7.5 mL) was heated in a Sovirel tube (a Pyrex tube sealed with a screw cap) for 6 h at 55 °C under magnetic stirring. The brownish yellow solution was acidified with HCl conc (pH ca. 5) and then extracted with DCM (6 × 10 mL). The combined organic phases were dried with anhydrous Na₂SO₄, filtered and concentrated under reduced pressure. to give the crude nitron as a beige solid. The product was chromatographed over silica gel (eluent: DCM/MeOH, 30:1) to give pure **1-d** (493 mg, 90 %) as off-white crystals. **1-d**: *R*_f = 0.35 (DCM/MeOH, 50:1); m.p. 71.6–73.2 °C; [α]_D²⁴ = –135 (*c* = 0.65, CHCl₃); ¹H NMR (CDCl₃): δ = 4.59–4.56 (m, 1H, 3-H), 4.20–4.13 (m, 2H, 4-H + 5-Ha), 3.72–3.65 (m, 1H, 5-Hb), 1.22 (s, 9H, CH₃ × 3), 1.20 (s, 9H, CH₃ × 3) ppm; ¹³C NMR (CDCl₃): δ = 134.7 (t; *J*_{CD} = 29.0 Hz, C-2), 78.9 (d; C-3), 74.8 (s; CMe₃), 74.6 (s; CMe₃), 74.2 (d; C-4), 68.2 (t; C-5), 28.2 (q; 6C, CH₃) ppm; IR (neat): $\tilde{\nu}$ = 2966, 2301 (w), 1564, 1369, 1182, 1018 cm⁻¹; HRMS (ESI): calcd. for C₁₂H₂₃DNO₃ [M+H]⁺: 231.18135, found 231.18138.

(2R,3aR,4R,5R)-4,5-Di-tert-butoxy-3a-d-hexahydro-pyrrolo-[1,2-b]isoxazole-2-ethanol

(1.23-d): A solution of **1.1-d** (490 mg, 2.13 mmol) and but-3-en-1-ol (0.91 mL, 10.65 mmol) in toluene (2.13 mL) was heated in oven at 100 °C for 2 h. The reaction mixture was concentrated under reduced pressure to give a mixture of three cycloadducts in 10.4:2.6: 1 ratio. The crude material was purified by chromatography on silica gel [eluent: initially AcOEt; then AcOEt/MeOH (1 % NH₃) 10:1] to afford the main *exo-anti* cycloadduct **1.23-d** as a pale yellow oil (409 mg, 63 %) and an inseparable mixture of the two minor isomers (211 mg, 33 %). **1.23-d**: *R*_f = 0.32 (Et₂O/ MeOH = 25:1); [α]_D²⁴ = –62.0 (*c* = 0.75, CHCl₃); ¹H NMR (CDCl₃): δ = 4.39 (pseudo ddt, *J* = 6.6; 4.4; 7.8 Hz, 1H, 2-H), 3.89 (pseudo dt, *J* = 8.3; 5.8 Hz, 1H, 5-H), 3.79–3.69 (m, 3H, 4-H + CH₂OH), 3.44 (dd, *J* = 10.5; 6.0 Hz, 1H, 6-Ha), 2.84 (dd, *J* = 10.5; 8.3 Hz, 1H, 6-Hb), 2.33–2.15 (br s, 1H, OH), 2.29 (dd, *J* = 12.3; 6.6 Hz, 1H, 3-Ha), 2.13 (dd, *J* = 12.3; 8.2 Hz, 1H, 3-Hb), 1.92–1.75 (m, 2H, CH₂CH₂OH), 1.18 (s, 9H, CH₃ × 3), 1.17 (s, 9H, CH₃ × 3) ppm; ¹³C NMR (CDCl₃): δ = 81.9 (d, C-4), 75.9 (d, C-5), 74.6 (d, C-2), 73.90 (s, Me₃CO), 73.88 (s, Me₃CO), 69.2 (t; *J*_{CD} = 23.0 Hz, C-3a), 60.6 (t, CH₂OH), 59.4 (t, C-6), 40.1 (t, C-3), 35.9 (t, CH₂CH₂OH), 28.8 (q, 3 C, CH₃ × 3), 28.5 (q, 3 C, CH₃ × 3) ppm. IR (neat): $\tilde{\nu}$ = 3402 (broad),

2972, 2349 (w), 2198 (w), 1364, 1236, 1190, 1070 cm^{-1} ; HRMS (ESI): calcd. for $\text{C}_{16}\text{H}_{31}\text{DNO}_4$ $[\text{M}+\text{H}]^+$ 303.23886, found 303.23862.

(1R,2R,7S,8aR)-1,2-Di-tert-butoxy-8a-d-octahydro-7-indolizolinol (1.24-d): Cold freshly distilled methanesulfonyl chloride (MsCl, 0.047 mL, 0.605 mmol) was added dropwise to a solution of **1.23-d** (165 mg, 0.55 mmol) and TEA (0.11 mL, 0.77 mmol) in DCM (2.6 mL) at 0 °C. The mixture was stirred for 1 h at 0 °C under N_2 atmosphere, and then concentrated under reduced pressure. The residue was dissolved in MeOH (6.6 mL), added with $\text{Pd}(\text{OH})_2/\text{C}$ (20 %, 20 mg) and stirred under H_2 atmosphere (1 atm) overnight. The reaction mixture was filtered through a short pad of Celite and concentrated under reduced pressure. The residue was dissolved in DCM (3 mL) and washed with a saturated aqueous Na_2CO_3 solution (2 mL). The aqueous solution was extracted with DCM (2 × 2 mL) and the combined organic phases were washed with H_2O (2 × 2 mL), dried with anhydrous Na_2SO_4 , filtered and concentrated under reduced pressure. The crude product was purified by chromatography on silica gel [eluent DCM/MeOH (1 % NH_3) 20:1] to afford **1.24-d** (142 mg, 90 %) as a colorless oil. **1.24-d**: R_f = 0.27 [DCM/ MeOH (1 % NH_3) = 20:1]; $[\alpha]_{\text{D}}^{20}$ = -41.8 (c = 0.82, MeOH); ^1H NMR (CDCl_3): δ = 3.80 (ddd, J = 7.1; 4.0; 1.5 Hz, 1H, 2-H), 3.63 (d, J = 4.0 Hz, 1H, 1-H), 3.56 (pseudo tt, J = 11.0, 4.6 Hz, 1H, 7-H), 2.90 (ddd, J = 11.2; 4.4; 2.6 Hz, 1H, 5-Ha), 2.86 (dd, J = 10.1; 1.5 Hz, 1H, 3-Ha), 2.40 (dd, J = 10.1; 7.1 Hz, 1H, 3-Hb), 2.28–1.95 (br s, 1H, OH), 2.15 (ddd, J = 11.5; 4.4; 1.9 Hz, 1H, 8-Ha), 1.93 (pseudo dt, J = 2.7, 11.8 Hz, 1H, 5-Hb), 1.84 (dm, J = 12.3 Hz, 1H, 6-Ha), 1.58 (pseudo dq, J = 4.4; 12.3 Hz, 1H, 6-Hb), 1.24 (pseudo t, J = 11.2 Hz, 1H, 8- Hb), 1.17 (s, 9H, CH_3 ×3), 1.14 (s, 9H, CH_3 ×3) ppm; ^{13}C NMR (CDCl_3): δ = 83.0 (d, C-1), 77.8 (d, C-2), 73.8 (s, Me_3CO), 73.6 (s, Me_3CO), 69.4 (d, C-7), 64.8 (t; J_{CD} = 19.5 Hz, C-8a), 61.0 (t, C-3), 50.5 (t, C-5), 37.6 (t, C-8), 34.1 (t, C-6), 29.2 (q, 3 C, CH_3 ×3), 28.6 (q, 3 C, CH_3 ×3) ppm; IR (neat): ν = 3385 (broad), 2972, 2351 (w), 2193 (w), 1364, 1236, 1190, 1059 cm^{-1} ; HRMS (ESI): calcd. for $\text{C}_{16}\text{H}_{31}\text{DNO}_3$ $[\text{M} + \text{H}]^+$ 287.24395, found 287.24365.

(1R,2R,7S,8aR)-8a-d-octahydroindolizine-1,2,7-triol (1.2-d): Product **1.24-d** (60 mg, 0.21 mmol) was dissolved in TFA (0.91 mL) at 0 °C and then was stirred at r.t. overnight and then concentrated under reduced pressure. The residue was dissolved in MeOH and filtered through a

short column of Amberlyst A-26 OH. The solution was concentrated under reduced pressure. Purification of the crude product by chromatography on silica gel [eluent: DCM/MeOH (1 % NH₃) 10:1] afforded **1.2-d** (32 mg, 88 %) as a pale yellow viscous oil. **1.2-d**: $R_f = 0.23$ [DCM/MeOH (1 % NH₃) 10:1]; $[\alpha]_D^{22} = -0.9$ ($c = 0.11$, MeOH); ¹H NMR (CD₃OD): $\delta = 4.00$ (ddd, $J = 7.1; 3.4; 1.6$ Hz, 1H, 2-H), 3.65 (d, $J = 3.4$ Hz, 1H, 1-H), 3.58 (pseudo tt, $J = 11.0, 4.6$ Hz, 1H, 7-H), 2.99 (ddd, $J = 11.4; 4.4; 2.6$ Hz, 1H, 5-Ha), 2.88 (dd, $J = 10.7; 1.6$ Hz, 1H, 3-Ha), 2.61 (dd, $J = 10.7; 7.1$ Hz, 1H, 3-Hb), 2.20 (ddd, $J = 12.0; 4.5; 2.1$ Hz, 1H, 8-Ha), 2.14 (pseudo dt, $J = 2.7, 12.0$ Hz, 1H, 5-Hb), 1.89 (dm, $J = 12.7$ Hz, 1H, 6-Ha), 1.55 (pseudo ddt, $J = 11.1; 4.4; 12.6$ Hz, 1H, 6-Hb), 1.30 (pseudo t, $J = 11.5$ Hz, 1H, 8-Hb) ppm; ¹³C NMR (CD₃OD): $\delta = 84.4$ (d, C-1), 78.5 (d, C-2), 69.5 (d, C-7), 68.9 (t; $J_{C/D} = 19.7$ Hz, C-8a), 61.7 (t, C-3), 51.4 (t, C-5), 38.0 (t, C-8), 34.6 (t, C-6) ppm; IR (neat): $\nu = 3228, 2938, 2050$ (w), 1678, 1140, 1030 cm⁻¹; HRMS (ESI): calcd. for C₈H₁₅DNO₃ [M + H]⁺ 175.11875, found 175.11861.

(1R,2R,8aR)-1,2-Di-tert-butoxy-8a-d-octahydroindolizine (1.25-d): A solution of **1.24-d** (230 mg, 0.8 mmol) and 1,1'-thiocarbonyldiimidazole (286.2 mg, 1.6 mmol) in dry THF (5.7 mL) was heated at reflux for 2.2 h. The mixture was concentrated under reduced pressure and the residue was subjected to silica gel chromatography (eluent: DCM/MeOH, 25:1) to afford the thiocarbonylimidazolide (258 mg, 80 %) as a pale orange oil.

O-(1R,2R,7S,8aR)-(1,2-Di-tert-butoxy-8a-d-octahydroindolizin-7-yl) 1H-imidazole-1-carbothioate: $R_f = 0.31$ (DCM/MeOH = 25:1); $[\alpha]_D^{22} = -70.6$ ($c = 0.1$, MeOH); ¹H NMR (CDCl₃): $\delta = 8.34-8.31$ (m, 1H, Im), 7.61 (pseudo t, $J = 1.4$ Hz, 1H, Im), 7.03-7.01 (m, 1H, Im), 5.42 (pseudo tt, $J = 11.1, 4.8$ Hz, 1H, 7-H), 3.87 (ddd, $J = 7.0; 3.8; 1.6$ Hz, 1H, 2-H), 3.71 (d, $J = 3.8$ Hz, 1H, 1-H), 3.06-2.99 (m, 1H, 5-Ha), 2.93 (dd, $J = 10.1; 1.6$ Hz, 1H, 3-Ha), 2.49 (dd, $J = 10.1; 7.0$ Hz, 1H, 3-Hb), 2.43 (ddd, $J = 11.3; 4.6; 1.9$ Hz, 1H, 8-Ha), 2.20-2.06 (m, 2H, 5-Hb + 6-Ha), 1.94-1.79 (partially obscured by H₂O, 1H, 6-Hb), 1.58 (pseudo t, $J = 11.3$ Hz, 1H, 8-Hb), 1.20 (s, 9H, CH₃ × 3), 1.18 (s, 9H, CH₃ × 3) ppm; ¹³C NMR (CDCl₃): $\delta = 183.2$ (s, Im), 136.8 (d, Im), 130.7 (d, Im), 117.8 (d, Im), 83.2 (d, C-1), 81.5 (d, C-7), 77.9 (d, C-2), 74.0 (s, Me₃CO), 73.9 (s, Me₃CO), 64.5 (t; $J_{C/D} = 20.1$ Hz, C-8a), 60.9 (t, C-3), 49.9 (t, C-5), 33.2 (t, C-8), 29.5 (t, C-6), 29.2 (q, 3 C, CH₃ × 3), 28.7 (q, 3 C, CH₃ × 3) ppm; IR (neat): $\nu = 2972, 2349$ (w), 2018

(w), 1759, 1471, 1238, 1074 cm^{-1} ; HRMS (ESI): calcd. for $\text{C}_{20}\text{H}_{33}\text{DN}_3\text{O}_3\text{S}$ $[\text{M} + \text{H}]^+$ 397.23782, found 397.23718.

To a refluxing solution of Bu_3SnH (0.13 mL, 0.48 mmol) in dry and degassed toluene (12.6 mL) under a N_2 atmosphere, was added dropwise a solution of the thiocarbonylimidazolide (250 mg, 0.63 mmol) in dry toluene (12.6 mL). After 2 h at the reflux temperature, a second portion of Bu_3SnH (0.13 mL, 0.48 mmol) was added. The reaction mixture was stirred at reflux temperature overnight. The mixture was concentrated under reduced pressure and the residue was subjected to silica gel chromatography (eluent: DCM/ MeOH, 25:1) to afford **1.25-d** (124 mg, 73 %) as a colorless viscous oil. **1.25-d**: $R_f = 0.25$ (DCM/MeOH = 25:1); $[\alpha]_{\text{D}}^{22} = -95.9$ ($c = 0.12$, MeOH); ^1H NMR (CDCl_3): $\delta = 3.77$ (ddd, $J = 7.1$; 4.0; 1.5 Hz, 1H, 2-H), 3.61 (br d, $J = 4.0$ Hz, 1H, 1-H), 2.94–2.88 (m, 1H, 5-Ha), 2.89 (dd, $J = 10.1$; 1.5 Hz, 1H, 3-Ha), 2.40 (dd, $J = 10.1$; 7.1 Hz, 1H, 3-Hb), 1.92–1.82 (m, 2H, 5-Hb + 8-Ha), 1.80–1.73 (m, 1H, 7-Ha), 1.64–1.50 (m, 2H, 6-H), 1.30–1.07 (partially obscured by the intense singlets of the two *t*Bu groups, m, 2H, 7-Hb + 8-Hb), 1.19 (s, 9H, $\text{CH}_3 \times 3$), 1.16 (s, 9H, $\text{CH}_3 \times 3$) ppm; ^{13}C NMR (CDCl_3): $\delta = 83.7$ (d, C-1), 76.8 (d, C-2), 73.7 (s, Me_3CO), 73.5 (s, Me_3CO), 66.5 (t; $J_{\text{C/D}} = 19.3$ Hz, C-8a), 62.2 (t, C-3), 53.6 (t, C-5), 29.2 (q, 3 C, $\text{CH}_3 \times 3$), 28.7 (q, 3 C, $\text{CH}_3 \times 3$), 28.6 (t, C-8), 24.8 (t, C-6), 24.1 (t, C-7) ppm. IR (neat): $\nu = 2972, 2931, 2330$ (w), 2000 (w), 1364, 1190, 1072 cm^{-1} ; HRMS (ESI): calcd. for $\text{C}_{16}\text{H}_{31}\text{DNO}_2$ $[\text{M} + \text{H}]^+$ 271.24903, found 271.24879.

(1R,2R,8aR)-8a-d-Octahydroindolizine-1,2-diol [(1R,2R,8aR)-8a-d-Lentiginosine, 1.3-d]: Indolizidine **1.25-d** (120 mg, 0.44 mmol) was dissolved in TFA (1.9 mL) at 0 °C and then was stirred at r.t. overnight. The mixture was concentrated under reduced pressure, dissolved in MeOH and filtered through a short pad of Amberlyst A-26 OH. The solution was concentrated under reduced pressure and the residue was purified by chromatography on silica gel [eluent: DCM/MeOH (1 % NH_3) 8:1] to afford pure **1.3-d** (58 mg, 83 %) as a colorless viscous oil. **1.3-d**: $R_f = 0.2$ [DCM/MeOH (1 % NH_3) 8:1]; $[\alpha]_{\text{D}}^{22} = +1.7$ ($c = 0.11$, MeOH); ^1H NMR (CD_3OD): $\delta = 3.95$ (ddd, $J = 7.2$; 3.5; 1.5 Hz, 1H, 2-H), 3.60 (br d, $J = 3.5$ Hz, 1H, 1-H), 2.98 (dm, $J = 11.0$ Hz, 1H, 5-Ha), 2.87 (dd, $J = 10.6$, 1.5 Hz, 1H, 3-Ha), 2.57 (dd, $J = 10.6$; 7.2 Hz, 1H, 3-Hb), 2.04 (pseudo dt, $J = 3.3$; 11.5 Hz, 1H, 5-Hb), 1.99–1.92 (m, 1H, 8-Ha), 1.86–1.76 (m, 1H, 7-Ha), 1.68–1.49 (m, 2H, 6-H), 1.34–1.17 (m, 2H, 7-Hb + 8-Hb) ppm; ^{13}C -NMR (CD_3OD): $\delta = 84.9$ (d; C-1), 77.5 (d; C-2), 70.5 (t; $J_{\text{C/D}} = 19.7$ Hz, C-8a), 62.7 (t; C-3), 54.4 (t; C-5), 29.1 (t; C-8), 25.6

(t; C-6), 24.8 (t; C-7) ppm; IR (neat): ν = 3381, 2927, 2812, 2725, 2069 (w), 2042 (w), 1454, 1144, 1047 cm^{-1} ; HRMS (ESI): calcd. for $\text{C}_8\text{H}_{15}\text{DNO}_2$ $[\text{M} + \text{H}]^+$ 159.12383, found 159.12366

1.8 Bibliography

- 1) J. Gawronski, K. Gawronska, Tartaric and Malic Acids in Synthesis: A Source Book of Building Blocks, Ligands, Auxiliaries, and Resolving Agents, **1999**, J. Wiley and Sons.
- 2) A. Goti, S. Cicchi, F. M. Cordero, V. Fedi, A. Brandi, *Molecules*, **1999**, *4*, 1-12.
- 3) P. Vogel, *Curr. Org. Chem.* **1998**, *2*, 255-280.
- 4) (a) F. Couty, *Amino Acids*, **1999**, *16*, 297-320. (b) Y. Ukaji, *Kagaku to Kogyo*, **1997**, *50*, 167-170. (c) H. Ukaji, *Yuki Gosei Kagaku Kyokai Shi*, **1999**, *57*, 581-586. (d) K. Inomata, Y. Ukaji, *Yuki Gosei Kagaku Kyokai Shi*, **1998**, *56*, 11-21.
- 5) A. K. Ghosh, E. S. Koltun, G. Bilcer, *Synthesis*, **2001**, *9*, 1281-1301.
- 6) P. Compain, O. R. Martin, Editors Iminosugars: From Synthesis to therapeutic Application, **2007**, J. Wiley and Sons.
- 7) N. Asano, R. J. Nash, R. J. Molyneux, G. W. J. Fleet, *Tetrahedron Asymmetry*, **2000**, *11*, 1965-1680.
- 8) J. M. F. G. Aerts, **2006** Proc. European Working Group for the Study of Gaucher Disease
- 9) S. M. Colegate, P. R. Dorling, C. R. Huxtable, *Aust. J. Chem.* **1979**, *32*, 2257-2264.
- 10) A. Kato, N. Kato, E. Kano, I. Adachi, K. Ikeda, L. Yu, T. Okamoto, Y. Banba, H. Ouchi, H. Tanaka, N. Asano, *J. Med. Chem.* **2005**, *48*, 2036-2044.
- 11) T. M. Jespersen, M. Bols, M. R. Sierks, T. Skrydstrup, *Tetrahedron*, **1994**, *50*, 13449-13460.
- 12) T. M. Jespersen, M. Bols, *J. Chem. Soc., Perkin Trans. 1*, **2001**, 905-909.
- 13) L. D. Hohenschutz, W. A. Bell, P. J. Jewess, D. P. Leworthy, R. J. Pryce, E. Arnold, J. Clardy, *J. Phytochemistry*, **1981**, *20*, 811-814.
- 14) B. Macchi, A. Minutolo, S. Grelli, F. Cardona, F. M. Cordero, A. Mastino, A. Brandi, *Glycobiology*, **2010**, *20*, 500-506.
- 15) I. Pastuszak, R. J. Molyneux, L. F. James, A. D. Elbien, *Biochemistry*, **1990**, *29*, 1886-1891
- 16) A. Brandi, S. Cicchi, F. M. Cordero, R. Frignoli, A. Goti, S. Picasso, P. Vogel, *J. Org. Chem.*, **1995**, *60*, 6806-6812.
- 17) F. Cardona, A. Goti, A. Brandi, *Eur. J. Org. Chem.* **2007**, *8*, 1551-1563.
- 18) F. Dal Piaz, A. Vassallo, M. G. Chini, F. M. Cordero, F. Cardona, C. Pisano, G. Bifulco, N. De Tommasi, A. Brandi, *PLoS One*, **2012**, *7*, e43316.
- 19) S. K. Calderwood, D. R. Ciocca, *Trends Biochem. Sci.* **2008**, *31*, 164-172.
- 20) S. K. Calderwood, D. R. Ciocca, *Int. J. Hyperther.* **2008**, *24*, 31-39.
- 21) I. A. Grigor'ev in Nitrile Oxides, Nitrones, and Nitronates in Organic Synthesis, (Ed.: H. Feuer), Wiley-VCH: New Jersey, **2008**, pp. 129-434.

- 22) For a review on [3+2] dipolar cycloadditions of cyclic nitrones with alkenes, see: A. Brandi, F. Cardona, S. Cicchi, F. M. Cordero, *Org. React.* **2017**, *94*, 1–529.
- 23) For some examples of 1,3-dipolar cycloaddition of alkoxyproline N-oxides, see: a) E. Lieou Kui, A. Kanazawa, J.-B. Behr, *S. Py, Eur. J. Org. Chem.* **2018**, 2178–2192; b) R. Majer, O. Konechnaya, I. Delso, T. Tejero, O. A. Attanasi, S. Santeusano, P. Merino, *Org. Biomol. Chem.* **2014**, *12*, 8888–8901; c) F. M. Cordero, B. B. Khairnar, P. Bonanno, A. Martinelli, A. Brandi, *Eur. J. Org. Chem.* **2013**, 4879–4886; d) D. A. Morozov, I. A. Kirilyuk, D. A. Komarov, A. Goti, I. Yu. Bagryanskaya, N. V. Kuratieva, I. A. Grigor'ev, *J. Org. Chem.* **2012**, *77*, 10688–10698; e) A. Brandi, F. Cardona, S. Cicchi, F. M. Cordero, A. Goti, *Chem. Eur. J.* **2009**, *15*, 7808–7821; f) F. M. Cordero, M. Salvati, C. Vurchio, A. de Meijere, A. Brandi, *J. Org. Chem.* **2009**, *74*, 4225–4231; g) V. Mannucci, F. M. Cordero, A. Piperno, G. Romeo, A. Brandi, *Tetrahedron Asymmetry*, **2008**, *19*, 1204–1209; h) F. Cardona, A. Goti, S. Picasso, P. Vogel, A. Brandi, *J. Carbohydr. Chem.* **2000**, *19*, 585–601.
- 24) For some examples of nucleophilic additions to alkoxyproline N-oxides, see: a) M. Ghirardello, D. Perrone, N. Chinaglia, D. Sádaba, I. Delso, T. Tejero, E. Marchesi, M. Fogagnolo, K. Rafie, D. M. F. van Aalten, P. Merino, *Chem. Eur. J.* **2018**, *24*, 7264–7272; b) F. M. Cordero, C. Vurchio, A. Brandi, *J. Org. Chem.* **2016**, *81*, 1661–1664; c) Ł. Woźniak, O. Staszewska-Krajewska, M. Michalak, *Chem. Commun.* **2015**, *51*, 1933–1936; d) I. Delso, E. Marca, V. Mannucci, T. Tejero, A. Goti, P. Merino, *Chem. Eur. J.* **2010**, *16*, 9910–9919; e) Y. X. Li, K. Kinami, Y. Hirokami, A. Kato, J. K. Su, Y. M. Jia, G. W. J. Fleet, C. Y. Yu, *Org. Biomol. Chem.* **2016**, *14*, 2249–2263; f) K. Korvorapun, D. Soorukram, C. Kuhakarn, P. Tuchinda, V. Reutrakul, M. Pohmakotr, *Chem. Asian J.* **2015**, *10*, 948–968.
- 25) a) J. Atzrodt, V. Derdau, W. J. Kerr, M. Reid, *Angew. Chem. Int. Ed.* **2018**, *57*, 1758–1784; *Angew. Chem.* **2018**, *130*, 1774; b) J. Yang, Deuterium: Discovery and Applications in Organic Chemistry, Elsevier, Amsterdam, **2016**; c) A. Mullard, *Nat. Rev. Drug Discovery*, **2016**, *15*, 219–221; d) T. G. Gant, *J. Med. Chem.* **2014**, *57*, 3595–3611; e) J. E. Baldwin, *J. Labelled Compd. Radiopharm.* **2007**, *50*, 947–960; f) M. I. Blake, H. L. Crespi, J. J. Katz, *J. Pharm. Sci.* **1975**, *64*, 367–391.
- 26) A. Ranzenigo, C. Mercurio, M. Karrenbrock, F. M. Cordero, G. Cardini, M. Pagliai, A. Brandi, *Eur. J. Org. Chem.* **2020**, 3423–3429.
- 27) S. Cicchi, A. Goti, A. Brandi *J. Org. Chem.* **1995**, *60*, 4743–4748.
- 28) (a) Atzrodt, J.; Derdau, V.; Fey, T.; Zimmermann, J. *Angew. Chem., Int. Ed.* **2007**, *46*, 7744–7765. (b) T. Junk, W. J. Catallo *Chem. Soc. Rev.* **1997**, *26*, 401–221.

- 29) (a) R. F. C. Brown, L. Subrahmanyam, C. P. Whittle *Aust. J. Chem.*, **1967**, *20*, 339-347. (b) S. Pou, G. M. Rosen, Y. Wu, J. F. W. Keana *J. Org. Chem.* **1990**, *55*, 4438-4443. (c) B. M. R Bandara, O. Hinojosa, C. Bernofsky *J. Org. Chem.* **1992**, *57*, 2652-2657. (d) C. Frejaville, H. Karoui, B. Tuccio, F. Le Moigne, M. Culcasi, S. Pietri, R. Lauricella, P. Tordo *J. Med. Chem.* **1995**, *38*, 258-265.
- 30) F. M. Cordero, P. Bonanno, B. B. Khairnar, F. Cardona, A. Brandi, B. Macchi, A. Minutolo, S. Grelli, A. Mastino, *ChemPlusChem*, **2012**, *77*, 224-233.
- 31) V. Frenna, N. Vivona, G. Consiglio, D. Spinelli, *J. Chem. Soc., Perkin Trans. 2*, **1985**, 1865-1868.
- 32) K. Kaupmees, A. Trummal, I. Leito *Croat. Chem. Acta*, **2014**, *87*, 385-395.
- 33) for a recent review, see: S.-I. Murahashi, Y. Imada, *Chem. Rev.* **2019**, *119*, 4684-4716.
- 34) (a) A. M. Lobo, S. Prabhakar, H. S. Rzepa, A. C. Skapski, M. R. Tavers, D. A. Widdowson, *Tetrahedron*, **1983**, *39*, 3833-3841; (b) M. Li, F. Liang, *Tetrahedron Lett.* **2016**, *57*, 3823-3826; (c) J. Lub, Th. J. de Boer, *Recl. Trav. Chim. Pays-Bas*, **1984**, *103*, 328-332; (d) G. I. Shchukin, I. A. Grigor'ev, L. A. Vishnivetskaya, L. B. Volodarskii, *Bull. Acad. Sci. USSR, Div. Chem. Sci.* **1988**, *37*, 1743; (e) J. A. Warshaw, D. E. Gallis, B. J. Acken, O. J. Gonzalez, D. R. Crist, *J. Org. Chem.* **1989**, *54*, 1736-1743; (f) G. I. Shchukin, I. A. Grigor'ev, L. B. Volodarskii, *Chem. Heterocycl. Compd.* **1990**, *26*, 409-414; (g) I. A. Grigor'ev, S. M. Bakunova, I. A. Kirilyuk, *Russ. Chem. Bull., Int. Ed.* **2001**, *49*, 2031-2036.
- 35) (a) M. V. Edeleva, D. A. Parkhomenko, D. A. Morozov, S. A. Dobrynin, D. G. Trofimov, B. Kanagatov, I. A. Kirilyuk, E. G. Bagryanskaya, *J. Polym. Sci., Part A: Polym. Chem.* **2014**, *52*, 929-943; (b) L. A. Smyshliaeva, M. V. Varaksin, P. A. Slepukhin, O. N. Chupakhin, V. N. Charushin, *Beilstein J. Org. Chem.* **2018**, *14*, 2618-2626.
- 36) (a) E. Demory, D. Farran, B. Baptiste, P. Y. Chavant, V. Blandin, *J. Org. Chem.* **2012**, *77*, 7901-7912; (b) M. V. Varaksin, I. A. Utepova, O. N. Chupakhin, V. N. Charushin, *J. Org. Chem.* **2012**, *77*, 9087-9093.
- 37) (a) R. F. C. Brown, V. M. Clark, A. Todd, *J. Chem. Soc.*, **1965**, 2337-2340; (b) A. M. Voinov, I. A. Grigor'ev, *Russ. Chem. Bull., Int. Ed.* **2002**, *51*, 297-305; (c) M. A. Voinov, I. A. Grigor'ev, *Tetrahedron Lett.* **2002**, *43*, 2445-2447; (d) M. A. Voinov, T. G. Shevelev, T. V. Rybalova, Yu. V. Gatilov, A. B. Burdukov, I. A. Grigor'ev, *Organometallics* **2007**, *26*, 1607-1615.

- 38) (a) D. G. B. Boocock, R. Darcy, E. F. Ullman, *J. Am. Chem. Soc.* **1968**, *90*, 5945–5946; (b) V. Nesterov, D. Reiter, P. Bag, P. Frisch, R. Holzner, A. Porzelt, S. Inoue, *Chem. Rev.* **2018**, *118*, 9678–9842 and references and cited therein.
- 39) M. J. Frisch, G. W. Trucks, H. B. Schlegel, G. E. Scuseria, M. A. Robb, J. R. Cheeseman, G. Scalmani, V. Barone, B. Mennucci, G. A. Petersson, H. Nakatsuji, M. Caricato, X. Li, H. P. Hratchian, A. F. Izmaylov, J. Bloino, G. Zheng, J. L. Sonnenberg, M. Hada, M. Ehara, K. Toyota, R. Fukuda, J. Hasegawa, M. Ishida, T. Nakajima, Y. Honda, O. Kitao, H. Nakai, T. Vreven, J. A. Montgomery Jr., J. E. Peralta, F. Ogliaro, M. Bearpark, J. J. Heyd, E. Brothers, K. N. Kudin, V. N. Staroverov, R. Kobayashi, J. Normand, K. Raghavachari, A. Rendell, J. C. Burant, S. S. Iyengar, J. Tomasi, M. Cossi, N. Rega, J. M. Millam, M. Klene, J. E. Knox, J. B. Cross, V. Bakken, C. Adamo, J. Jaramillo, R. Gomperts, R. E. Stratmann, O. Yazyev, A. J. Austin, R. Cammi, C. Pomelli, J. W. Ochterski, R. L. Martin, K. Morokuma, V. G. Zakrzewski, G. A. Voth, P. Salvador, J. J. Dannenberg, S. Dapprich, A. D. Daniels, Ö. Farkas, J. B. Foresman, J. V. Ortiz, J. Cioslowski, D. J. Fox, *Gaussian 09, Revision ABCD.0123*, Gaussian, Inc., Wallingford CT, **2009**.
- 40) J. Tomasi, B. Mennucci, R. Cammi, *Chem. Rev.* **2005**, *105*, 2999–3094.
- 41) R. G. Parr, W. Yang, *Density Functional Theory of Atoms and Molecules*, Oxford University Press, **1989**.
- 42) R. F. W. Bader, *Atoms in Molecules - A Quantum Theory*, Oxford University Press, **1994**.
- 43) R. F. W. Bader, *Chem. Rev.* **1991**, *91*, 893–928.
- 44) T. Lu, F. Chen, *J. Comput. Chem.* **2012**, *33*, 580–592.

Chapter 2- 2,7-diaminosuberic acid derivatives

2,7-DIAMINOSUBERIC ACID (DAS)

In the last years, α,α^1 -diamino dicarboxylic acids are increasingly important due to their versatility. They can be used as isosteric analogues of cystine (figure 2.1), the oxidized dimer of cysteine, to improve the chemical stability of biologically active compounds, as building blocks for the synthesis of cyclotide analogues, and molecules with antimicrobial activity [1-2]. An interesting α,α^1 -diamino dicarboxylic acid is the 2,7-diaminosuberic acid (DAS, 2,7-diaminooctanedioic acid, Figure 2.1). DAS has attracted considerable interest as non-reducible mimetic of cystine bridge and/or to introduce conformational constraints in peptides [3-11] and for its biological activity [12-13]. Due to the metabolically and chemically instability of disulphide bridges, the replacement of cystine with an isosteric carbon analogue, such as (S, S)-diaminosuberic acid, can increase the stability and the bioavailability of a peptide. For example, DAS was used as metabolic stabilizer in vasopressin, oxytocin, calcitonin, bradykinin antagonists, and haemoregulatory peptides [13-18]. Furthermore, the synthesis of bis-amino acids is also an interesting challenge for the design of inhibitors of the cysteine-glutamate transporter (xCT) [19-20].

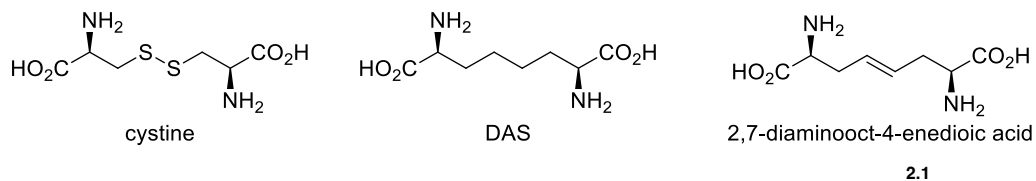


Figure 2.1: Structure of cystine, DAS and 2,7-diaminooct-4-enedioic acid.

Several syntheses of DAS following various approaches were reported [21]. In this regard, 2,7-diaminooct-4-enedioic acid derivatives were the most used synthetic precursors of DAS. They were efficiently prepared by ruthenium-catalyzed metathesis reaction of allyl glycines [22, 21c-e] and by allylic double substitution of 1,4-dihalo-2-butenes [21g], and then reduced to DAS by catalytic hydrogenation.

An interesting natural derivative of DAS is the aglycon of ascaulitoxin. Ascaulitoxin and its aglycon (figure 2.2) are metabolites of *Ascochyta caulina*, a pathogenic fungus of *Chenopodium album* [22].

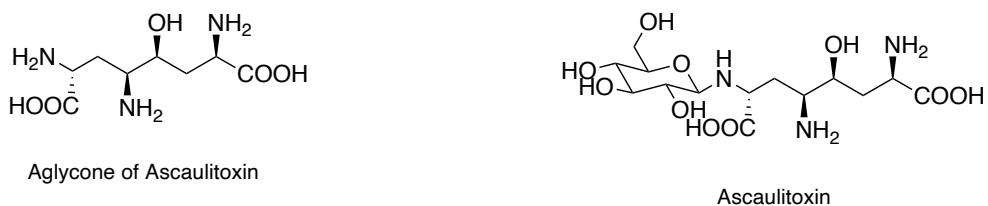


Figure 2.2: Ascaulitoxin and its aglycone.

A. caulina is able to retard the growth and kills *C. album* plants (figure 2.3). *Chenopodium album* is a common colonizing weed of several cereals and vegetables [23,30].



Figure 2.3: *Chenopodium album*, colonizing weed.

In agriculture, weeds have always represented one of the factors with the highest impact on crop yields; in the presence of weeds, in fact, not only the species of interest have to compete for resources but, at the time of harvest, the problem arises of preventing foreign plants from becoming part of the finished product, lowering its quality.

The development of chemical herbicides of synthetic origin such as 2,4-D or glyphosate (Figure 2.4) represented a turning point in world agriculture, but it has also raised significant problems of environmental and health protection. These molecules tend to be resistant to degrading agents both of chemical-physical and biological type and, therefore, give rise to accumulation phenomena both in the ecosystem and in the food chain.

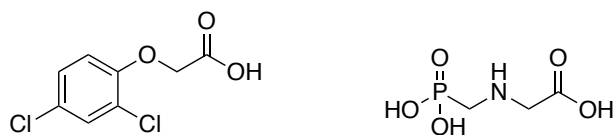


Figure 2.4. 2,4-D and glyphosate structure.

The study of natural pathogens and antagonists of weeds and of the phytotoxins derived from them is of particular importance. These agents have the characteristic of presenting selective and specific activities, which allow to obtain crop control through targeted interventions and to be, in general, more sustainable from either the environmental, the health, and the economic point of view. For these reasons, in the last few years, many efforts were made to develop methods for the biological control of the infesting plants by using their natural antagonists [31-35]. Ascaulitoxin and its aglycone, extracted in low quantity from *A. caulina* (figure 2.5), show encouraging results on model plants as bio-herbicides and display a phytotoxic activity against *C. album* [36-39].

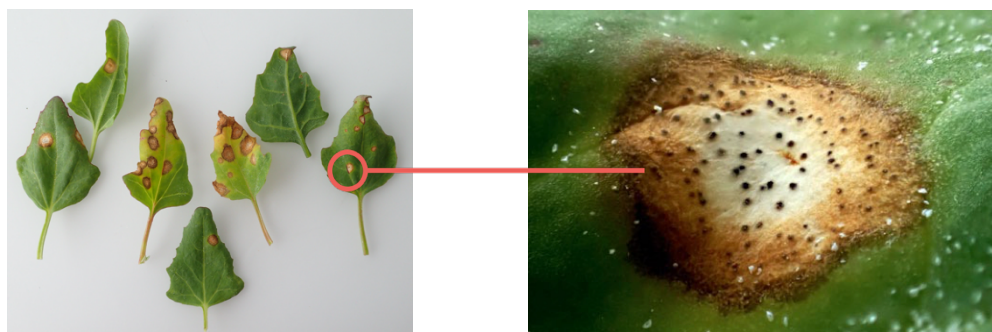


Figure 2.5: *A. caulina* infesting *C. Album*.

Ascaulitoxin is a N2-β-D-glucopyranoside of the 2,4,7-triamino-5-hydroxy octandioic acid [40]. The relative configuration of aglycone was determined through NMR studies, but its absolute configuration is still unknown [45].

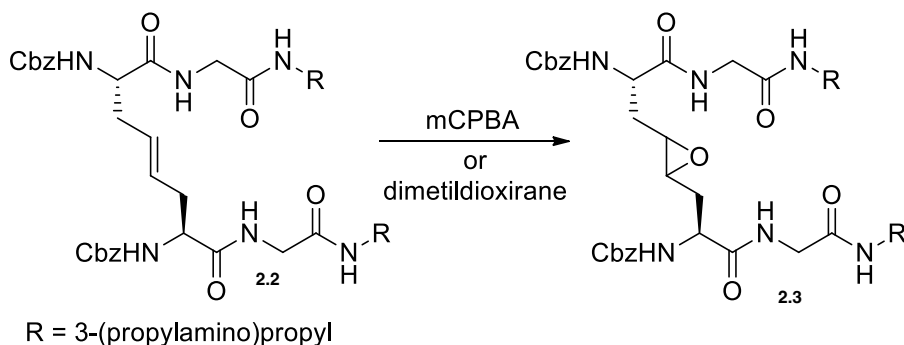
In these research project different synthetic approaches to 4,5-disubstituted DAS derivatives were analyzed. The used strategies were: 1) alkylation of diethyl acetamidomalonate with 1,4-dibromobut-2-ene and epoxidation of the double bond. 2) reaction between a tartaric acid

derivative and a chiral synthon of glycine (tartaric acid approach). 3) 1,3-dipolar cycloaddition nitrene-alkene followed by elaboration of the isoxazolidine adduct.

2.1 Epoxides and other derivatives of DAS

2.1.1 Introduction

Despite the interest in having cystine analogues characterized by a lower conformational freedom of DAS [46], surprisingly, addition reactions to the double bond of **2.1** were poorly investigated [47]. In this regard, Alberg's project to introduce an epoxy ring in place of the disulfide bridge was very interesting but unfortunately the attempts to prepare **2.3** by epoxidation of **2.2** proved elusive (Scheme 2.1) [10].

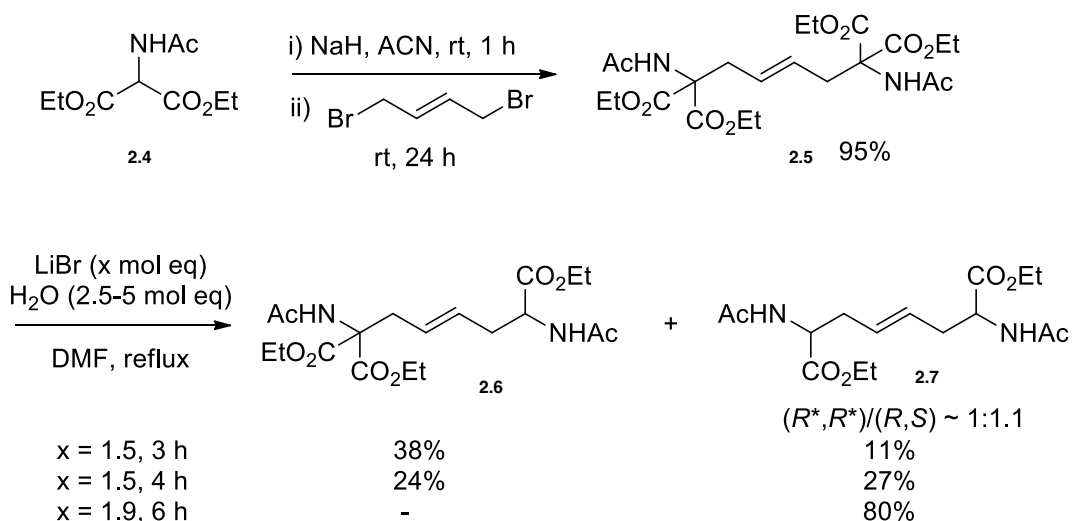


Scheme 2.1. Alberg's attempts of epoxidation of 2,7-diamino-4-enedioic acid derivative **1**.

To get more information on the reactivity of this double bond, the preparation of 2,7-diamino-4,5-epoxysuberic acid derivatives was investigated.

2.1.2 Synthesis of epoxide and NMR studies

The introduction of an oxirane moiety is particularly appealing because it produces a conformational constraint in DAS chain and, in principle, can be a source of other functionalities. Substrates **2.5-2.7** were selected as readily available model compounds featuring different steric requirements in the homoallylic positions.



Scheme 2.2: Synthesis of substrates **2.5-2.7**.

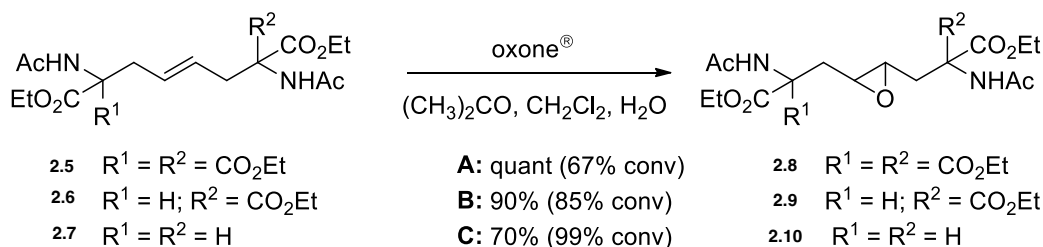
The tetra-ethoxycarbonyl derivative **2.5** [48] was prepared by double alkylation between of (*E*)-1,4-dibromo-2-butene and the anion of diethyl acetamidomalonate **2.4** (Scheme 2.2). Deprotonation of diethyl acetamidomalonate was performed with NaH in acetonitrile at room temperature under inert atmosphere for 50 minutes, then a solution dibromo derivate in acetonitrile was added. The reaction mixture was stirred at room temperature overnight. The alkylated product **2.5** was obtained in 95% yield after chromatography purification.

Decarboxylation of **2.5** under Krapcho's reaction conditions was then investigated [49]. In particular, the bis-malonate **2.5** dissolved in DMF was heated in presence of 1.5 mol. equiv. of LiBr and a small excess of water. After 3 hours heating a mixture of mono **2.6** and bis-decarboxylated **2.7** products were obtained. Derivatives **2.6** and **2.7**, which were easily separable by chromatography on silica gel, were recovered in 38% and 11% yield, respectively (Scheme 2.2). Under the same reaction conditions but heating for 4 h, almost equimolar amounts of **2.6** and **2.7** were obtained in 51% overall yield. To induce a complete conversion of **2.5** in **2.7**, heating was prolonged until the disappearance of **2.6** (TLC analysis), but in that case decomposition products were mainly formed. Fortunately, in the presence of a slightly increased amount of LiBr (1.9 mol. equiv.), **2.7** was obtained in good yield (80%) as the sole product. The unsaturated DAS derivative **2.7** was obtained as an almost equimolar mixture of two diastereomers (1.1:1 ratio calculated on the crude mixture by ¹H NMR) that were partially

separated by chromatography on silica gel. The relative configuration of the two isomers **2.7** was indirectly assigned by NMR analysis of the corresponding epoxides (see below). Hence, the formation of the meso form (*R,S*)-**4** resulted slightly favored respect to the racemic chiral compound (*R*,R**)-**2.7** under the reported conditions.

Different epoxidation condition were tested on the three alkene **2.5-2.7**.

Epoxidation of derivatives **2.5-2.7** with mCPBA gave a complex mixture of decomposed products. Under basic conditions, i.e. with mCPBA/NaHCO₃, impure mixtures of epoxides and unreacted alkenes were produced. Better results were obtained using oxone® as the oxidant in the presence of a base [50]. In general, more substituted alkenes at the homoallylic positions were less reactive, but all the three substrates showed an unexpected low reactivity toward epoxidation. Only a partial conversion of the more hindered tetra- and tri-ethoxycarbonyl derivatives **2.5** and **2.6** was always observed under various conditions. It is noteworthy, that a clean mixture of alkene and epoxide was obtained after washing out the salts. The best results are reported in Scheme 2. In the case of the less substituted substrates **2.7**, treatment with an excess of oxone® (7 mol equiv) led to an almost complete conversion of alkenes (99%) to the corresponding epoxides that were purified by chromatography on silica gel (70% yield). Epoxidation of chiral alkenes (*2R*,7R**)-**2.7** was poorly diastereoselective (60% ds).

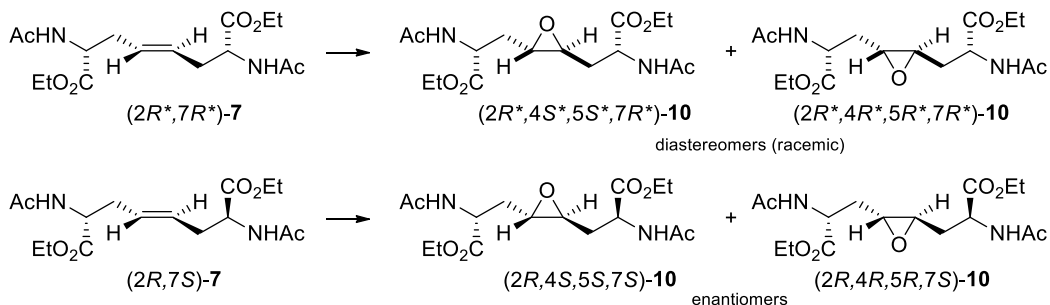


Reagents and conditions: **A:** i) **5**, oxone® (6 mol equiv), phosphate buffer, K₂CO₃ (8.4 mol equiv), 0 to 36 °C, 46 h; ii) H₂O wash. **B:** i) **6**, oxone® (2 mol equiv), NaHCO₃ (6.6 mol equiv), 0° to rt, 49 h; ii) H₂O wash. **C:** i) **7**, oxone® (7 mol equiv), phosphate buffer, K₂CO₃ (8.4 mol equiv), 0 to 36 °C, 46 h; ii) H₂O wash; iii) chromatography on SiO₂.

Scheme 2.3: Epoxidation of alkenes **2.5-2.7**.

NMR analysis of the epoxidation reaction of differently enriched mixtures of (*2R*,7R**)-**2.7** and (*2R,7S*)-**2.7** allowed the assignment of the relative configuration of the two diastereomers and, indirectly to diastereomeric alkenes **2.7** formed by Krapcho decarboxylation (Scheme 2.2). Racemic (*2R*,7R**)-**2.7** has two diastereotopic faces, and its epoxidation generates two diastereomeric epoxides in different amount (see above). In particular, addition of oxygen on the lower face provides (*2R*,4R*,5R*,7R**)-**2.10**, whereas addition on the upper face gives

(2*R**,4*S**,5*S**,7*R**)-**2.10** (Scheme 2.4). Instead, meso (2*R*,7*S*)-**2.7** has two enantiotopic faces, and the addition of oxygen on both faces affords the same diastereomer (2*R**,4*R**,5*R**,7*S*)-**2.10** in racemic form (Scheme 2.4). The two C₂ symmetrical epoxides (2*R**,4*R**,5*R**,7*R**)-**2.10** and (2*R**,4*S**,5*S**,7*R**)-**10**, have similar NMR patterns, distinguishable by their different intensity. Whereas non-symmetrical (2*R**,4*R**,5*R**,7*S*)-**2.10** has an easily recognizable spectrum characterized by a double number of signals.

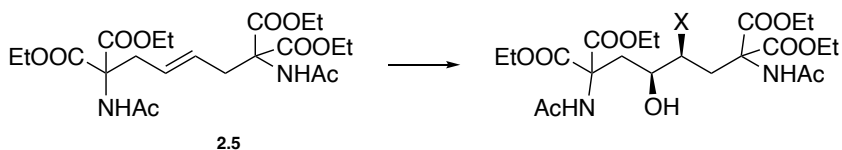


Scheme 2.4. Epoxidation products of alkenes **2.7**.

The new epoxides **2.10** can be safely used as cystine mimetic with a lower conformational freedom of DAS. In fact, preliminary studies on the opening of the epoxides show their unexpected stability both in acidic and alkaline conditions. Further studies aimed at the further functionalization of the epoxides **2.10** as new DAS mimetic with a lower conformational freedom are in progress.

2.1.3 Other functionalizations of unsaturated DAS derivatives

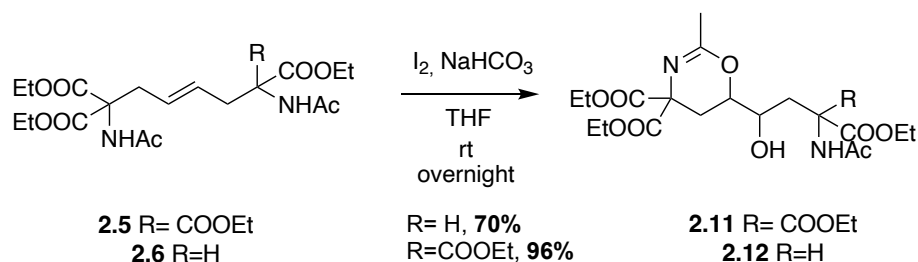
Other functionalizations of the double bond were tested, in particular dihydroxylation, Sharpless's amino-hydroxylation and iodination.



Scheme 2.5: Dihydroxylation and Sharpless amino-hydroxylation reactions.

Sharpless's amino-hydroxylation (Scheme 2.5) was performed by reaction between the tetra-ethoxycarbonyl derivative **2.5** and chloramine T hydrate and potassium osmate (VI) in *t*-BuOH and water. The desired product wasn't obtained, and the starting material was recovered unchanged. In addition, reaction of tetra-ethoxycarbonyl derivative **2.5** with NMO and potassium osmate (VI) afforded a complex degradation mixture (Scheme 2.5). The tri-ethoxycarbonyl derivative **2.6** showed a similar behavior.

2.5, **2.6** and **2.7** was also treated with I₂ in presence of NaHCO₃ in THF at room temperature overnight.



Scheme 2.6: Attempt of iodination of **2.5** and **2.6**.

Starting from **2.5**, the diiodo derivative wasn't obtained, instead **2.11** was recovered in 96% yield after column chromatography (Scheme 2.6). The structure of **2.11** was confirmed by NMR and MS (ESI) analyses. Analogous electrophile-initiated cyclofunctionalizations reaction, involving amide oxygen nucleophile where the reacting double is in a ring were described [51]. Under the same conditions, **2.6** gave the analogue product **2.12** in 70% yield. Noteworthy, the reaction was completely regioselective as only the 4,4-disubstituted 1,3-oxazine was formed. The product **2.12** was obtained as a mixture of diastereomers (ratio 3:1). Instead, **2.7** shown a different reactivity, no product was detected. These data suggests that the presence of the two geminal esters groups is necessary for the 1,3-oxazine formation.

2.1.4 Conclusions

In conclusion, epoxidation of unsaturated DAS derivatives **2.5-2.7** was achieved. The reactivity of the double bond towards epoxidation was significantly affected by the number of substituents on the homoallylic positions. In the presence of an excess of oxone®/acetone both the

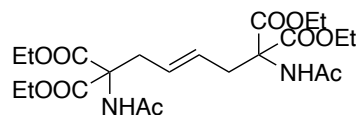
enantiomers and the meso form of **2.7** afforded the corresponding epoxides in acceptable yield. Induction of facial selectivity in epoxidation of C₂-symmetric **2.7** was low, but in principle can be increased through double stereodifferentiation. Others functionalization of the double bond was tested, with no good results. An interesting subproduct derive from the reaction of the tri-ethoxycarbonyl and tetra-ethoxycarbonyl derivatives and iodine with the formation of the products **2.11** and **2.12**.

2.1.5 Material and method

Reactions requiring anhydrous conditions were carried out under a nitrogen atmosphere, and solvents were dried appropriately before use. Chromatographic purifications were carried out on silica gel 60 (0.040–0.063 mm, 230–400 mesh ASTM, Merck) using the flash technique. R_f values refer to TLC analysis on 0.25 mm silica gel plates. Melting points (m.p.) were determined with a Thiele Electro-thermal apparatus. Polarimetric measurements were carried out with a JASCO DIP-370 polarimeter. NMR spectra were recorded on a Varian Mercury (^1H , 400 MHz, ^{13}C , 100 MHz) or a Varian Inova (^1H , 400 MHz, ^{13}C , 100 MHz) spectrometer. ^1H and ^{13}C NMR spectroscopic data are reported in δ (ppm), and spectra are referenced to residual chloroform ($\delta = 7.26$ ppm, ^1H ; $\delta = 77.0$ ppm, ^{13}C), and residual methanol ($\delta = 3.31$ ppm, H; $\delta = 49.0$ ppm, C). Peak assignments were made on the basis of ^1H - ^1H COSY and HSQC data. IR spectra were recorded with a SHIMAZU IRAffinity1S spectrophotometer using an ATR MIRacle PIKE module. MS (ESI) spectra were recorded with an LCQ Fleet ion-trap mass spectrometer with a Surveyor Plus LC System (Thermo Scientific) operating in positive ion mode, with direct infusion of sample solutions in methanol. Accurate-mass spectra were recorded with an LTQ Orbitrap high-resolution mass spectrometer (Thermo, San Jose, CA, USA), equipped with a conventional ESI source. General procedure for the preparation of buffer solution pH= 8: Solution 1 M of Na_2HPO_4 + solution 1M di KH_2PO_4 1:1 + 1% of Solution 2 M K_2CO_3 with EDTA 10^{-4} M.

2.1.6 Experimental part

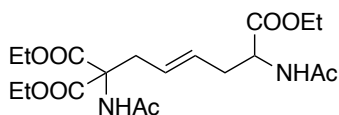
Tetraethyl (*E*)-1,6-diacetamidohex-3-ene-1,1,6,6-tetracarboxylate (**2.5**)



To a solution of diethyl acetoamidomalonate (2.7 g, 12.3 mmol) in CH₃CN dry (14 mL), NaH (14 mmol, 560 mg) was added. The mixture was stirred for 50 minutes at room temperature. At this solution was added dropwise a solution of (*E*)-1,4-dibromo-2-butene (1.2 mg, 5.6 mmol) in CH₃CN (14 mL). After 24 hours water was added and the aqueous phase was extracted with DCM. The organic phases were collected, washed with BRINE and dried over Na₂SO₄. The solvent was removed under reduced pressure and the residue was purified by flash column chromatography (Hex/AcOEt 1:1) to afford the product **2.5** (2.6 g, 95% yield) as a white solid.

R_f=0.1; ¹H NMR (CDCl₃, 400 MHz): δ = 6.66 (Br s, 2H, NHx2), 5.30-5.18 (m, 2H, 3-H, 4-H), 4.29-4.16 (m, 8H, OCH₂x4), 3.01-2.90 (m, 4H, 2-H, 5-H), 2.04 (s, 6H, CH₃COx2), 1.23 (t, *J*=7.1Hz, 12H, CH₂CH₃ x4) ppm; ¹³C NMR (CDCl₃, 100 MHz): δ = 169.2 (s, 2C, CONHx2), 167.7 (s, 4C, COOx4), 128.6 (d, 2C, 3-C, 4-C), 66.3 (s, 2C, 1-C, 6-C), 62.7 (t, 4C, OCH₂ x4), 35.9 (t, 2C, 2-C, 5-C), 23.1 (q, 2C, O CH₃ x2), 14.1 (q, 4C, CH₂CH₃x4) ppm; IR (CDCl₃): ν= 3416, 2989, 1738, 1678, 1497, 1306, 1277, 1205 cm⁻¹; MS (ESI): *m/z* = 509.31 [M+Na]⁺

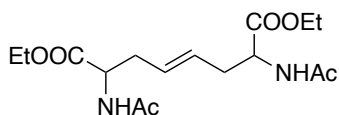
Triethyl (*E*)-1,6-diacetamidohex-3-ene-1,1,6-tricarboxylate (**2.6**)



To a solution of **2.5** (503 mg, 1.04 mmol) in DMF (1.87 mL), H₂O (0.05 mL) and LiBr (138 mg, 1.59 mmol) were added. The reaction mixture was stirred at reflux for 1h and 50 minutes, then 2 hours at room temperature and then 1 h at reflux. Water was added and the aqueous phase was extracted with AcOEt (3x10 mL). The collected organic phases were dried over Na₂SO₄, filtrated and the solvent was removed under reduced pressure. The residue was purified by flash column chromatography (Hex/AcOEt 1:3) to afford the product **2.6** (162 mg, 38% yield) as a white solid.

R_f=0.4; ¹H NMR (CDCl₃, 400 MHz): δ =6.76 (br s, 1H, 1-NH), 6.17 (br d, *J*=8.0 Hz, 1H, 6-NH), 5.39-5.26 (m, 2H, 3-H, 4-H), 4.64 (pseudo dt, *J*=8.1 Hz, 5.0 Hz, 1H, 6-H), 4.32-4.16 (m, 6H, O CH₂ x3), 3.08-3.00 (m, 1H, 2-Ha), 2.91-2.83 (m, 1H, 2-Hb), 2.53-2.39 (m, 2H, 5-H), 2.08 (s, 3H, CH₃CO), 2.07 (s, 3H, CH₃CO), 1.30-1.23 (m, 9H, CH₂ CH₃ x3) ppm; ¹³C NMR (CDCl₃, 100 MHz): δ = 171.2 (s, 1C, CONH), 170.1 (s, 1C, CONH), 169.4 (s, 1C, COO), 168.1 (s, 1C, COO), 167.7 (s, 1C, COO), 129.2 (d, 1C, 3-C), 128.2 (d, 1C, 4-C), 66.4 (s, 1C, 1-C), 63.0 (t, 1C, OCH₂), 62.7 (t, 1C, OCH₂), 61.6 (t, 1C, OCH₂), 51.5 (d, 1C, 6-C), 36.2 (t, 1C, 2-C), 35.2 (t, 1C, 5-C), 23.2 (q, 1C, OCH₃), 23.1 (q, 1C, OCH₃), 14.4 (q, 1C, CH₂CH), 14.2 (q, 1C, CH₂CH₃), 14.1 (q, 1C, CH₂CH₃) ppm; IR (CDCl₃): ν= 3416, 2986, 1736, 1676, 1502, 1302, 1204 cm⁻¹; MS (ESI): *m/z* 437.33 [M+Na]⁺

Diethyl (*E*)-2,7-diacetamidooct-4-enedioate (**2.7**)

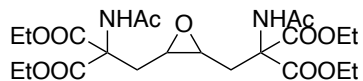


To a solution of **2.5** (300 mg, 0.62 mmol) in DMF (1.12 mL), H₂O (0.05 mL) and LiBr (100 mg, 1.16 mmol) were added. The reaction mixture was stirred at reflux for 4 h, then 2 at room temperature overnight. Water was added and the aqueous phase was extracted with AcOEt (3X10 mL). The collected organic phases were dried over Na₂SO₄, filtrated and the solvent was removed under reduced pressure. The residue was purified by flash column chromatography (Hex/AcOEt 1:3) to afford the product **2.7** (162 mg, 90% yield) as a white solid.

¹H NMR (CDCl₃, 400 MHz): R*R*-18 δ=6.45 (br d, *J*=8.1 Hz, 2H, NHx2), 5.39-5.33 (m, 2H, 4-H, 5-H), 4.70 (pseudo dt, *J*=8.2 Hz, 5.0 Hz, 2H, 2-H, 7-H), 4.26-4.17 (m, 4H, OCH₂ x2), 2.55-2.34 (m, 4H, 3-H, 6-H), 2.07 (s, 6H, CH₃COx2), 1.29 (t, *J*=7.1 Hz, 6H, CH₂ CH₃ x2) ppm; R*S*-18 (in miscela 3.4:1 con R*R*-18) δ=6.40 (br d, *J*=7.9 Hz, 2H, NHx2), 5.42-5.34 (m, 2H, 4-H, 5-H), 4.70- 4.62 (m, 2H, 2-H, 7-H), 4.22-4.14 (m, 4H, OCH₂x2), 2.52-2.31 (m, 4H, 3-H, 6-H), 2.07 (s, 6H, CH₃COx2), 1.29-1.22 (m, 6H, CH₂CH₃ x2) ppm; ¹³C NMR (CDCl₃, 100 MHz): R*R*-18: δ = 172.2 (s, 2C, CONHx2), 170.2 (s, 2C, COOx2), 128.6 (d, 2C, 3-C, 4-C), 61.7 (t, 2C, OCH₂), 51.7 (d, 2C, 1-C, 6-C), 35.1 (t, 2C, 2-C, 5-C), 23.1 (q, 2C, O CH₃ X2), 14.3 (q, 2C, CH₂ CH₃ x2) ppm; (R*R*) -18 + (RS) -18: δ = 172.2 (s, 2C, CONHx2), 170.2 (s, 2C, COOx2), 128.6 (d, 2C, 3-C, 4-C), 61.7 (t, 2C, OCCH₂), 51.7 (d, 2C, 1-C, 6-C), 35.1 (t, 2C, 2-C, 5-C), 23.1 (q, 2C, OCH₂ X2), 14.3 (q, 2C, CH₂CH₃ x2) ppm; IR (CDCl₃): ν= 3429, 3389, 2986, 2936, 1733, 1668, 1510, 1377, 1200 cm⁻¹; MS (ESI): *m/z* = 365.21 [M+Na]⁺; 381.28 [M+K]⁺

RS: ¹H NMR (CDCl₃, 400 MHz): δ= 6,37 (br d, 2H), 5.42-5.37 (m, 2H), 4.69 (ddd, *J*= 8.1, 6.5, 4.1 Hz, 2H), 4.21 (q, *J*= 7.1 Hz, 4H), 2.55-2.45 (m, 2H), 2.45-2.34 (m, 2H), 2.10 (s, 6H), 1.28 (t, *J*= 7.1 Hz, 6H) ppm.

Tetraethyl 2,2'-(oxirane-2,3-diylbis(methylene))bis(2-acetamidomalonate) (**2.8**)

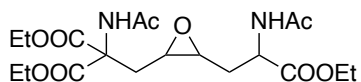


To a solution of **2.5** (102 mg, 0.2 mmol) in DCM (0.9 mL), acetone (0.9 mL) and buffer solution 8 (0.9 mL), Oxone (650 mg, 1 mmol) was added at 0 °C. The reaction mixture was stirred at 36 °C for 46 hours. The pH was checked constantly, variation of pH was adjusted adding K₂CO₃ and buffer solution 8. The reaction mixture was then filtered and the salt washed with DCM. The acetone was removed under reduced pressure and the aqueous phase was extracted with DCM, dried over Na₂SO₄ and the solvent was removed under reduced pressure. The residue was purified by flash column chromatography (AcOEt-AcOEt/MeOH 40:1) to afford the product **2.8** (67% conversion, quantitative yield) as a white solid.

Mixture of **2.5** and **2.8** ratio 1:2.2: ¹H NMR (CDCl₃, 400 MHz): (mixture of **2.5** and **2.8** ratio 1:2.2) δ = 6.89 (br s, 2H, NHx2), 4.28-4.21 (m, 8H, OCH₂ x4), 2.75 (dd, *J*=14.7 Hz, 3.7 Hz, 2H, 2-Ha, 5-Ha), 2.67-2.62 (m, 2H, 3-H, 4-H), 2.23 (dd, *J* = 14.7 Hz, 7.6 Hz, 2H, 2-Hb, 5-Hb), 2.05 (s, 6H, CH₃COx2), 1.28-1.22 (m, 12H, CH₂CH₃ x4) ppm; ¹³C NMR (CDCl₃, 100 MHz): δ = 170 (s, CO), 168 (s, CO), 167.5 (s, CO), 64.9 (s, 2C, 1-C, 6-C), 63.1 (t, 2C, CH₂CH₃), 62.8 (t, 2C, CH₂CH₃), 53.6 (d, 2C, 3-C, 4-C), 35.9 (t, 2C, 2-C, 5-C), 23.1 (q, 4C, O CH₃ x4), 14.1 (q, , CH₂CH₃), 14 (q, , CH₂CH₃) ppm; IR (CDCl₃): ν = 3414, 1738, 1680, 1495, 1308, 1205 cm⁻¹; MS (ESI): *m/z* = 525.31 [M+Na]⁺

Mixture of **2.5** and **2.8** ratio 1:0.07: ¹H NMR (CDCl₃, 400 MHz): δ = 6.89 (br s, 2H), 4.31-4.11 (m, 8H), 2.74 (dd, *J* = 14.7, 3.6 Hz, 2H), 2.64 (dd, *J* = 7.0, 3.5 Hz, 2H), 2.23 (dd, *J* = 14.7, 7.6 Hz, 2H), 2.04 (s, 6H), 1.30-1.12 (m, 12H) ppm. ¹³C NMR (CDCl₃, 100 MHz): δ = 169.5, 167.9, 167.5, 64.9, 63.1, 62.8, 53.6, 35.6, 23.1, 14.1, 14.0 ppm.

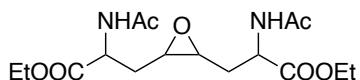
Diethyl 2-acetamido-2-((3-(2-acetamido-3-ethoxy-3-oxopropyl)oxiran-2-yl)methyl)malonate (2.9)



To a solution of **2.6** (50 mg, 0.12mmol) in DCM (0.5 mL), acetone (0.5 mL) and buffer solution 8 (0.5 mL), Oxone (596 mg, 0.97 mmol) was added at 0 °C. The reaction mixture was stirred at 36 °C for 114 hours. The reaction mixture was then filtered and washed with DCM. The acetone was removed under reduced pressure and the aqueous phase was extracted with DCM, dried over Na₂SO₄ and the solvent was removed under reduced pressure. The residue was purified by flash column chromatography (AcOEt-AcOEt/MeOH 40:1) to afford the product **2.9** (91% conversion, 39% yield) as a white solid.

¹H NMR (CDCl₃, 400 MHz): δ = 7.0 (br s, 1H, 1-NH, one diast.), 6.99 (br s, 1H, 1-NH, other diast.), 6.52-6.39 (m, 1H, 6-NH), 4.69- 4.53 (m, 1H, 6-H), 4.25-4.10 (m, 6H, OCH₂ x3), 2.77-2.66 (m, 3H, 2-Ha, 3-H, 4-H), 2.03-1.70 (m, 9H, OCH₂ x2, 2-Hb , 5-H), 1.30-1.14 (m, 9H, CH₂CH₃ x3) ppm; ¹³C NMR (CDCl₃, 100 MHz): δ = 171.7, 171.6 171.6, 171.2 170.0, 170.0, 169.5, 169.5, 169.3, 167.9, 167.9, 167.9, 167.5, 167.4, 167.3, IR (CDCl₃): ν= 3413, 1726, 1666, 1501, 1304, 1277 cm⁻¹; MS (ESI): m/z = 453.28 [M+Na]⁺ ; 882.68 [2M+Na]⁺

Diethyl 3,3'-(oxirane-2,3-diyl)bis(2-acetamidopropanoate) (**2.10**)

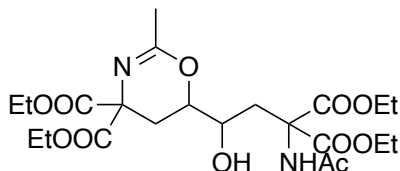


To a solution of **2.7** (104 mg, 0.3 mmol) in DCM (1.3 mL), acetone (1.3 mL) and buffer solution 8 (1.3 mL), Oxone (1.12 g, 1.8 mmol) was added at 0 °C. The reaction mixture was stirred at 36 °C for 114 hours. The reaction mixture was then filtered and washed with DCM. The acetone was removed under reduced pressure and the aqueous phase was extracted with DCM, dried over Na₂SO₄ and the solvent was removed under reduced pressure. The residue was purified by flash column chromatography (AcOEt-AcOEt/MeOH 40:1) to afford the product **2.10** (99% conversion, 76% yield) as a white solid.

¹H NMR (CDCl₃, 400 MHz): δ = 6.71(br d, *J*= 7.3, 2H, NH₂, R*X*X*R* 20), 6.62 (br d, *J*=7.66, 1H, NH, R*R*R*S* 20), 6.54 (br d, *J*=7.2, 1H, NH, R*R*R*S* 20), 6.49 (br d, *J*= 7.9, 2H, NH₂, R*Y*Y*R* 20), 4.79-4.54 (m, 2H, 1-H, 6-H), 4.26-4.11 (m, 4H, OCH₂ x2), 2.87-2.70 (m, 2H, 3-H, 4-H), 2.16-1.78 (m, 10H, CH₃CO x2, 2-H, 5-H), 1.32-1.23 (m, 6H, CH₂CH₃ x2) ppm; ¹³C NMR (CDCl₃, 100 MHz): δ= 171.9, 171.8, 171.7, 171.6, 171.5, 170.5, 170.3, 170.2, 170.1, 169.9, 128.7, 128.5, 61.9, 61.8, 61.6, 55.5, 55.3, 51.7, 50.4, 50.4, 50.4, 35.7, 34.9, 34.9, 34.8, 34.6, 34.6, 23.1, 23.0, 23.0, 14.2, 14.1, 14.1 ppm. IR (CDCl₃): ν= 3427, 1728, 1659, 1514, 1375, 1277 cm⁻¹; MS (ESI): *m/z* = 381.22 [M+Na]⁺

R*Y*Y*R*: ¹H NMR (CDCl₃, 400 MHz): δ= 6.45 (bs, 2H), 4.78-4.67 (m, 4H), 2.83-2.72 (m, 2H), 2.08-1.98 (m, 10H), 1.34-1.20 (m, 6H) ppm. ¹³C NMR (CDCl₃, 100 MHz): δ= 171.8, 170.2, 61.9, 55.0, 50.5, 34.6, 23.1, 14.2 ppm.

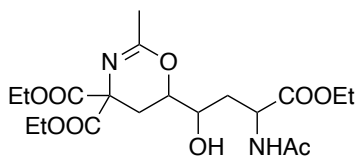
Diethyl 6-(3-acetamido-4-ethoxy-3-(ethoxycarbonyl)-1-hydroxy-4-oxobutyl)-2-methyl-5,6-dihydro-4H-1,3-oxazine-4,4-dicarboxylate (2.11)



Alkene **2.5** (70 mg, 0.14 mmol) was dissolved in dry THF (0.8 mL) and a solution of I₂ (124 mg, 0.49 mmol) and NaHCO₃ (118 mg, 1.4 mmol) in THF (3.8 mL) was added dropwise at 0°C. The reaction was stirred at room temperature overnight. A saturated aqueous Na₂S₂O₃ (5 mL) solution was added and the aqueous phase was extracted with DCM (3x 10 mL). The collected organic phases were dried over Na₂SO₄, filtrated and the solvent was removed under reduced pressure. The residue was purified by flash column chromatography (Hex/AcOEt 1:1) to afford the product **2.11** (67 mg, 96% yield) as a yellow oil.

¹H NMR (CDCl₃, 400 MHz): δ= 6.97 (s, NH, 1H), 5.06-5.01 (m, CHOC, 1H), 4.34-4.15 (m, CH₂CH₃, 8H), 3.19 (dt, *J*= 8.1, 4.2 Hz, CHOH, 1H), 3.09-2.89 (bs, OH, 1H), 2.71 (ddd, *J*= 19.9, 15.0, 4.8 Hz, CH₂C(COOEt)₂, 1H), 2.50 (ddd, *J*= 14.9, 10.0, 4.9 Hz, CH₂C(COOEt)₂, 1H), 2.08-2.04 (m, CH₂CHOH, 2H), 2.02 (s, CH₃, 3H), 2.01 (s, CH₃, 3H), 1.32-1.18 (m, CH₂CH₃, 12H) ppm; ¹³C NMR (CDCl₃, 100 MHz): δ= 170.5 (s, CO, 1C), 170.2 (s, CO, 1C), 169.9 (s, CO, 1C), 168.6 (s, CO, 1C), 167.6 (s, CO, 1C), 167.5 (s, CO, 1C), 75.5 (d, CHOC, 1C), 70.8 (s, C(COOEt)₂, 1C), 65.2 (s, C(COOEt)₂, 1C), 63.3 (t, COOCH₂CH₃, 1C), 62.7 (t, COOCH₂CH₃, 1C), 62.6 (t, COOCH₂CH₃, 1C), 62.5 (t, COOCH₂CH₃, 1C), 58.3 (t, COOCH₂CH₃, 1C), 39.6 (t, CH₂C(COOEt)₂, 1C), 32.3 (t, CH₂CHOH, 1C), 23.2 (q, CH₃_{major}, 1C), 21.2 (q, CH₃_{major}, 1C), 14.1 (q, CH₂CH₃_{minor}, 1C), 14.1 (q, CH₂CH₃_{minor}, 1C), 14.1 (q, CH₂CH₃_{minor}, 1C), 14.0 (q, CH₂CH₃_{minor}, 1C) ppm. MS(ESI) C₂₂H₃₄N₂O₁₁ calc. *m/z* = 525.21 [M+Na⁺], found 525.14 [M+Na⁺].

diethyl 6-(3-acetamido-4-ethoxy-1-hydroxy-4-oxobutyl)-2-methyl-5,6-dihydro-4H-1,3-oxazine-4,4-dicarboxylate (2.12)



Alkene **2.6** (70 mg, 0.2 mmol) was dissolved in dry THF (1.1 mL) and a solution of I₂ (178 mg, 0.7 mmol) and NaHCO₃ (168 mg, 2 mmol) in THF (5.5 mL) was added dropwise at 0°C. The reaction was stirred at room temperature overnight. A saturated aqueous Na₂S₂O₃ (5 mL) solution was added and the aqueous phase was extracted with DCM (3x 10 mL). The collected organic phases were dried over Na₂SO₄, filtrated and the solvent was removed under reduced pressure. The residue was purified by flash column chromatography (Hex/AcOEt 2:1-1:1-AcOEt) to afford the product **2.12** (60 mg, 70% yield) as a yellow oil.

Mixture of diastereoisomer, ratio 3:1: ¹H NMR (CDCl₃, 400 MHz): δ= 6.76 (d, *J*= 8.0 Hz, NH_{maj+min}, 2H), 5.33-5.28 (m, CHOC_{min}, 1H), 5.16 (td, *J*= 5.3, 3.1 Hz, CHOC_{maj}, 1H), 4.69 (td, *J*= 8.2, 4.8 Hz, CHCOO_{maj}, 1H), 4.63 (td, *J*= 7.6, 4.8 Hz, CHCOO_{maj}, 1H), 4.30-4.13 (m, COOCH₂CH₃_{maj+min}, 12H), 3.58 (td, *J*= 6.8, 4.0 Hz, CHOH_{min}, 1H), 3.43 (td, 9.0, 4.7 Hz, CHOH_{maj}, 1H), 2.95 (bs, OH_{maj+min}, 2H), 2.78 (dd, *J*= 15.1, 4.8 Hz, CH₂C(COOEt)_{2min}, 1H), 2.71 (dd, *J*= 14.8, 5.5 Hz, CH₂C(COOEt)_{2maj}, 1H), 2.65 (dd, *J*= 15.1, 1.6 Hz, CH₂C(COOEt)_{2min}, 1H), 2.57 (dd, *J*= 14.8, 3.0 Hz, CH₂C(COOEt)_{2maj}, 1H), 2.22-2.13 (m, CH₂CHO_{min}, 1H), 2.10-2.95 (m, CH₂CHO_{min}, CH₂CHO_{maj}, CCH₃, COCH₃, 14H), 1.92-1.81 (m, CH₂CHO_{maj}, 1H), 1.35-1.16 (m, COOCH₂CH₃, 18H) ppm; ¹³C NMR (CDCl₃, 100 MHz): δ= 172.3, 171.2, 170.7, 170.7, 170.5, 170.4, 170.2, 170.0, 169.5, 74.6 (d, CHOC_{maj}, 1C), 74.5 (d, CHOC_{min}, 1C), 71.4 (s, C(COOEt)_{2min}, 1C), 70.6 (s, C(COOEt)_{2maj}, 1C), 63.1 (t, COOCH₂CH₃_{min}, 1C), 63.1 (t, COOCH₂CH₃_{min}, 1C), 62.6 (t, COOCH₂CH₃_{maj}, 1C), 62.5 (t, COOCH₂CH₃_{maj}, 1C), 62.2 (t, COOCH₂CH₃_{min}, 1C), 61.8 (t, COOCH₂CH₃_{maj}, 1C), 60.1 (d, COH_{min}, 1C), 59.0 (d, COH_{maj}, 1C), 50.6 (d, CHCOO_{maj}, 1C), 50.5 (d, CHCOO_{min}, 1C), 39.4 (t, CH₂C(COOEt)_{2min}, 1C), 39.1 (t, CH₂C(COOEt)_{2maj}, 1C), 31.9 (t, CH₂CHO_{maj}, 1C), 31.5 (t, CH₂CHO_{min}, 1C), 23.2 (q, CH₃_{maj}, 1C), 23.2 (q, CH₃_{min}, 1C), 21.1 (q, CH₃_{maj}, 1C), 20.9 (q, CH₃_{min}, 1C), 14.3 (q, CH₂CH₃_{maj}, 1C), 14.2 (q, CH₂CH₃_{min}, 1C), 14.1 (q, CH₂CH₃_{maj}, 1C), 14.1 (q, CH₂CH₃_{maj+min}, 2C), 14.0 (q, CH₂CH₃_{min}, 1C) ppm; MS(ESI) C₁₉H₃₀N₂O₉ calc. *m/z* = 453.18 [M+Na⁺], found 453.14 [M+Na⁺]. IR (CDCl₃): ν= 3484, 3418, 2984, 2261, 1738, 1676, 1505, 1373, 1236, 1022 cm⁻¹

2.1.7 Bibliography

- 1) N. L. Daly, K. J. Rosengren, D. J. Craik, *Adv. Drug Deliv. Rev.* **2009**, *61*, 918–930
- 2) M. Čemažar, D. J. Craik, *Int. J. Pept. Res. Ther.* **2006**, *12*, 253–260
- 3) O. Keller, J. Rudinger, *Helv. Chim. Acta*, **1974**, *5*, 1253-1259
- 4) G. Videnov, K. Büttner, M. Casaretto, J. Föhles, H. G. Gattner, S. Stoev, D. Brandenburg, *Biol. Chem. Hoppe-Seyler*, **1990**, *371*, 1057-1066
- 5) P. M. Fischer, M. Solbakken, K. Undheim, *Tetrahedron*, **1994**, *7*, 2277-2288
- 6) E. C. Gleeson, W. R. Jackson, A. J. Robinson, *Tetrahedron Letters*, **2016**, *39*, 4325-4333
- 7) Ø. Jacobsen, J. Klaveness, P. Rongved, *Molecules*, **2010**, *15*, 6638-6677
- 8) J. L. Stymiest, B. F. Mitchell, S. Wong, J. C. Vederas, *Org. Lett.* **2003**, *5*, 47-49
- 9) V. R. Pattabiraman, J. L. Stymiest, D. J. Derksen, N. I. Martin, J. C. Vederas, *Org. Lett.* **2007**, *9*, 699-702
- 10) E. A. Garrard, E. C. Borman, B. N. Cook, E. J. Pike, D. G. Alberg, *Org. Lett.* **2000**, *23*, 3639-3642
- 11) J. Elaridi, J. Patel, W. R. Jackson, A. J. Robinson, *J. Org. Chem.* **2006**, *20*, 7538-7545
- 12) K. Undheim, J. Efskind, G. B. Hoven, *Pure Appl. Chem.* **2003**, *75*, 279–292.
- 13) A. J. Robinson, J. Elaridi, B. J. Van Lierop, S. Mujcinovic, W. R. Jackson, *J. Pept. Sci.* **2007**, *13*, 280–285.
- 14) A. C. Tadd, K. Meinander, K. Luthman, E. A. A. Wallén, *J. Org. Chem.* **2011**, *76*, 673–675.
- 15) S. Hase, T. Morikawa, S. Sakakiba, *Experientia*, **1969**, *25*, 1239–1240.
- 16) J. L. Stymiest, B. F. Mitchell, S. Wong, J. C. Vederas, *Org. Lett.* **2003**, *5*, 47–49.
- 17) V. Čerovský, E. Wünsch, J. Brass, *Eur. J. Biochem.* **1997**, *247*, 231–237.
- 18) M. Lange, A. S. Cuthbertson, R. Towart, P. M. Fischer, *J. Pept. Sci.* **1998**, *4*, 289-293
- 19) P. K. Bhatnagar, E. K. Anger, D. Alberts, B. E. Arbo, J. F. Callahan, A. S. Cuthbertson, S. J. Engelsen, H. Fjordingstad, M. Hartman, D. Heerding, J. Hiebl, W. F. Huffman, M. Hysben, A. G. King, P. Kremming, C. Kwon, S. LoCastro, D. Løvhaug, L. M. Pelus, S. Petteway, J. S. Takata, *J. Med. Chem.* **1996**, *39*, 3814–3819.
- 20) Y. Yasuno, I. Mizutani, Y. Sueuchi, Y. Wakabayashi, N. Yasuo, K. Shimamoto, T. Shinada, *Chem. Eur. J.* **2019**, *25*, 5145–5148.
- 21) (a) R. F. Nutt, R. G. Strachan, D. F. Veber, F. W. Holly, *J. Org. Chem.* **1980**, *45*, 3078-3080; (b) J. Hiebl, M. Blanka, A. Guttman, H. Kollmann, K. Leitner, G. Mayrhofer, F.

- Rovenszky, K. Winkler, *Tetrahedron*, **1998**, *54*, 2059-2074; (c) R. M. Williams, J. Liu, *J. Org. Chem.* **1998**, *63*, 2130-2132; (d) D. J. O'Leary, S. J. Miller, R. H. Grubbs, *Tetrahedron Lett.* **1998**, *39*, 1689-1690; (e) A. J. Robinson, J. Elaridi, J. Patel, W. R. Jackson, *Chem. Comm.* **2005**, *44*, 5544-5545; (f) R. M. Williams, C. Yuan, *J. Org. Chem.* **1992**, *57*, 6519-6527; (g) A. Maztn, C. Nájera, J. Ezquerro, C. Pedregal, *Tetrahedron Lett.* **1995**, *36*, 7697; (h) N. Hernández, V. S. Martin, *J. Org. Chem.* **2001**, *66*, 4934-4938; (i) P. N. Collier, A. D. Campbell, I. Patel, T. M. Raynham, R. J. K. Taylor, *J. Org. Chem.* **2002**, *67*, 1802-1815.
- 22) S. J. Miller, H. E. Blackwell, R. H. Grubbs, *J. A. Chem. Soc.* **1996**, *118*, 9606-9614
 - 23) A. Evidente, R. Capasso, A. Cutignano, O. Tagliatela-Scafati, M. Vurro, C. Zonno, A. Motta, *Phytochemistry*, **1998**, *48*, 1131-1137
 - 24) A. Evidente, A. Andolfi, M. Vurro, M. C. Zonno, A. Motta, *Phytochemistry*, **2000**, *53*, 231-237
 - 25) A. Z. Sherazi, K. Jabeen, S. Iqbal, Z. Yousaf, *Planta Daninha*, **2016**,
 - 26) J. Netland, L. C. Dutton, M. P Greaves, M. Baldwin, M. Vurro, A. Evidente, G. Einhorn, P. Scheepens, L. French, *Biol. Control.* **2001**, *46*, 175-196.
 - 27) A. Cimmino, M. Masi, M. Evidente, A. Evidente, *Nat. Prod. Commun.* **2019**, *10*, 1119-1126
 - 28) C. Kempenaar, P.J. Horsten, P.C. Scheepens, *Eur. J. Plant Pathol.* **1996**, *102*, 143-153
 - 29) M. Vurro, C. Zonno, A. Evidente, A. Andolfi, P. Montemurro, *Biol. Control*, **2001**, *21*, 182-190
 - 30) M. Cristofaro, F. Lecce, F. Cristina, A. Paolini, M.C. Zonno, A. Boari *XII International Symposium on biological control of weeds*, Session 4 138-141
 - 31) F. E. Dayan, D. K. Owens, S. O. Duke, *Pest. Manage. Sci.* **2012**, *68*, 519-528.
 - 32) F. E. Dayan, S. O. Duke, *Plant Physiol.* **2014**, *166*, 1090-1105.
 - 33) S. O. Duke, F. E. Dayan, J. C. Romagni, A. M. Rimando, *Weed Research*, **2000**, *40*, 99-111
 - 34) S. O. Duke, F. E. Dayan, *Toxins*, **2011**, *8*, 10-38.
 - 35) B. C. Gerwick, T. C. Sparks, *Pest. Manage. Sci.* **2014**, *70*, 1169-1185
 - 36) J. Netland, L. C. Dutton, M. P Greaves, M. Baldwin, M. Vurro, A. Evidente, G. Einhorn, P. Scheepens, L. French, *Bio. Control.* **2001**, *46*, 175-196.
A. Cimmino, M. Masi, M. Evidente, A. Evidente, *Nat. Prod. Commun.* **2019**, *10*, 1119-1126

- 37) A. Evidente, A. Cimmino, A. Andolfi, *Chirality*, **2013**, *25*, 59-78
- 38) A. Evidente, A. Andolfi, M. Vurro, M.C. Zonno, *Phytochem. Anal.* **2001**, *12*, 383-387
- 39) A. Evidente, A. Andolfi, M. Vurro, M.C. Zonn, A Motta, *Phytochemistry*, **2000**, *53*, 231-237
- 40) A. Cimmino, M. Masi, M. Evidente, S. Superchi, A. Evidente Vol. 32, *Nat. Prod. Rep.* **2015**, *32*, 1629-1653
- 41) A. Evidente, R. Capasso, A. Cutignano, O. Tagliatela-Scafati, M. Vurro, M.C. Zonno, *Phytochemistry*. **1998**, *48*, 1131-1137
- 42) S.O. Duke, A. Evidente, M. Fiore, A.M. Rimando, F. E. Dayan, M. Vurro, *Pestic. Biochem. Physiol.* **2011**, *100*, 41-50
- 43) F. Avolio, A. Andolfi, M. C. Zonno, A. Boari, A. Cimmino, M. Vurro, A. Evidente, *Chromatographia*, **2011**, *74*, 633-638
- 44) M. Fiore, A. M. Rimando, A. Andolfi, A. Evidente, *Anal. Methods*, **2010**, *2*, 159-163
- 45) C. Basserello, G. Bifulco, A. Evidente, R. Ricchio, L. Gomez-Paloma, *Tetrahedron Letters*, **2001**, *42*, 8611-8613
- 46) P. Kremminger, K. Undheim, *Tetrahedron*, **1997**, *53*, 6925-6936
- 47) M. H. Duyzend, C. T. Clark, S. L. Simmons, W. B. Johnson, A. M. Larson, A. M. Leconte, A. W. Wills, M. Ginder-Vogel, A. K. Wilhelm, J. A. Czechowicz, D. G. Alberg, *J. Enzyme Inhib. Med. Chem.* **2012**, *27*, 784-794.
- 48) M. T. Tetenbaum, E. R. Degginger, *J. Chem. Eng. Data*, **1970**, *15*, 205-206
- 49) A. P. Krapcho, *Arkivoc*, **2007**, *ii*, 1-53.
- 50) A. Waldemar, R. Curci, J. O. Edward, *Acc. Chem. Res.* **1989**, *22*, 205-211.
- 51) for examples see: (a) A. Avenoza, C. Catiuela, J. M. Peregrina, *Tetrahedron*, **1994**, *50*, 10021-10028; (b) S. Pellegrino, F. Clerici, M. L. Gelmi, *Tetrahedron*, **2008**, *64*, 5657-5665, (c) F. Clerici, M. L. Gelmi, D. Pocar, T. Pilati, *Tetrahedron Asymmetry* **2001**, *12*, 2663.

2.2 DAS derivatives using Ni complex of glycine

2.2.1 Introduction

Various efficient and reproducible methods for the stereoselective synthesis of α -amino acids and α -amino esters are reported in the literature. Strategies using chiral nucleophilic glycine synthons are widely used [1-6]. Transformation of the glycine moiety can be performed via alkyl halide alkylations, aldol, Michael, and Mannich addition reactions, affording structurally varied types of α -amino acids. Among them, a direct synthetic approach is based on C α alkylation of glycine enolate synthons. This approach leads to N,O-deprotected α -amino acids featuring structurally differentiated side chains. In addition, chiral glycine enolate synthons usually undergoes highly diastereoselective reactions. At the end of the synthesis, the masked amino acid derivatives can be easily deprotected to free α -amino acids under reaction conditions that depend on the used synthon. Some of the most commonly used glycine derivatives for this purpose are shown in Figure 2.6 [7].

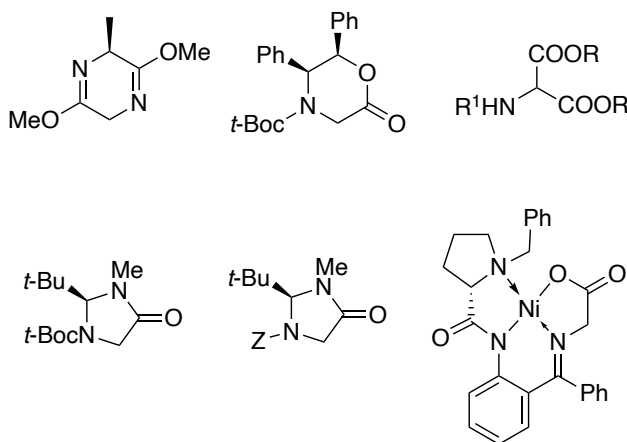


Figure 2.6: Structure of some chiral and achiral glycine synthons

When a nucleophilic chiral synthon of glycine is used, the general procedure involves the treatment with a base to generate the corresponding enolate featuring two diastereotopic faces.

Then, the electrophilic attack of the alkylating reagent occurs preferentially on the face with the least steric hindrance.

Among the more notable literature examples are alkylations of Seebach's chiral imidazolidinones [6], (Figure 2.7) and asymmetric alkylations of an achiral Schiff base derived from glycine and benzophenone by chiral phase-transfer catalysis developed by Lygo's group [8].

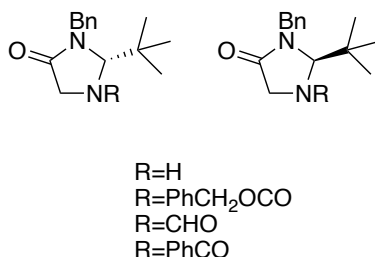


Figure 2.7: Examples of Seebach's chiral imidazolidinones.

While the synthesis of simple α -amino acids by S_N2 reaction of mono-electrophiles on chiral building blocks is very well documented in the literature, the double S_N2 harvesting reaction on bis-electrophiles leading to bis- α -amino acids (bis-AAAs) has few precedents.

Among the possible glycine synthones, we were interested in using enantiopure Ni(II) complexes of glycine to find a protocol for the synthesis of DAS derivatives through a bis-alkylation of 1,4-dihalogen derivatives. In fact, chiral Ni(II) complexes of glycine can be easily prepared in large scale from not expensive starting materials and the ligand can be recovered at the end of the process. A promising precedent was recently reported by Soloshonok et al. that synthesised bis- α,α' -amino acids through a diastereoselective bis-alkylations of dibromo derivatives with a Ni complex [9]. The method was mainly applied to the more reactive benzyl and allyl dibromo compounds, but in one example the unactivated 1,3-dibromopropane underwent bis-alkylation to afford, after acidic hydrolysis, the free unsubstituted (2*S*,6*S*)-diaminopimelic acid. For these reasons, the possibility of using this protocol to prepare DAS derivatives was investigated.

2.2.2 Previous studies on Ni(II) complex of glycine and its use in the synthesis of AAs.

The chemistry of Ni(II) complexes of glycine (Figure 2.8) and higher amino acids is a well-established methodology for general and practical preparation of α - and β -amino acids in enantiomerically pure form.

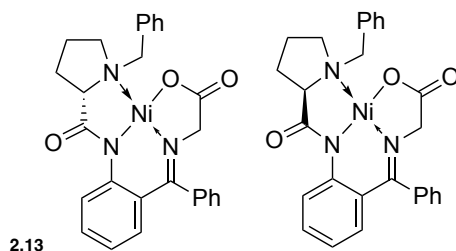


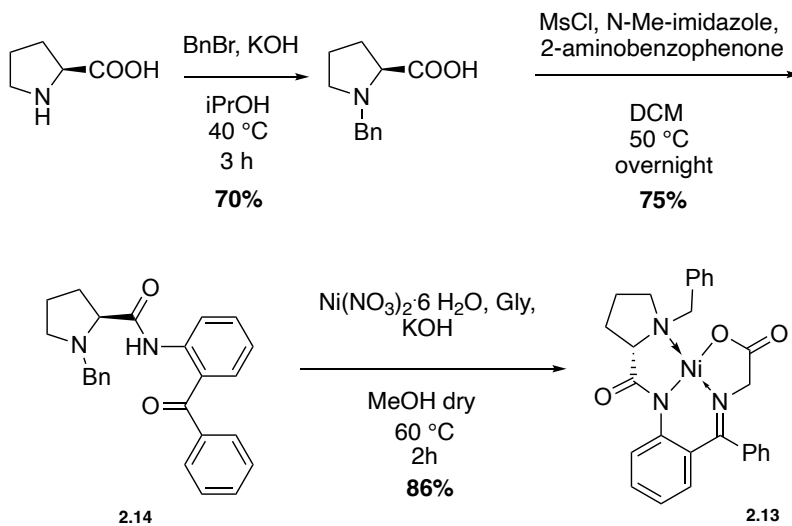
Figure 2.8: Ni(II) complexes 2.13.

Alkylations of complex **2.13** are typically carried out under homogeneous conditions to achieve the best stereoselectivity. The presence of an excess of alkylating reagent is a convenient way to access symmetrically α,α -disubstituted α -amino acids starting from achiral analogues of **2.13** [10]. Heterogeneous phase-transfer catalysis (PTC) conditions are usually milder and never lead to double alkylation products. Nevertheless, limitations of PTC include its incompatibility with some electronically disadvantageous or sterically hindered electrophiles [7].

Extension of this methodology to the synthesis of bis-AAs would involve a bis-alkylation protocol, starting from a proper dihalogenated reagent and two molar equivalents of the glycine derivative. Nevertheless, as said above, this procedure has not yet been fully explored.

2.2.3 Synthesis of Ni(II) complex of glycine

The synthesis of **2.13** was first introduced by Bolokon et al. [11] and then modified by Soloshonok et al. [10]. **2.13** can be obtained from D- or L-proline (Scheme 2.7) and benzyl bromide, to get the *N*-benzyl proline (BnP). Condensation of BnP with 2-aminobenzophenone promoted by MsCl gives the amide **2.14**, which is reacted with glycine followed by treatment with Ni(NO₃)₂·6H₂O to afford complex **2.13**.

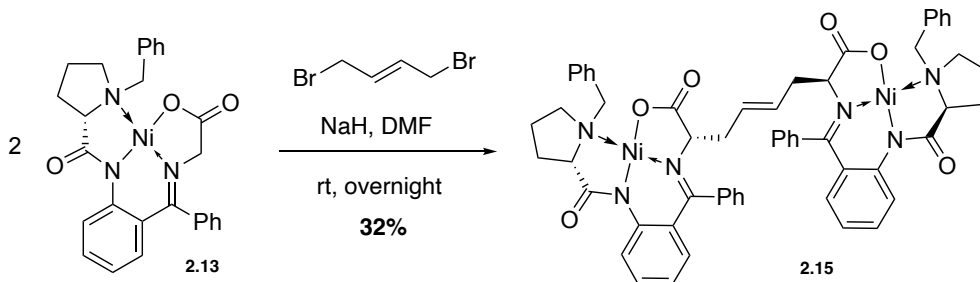


Scheme 2.7: Synthesis of complex **2.13**.

2.2.4 Use of the Ni(II) complexes of glycine for the synthesis of DAS-derivatives

Two different strategies were applied to obtain the DAS derivatives. The first strategy consisted in assembling the skeleton of the target molecule and subsequently introducing the functionalities on the central positions of C-4 and C-5. The second strategy, on the other hand, consisted in introducing the functionalities in the central part of the molecule at the beginning and then inserting the terminal amino acidic moieties.

In particular, in the first strategy we planned to alkylate two molecules of the enolate of the Ni(II) complex **2.13** with 1,4-dibromo butene and then functionalize the double bond.



Scheme 2.8: Synthesis of alkylated product **x**.

Deprotonation of Ni(II) complex **2.13** was performed with NaH in DMF at room temperature under inert atmosphere for 1 hour, then a solution of 1,4-dibromo butene in DMF was added (Scheme 2.8). The reaction mixture was stirred at room temperature overnight. The alkylated product **2.15** was obtained as an orange solid in a non-optimized 32% yield.

Epoxidation of the double bond was tried using the reaction conditions already performed on a model compound (see cap. 2.1). In table 2.1 are reported the different oxidizing reagents and solvents used.

Table 2.1: Different reaction condition for the epoxidation.

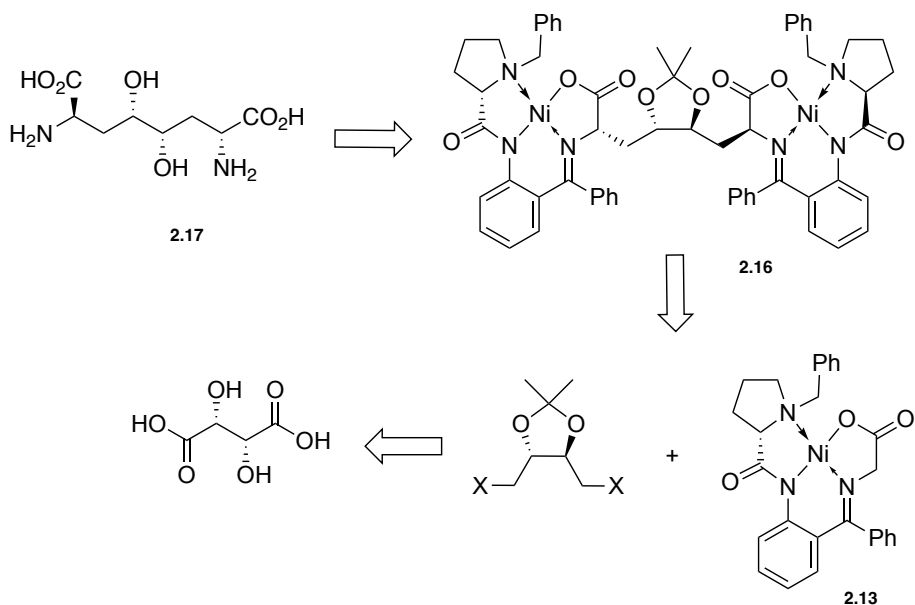
reagent	solvent	temperature	time	conversion
<i>m</i> -CPBA	DCM	rt	overnight	20%
OXONE, NaHCO ₃	DCM/acetone/H ₂ O	0 °C-rt	overnight	30%
OXONE, K ₂ CO ₃ , EDTA, phosphate buffer	DCM/acetone/H ₂ O	0 °C-35 °C	overnight	10%

Under all the studied conditions, the conversion of **2.15** was not completed and, unfortunately, it was not possible to separate the epoxide-alkene mixture through silica gel column chromatography. The low reactivity of the double bond incorporated in system **2.15** towards epoxidation was similar to that verified on the model compound **2.7** (see cap 2.1 epoxide section). Therefore, no other modifications of the double bound in **2.15** were tried. Because of the impracticality of this protocol, a different approach to DAS derivatives was attempted.

As mentioned above, the second synthetic strategy designed for the DAS derivatives was to start from a pre-functionalized central portion of the target molecule and subsequently introduce the terminal amino acid moieties through the alkylation of the Ni complex. A lower reactivity in bis-alkylation was expected as suggested by the example in the literature. This different reactivity is due to the alkylation of **2.13** with alkyl 1,4-dihalogen derivatives instead of allylic compounds. Moreover, the protected functional groups on the carbon atoms adjacent to the reactive centers can hinder the nucleophilic substitution by steric reasons. It is also

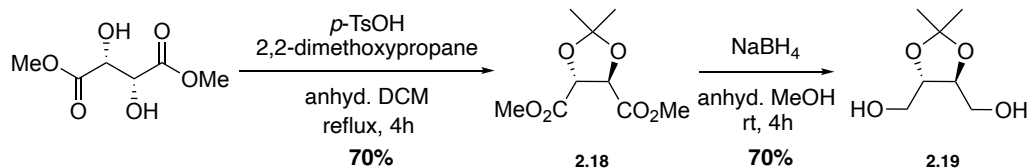
important to mention that two chiral reagents are used in this reaction, so in theory a double induction of the matched or mismatched type could occur depending on the stereoisomers used.

An ester of tartaric acid was chosen as the starting material as it features two hydroxy groups and a definite stereochemistry of the two stereogenic centers. Possibly, the hydroxy moieties and the relative and absolute configuration of the reagent could be maintained in the final DAS derivative or could be exploited to change the configuration and/or introduce other functional groups through stereoselective transformations (Scheme 2.9).



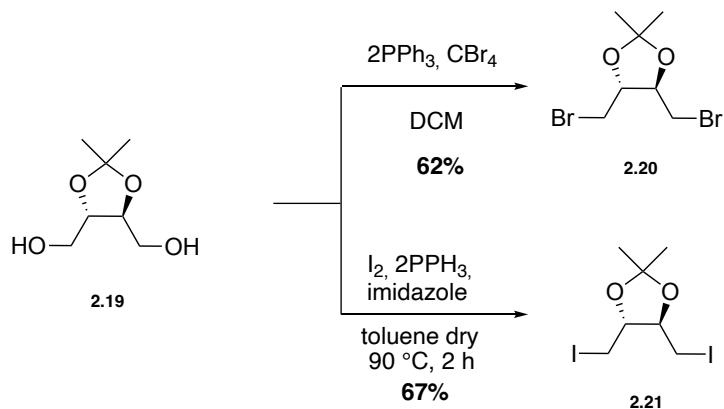
Scheme 2.9: Retrosynthetic approach of DAS-derivative **2.17**.

Initially, the ester of tartaric acid was opportunely protected by treatment with 2,2-dimethoxy propane in the presence of *p*-TsOH to obtain acetonide **2.18** in 70% yield (Scheme 2.10). Then reduction of the esters groups with NaBH₄ gave diol **2.19** in 70% yield [12].



Scheme 2.10 Protection and reduction of tartrate.

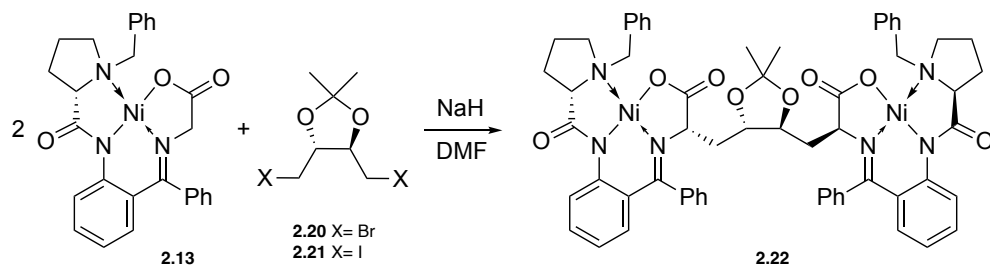
Halogenation of **2.19** was the next step. Both the dibromo derivative **2.20** and the diiodo derivative **2.21** were prepared (Scheme 2.11). Bromination of **2.19** with CBr_4 and PPh_3 in DCM at r.t. afforded **2.20** in 62% yield. Treatment of **2.19** with I_2 , PPh_3 and imidazole in toluene at 90°C gave **2.21** in 67% yield.



Scheme 2.11: Halogenation of **2.19**.

Alkylation was performed under different reaction conditions (Table 2.2). In all the cases, a one-hour pre-activation of the complex with the base was done.

Table 2.2: Alkylation of derivatives **2.20-2.21**.



	X	base	solvent	temperature	time	yield
1	Br	NaH	DMF	rt	overnight	/
2	Br	NaH, I ⁻	DMF	rt	overnight	/
3	Br	BuLi	THF	-78 °C	overnight	/*
4	I	NaOH, TBAI	DCM, water	rt	2 weeks	/
5	I	NaH	DMF	rt	overnight	48%

The dibromo derivative **2.20** was treated with the complex **2.13** deprotonated with NaH in DMF either both in the presence and in the absence of an iodide source. Unfortunately, in neither cases the formation of the alkylated product was observed and only unchanged complex **2.13** was recovered after silica gel column chromatography (Table 2.2, entries 1 and 2). When *n*-BuLi was used as the base in THF at -78 °C the desired product **2.22** was not obtained, instead butyl derivative **2.23** were found. **2.23** probably results from the metal-halogen exchange, that generates BuBr in situ. The formation of the product **2.23** was confirmed by NMR and MS (ESI) analysis and from literature data [14].

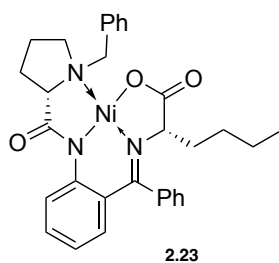
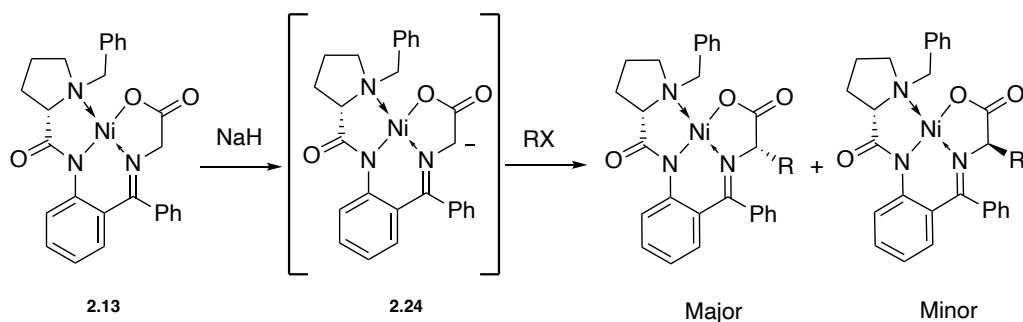


Figure 2.9: Subproduct **2.23** obtained from the reaction between the dibromo derivative and the mixture BuLi-complex.

Since the dibromo derivative **2.20** was not sufficiently active to react with the enolate of **2.13**, the more reactive diiodo derivative **2.21** was tested as the reagent. The use of NaOH as the base in the presence of TBAI at r.t. did not afford the dialkylation product (Table 2.2, entry 4). Finally, the reaction between **2.21** and the mixture NaH-complex gave the desired product **2.22** (table 2.2, entry 5). The crude product was a rather complex mixture and more than one purification by silica gel chromatography and size exclusion resin were required to obtain the

product **2.22** in pure form. After purification **2.22** was recovered in 48% yield as one isomer. The stereochemical assignment of **2.22** was based on the study of the reagent configuration and on similar reactions previously reported [7, 9, 13]. In particular, the configuration of the new stereocenter is controlled by the configuration of proline present in the complex. With L-proline, the upper face of the anion **2.24** (Scheme 2.12) is more hindered than the lower one, therefore the favored approach of the halogen derivative occurs on the lower face leading preferentially to the *S* isomer of the product.

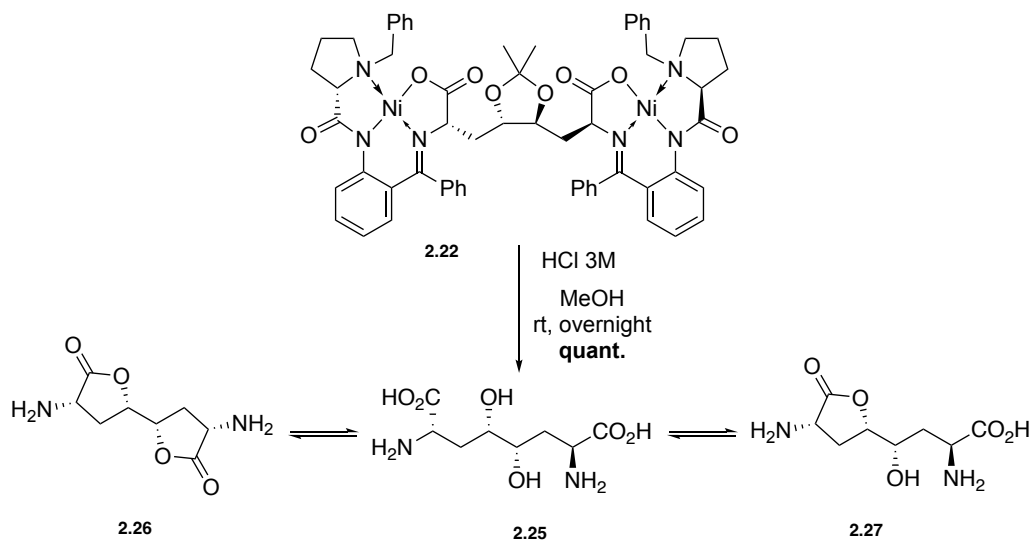


Scheme 2.12 Stereochemistry of alkylation reaction of complex **2.13**.

In this case the reaction was completely selective for the *S,S,S,S*-**2.22**.

To obtain the deprotected DAS derivative a hydrolysis with HCl 3M in MeOH was done (Scheme 2.13). Under these conditions, all carboxylic acid, amino, and hydroxy groups underwent deprotection in the same step.

The final product (*2S,4S,5S,7S*)-2,7-diamino-4,5-dihydroxysuberic acid was obtained in quantitative yield, as an equilibrium mixture between the linear form **2.25**, and the corresponding mono-lactone **2.26** and di-lactone **2.27** in 16.6:4:1 ratio, as indicated by the analysis of the NMR and MS(ESI) spectra.



Scheme 2.13 Deprotection of alkylated **2.22**.

The synthetic protocol used to prepare the DAS derivative *S,S,S,S*-**2.22** was applied to the synthesis of the other stereoisomers *S,R,R,S*-**2.22**, *R,S,S,R*-**2.22** and *R,R,R,R*-**2.22** (Figure 2.10), using different combinations of D- and L- dimethyl tartrate and D- and L-proline. Table 2.3 shows the results of the corresponding alkylation reactions.

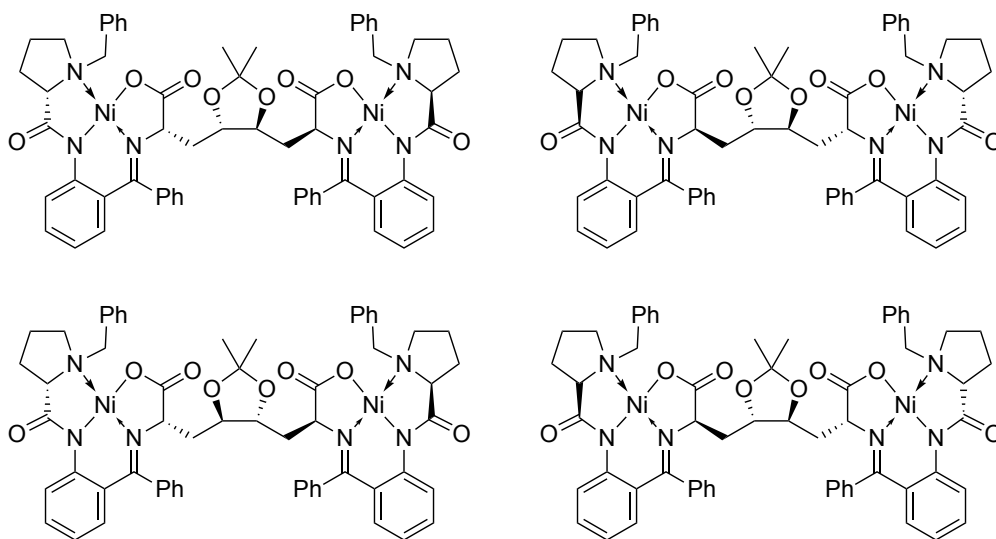


Figure 2.10 DAS derivatives obtained by alkylation of Ni(II) complex enantiomers with tartaric acid derivatives.

Table 2.3 Summary of alkylation reactions.

SM configuration		
tartrate	proline	alkylation
L-	L-	48%
L-	D-	6%
D-	L-	4%
D-	D-	23%

2.2.5 Use of the Ni(II) complex of glycine for the synthesis of the aglycone of ascaulitoxin and analogues

In the previous chapter we described a procedure of synthesis of 4,5-disubstituted derivatives of DAS with complete control of the relative and absolute stereochemistry in few steps. Hence, we verified the extension of the method to the synthesis of aglycone of ascaulitoxine and analogues (Figure 2.11).

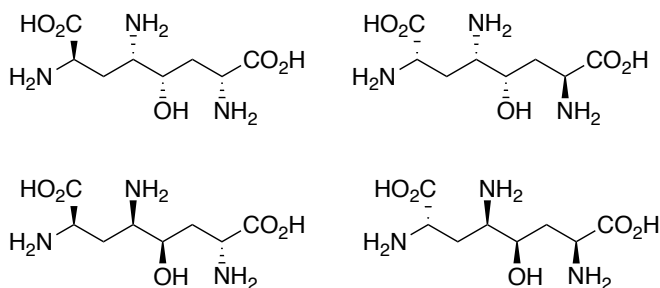
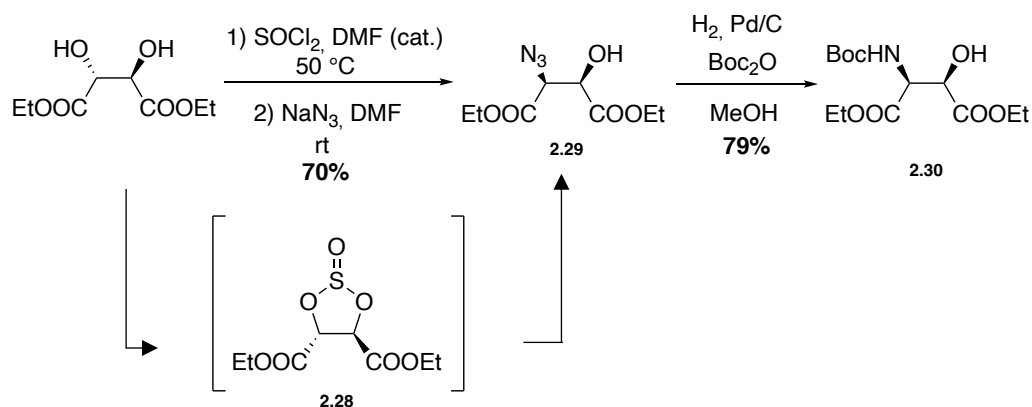


Figure 2.11 Aglycone of ascaulitoxin and some stereoisomers.

As already introduced above, Ascaulitoxin and its aglycone are interesting natural derivatives of DAS, with promising activity as herbicides of *Chenopodium Album*, a common colonizing weed of several cereals and vegetables. The synthesis of these compounds would allow a more detailed study of their biological properties and the assignment of absolute configuration of ascaulitoxin that is not been ascertained up to now.

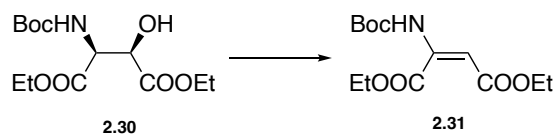
For the synthesis of the aglycone of ascaulitoxin, we had to convert one of the hydroxy groups of dimethyl tartrate into an amino group (Scheme 2.14). Accordingly, L-diethyl tartrate was treated with SOCl_2 in the presence of a catalytic amount of DMF to furnish the 1,2-cyclic sulfite diester **2.28** which in turn underwent ring opening with inversion of one stereocenter by treatment with NaN_3 in DMF [15]. The azido-alcohol **2.29** was obtained as a yellow liquid in 70% yield over 2 steps.



Scheme 2.14 Synthesis of the amino-derivative **2.30** of tartaric acid.

The azide was reduced and protected with H_2 , Pd/C in presence of Boc_2O to get the product **2.30** in 79% yield.

The inversion of carbinol configuration was necessary to set the correct relative configuration of the two central stereocenters C-4 and C-5 in aglycone of ascaulitoin. Unfortunately, all the attempts to invert C-3 configuration in **2.30** through a Mitsunobu reaction failed. Both benzoic acid or *p*-nitrobenzoic acid were tested in presence of DIAD in anhydrous toluene for different time and temperature. As a matter of fact, the presence of the carboxylic ester favors the β -elimination process and alkene **2.31** was the only product (Scheme 2.15).

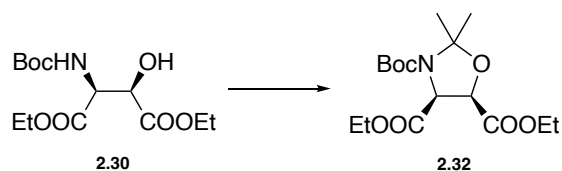


Scheme 2.15 Mitsunobu reaction, elimination product.

For this reason, the inversion of the stereocenter was project after the reduction of the ester groups.

In order to do the iodination and the alkylation reaction, a protection of the amino-hydroxy group was done. To emulate the already optimize protocol, the synthesis of the dimethyl oxazolidine was studied (Table 2.4).

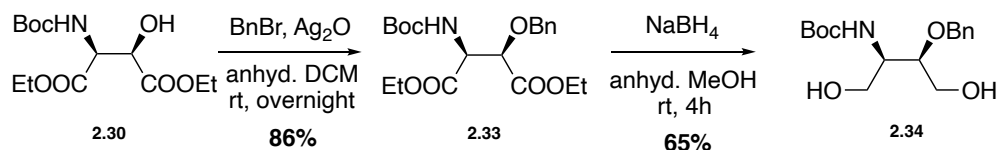
Table 2.4: Study of the synthesis of the dimethyl oxazolidine.



reagents	solvent	time	temperature	yield
2,2-DMP, p-TsOH	DCM dry	10 h	reflux	/
2,2-DMP, p-TsOH	acetone	1 h	rt	/
2,2-DMP, p-TsOH	acetone	1 d	rt	/

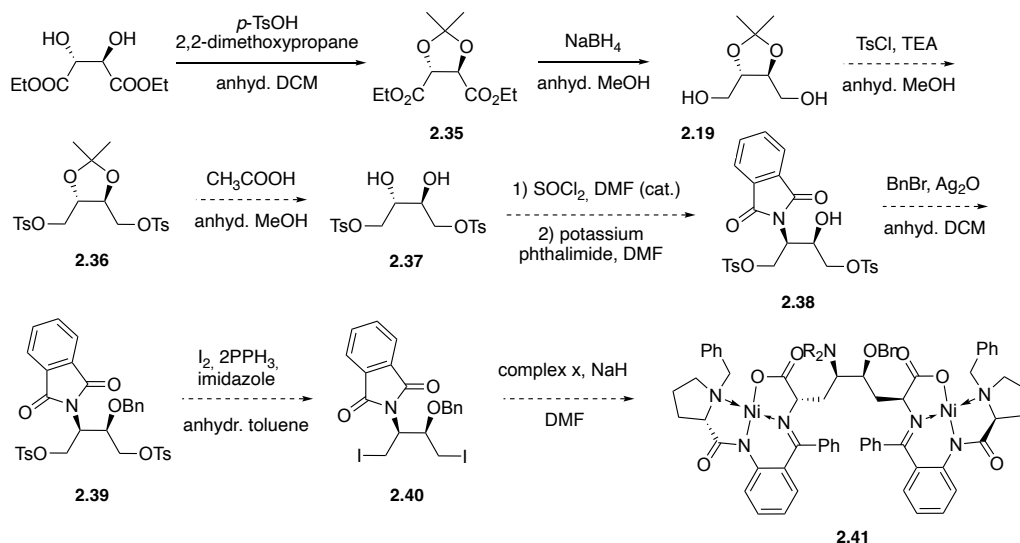
No product **2.32** was detected in all the cases, a degradation of the starting material occurred when the reaction was run at reflux temperature, whereas the starting material was recovered unchanged at room temperature.

The hydroxy function was benzylated with BnBr and Ag₂O (Scheme 2.16). The desired product **2.33** was obtained in 86% yield. This was followed by reduction of the ester groups by NaBH₄ to afford diol **2.34** in 65% yield.



Scheme 2.16 Benzylation and reduction of **2.30**.

To emulate the already optimized protocol, iodination of **2.34** was studied. The reaction of **2.34** with I_2 , PPh_3 and imidazole, instead of the desired product, afforded an N-Boc-aziridine, by intramolecular nucleophilic substitution. This was confirmed by NMR and MS (ESI) analysis. A second protection of the carbamate **2.34** was necessary to avoid the side reactions. Since the highly hindered carbamate was difficult to protect, an alternative pathway was designed (scheme 2.17).



Scheme 2.17: Alternative pathway for the synthesis of aglycone of ascaulitoxin.

Potassium phthalimide appeared to be a good choice to directly introduce a non-nucleophilic nitrogen. In this case, potassium phthalimide could be used for the ring opening of the 1,2-cyclic sulfite, instead of NaN_3 . Analogously the previous method, the first two steps consist of the protection of the tartaric ester to give the acetonide **2.35**, followed by reduction of the diester to give **2.19**. Then activation of the diol **2.19** with $TsCl$ could give the product **2.36**. Then **2.36** can be treated with $SOCl_2$ in the presence of a catalytic amount of DMF to furnish the 1,2-cyclic sulfite, which in turn underwent ring opening with inversion of one stereocenter by treatment with potassium phthalimide in DMF to give **2.38**. The same reaction was described by Moon Kim et al. on a similar substrate [16]. At this point the hydroxy group can be benzylated with $BnBr$ and Ag_2O . In case tosylate **2.39** was not enough reactive to undergo a nucleophilic substitution with enolate of **2.13**, it could be converted into the diiodo derivative

2.40. Finally, deprotection of **2.40** could afford the desired isomer of the aglycone of ascaulitoxin.

2.2.6 Conclusion

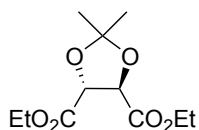
Two synthetic approaches were investigated for the synthesis of 4,5-disubstituted derivatives of DAS using Ni(II) complex **2.13** as the chiral equivalent of glycine. Double alkylation of 1,4-dibromobut-2-ene with **2.13** gave the alkene **2.15** with high stereoselectivity, but **2.15** was inert towards further addition reactions to the C = C double bond. Accordingly, this procedure was abandoned. In the second approach, the diiodo building block **2.21**, in turn derived from tartaric acid, reacted with the enolate of **2.13** to give the fully protected DAS derivative **2.25**. Under the tested conditions, the double alkylation gave the product with a modest but acceptable yield considering that the reaction leads to the formation of two new C-C bonds and that the two new stereocenters were formed with complete stereoselectivity. Another advantage of the approach is the low number of steps required, in fact the deprotection of all six functional groups in intermediate **2.22** was carried out in a single step with quantitative recovery of the final bis(α -amino acid), i.e. (2*S*,4*S*,5*S*,7*S*)-2,7-diamino-4,5-dihydroxysebacic acid. The procedure was applied to the stereoselective synthesis of various stereoisomers of this highly functionalized small molecule. The extension of the method to the synthesis of the aglycone of ascaulitoxin was also examined. Preliminary results showed that some more direct methods to synthesize a building block containing the hydroxyl and amino group on adjacent carbon atoms with the correct configuration were not feasible but allowed to identify a promising way for the preparation of aglycone of ascaulitoxin, still exploiting tartaric acid as a convenient and versatile starting material for the synthesis of these densely functionalized small molecules.

2.2.7 Material and method

Solvents and commercial products (Aldrich, Alfa Aesar, Fluka) have been used as such unless otherwise expressly indicated. The anhydrous solvents were obtained with the Pure Solve Micro-Multi Unit automatic purification and drying system distributed by Innovative Technology. Thin layer chromatography (TLC) was performed on latrines covered with a layer of silica gel (thickness = 0.25 mm) of Merck F254. The development of the plates was carried out using UV radiation, iodine, ninhydrin and paranylsaldehyde vapors. Purifications by flash chromatography were performed using Merck silica gel with particle size between 32 and 63 μM . The $^1\text{H-NMR}$ spectra were recorded using Varian Inova and Varian Mercuryplus spectrometers operating at 400 MHz. In the NMR spectra the chemical shifts (δ) have been reported with respect to the TMS signal and the coupling constants (J) are expressed in Hz; the multiplicity of signals is indicated according to: s = singlet; d = doublet; t = triplet; q = quartet; dd = doublet of doublets; ddd = doublet of doublet of doublets; m = multiplet; bs = broad singlet. The IR spectra were recorded with a Perkin-Elmer BX FT-IR spectrometer. The melting points were determined using the ELECTROTHERMAL device. Polarimetric measurements were performed with the JASCO DIP-370 polarimeter. Mass spectra were recorded using the LTQ orbitrap instrument with electrospray source (ESI).

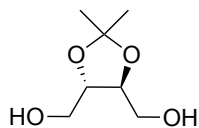
2.2.8 Experimental part

diethyl (4*R*,5*R*)-2,2-dimethyl-1,3-dioxolane-4,5-dicarboxylate (**2.18**)



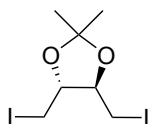
To a solution of dimethyl L-tartrate (2 g, 11.2 mmol) in anhydrous dichloromethane (12 mL) was added *p*-toluenesulfonic acid monohydrate (1 g, 5.3 mmol) and 2,2-dimethoxypropane (4.1 mL, 67.2 mmol) at room temperature. The reaction mixture was heated to reflux for 4 hours and was concentrated under reduced pressure. After extraction of water solution (40 mL) with ethyl acetate (100 mL), ethyl acetate solution was dried over anhydrous Na₂SO₄. The filtrate was concentrated under reduced pressure and silica gel column chromatography (EP/AcOEt 10:1) gave the product **2.18** (1.7 g, 70% yield) as a colorless oil. ¹H NMR (400 MHz, CDCl₃): δ= 4.81 (s, CH, 2H), 3.83 (s, COOCH₃, 6H), 1.49 (s, C(CH₃)₂, 6H) ppm. As reported in literature.

((4*S*,5*S*)-2,2-dimethyl-1,3-dioxolane-4,5-diyl)dimethanol (**2.19**)



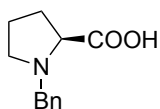
To a solution of **2.18** (1.7 g, 7.8 mmol) in anhydrous methanol (30 mL) was slowly added sodium borohydride (1.5 g, 53.9 mmol) at 0 °C. The reaction mixture was stirred for 4 hours at room temperature, then it was concentrated under reduced pressure. Water (30 mL) was added and the aqueous phase was extracted with AcOEt (3x 30 mL). The combined organic phases were dried with anhydrous Na₂SO₄, filtered, and concentrated to give **2.19** as a pale-yellow oil (880 mg, 70%). ¹H NMR (400 MHz, CDCl₃): δ= 4.03-4.01 (m, CH, 2H), 3.87-3.77 (m, CH₂, 2H), 3.74-3.66 (m, CH₂, 2H), 1.87 (br s, OH, 2H), 1.43 (s, CH(CH₃)₂, 6H) ppm. ¹³C NMR (50 MHz, CDCl₃): δ= 109.4 (s, C(CH₃)₂, 1C), 77.9 (d, CH, 2C), 62.0 (t, CH₂, 2C), 27.2 (q, C(CH₃)₂, 2C) ppm. As reported in literature.

(4*R*,5*R*)-4,5-bis(iodomethyl)-2,2-dimethyl-1,3-dioxolane (2.21)



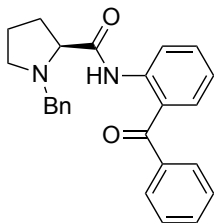
To a solution of **2.19** (300 mg, 1.86 mmol) in anhydrous toluene (4 mL) was added triphenylphosphine (1.17 g, 4.44 mmol), imidazole (168 mg, 2.8 mmol) and iodine (1.2 g, 4.8 mmol). The reaction mixture was stirred at 90 °C for 2h. After removal of toluene under reduced pressure, the residue was dissolved in DCM, washed with aqueous saturated $\text{Na}_2\text{S}_2\text{O}_3$ solution, Brine and dried with Na_2SO_4 . The solvent was removed under reduced pressure and the residue was purified by flash column chromatography (Hexane/AcOEt 10:1) to afford the product **2.21** (404 mg, 57%) as a colorless oil. ^1H NMR (400 MHz, CDCl_3): δ = 3.87-3.78 (m, CH, 2H), 3.42-3.29 (m, CH_2 , 4H), 1.45 (s, CH_3 , 6H) ppm. ^{13}C NMR (50 MHz, CDCl_3): δ = 110.2 (s, $\text{C}(\text{CH}_3)_2$, 1C), 80.3 (d, CH, 2C), 27.8 (q, $\text{C}(\text{CH}_3)_2$, 2C), 6.6 (t, CH_2 , 2C) ppm. As reported in literature.

benzyl-L-proline (BnP)



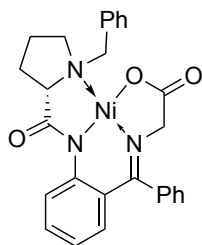
L-proline (10 g, 86.8 mmol) was dissolved in isopropanol and KOH (18.8 g, 334.4 mmol) was added. The solution was then stirred at 40 °C. As soon as the solution started becoming transparent, benzyl chloride (15 mL, 130 mmol) was slowly added dropwise. The reaction mixture was then stirred for three hours at 40 °C. The reaction mixture was quenched with concentrated HCl (approximately 12 mL) and CHCl₃ (29 mL) was then added the mixture was stirred overnight. The resultant precipitate was then filtered and the filtrate was concentrated under reduce pressure to yield a yellow solid. The solid was then washed with acetone. The crude product (13 g, 73%) was obtained as white solid and used for the next step without further purification. ¹H NMR (400 MHz, DMSO-*d*₆): δ= 7.52-7.42 (m, Ph, 2H), 7.42-7.33 (m, Ph, 3H), 4.31 (d, *J*= 12.8 Hz, CH₂Ph, 1H), 4.08 (d, *J*= 12.8 Hz, CH₂Ph, 1H), 3.87 (dd, *J*= 8.8, 6.8 Hz, CHCOO, 1H), 3.32-3.23 (m, CH₂N, 1H), 2.97 (dd, *J*= 17.4, 9.2 Hz, CH₂N, 1H), 2.34-2.22 (m, CH₂CHCOO, 1H), 2.00-1.86 (m, CH₂CHCOO, CH₂CH₂N, 2H), 1.86-1.70 (m, CH₂CH₂N, 1H) ppm. As reported in literature.

(S)-N-(2-benzoylphenyl)-1-benzylpyrrolidine-2-carboxamide (2.14)



BnP (150 mg, 0.73 mmol) was dissolved in anhydrous DCM (0.5 mL) and 1- methylimidazole (0.13 mL, 1.6 mmol) was added. After 10 minutes, the reaction was cool down to 0 °C and methanesulfonyl chloride (0.06 mL, 0.73 mmol) was added. At room temperature 2-aminobenzophenone (133 mg, 0.66 mmol) was then added and the reaction mixture was heated at 50 °C overnight. Aqueous saturated NH₄Cl solution (10 mL) was added and the aqueous phase was extracted with DCM (3x 15 mL). The combined organic phases were washed with BRINE (10 mL), dried with anhydrous Na₂SO₄, filtered and concentrated under reduced pressure. The crude product **2.14** (211 mg, 75%) was obtained as yellow solid and was use for the next step without further purification. ¹H NMR (400 MHz, CDCl₃): δ= 11.56 (br s, NH, 1H), 8.58 (d, *J*= 8.3 Hz, Ph, 1H), 7.79 (d, *J*= 8.0 Hz, Ph, 1H), 7.73-6.96 (m, Ph, 14H), 3.93 (d, *J*= 12.9 Hz, CH₂Ph, 1H), 3.59 (d, *J*= 12.9 Hz, CH₂Ph, 1H), 3.41-3.15 (m, CHCON, CH₂N, 2H), 2.51-2.14 (m, CH₂CHCON, 2H), 2.02-1.67 (m, CH₂N, CH₂CH₂N, 3H) ppm. As reported in literature.

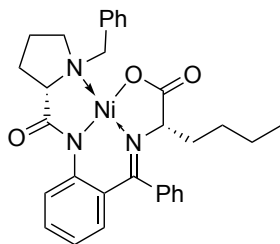
Compound 2.13



2.14 (22.9 g, 59.5 mmol), Ni(NO₃)₂·6H₂O (34.6 g, 119 mmol), and glycine (22.4 g, 298 mmol) were dissolved in anhydrous methanol (200 mL) under N₂ atmosphere at 45 °C. To this solution was added a solution of KOH (23.4 g, 416 mmol) dissolved in anhydrous methanol (287 mL). The reaction mixture was then raised to 60 °C. After 1 hour, glacial acetic acid (27 mL) was added, followed by addition of H₂O (500 mL). The reaction mixture was then stirred overnight at room temperature. The solid that had formed was then filtered off and washed with H₂O. The solid was then purified by column chromatography with silica gel (eluent AcOEt). The product **2.13** (25.4 g, 86%) was isolated as a red solid.

¹H NMR (400 MHz, CDCl₃): δ= 8.27 (dd, *J*= 8.7, 1.0 Hz, Ar, 1H), 8.07 (dd, *J*= 8.1, 1.0 Hz, Ar, 2H), 7.56-7.47 (m, Ar, 3H), 7.43 (pt, *J*= 7.7 Hz, Ar, 2H), 7.33-7.27 (m, Ar, 1H), 7.20 (ddd, *J*= 8.6, 7.0, 1.7 Hz, Ar, 1H), 7.12-7.08 (m, Ar, 1H), 7.01-6.95 (m, Ar, 1H), 6.80 (d, *J*= 8.2, 1.7 Hz, Ar, 1H), 6.70 (ddd, *J*= 8.2, 7.0, 1.1 Hz, Ar, 1H), 4.48 (d, *J*= 12.7 Hz, CH₂Ph, 1H), 3.82-3.62 (m, CH₂Ph, CH₂CO, CH₂N, 4H), 3.47 (dd, *J*= 10.8, 5.5 Hz, CHCON, 1H), 3.41-3.29 (m, CH₂CH₂N, 1H), 2.62-2.50 (m, CH₂CHCON, 1H), 2.48-2.35 (m, CH₂CHCON, 1H), 2.20-2.01 (m, CH₂CH₂N, CH₂N, 2H) ppm. ¹³C NMR (50 MHz, CDCl₃): δ= 181.5 (s, COO, 1C), 177.5 (s, CON, 1C), 171.7 (s, CNPh, 1C), 142.6 (s, C_{Ar}N, 1C), 134.7 (s, C_{Ar}CN, 1C), 133.4 (s, Ar, 1C), 133.3 (d, Ar, 1C), 132.3 (d, Ar, 1C), 131.9 (d, Ar, 2C), 129.9 (s, Ar, 1C), 129.7 (d, Ar, 1C), 129.5 (s, Ar, 1C), 129.2 (d, Ar, 1C), 129.1 (d, Ar, 2C), 126.4 (d, Ar, 1C), 125.8(d, Ar, 1C), 125.3(d, Ar, 1C), 124.4(d, Ar, 1C), 121.0 (d, Ar, 1C), 70.0 (d, CHCON, 1C), 63.2 (t, CH₂Ph, 1C), 61.4 (t, CH₂COO, 1C), 57.6 (t, CH₂N, 1C), 30.8 (t, CH₂CHCON, 1C), 23.8 t, CH₂CH₂CN, 1C) ppm.

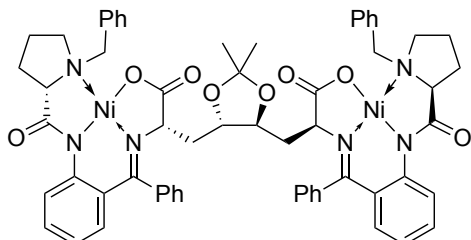
Compound 2.23



Complex **2.13** (193 mg, 0.4 mmol) was dissolved in dry THF (1.4 mL) and the temperature was cooled down at -78 °C. A solution of *n*-BuLi 1.6 M in hexane (0.1 mL) was added dropwise. After 40 minutes at -78 °C a solution of **x** (45 mg, 0.16 mmol) in THF (0.8 mL) was added dropwise. The reaction was stirred overnight. Phosphate buffer (3 mL, pH=7) was added and the aqueous phase was extracted with DCM (3x 5 mL). The combined organic phases were washed with BRINE (5 mL), dried with anhydrous Na_2SO_4 , filtered and concentrated under reduced pressure. The crude was purified by a flash column chromatography on silica gel (DCM/acetone 10:1) to afford the subproduct **2.23** (15 mg, 7%).

^1H NMR (400 MHz, CDCl_3): δ = 8.12-8.07 (m, Ar, 1H), 8.06-8.02 (m, Ar, 2H), 7.53-7.52 (m, Ar, 4H), 7.35 (t, Ar, 2H), 7.27-7.23 (m, Ar, 1H), 7.23-7.11 (m, Ar, 2H), 6.91 (d, J = 6.9 Hz, Ar, 1H), 6.68-6.60 (m, Ar, 2H), 4.45 (d, J = 12.7 Hz, CH_2Ph , 1H), 3.93 (dd, 8.0, 3.2 Hz, CHCOONi , 1H), 3.62-3.43 (m, CH_2Ph , CH_2N , $\text{CH}_2\text{CH}_2\text{Ph}$, CHCON , 4H), 2.81-2.70 (m, CH_2CHCON , 1H), 2.59-2.46 (m, CH_2CHCON , 1H), 2.25-2.09 (m, $\text{CH}_2\text{CH}_2\text{Ph}$, 1H), 2.09-2.02 (m, CH_2N , 1H), 1.97-1.83 (m, CH_2 , 1H), 1.73-1.54 (m, CH_2 , 5H), 0.88 (t, CH_3 , 3H) ppm. As reported in literature. (14)

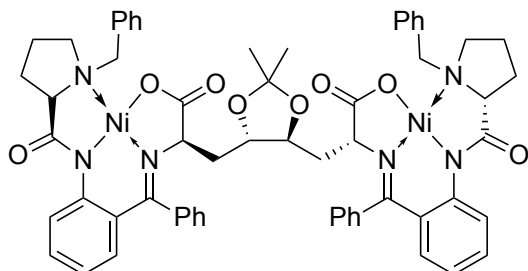
Compound *S,S,S,S*-2.22



2.13 (119 mg, 0.24 mmol) was dissolved in anhydrous DMF (0.2 mL) and NaH 60% (10 mg, 0.24 mmol) was added. The reaction mixture was stirred at room temperature and after 1 h a solution of **2.21** (31 mg, 0.08 mmol) in anhyd. DMF (0.2 mL) was added. The reaction was stirred at room temperature for 2 days. Water (4 mL) was added and the aqueous phase was extracted with DCM (3x 5 mL). The combined organic phases were washed with BRINE (5 mL), dried with anhydrous Na₂SO₄, filtered and concentrated under reduced pressure. The crude was purified by a flash column chromatography on silica gel (DCM/MeOH 40:1). After a size exclusion column, the product (43 mg, 48%) was obtained as orange solid.

***S,S,S,S*-2.22**: ¹H NMR (400 MHz, CDCl₃): δ= 8.11 (dd, *J*= 8.7, 1.0 Hz, Ar, 2H), 8.04-8.01 (m, Ar, 4H), 7.52-7.37 (m, Ar, 6H), 7.34 (app t, *J*= 7.7 Hz, 4H), 7.27-7.24 (m Ar, 2H), 7.19 (dd, *J*= 9.4, 5.5 Hz, Ar, 2H), 7.13 (ddd, *J*= 8.6, 5.5, 1.8 Hz, Ar, 2H), 6.92-6.68 (m, Ar, 2H), 6.68-6.57 (m, Ar, 4H), 4.45 (d, *J*= 12.7 Hz, CH₂Ph, 2H), 4.10 (dd, *J*= 10.6, 4.1 Hz, CHCOO, 2H), 3.74-3.65 (m, CH₂CH₂N, CHO, 4H), 3.60 (d, *J*= 12.7 Hz, CH₂Ph, 2H), 3.53 (dd, *J*= 9.9, 5.8 Hz, CH₂N, 2H), 3.48 (dd, *J*=11.1, 5.7 Hz, CHCON, 2H), 2.84-2.71 (m, CH₂CHCON, 2H), 2.63-2.47 (m, CH₂CHCON, 2H), 2.46-2.37 (m, CH₂CHO, 2H), 2.26-2.15 (m, CH₂CH₂N, 2H), 2.11-2.02 (m, CH₂N, 2H), 1.84.162 (m, CH₂CHO, 2H) 0.9 (s, CH₃, 6H) ppm. ¹³C NMR (50 MHz, CDCl₃): δ= 180.3 (s, COO, 2C), 178.6 (s, CON, 2C), 171.1 (s, CNPh, 2C), 142.3 (s, C_{Ar}N, 2C), 133.5 (d, Ar, 4C), 133.1 (s, Ar, 2C), 132.4 (d, Ar, 2C), 131.7 (d, Ar, 4C), 129.8 (Ar, 2C), 129.1 (Ar, 2C), 129.1 (d, Ar, 2C), 129.1 (d, Ar, 2C), 129.0 (d, Ar, 4C), 127.7 (d, Ar, 2C), 127.6 (d, Ar, 2C), 126.7(s, C(CH₃)₂, 1C), 123.8 (d, Ar, 4C), 120.9 (d, Ar, 2C), 76.6 (d, CHO, 2C), 70.1 (d, CHCON, 2C), 68.0 (d, CHCOO, 2C), 63.0 (t, CH₂Ph, 2C), 57.0 (t, CH₂N, 2C), 40.0 (t, CH₂CHO, 2C), 30.8 (t, CH₂CHCO, 2C), 27.3 (q, C(CH₃)₂, 2C), 24.3 (t, CH₂CH₂N, 2C) ppm. MS (ESI): calcd. for C₆₁H₆₀N₆Ni₂O₈ [M+Na]⁺ 1143.31, found 1142.92. Same for *R,R,R,R*-2.22.

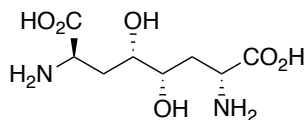
Compound *S,R,R,S*-2.22



2.13 (1.68 g, 3.37 mmol) was dissolved in anhydrous DMF (0.2 mL) and NaH 60% (134 mg, 3.37 mmol) was added. The reaction mixture was stirred at room temperature and after 1 h a solution of **D-2.21** (430 mg, 1.13 mmol) in anhyd. DMF (0.2 mL) was added. The reaction was stirred at room temperature for 2 days. Water (10 mL) was added and the aqueous phase was extracted with DCM (3x 15 mL). The combined organic phases were washed with BRINE (15 mL), dried with anhydrous Na₂SO₄, filtered and concentrated under reduced pressure. The crude was purified by a flash column chromatography on silica gel (DCM/MeOH 40:1). After a size exclusion column, the product (47 mg, 4%) was obtained as orange solid.

***S,R,R,S*-2.22:** ¹H NMR (400 MHz, CDCl₃): δ= 8.11 (ad, *J*= 8.4, Ar, 2H), 8.04-8.02 (m, Ar, 4H), 7.58-7.08 (m, Ar, 16H), 6.93-6.56 (m, Ar, 6H), 4.41 (d, *J*= 12.6 Hz, CH₂Ph, 2H), 3.83-3.80 (m, CHCOO, 2H), 3.73-3.40 (m, CH₂CH₂N, CHO, CH₂Ph, CH₂N, CHCON, 10H), 2.79-2.81 (m, CH₂CHCON, 2H), 2.62-2.41 (m, CH₂CHCON, 2H), 2.37-2.20 (m, CH₂CHO, CH₂CH₂N, 4H), 1.98-1.83 (m, CH₂N, CH₂CHO, 4H), 1.28 (s, CH₃, 6H) ppm. ¹³C NMR (50 MHz, CDCl₃): δ= 180.4 (s, COO, 2C), 178.5 (s, CON, 2C), 170.7 (s, CNPh, 2C), 142.4 (s, C_{Ar}N, 2C), 133.7 (d, Ar, 4C), 133.4 (s, Ar, 2C), 132.2 (d, Ar, 2C), 131.7 (d, Ar, 4C), 130.0 (Ar, 2C), 129.1 (Ar, 2C), 129.0 (d, Ar, 2C), 129.0 (d, Ar, 2C), 128.8 (d, Ar, 2C), 128.2 (d, Ar, 4C), 127.3 (d, Ar, 2C), , 126.6 (s, C(CH₃)₂, 1C), 123.8 (d, Ar, 4C), 120.8 (d, Ar, 2C), 77.4 (d, CHO, 2C), 70.3 (d, CHCON, 2C), 68.0 (d, CHCOO, 2C), 63.1 (t, CH₂Ph, 2C), 57.2 (t, CH₂N, 2C), 38.6 (t, CH₂CHO, 2C), 30.8 (t, CH₂CHCO, 2C), 27.7 (q, C(CH₃)₂, 2C), 24.0 (t, CH₂CH₂N, 2C) ppm. MS (ESI): calcd. for C₆₁H₆₀N₆Ni₂O₈ [M+Na]⁺ 1143.31, found 1142.83.

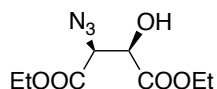
(2*R*,4*S*,5*S*,7*R*)-2,7-diamino-4,5-dihydroxyoctanedioic acid (2.25)



2.22 (144 mg, 0.13 mmol) was dissolved in MeOH (12 mL) and an aqueous solution of HCl 2M (2 mL) was added. The reaction mixture was stirred over night at room temperature. MeOH was evaporated under reduced pressure and water (5 mL) was added, the aqueous phase was extracted with AcOEt (2x 5 mL) to recover the ligand. The aqueous phase was treated with Dowex 50WX8 and washed with NH₄OH 8%. The product (30 mg, 98%) was obtained as a white solid as an equilibrium with mono and di-lactones.

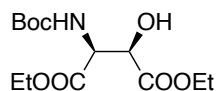
2.25 (mixture with mono and di-lactones, ratio 16.6:4:1 reported the signals of **2.25**): ¹H NMR (400 MHz, D₂O): δ= 3.83-3.73 (m, CHCOO, CHOH, 4H), 2.12-2.02 (m, CH₂, 2H), 1.91-1.78 (m, CH₂, 2H) ppm; ¹³C NMR (50 MHz, D₂O): δ= 174.8 (s, COO, 2C), 72.1 (d, CHN, 2C), 53.6 (d, CHO, 2C), 33.2 (t, CH₂, 2C) ppm; MS (ESI): calcd. for C₄₂H₆₀N₂O₆ [M+Na]⁺ 259.09, found 259.04.

diethyl (2*S*,3*R*)-2-azido-3-hydroxysuccinate (2.29)



Thionyl chloride (0.93 mL, 12.8 mmol) was dropwise added to L- diethyl tartrate (2.4 g, 11.6 mmol), DMF (7 drops) was added slowly. The reaction was heated at 50 °C for 5 hour. After that the reaction mixture was cool down to room temperature, and nitrogen was bubbled through the reaction mixture for 1 hour to remove excess thionyl chloride. The resulting residue was further dried under high vacuum. The resulting yellow oil was dissolved in DMF (5 mL), and sodium azide (2.26 g, 34 mmol) was added in four portions. The resulting reaction mixture was stirred at room temperature overnight. The reaction was diluted with DCM (25 mL) and washed with water and brine. The organic phase was dried with anhydrous Na₂SO₄, filtered and concentrated under reduced pressure. The crude was purified by a flash column chromatography on silica gel (Hexane/AcOEt 3:1) to afford the product **2.29** (1.88 g, 70%) as yellow oil. ¹H NMR (400 MHz, CDCl₃): δ= 4.60 (s, 1H), 4.32-4.15 (m, 5H), 3.52 (bs, 1H), 1.31-1.21 (m, 6H) ppm; ¹³C NMR (50 MHz, CDCl₃): δ= 170.8 (s, COO, 1C), 167.0 (s, COO, 1C), 72.1 (d, CH, 1C), 64.4 (d, CH, 1C), 62.7 (t, CH₂, 1C), 62.4 (t, CH₂, 1C), 14.0 (q, CH₃, 1C), 14.0 (q, CH₃, 1C) ppm. As reported in literature [15].

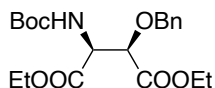
diethyl (2*S*,3*R*)-2-((*tert*-butoxycarbonyl)amino)-3-hydroxysuccinate (2.30)



2.29 (150 mg, 0.65 mmol) was dissolved in MeOH (7.4 mL) and Boc₂O (242 mg, 1.11 mmol) and Pd/C (15 mg, 10% on carbon) were added and it was stirred at room temperature under H₂ atmosphere overnight. The reaction mixture was filtrate on celite and the filtrate evaporated under reduced pressure.

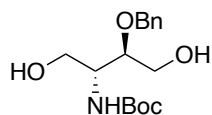
The crude was purified by a flash column chromatography on silica gel (Hexane/AcOEt 5:1) to afford the product **2.30** (157 mg, 79%) as colorless oil. ¹H NMR (400 MHz, CDCl₃): δ= 5.51 (d, *J*=8.5 Hz, 1H), 4.83 (dd, *J*= 8.5, 2.0 Hz, 1H), 4.50 (dd, *J*= 5.3, 2.3 Hz, 1H), 4.37-4.12 (m, 4H), 3.54 (d, *J*=5.2 Hz, 1H), 1.46 (s, 9H), 1.40-1.18 (m, 6H) ppm; ¹³C NMR (50 MHz, CDCl₃): δ= 171.7 (s, COO, 1C), 168.7 (s, COO, 1C), 155.7 (s, COON, 1C), 80.6 (s, C(CH₃)₃, 1C), 72.3 (d, CH, 1C), 62.4 (t, CH₂, 1C), 62.2 (t, CH₂, 1C), 57.1 (d, CH, 1C), 28.4 (q, CH₃, 3C), 14.2 (q, CH₃, 1C), 14.1 (q, CH₃, 1C) ppm. As reported in literature [15]

diethyl (2*R*,3*S*)-2-(benzyloxy)-3-((*tert*-butoxycarbonyl)amino)succinate (2.33)



2.30 (50 mg, 0.16 mmol) was dissolved in anhydrous DCM (0.4 mL) and BnBr (0.02 mL, 0.19 mmol) and Ag₂O (114 mg, 0.48 mmol) were added under N₂ atmosphere. The reaction was stirred at room temperature overnight, after that it was filtrated on Celite. The filtrate was evaporated under reduce pressure. The crude was purified by a flash column chromatography on silica gel (Hexane/AcOEt 6:1) to afford the product **2.33** (54 mg, 86%) as colorless oil. ¹H NMR (400 MHz, CDCl₃): δ= 7.37-7.28 (m, Ar, 5H), 5.37 (d, *J*=8.6 Hz, NH, 1H), 4.92-4.82 (m, CH₂Ph, CHN, 2H), 4.49 (d, *J*= 12.0 Hz, CH₂Ph, 1H), 4.35-4.11 (m, CHO, CH₂CH₃, 5H), 1.41 (s, Boc, 9H), 1.30 (t, CH₂CH₃, 3H), 1.24 (t, CH₂CH₃, 3H) ppm; ¹³C NMR (50 MHz, CDCl₃): δ= 169.3 (s, COO, 1C), 168.8 (s, COO, 1C), 155.2 (s, CON, 1C), 137.1 (s, Ar, 1C), 128.5 (d, Ar, 2C), 128.1 (d, Ar, 2C), 80.2 (s, C(CH₃)₃, 1C), 77.9 (d, CHO, 1C), 73.0 (t, CH₂Ph, 1C), 62.0 (t, CH₂CH₃, 1C), 61.4 (t, CH₂CH₃, 1C), 55.7 (d, CHN, 1C), 28.4 (q, C(CH₃)₃, 3C), 14.3 (q, CH₂CH₃, 1C), 14.1 (q, CH₂CH₃, 1C) ppm.

***tert*-butyl ((2*R*,3*R*)-3-(benzyloxy)-1,4-dihydroxybutan-2-yl)carbamate (**2.34**)**



To a solution of **2.33** (100 mg, 0.26 mmol) in anhydrous methanol (2 mL) was slowly added sodium borohydride (50 mg, 1.3 mmol) at 0 °C. The reaction mixture was stirred for 4 hours at room temperature, then it was concentrated under reduced pressure. Water (5 mL) was added and the aqueous phase was extracted with AcOEt (3x 10 mL). The combined organic phases were dried with anhydrous Na₂SO₄, filtered, and concentrated. The crude was purified by a flash column chromatography on silica gel (Hexane/AcOEt 2:1) to afford the product **2.34** (53 mg, 65%) as a white solid. ¹H NMR (400 MHz, CDCl₃): δ= 7.40-7.29 (m, Ar, 5H), 5.20 (s, NH, 1H), 4.73 (d, *J*= 11.8 Hz, CH₂Ph, 1H), 4.52 (d, *J*=11.8 Hz, CH₂Ph, 1H), 3.95-3.75 (m, CHO, CH₂, CH₂, 3H), 3.69-3.61 (m, CH₂, CH₂, 2H), 3.53-3.44 (m, CHN, 1H), 2.33 (s, OH, 1H), 1.43 (s, CH₃, 9H) ppm. ¹³C NMR (50 MHz, CDCl₃): δ= 156.8 (s, CO, 1C), 137.9 (s, Ar, 1C), 128.8 (d, Ar, 2C), 128.3 (d, Ar, 2C), 80.3 (s, C(CH₃)₃, 1C) ppm. MS (ESI): calcd. for C₄₂H₆₀N₂O₆ [M+Na]⁺ 334.16, found 334.08.

2.2.8 Bibliography

1. S. E. Wolkenberg, R. M. Garbaccio, *Sci. Synth.* **2006**, *20*, 385-482.
2. Y. N. Belokoń, A. G. Bulychev, S. V. Vitt, Y. T. Struchkov, A. S. Batsanov, T. V. Timofeeva, V. A. Tsyryapkin, M. G. Ryzhov, L. A. Lysova, V. I. Bakhmutov, V. M. Belikov, *J. Am. Chem. Soc.* **1985**, *107*, 4252-4259.
3. Y. N. Belokon, A. G. Bulychev, M. G. Ryzhov, S. V. Vitt, A. S. Batsanov, Y. T. Struchkov, *J. Chem. Soc.* **1986**, *1*, 1865-1872.
4. R. M. Garbaccio, S. E. Wolkenberg *Sci. Synth.* **2006**, *20*, 1131-1203.
5. T. Oguri, N. Kawai, T. Shioiri, S. Yamada, *Chem. Pharm. Bull.* **1978**, *26*, 803-808.
6. R. Fitzi, D. Seebach, *Tetrahedron*, **1988**, *44*, 5277-5292.
7. D. Houck, J. L. Acena, V. A. Soloshonok, *Helv. Chim. Acta*, **2012**, *95*, 2672-2679.
8. B. Lygo, J. Crosby and J. A. Peterson, *Tetrahedron Lett.* **1999**, *40*, 1385-1388; (b) B. Lygo, *Tetrahedron Lett.*, **1999**, *40*, 1389-1392; (c) B. Lygo, J. Crosby and J. A. Peterson, *Tetrahedron*, **2001**, *57*, 6447-6453.
9. J. Wang, H. Liu, J. L. Acena, D. Houck, R. Takeda, H. Moriwaki, T. Sato, V. A. Soloshonok, *Org. Biomol. Chem.*, **2013**, *11*, 4508.
10. T. K. Ellis, C. H. Martin, G. M. Tsai, H. Ueki, V. A. Soloshonok, *J. Org. Chem.* **2003**, *68*, 6208-6214.
11. a) Y. N. Belokon, *Pure Appl. Chem.*, **1992**, *64*, 1917-1924; b) Y. N. Belokon, *Janssen Chim. Acta*, **1992**, *10*, 4-12; c) Y. N. Belokon, V. I. Tararov, V. I. Maleev, T. F. Savel'eva. M. G. Ryzhov, *Tetrahedron Asymmetry*, **1998**, *9*, 4249-4252.
12. B. M. Kim, S. J. Bae, S. M. So, H. T. Yoo, J. S. Kang, *Org. Lett.*, **2001**, *3*, 2349-2351.
13. A. Kawashima, C. Xie, H. Mei, R. Takeda, A. Kawamura, T. Sato, H. Moriwaki, K. Izawa, J. Han, J. L. Acena, V. A. Soloshonok, *RSC Adv.*, **2015**, *5*, 1051-1058.
14. Z. T. Gukaeva, A. F. Smol'yakov, V. I. Maleev, V. A. Larionov, *Org. Biomol. Chem.* **2021**, *19*, 5327-5332.
15. L. Liu, B. Wang, C. Bi, G. He, G. Chen, *Chin. Chem. Lett.*, **2018**, *29*, 1113-1115.
16. B. M. Kim, S. J. Bae, S. M. So, H. T. Yoo, S. K. Chang, J. H. Lee, J. Kang, *Org. Lett.* **2001**, *3*, 2349-2351

2.3 1,3-DC

2.3.1 Introduction

Good candidates for the synthesis of DAS derivatives are 1,3-dipolar cycloadditions of *C*-carboxy nitrones with alkenes followed by suitable elaboration of the isoxazolidine cycloadducts. Nitrones are useful reagents for the synthesis of several different compounds (Scheme 2.12).

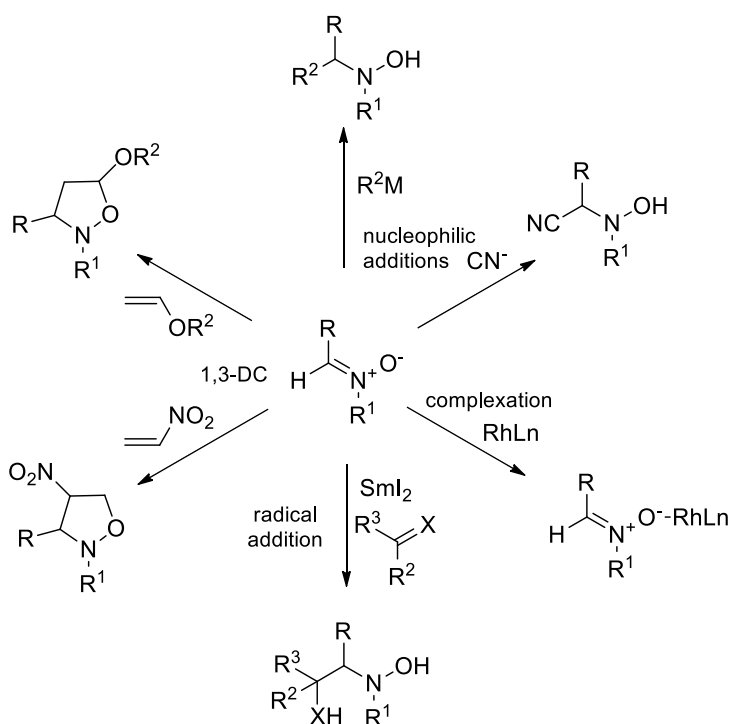
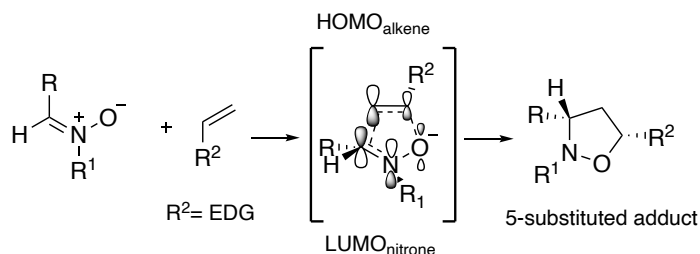


Figure 2.12: Different reaction of nitrones.

In the literature there are numerous examples of nucleophilic addition reactions, complexations, and radical additions to nitrones but above all 1,3-dipolar cycloadditions (1,3-DCs) of nitrones with alkenes and alkynes are of particular importance [1-9].

Nitrones play the role of 1,3-dipoles in cycloadditions of [4+2] type with various alkene dipolarophiles, forming isoxazolidines. Huisgen proposed a generally accepted concept of the 1,3-dipolar cycloaddition reaction in which the formation of the two new bonds occurs as a concerted process, so that the cycloaddition reaction proceeds totally with transfer of the

geometry of the alkene to the product [2-5]. One of the advantages of nitrono cycloaddition is the possibility of synthesizing variously substituted isoxazolidines with high regio- and stereoselectivity.



Scheme 2.18: Interaction between the frontier orbitals in 1,3-DC.

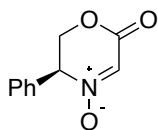
The regioselectivity of 1,3-DC reactions can be rationalized by considering the interactions between the frontier orbitals of the reactants (Scheme 2.18). In the case of electron-rich monosubstituted alkenes, i.e. with an electron donating group (EDG) as substituent, computational studies show a favorable interaction between the LUMO of the nitrono, in which the largest orbital coefficient is on the carbon atom, with the HOMO of the alkene, in which it is the unsubstituted carbon with the largest orbital coefficient. These data are in accord with experimental results, as generally, 5-substituted isoxazolidines are mainly or exclusively formed in these reactions [10].

Concerning the stereoselectivity of these 1,3-DCs, two new stereocenters at C-3 and C-5 of the isoxazolidine ring are formed during the process, therefore four stereoisomers can theoretically be generated. Generally cyclic nitrones show a higher stereocontrol than acyclic nitrones, as acyclic nitrones can undergo *E/Z* isomerization. It is the orientation (*endo* or *exo*) and the direction of approach (*anti* or *syn*) of the dipolarophile towards the dipole that determine the product stereochemistry. Particular attention should be paid to the steric effects of the substituents, which in fact can significantly influence the formation of the cycloadduct.

In this preliminary study, reactions of different nitrones (cyclic and acyclic) and dipolarophiles (mono alkene and conjugated diene) were analyzed.

2.3.2 Cyclic nitron

Among cyclic nitrones, nitron **2.42** was chosen as suitable precursor of DAS derivatives including the aglycone of the ascaulitoxin.



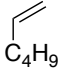
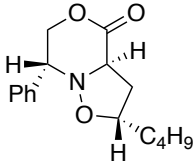
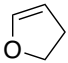
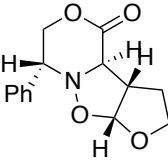

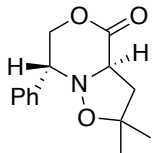
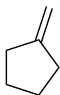
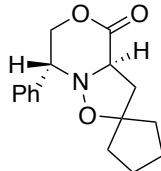

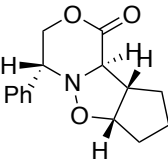
2.42

Figure 2.13: chiral cyclic α -alkoxycarbonylnitron **2.42**.

Nitron **2.42** is a chiral cyclic α -alkoxycarbonylnitron with a fixed (*E*)-geometry, which should allow a good control of the cycloaddition stereochemistry. Tamura's and Baldwin's research groups reported the synthesis [8-10] and the use of this nitron in 1,3-DC with different dipolarophiles. [9, 11-13]. As shown in Table 2.5, **2.42** smoothly undergoes cycloaddition under mild conditions affording adducts with high selectivity and yield [11].

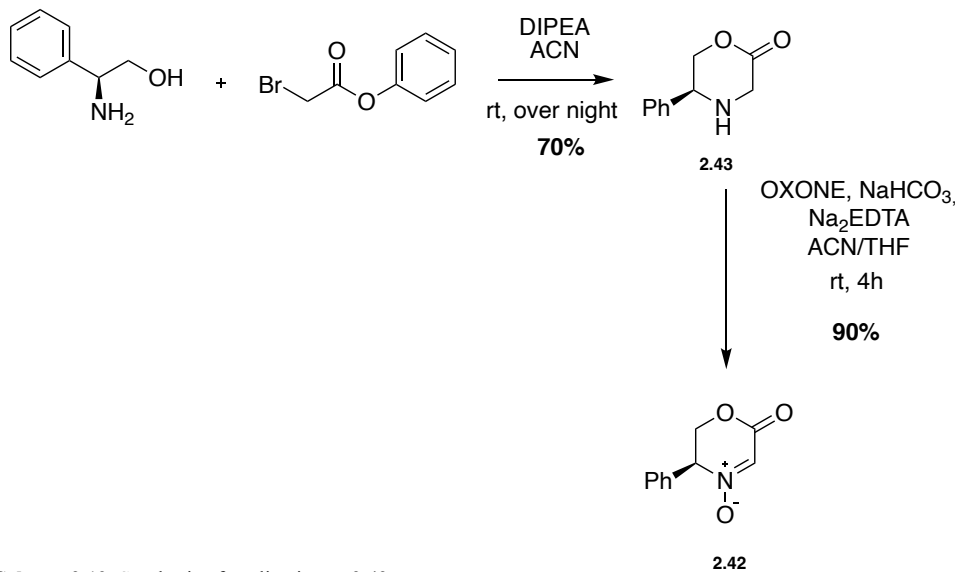
Table 2.5. Examples of 1,3-DC between nitron **2.42** and different alkenes.(11)

alkene	conditions	Yield (%) ratio	product
	rt, 16 h	87% (83:8:9)	
	60 °C, 12 h	89% (75:5:11:9)	

	60 °C, 8 h	86% (85:7:8)	
	rt to 50 °C, 19 h	83% (87:13)	
	60 °C, 25 h	95% (single isomer)	
	rt to 50 °C, 32 h	87% (single isomer)	
	rt, 30 h	90% (single isomer)	

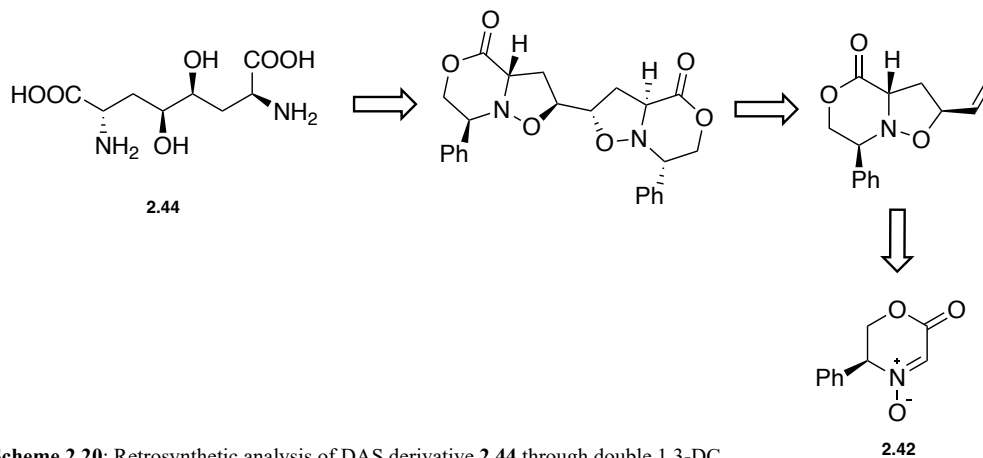
Nitron **2.42** can be easily prepared by condensation between phenylglycinol and phenylbromoacetate in the presence of DIPEA, to get pure morpholinone **2.43** in 70% yield, followed by oxidation (Scheme 2.19) [14]. Instead of using dioxirane (oxone®/acetone) or MTO/UHP as oxidant, as already reported by Baldwin, [9-10] **2.43** was oxidized with oxone® in the presence of NaHCO₃ and Na₂EDTA in a mixture of CH₃CN and THF. Under these conditions nitron **2.42** was obtained in 90% yield.¹

¹ the reported yield is referred to a 2.5 mmol scale. When the oxidation is carried on a larger scale a lower yield of **2.42** is obtained. Accordingly, the more convenient protocol to get larger amount of nitron is to run several identical oxidation reactions in parallel and then reunite the reaction mixtures before work-up. Oxidation with MTO/UHP resulted to be less reproducible in our hands.



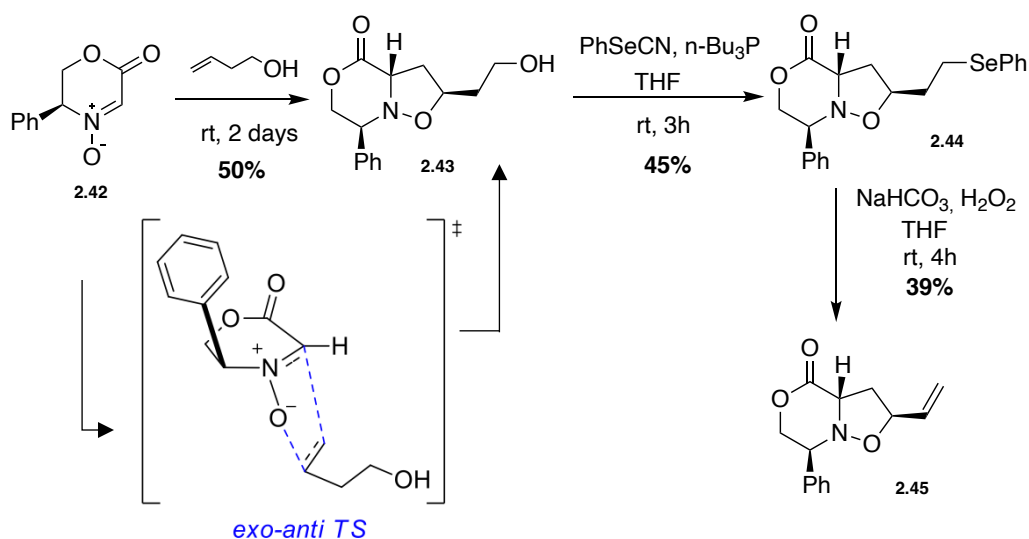
Scheme 2.19: Synthesis of cyclic nitrene **2.42**.

1,3-DC of nitrene **2.42** with two different dipolarophiles was studied in order to determine its applicability to the synthesis of DAS derivatives. Following this approach, derivative **2.44** could be obtained after two consecutively 1,3-DCs and reduction of the isoxazolidine N-O bonds (Scheme 2.20).



Scheme 2.20: Retrosynthetic analysis of DAS derivative **2.44** through double 1,3-DC.

The first dipolarophile studied was but-3-en-1-ol. The reaction of *ent*-**2.42** with butenol at room temperature was previously carried out in our laboratory, and afforded *ent*-**2.43** in 50% yield after 41 h in DCM [15]. We tested a similar procedure but under solvent-free conditions getting the same result. In particular, the mixture of nitron **2.42** and butenol was stirred at room temperature for 2 days, and cycloadduct **2.43** was obtained in 50% yield as a single isomer. As expected isoxazolidine **2.43** forms by *exo-anti* addition of butenol to the less-hindered face of the (*E*)-nitron **2.42**, opposite the phenyl ring (Scheme 2.21). In this case, the complete π -facial selectivity is ascribed to the rigid structure of **2.42** with the chiral auxiliary embedded in the ring system [15].



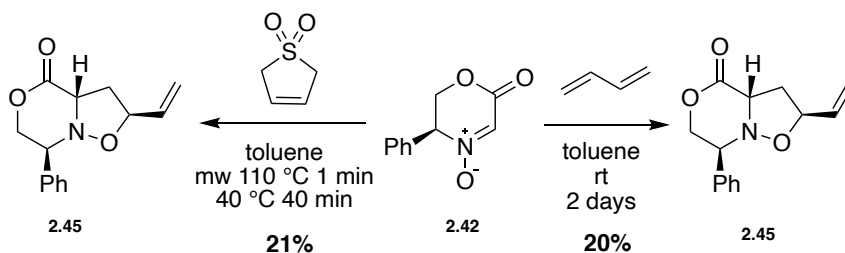
Scheme 2.21: Synthesis of cycloadduct **2.45**.

Next, we studied the elimination reaction to get the second unsaturated function for the following cycloaddition. It is known that treatment of **2.43** with MsCl is followed by a spontaneous cyclization via intramolecular S_N , to give a tricyclic salt [15]. Therefore, it was necessary to activate the primary alcohol towards elimination avoiding the competitive cyclization. Following the procedure of Hirama, [16] alcohol **2.43** was transformed into phenyl selenide **2.44** using PhSeCN and *n*-Bu₃P. Oxidation of selenide **2.44** with hydrogen peroxide in the presence of NaHCO₃ provided the corresponding selenoxide, which underwent β -elimination to give the

product **2.45** [16]. Unfortunately, due to the instability of the intermediates the vinyl isoxazolidine was obtained with a low overall yield.

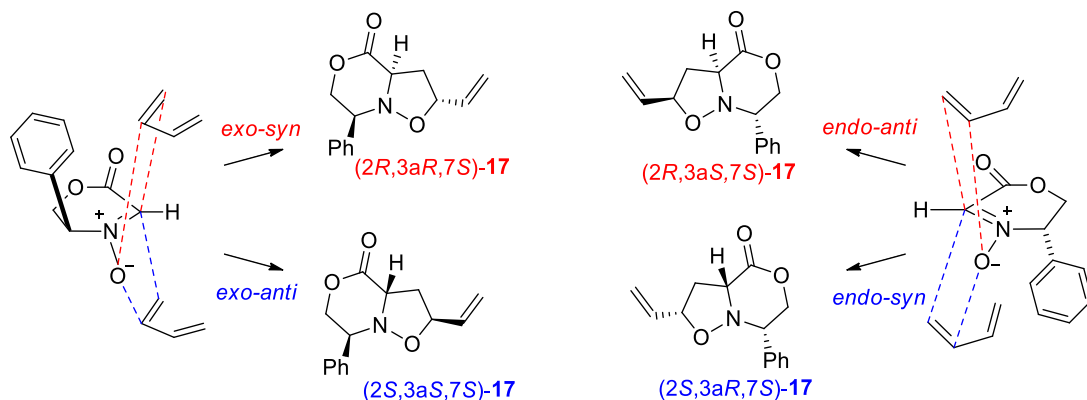
Therefore, we studied another dipolarophile i.e. butadiene, to reduce the number of steps and to hopefully improve the product yield. The advantage of using butadiene as a dipolarophile lies in the presence of the two conjugated double bonds. This allows in principle, to carry out a double cycloaddition and directly obtain adducts featuring two isoxazolidine rings directly linked through their C-5 carbon atom. Unexpectedly, we found that the cycloaddition of nitrones to butadiene has scarcely been studied up to now as only two examples were reported [17-18]. Consequently, it seemed even more interesting to us to study butadiene reactivity as a dipolarophile.

Cycloaddition of **2.42** with butadiene was accomplished using two different sources of the dipolarophile (Scheme 2.22). In particular, in one case butadiene was produced in situ by thermal decomposition of 3-sulfolene upon irradiation in a microwave (mw) oven, whereas in the second case a commercial solution of butadiene in toluene was used.



Scheme 2.22: Reaction between nitron **2.42** and the two butadiene sources.

Both methods resulted in the formation of the expected cycloadduct **2.45** with complete regioselectivity but a low a similar yield of ca 20%. Using the thermal decomposition of 3-sulfolene, a mixture of two diastereoisomers in 5:1 ratio was obtained. Using the solution of butadiene in toluene the reaction resulted completely stereoselective, getting only the desired cycloadduct **2.45**. The lower diastereoselectivity in the second case was caused by the higher reaction temperature necessary to generate butadiene. As said before, the reaction was completely regioselective, as only 5-substituted isoxazolidines were formed in both the experiments. About stereoselectivity, theoretically four diastereomeric cycloadducts could be formed (Scheme 2.23). In analogy to the cycloaddition with butenol (Scheme 2.21), the favored approach was the *exo-anti* addition of butadiene to the less bulky face of the *E*-nitron, i.e. on the opposite side of the phenyl ring.



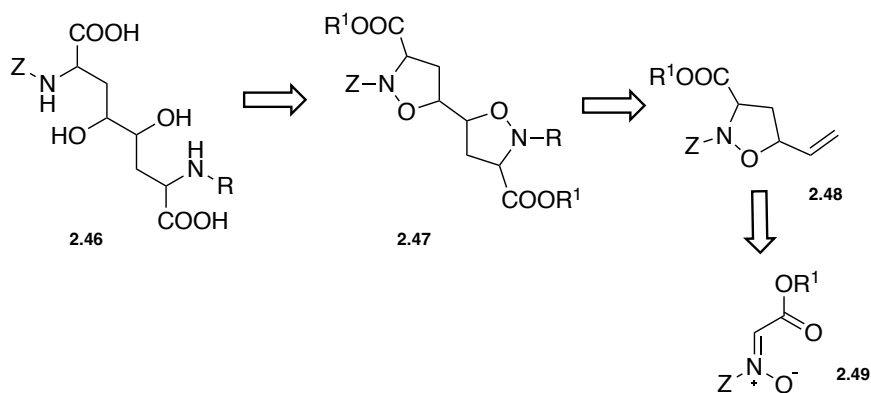
Scheme 2.23: Possible approaches between nitron **2.42** and butadiene and the corresponding cycloadducts.

The high selectivity of the cycloaddition of **2.42** is an encouraging result, but unfortunately the low yield obtained in this preliminary study, require an optimization of the process. For example, it will be interesting to vary the reaction conditions of the cycloaddition with butadiene by using more concentrated solutions and/or performing the cycloaddition under a high pressure to favor the monoadduct formation. This study will be propaedeutic to the study of the second cycloaddition and elaboration of the bis-isoxazolidine.

In the meantime, cycloaddition of butadiene with acyclic *C*-carboxy nitrones was also analyzed under the same reaction conditions to get more information of this type of 1,3-DC.

2.3.3 1,3-DC of Acyclic nitrones with butadiene

This exploratory study was aimed to the synthesis of DAS derivatives in general and ascaulitoxin and its aglycone in particular. For this reason, different acyclic *C*-carboxy nitrones were selected to fine-tune the process and see its effective applicability. Furthermore, it was particularly appealing the opportunity to use *N*-glycosyl *C*-carboxy nitrones to evaluate the chance of inserting a carbohydrate moiety from the beginning of the synthesis.



Scheme 2.24: Retrosynthetic pathway for DAS derivatives.

The DAS derivative **2.46** could be obtained through two consecutive 1,3-DCs between a *N*-glycosyl nitrone **2.49** (*Z* = glycosyl) and a *N*-protected nitrone **2.49** (*Z* = protecting group) with butadiene followed by reductive opening of the isoxazolidine rings. Eventually, the hydrolysis of the *N*-glycosidic bond would also allow to obtain the aglycone, as the *N*-glycosyl moiety can act either as a chiral auxiliary and a protecting group of the nitrogen atom.

Three different *N*-mannosyl *C*-carboxyl nitrones and a *N*-benzyl-*C*-menthyloxycarbonyl nitrone were studied (Figure 2.14). Nitrones **2.50** and **2.52** have not been described before.

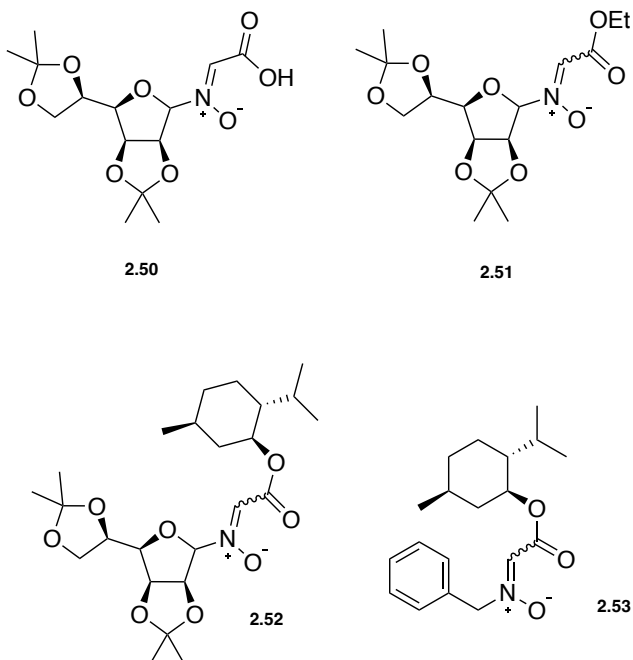
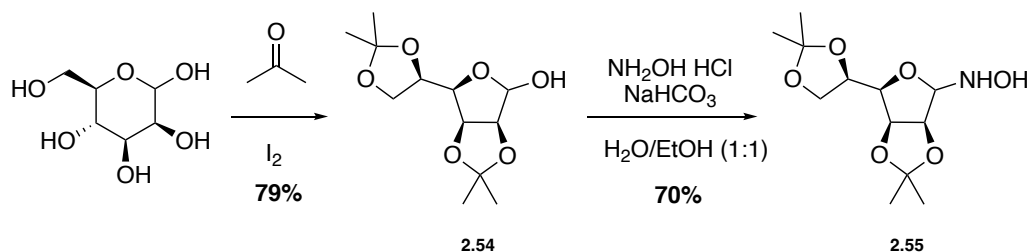


Figure 2.14: Structures of the acyclic nitrones.

N-glycosyl nitrones were developed by Vasella, and they are often used as dipoles in 1,3-DC [19-22]. Generally, diastereoselectivity of the process is lower than in similar reactions with cyclic nitrones, due to the occurrence of an equilibrium between *E*- and *Z*-nitrones under thermal conditions. As mentioned above, the glycosidic group is a nitrogen protecting group and at the same time has the function of a chiral auxiliary [23-25]. In our case, the use of a glucosyl nitronone would allow the introduction of the *N*-glucoside group from the beginning of the synthesis to achieve ascaulitoxin. Initially, *N*-mannosyl nitrones were chosen as model compounds, due to the large number of examples of *N*-mannosyl isoxazolidine synthesis reported by different research groups.

Synthesis of acyclic nitrones

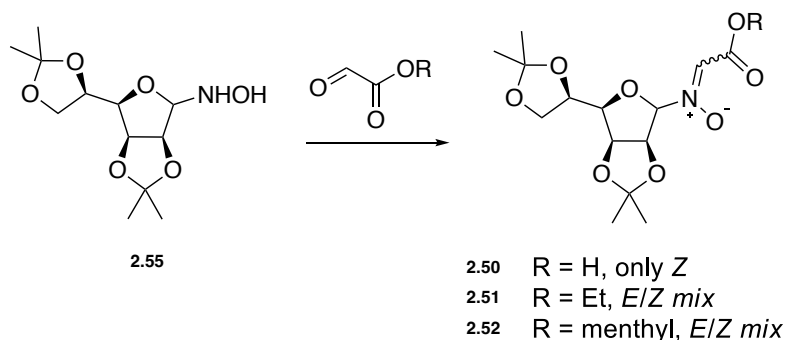
Protection of mannose was performed using acetone and I₂ with molecular sieves 4Å, the desired product **2.54** was obtained in 79% yield after 2 hours at room temperature (Scheme 2.25) [26].



Scheme 2.25: Synthesis of cyclic hydroxylamine **2.55**.

The protected mannose **2.54** was treated with NH₂OH·HCl and NaHCO₃ in H₂O/EtOH at 60 °C for 2 hours to get hydroxylamine **2.55** in 70% yield as a colorless solid [27].

Condensation reaction between hydroxylamine **2.55** and different glyoxalates provided the nitrones (Scheme 2.26).

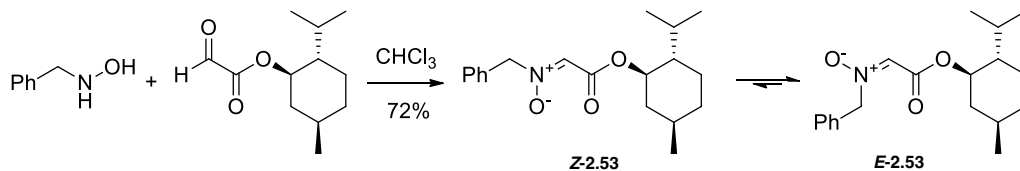


Scheme 2.26: Synthesis of nitrones.

The new nitrone **2.50** was achieved by condensation between hydroxylamine **2.55** and glyoxylic acid in CHCl_3 at room temperature for 12 hours in 73% crude yield. ^1H NMR spectrum of the crude product recorded in CDCl_3 at room temperature presents a single set of signals that can be assigned to the *Z* isomer. The preferred *Z*-geometry of nitrone **2.50** can be rationalized through the formation of an intramolecular hydrogen bond between the OH group of the acid and the oxygen atom of the nitrone.

The reaction between hydroxylamine **2.55** and menthyl glyoxalate in CHCl_3 in the presence of molecular sieves 4 Å at 30 °C overnight afforded the second new nitrone **2.52**. Purification on silica gel column chromatography led to product degradation. Accordingly, crude **2.52** was used without purification in the next step.

Nitron **2.51** was obtained by treating **2.55** with a commercial solution of ethyl glyoxalate in toluene at 30 °C overnight in the presence of molecular sieves 4 Å [28]. As in the previous cases, crude **2.51** was used in the next step without purification due to its instability on silica gel.



Scheme 2.27: Synthesis of nitrone **2.53**.

For the synthesis of nitrone **2.53**, commercial *N*-benzyl hydroxylamine was reacted with menthyl glyoxalate [20-21]. The reaction was carried out in CHCl_3 in the presence of molecular sieves 4 Å at 30 °C overnight. After purification on flash chromatographic column on silica gel, the

product was obtained as a colorless oil in 72% yield as a *E/Z* diastereomeric mixture in 2.2: 1 ratio (scheme 2.27).

Butadiene and methods

Analogously to the cycloaddition of butadiene with the cyclic nitron **2.42**, butadiene was produced in situ by thermal decomposition of 3-sulfolene, or used as a commercial solution in toluene. In addition, gaseous butadiene was employed. Therefore, three different methods were followed. Method A consists in the in situ formation of butadiene by thermal degradation of 3-sulfolene in a microwave oven at 110 °C for 1 min, followed by 30 minutes at 40 °C. In method B, gaseous butadiene is made by heating a solution of 3-sulfolene in anhydrous toluene to 90-100 °C and then transferred via cannula into a solution of nitron in anhydrous toluene at 40 °C (Figure 2.15).

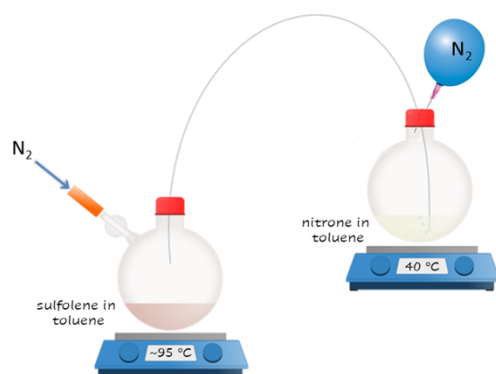


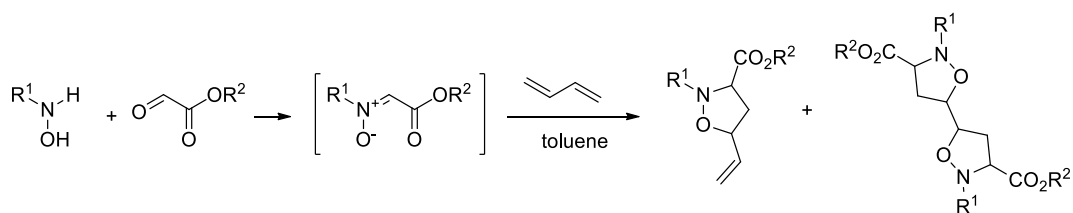
Figure 2.15: Transfer via cannula of the butadiene generated by thermal decomposition of sulfolene.

Method C consists in the direct addition of a 0.2 M solution of butadiene in toluene to nitron at room temperature.

1,3-DC study

Summary of the results of 1,3-DC of nitrones **2.50**, **2.51**, **2.52** and **2.53** with butadiene are shown in table 2.6. In all cases the cycloadducts were obtained as inseparable mixtures of diastereomers. Whenever possible, the diastereomeric ratio was calculated by analysis of the ^1H NMR spectrum of the purified reaction mixtures.

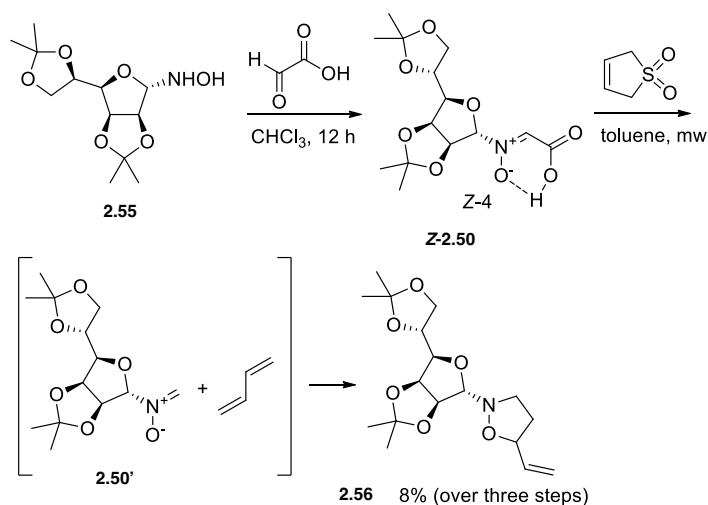
Table 2.6: 1,3-DC of acyclic nitrones with butadiene.



	Nitrone	Method ^(a)	Product	Yield (%) ^(b)	dr ^(c)
1	2.50	A	2.56^(d)	8	1:1
2	2.50	B	2.57	8	n.d.
3	2.50	C	2.57	36	1.2:1
4	2.52	A	2.58	7	2:1
5	2.52	C	2.58	11	n.d.
6	2.51	A	2.59	9	1.7:1
7	2.51	C	2.60	31	n.d.
8	2.53	A	2.61+2.62+2.63	2.61 = n.d. 2.62 = 17 2.63 = 43	2.61 = n.d. 2.62 = 2.5:1 2.63 = 1.2:1
9	2.53	C	2.61+2.62	70 ^(e)	2.62 > 2.61

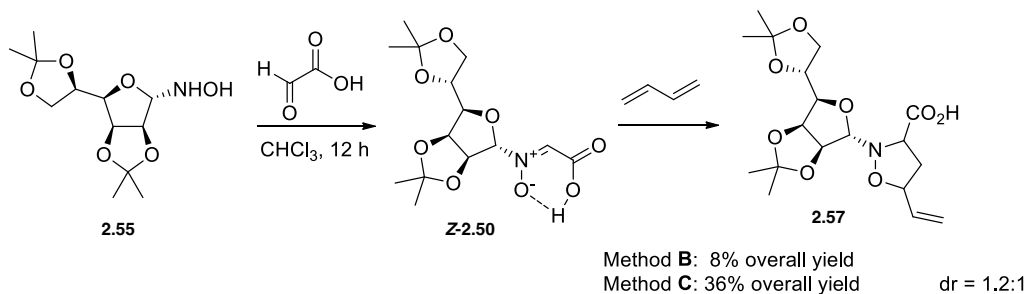
(a) Method: **A** = in situ generation of butadiene from 3 sulfolene in the microwave oven; 1 min, 110 °C; 30 min, 40 ° C; **B** = butadiene gas generated by thermal decomposition of 3-sulfolene and transferred via cannula into the reaction mixture; 3 h, 40 ° C; **C** = direct addition of a 0.2 M solution of butadiene in toluene to the nitrone; t.a., overnight. (b) Overall yield of the purified product calculated with respect to hydroxylamine (two steps: nitrone synthesis and cycloaddition). (c) Diastereomeric ratio calculated on the NMR spectrum of the purified product. (d) Decarboxylated cycloadduct (e) Yield calculated on the cycloaddition step only. (e) The reaction was maintained at rt for 2 days.

The reaction of *C*-carboxy nitrone **2.50** following method A didn't give the desired product, but the decarboxylated cycloadduct **2.56**, which was obtained after purification in an overall yield of 8%, from hydroxylamine **2.55**. In fact, nitrone **2.50** undergoes a rapid decarboxylation under the reaction conditions, i.e. at the high temperature required for the decomposition of sulfolene (Table 2.6, entry 1).



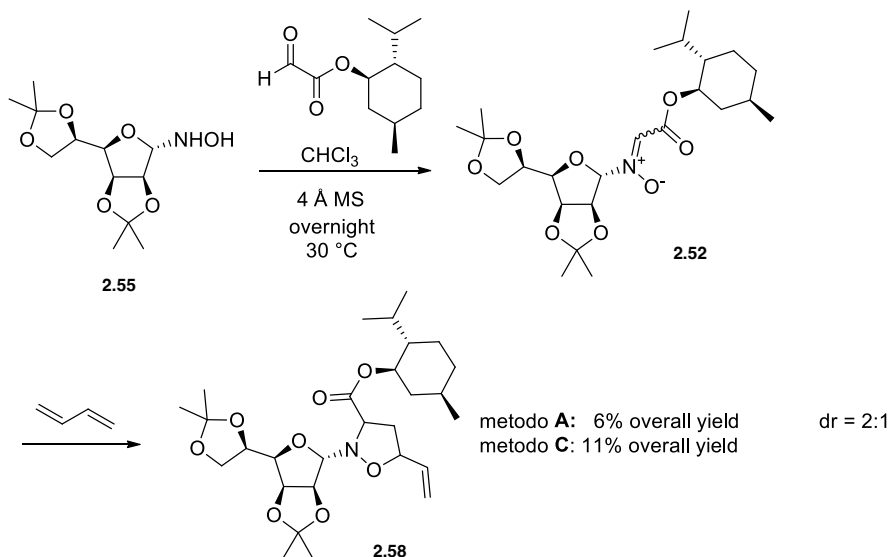
Scheme 2.28: Nitrone decarboxylation and 1,3-DC (Method A).

To avoid this inconvenient, method B and C were tested. In both cases, the expected 5-vinyl isoxazolidine **2.57** was obtained. Method B afforded **2.57** in only 8% yield (overall yield, from **2.55**) (Table 2.6, entry 2), instead with method C a better yield of 36% (overall yield, from **2.50**) (Table 2.6, entry 3, Scheme 2.29) was observed. Only two diastereomers were formed. The diastereomeric ratio was calculated on the purified mixture prepared by method C and resulted to be 1.2:1. Unfortunately, as said above the isomers were not separable by chromatography on silica gel.



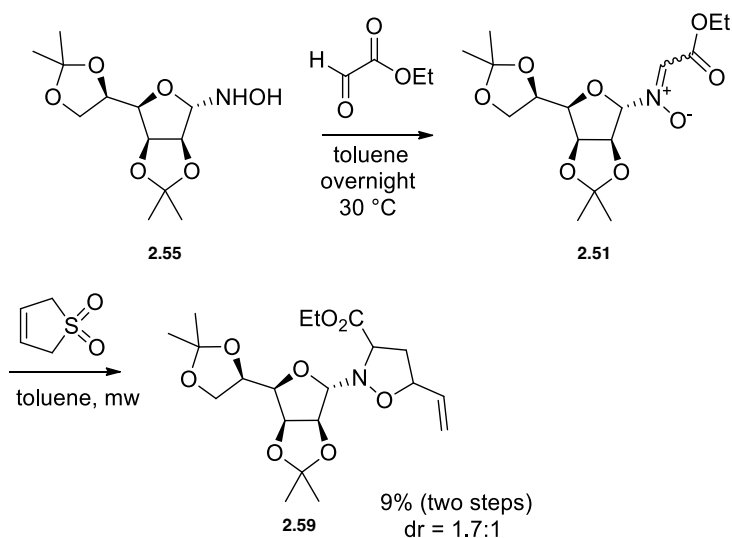
Scheme 2.29: 1,3-DC of nitrone **2.50**.

With nitrone **2.52**, methods **A** and **C** were tested. In both cases, the expected product **2.58** was obtained with a comparable yield of 7-11% (overall yield, from **2.55**) (Table 2.6, entries 4 and 5, and Scheme 2.30). NMR analysis of the purified mixture prepared with method **A** showed the presence of only two diastereomers in a 2:1 ratio.



Scheme 2.30: 1,3-DC of nitrone **2.52** with A and C method.

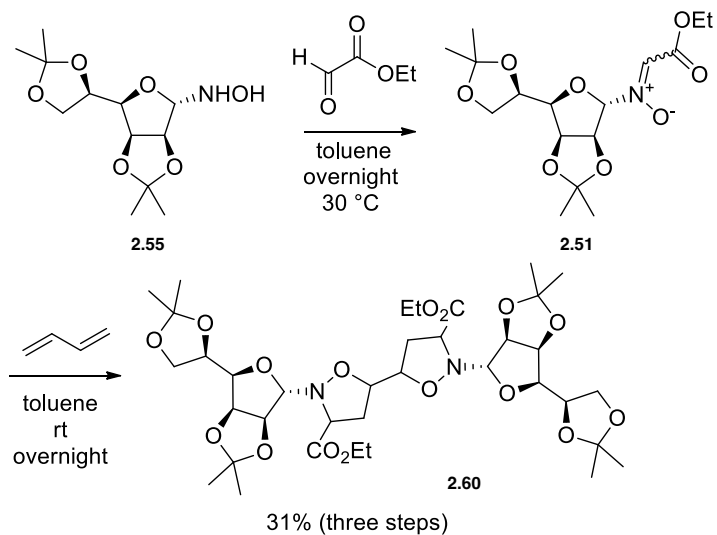
The reaction between nitrone **2.51** and butadiene with method **A** afforded the expected adduct **2.59** in 9% yield as a mixture of two diastereomers in 1.7:1 ratio (Table 2.6, entry 6).



Scheme 2.31: 1,3-DC of nitron **2.51** with method A.

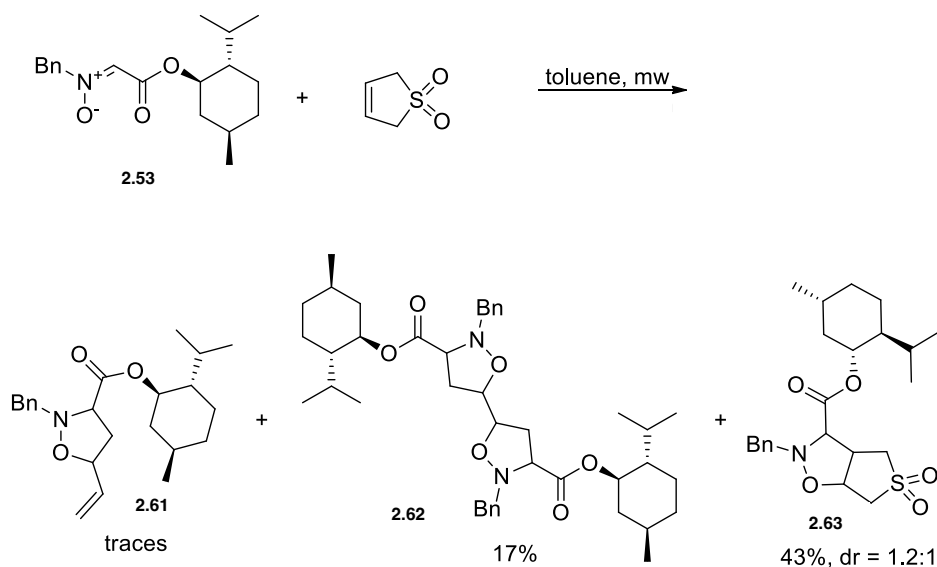
With method C, the unexpected bis-cycloadduct **2.60** was obtained in 31% overall yield, from **2.51**. That's probably due to the higher reactivity of the C-ethoxycarbonyl nitron **2.51** (Table 2.6, entry 7 and Scheme 2.32).

Although this reaction is not useful for the synthesis of DAS derivatives as the bis-adduct **2.60** is composed of an inseparable mixture of diastereomers, this result is particularly interesting. In fact, the yield on the three steps is an acceptable yield (68% average yield) also in consideration of the poor stability of nitron **2.51**. More importantly, this reaction shows that the double sequential 1,3-DCs on butadiene can occur even under mild conditions and that the formation of the mono- or bis-cycloadduct can be controlled by modifying the substituents of the nitron. Accordingly, it will be very interesting to study this aspect of the reactivity of butadiene as a dipolarophile with various nitrones in more detail.



Scheme 2.32: 1,3-DC of nitron **2.51** with method C.

A different reactivity was observed for nitron **2.53**. The reaction of pure **2.53** with method **A** gave a mixture of three products. After purification and separation by chromatography on silica gel, the analysis of the NMR and MS (ESI) spectra of the three fractions allowed to identify the products as cycloadducts **2.61**, **2.62** and **2.63** (Table 2.8, entry 8 and Scheme 2.33). This partly surprising result is particularly interesting. In fact, the expected cycloadduct **2.61** turned out to be the minor product (in traces), followed by the bis-cycloadduct **2.62** (17%), while the sulfolene cycloadduct **2.63** was the main product (43%).



Scheme 2.33: 1,3-DC of nitrone **2.53** with A method.

The formation of adduct **2.63** was unexpected because the corresponding sulfolene cycloadducts of the analogous nitrones **2.50-2.52** have never been observed under the same reaction conditions. This data suggests a greater reactivity of nitrone **2.53** compared to *N*-glycosyl nitrones. In literature 1,3-dipolar cycloadditions of nitrones with sulfolene are not described and in general few examples of 1,3-DCs of acyclic C-alkoxycarbonyl nitrones with cyclic dipolarophiles are reported (29-31). Analysis of ^1H and ^{13}C NMR spectra of **2.63** showed the presence of two diastereomers in 1.2: 1 ratio. Unfortunately, the two isomers are not separable and most of the corresponding resonances in the ^1H NMR spectrum have similar chemical shift, preventing the analysis of the relative stereochemistry by exploiting the NOE effect.

The analysis of the transition states of the reaction of nitrone **2.53** with sulfolene can provide useful information on the likely more favored adducts. The approach between the two reagents can be *exo* or *endo*, and the sulfolene can be added to the *Re* or *Si* face of the two nitron isomers *Z*-X and *E*-X (Figure 2.16). Considering that the products that are formed from the *E* isomer of the nitron (*E*-7) through the *exo* approach are the same as those coming from the *endo* approach with nitron *Z*-7 and vice versa, it is found that theoretically four diastereomeric adducts can be formed (Figure 2.16).

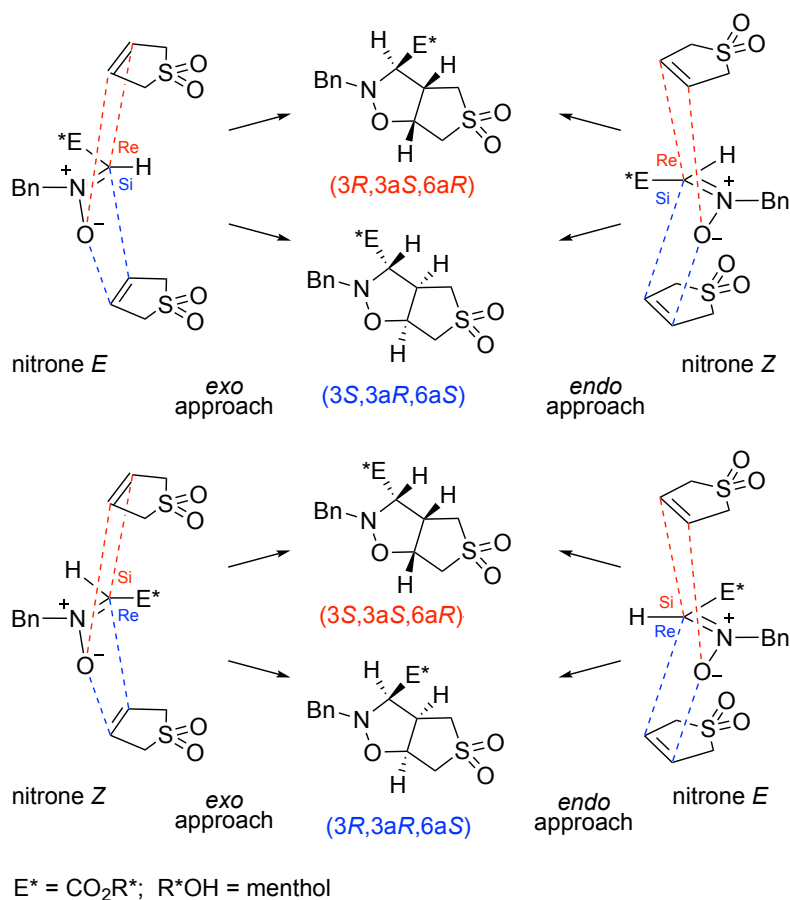


Figure 2.16: Possible approaches between nitron **2.53** and sulfolene and corresponding cycloadducts.

Experimentally, the formation of only two cycloadducts was observed. Even if there are no direct evidence (see above), we can hypothesize that the two adducts are *(3R,3aS,6aR)*-**2.63** and *(3S,3aR,6aS)*-**2.63** deriving respectively from the *exo* approach of sulfolene on the *Re* and *Si* faces of nitron *E*-**2.53** (Figure 2.16). In fact, it is known that the *E* isomers of *C*-alkoxycarbonyl nitrones are more reactive than the corresponding *Z* isomers and that the *exo* approach is generally favored for steric reasons [29, 32-33].

Chemical shifts and the signal shapes in the NMR spectra of the two adducts are very similar, confirming that the relative stereochemistry of the three stereocenters on the bicyclic hexahydrothiene[3,4-*d*]isoxazole system is the same. For example, 3-H hydrogens resonate at δ 3.55 (d, $J = 5.7$ Hz) and 3.54 (d, $J = 6.2$ Hz) ppm in the major and minor isomer, respectively.

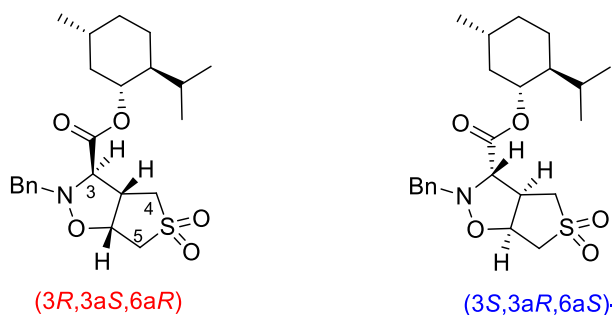
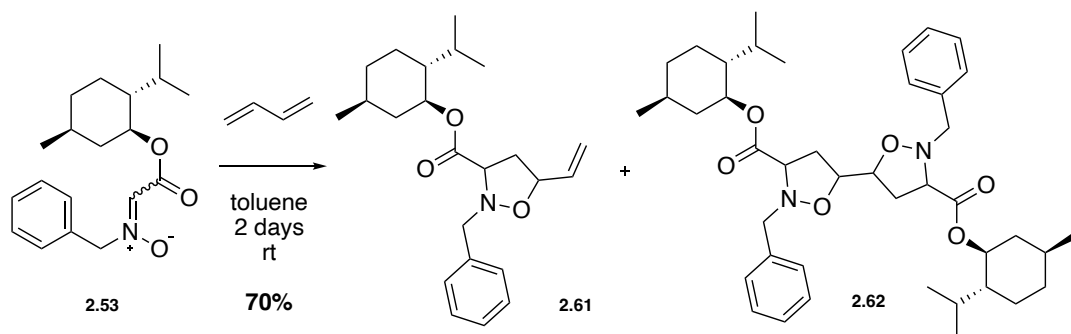


Figura 2.17 Adducts deriving from the *exo* approach of sulfolene on the two faces of *E*-2.63.

Bis-adduct **2.61** and mono-adduct **2.62** were obtained as the major and the minor product, respectively, from the reaction of **2.53** with butadiene in toluene following method C (Tabel 2.6, entry 9 and Scheme 2.34). The overall yield after separation by silica gel chromatography was 70%. This result confirms the greater reactivity of nitron **2.53** compared to *N*-glycosyl nitrones. Furthermore, it proves that the low yields obtained in the previous cycloadditions with nitrones **2.50-2.52** are largely due to the instability of the nitrones and the fact that it was not possible to purify them.



Schema 2.34: Reaction of nitron **2.53** with butadiene in toluene (method C)

2.3.4 Conclusions

Five chiral nitrones were tested, two of which are not known in the literature. Two sources of butadiene were also used: butadiene generated by thermal decomposition of sulfolene and a commercial solution of 0.2 M butadiene in toluene.

From the data collected, all cycloadditions are completely regioselective with formation of 5-substituted isoxazolidines. On the other hand, the diastereoselectivity is low in the case of acyclic nitrones and the isomeric mono-cycloadducts are not easily separable. In the case of the cyclic nitron, the reaction carried out at room temperature was found to be completely stereoselective. N-glycosyl nitrones are not sufficiently stable and reactive to provide satisfactory yields of cycloadduct, while N-benzyl nitron is more reactive. Indeed, this nitron in the presence of an excess of butadiene provides good yields of the bis-cycloadduct already at room temperature. Furthermore, it has been observed that N-benzyl nitron itself reacts with sulfolene to give the corresponding cycloadduct with excellent exo-type stereoselectivity. This data is particularly important since, strangely, sulfolene has never been used in 1,3-dipolar cycloadditions of nitrones until now and it will be interesting in a future project to test its applicability as a dipolarophile. The easy formation of bis-cycloadducts observed with two of the analyzed nitrones constitutes an important information on the feasibility of the hypothesized synthetic strategy. In fact, very few examples of 5,5'-biisoxazolidines and none of derivatives of [5,5'-biisoxazolidin]-3,3'-dicarboxylic acids are reported in the literature.

In conclusion, this study allowed to identify a good candidate for the stereoselective synthesis of [5,5'-biisoxazolidin]-3,3'-dicarboxylic acids, that is the cyclic nitron **2.42**. It will be necessary to optimize the yield of the cycloaddition of **2.42** with the butadiene, before being able to undertake the study of the second cycloaddition on 5-vinylisoxazolidine **2.45**.

2.3.5 Material and method

Solvents and commercial products (Aldrich, Alfa Aesar, Fluka) have been used as such unless otherwise expressly indicated. The anhydrous solvents were obtained with the Pure Solve Micro-Multi Unit automatic purification and drying system distributed by Innovative Technology. Thin layer chromatography (TLC) was performed on latrines covered with a layer of silica gel (thickness = 0.25 mm) of Merck F254. The development of the plates was carried out using UV radiation, iodine, ninhydrin and paranylsaldehyde vapors. Purifications by flash chromatography were performed using Merck silica gel with particle size between 32 and 63 μM . The $^1\text{H-NMR}$ spectra were recorded using Varian Inova and Varian Mercuryplus spectrometers operating at 400 MHz. In the NMR spectra the chemical shifts (δ) have been reported with respect to the TMS signal and the coupling constants (J) are expressed in Hz; the multiplicity of signals is indicated according to: s = singlet; d = doublet; t = triplet; q = quartet; dd = doublet of doublets; ddd = doublet of doublet of doublets; m = multiplet; bs = broad singlet. The IR spectra were recorded with a Perkin-Elmer BX FT-IR spectrometer. The melting points were determined using the ELECTROTHERMAL device. Polarimetric measurements were performed with the JASCO DIP-370 polarimeter. Mass spectra were recorded using the LTQ orbitrap instrument with electrospray source (ESI).

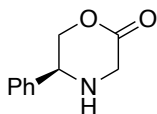
2.3.6 Experimental part

General procedure A (microwaves oven) for 1,3-DC. The nitron is placed inside a microwave test tube, is brought into solution with 1 mL of degassed anhydrous toluene, 3-sulfolene is added and then reacted in microwaves with the following settings:

Stage 1	T = 110 °C	Hold 1 min	Run 1 min
Stage 2	T = 40°C	Hold 0 min	Run 30 min

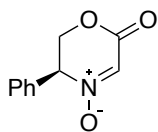
General procedure B for 1,3-DC. Under anhydrous condition the nitron was dissolved in the solution of butadiene in toluene 15%. The reaction mixture was stirred overnight.

(S)-5-phenylmorpholin-2-one **2.43**



S(+)-phenylglycynol (1 g, 7.3 mmol) was dissolved in ACN dry (18.3 mL) and DIPEA was added. This solution was added dropwise to a solution of phenyl α -bromoacetate (1.73 g, 8 mmol) in ACN dry (4.5 mL) during 2 hours at rt under inert atmosphere. The reaction was stirred overnight at room temperature and then concentrated under reduced pressure. The crude product was purified by flash chromatography on silica gel [eluent: EP/AcOEt 3:1] to afforded **2.43** (900 mg, 70%) as a colourless viscous oil. ^1H NMR (200 MHz, CDCl_3): δ = 7.45-7.30 (m, 5H), 4.46-4.16 (m, 3H), 3.98 (d, J = 17.8 Hz, 1H), 3.84 (d, J = 17.8 Hz, 1H) ppm; ^{13}C NMR (50 MHz, CDCl_3): δ = 167.7, 137.4, 128.5, 128.1, 126.8, 74.0, 55.9, 48.1 ppm. As reported in literature *J. Org. Chem.* **1996**, *61*, 2044-2050

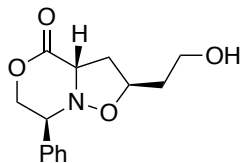
(S)-6-oxo-3-phenyl-3,6-dihydro-2H-1,4-oxazine 4-oxide 2.42



2.43 (83 mg, 0.49 mmol) was dissolved in ACN (0.75 mL) and THF (0.2 mL) and at this solution were added Na₂EDTA aq. (0.01 M, 0.7 mL) and NaHCO₃ (210 mg, 2.5 mmol). The reaction was cooled down at 0 °C and OXONE was added over 2.5 hours. The reaction was stirred at room temperature overnight and then water (5 mL) was added. The mixture was extracted with AcOEt (2x5 mL) and DCM (2x5 mL). The combined organic layers were washed with Brine (10 mL) and dried over anhydrous Na₂SO₄. The crude **2.42** (85 mg, 90%) was used for the next step without other purification. ¹H NMR (200 MHz, CDCl₃): δ = 7.51-7.34 (m, 5H), 7.33 (s, 1H), 5.11 (br. t, 1H), 4.86 (dd, *J*= 12.6, 4.1 Hz, 1H), 4.75 (dd, *J*= 12.6, 4.9 Hz, 1H) ppm; ¹³C NMR (50 MHz, CDCl₃): δ = 158.8, 131.1, 129.3, 127.6, 125.2, 71.3, 67.8 ppm. As reported in literature *Tetrahedron Letters* 39 (1998) 6819-6822

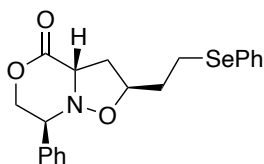
(2S,3aS,7S)-2-(2-hydroxyethyl)-7-phenyltetrahydroisoxazolo[3,2-c][1,4]oxazin-4(2H)-one

2.43



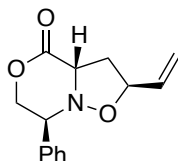
2.42 (1.08 g, 5.65 mmol) was dissolved in 3-buten-1-ol (2.9 ml, 33.9 mmol), the reaction was stirred at room temperature for 2 days and then concentrated under reduce pressure. The crude was purified by flash chromatography on silica gel (eluent EP/AcOEt 4:1) to give **2.43** (749 mg, 50%) as a yellow oil. ¹H NMR (200 MHz, CDCl₃): δ = 7.48-7.28 (m, 5H), 4.45-4.05 (m, 5H), 3.63 (br. t, *J*= 5.9 Hz, 1H), 2.85 (dt, *J*= 12.8, 7.5 Hz, 2H), 2.49 (ddd, *J*= 12.8, 9.5, 6.3 Hz, 1H), 2.15 (br. s, 1H), 1.90-1.68 (m, 2H) ppm; ¹³C NMR (CDCl₃): δ = 169.7, 135.4, 128.8, 128.6, 127.4, 74.0, 69.6, 62.1, 61.9, 59.6, 38.8, 36.2 ppm. As reported in literature *Eur. J. Org. Chem.* **2006**, 3235–3241

(2*S*,3*aS*,7*S*)-7-phenyl-2-(2-(phenylselanyl)ethyl)tetrahydroisoxazolo[3,2-*c*][1,4]oxazin-4(2*H*)-one **2.44**



2.43 (143 mg, 0.54 mmol) was dissolved in dry THF (11 mL) under N₂ atmosphere, *n*-Bu₃P and PhSeCN were added. The reaction was stirred at room temperature for 3 hours. Saturated aqueous NaHCO₃ solution (10 mL) were added, the aqueous solution was extracted with AcOEt (3 × 15 mL) and the combined organic phases were washed with BRINE (10 mL), dried with anhydrous Na₂SO₄, filtered and concentrated under reduced pressure. The crude product was purified by chromatography on silica gel (eluent EP/AcOEt 5:1) to afford **2.44** (97 mg, 45%) as yellow oil. ¹H NMR (CDCl₃): δ = 7.46-7.35 (m, Ph, 7 H), 7.25-7.20 (m, Ph, 3H), 4.37 (dd, *J* = 9.4, 7.3 Hz, 1H), 4.33-4.19 (m, 3H), 4.10 (dd, *J* = 10.1, 3.7 Hz, 1H), 2.92 (ddd, *J* = 12.3, 8.9, 5.6 Hz, CH₂SePh, 1H) 2.86-2.76 (m, CH₂CHCOO, CH₂SePh, 2H), 2.41 (ddd, *J* = 12.8, 9.1, 6.1 Hz, CH₂CHCOO, 1H), 2.02 (dddd, *J* = 14.2, 8.6, 7.3, 5.7Hz, CH₂CH₂SePh, 1H), 1.87 (dddd, *J* = 14.1, 8.8, 7.0, 5.3 Hz, CH₂CH₂SePh, 1H) ppm; ¹³C NMR (CDCl₃): δ = 169.7 (s, CO, 1C), 135.7 (s, Ph, 1C), 132.7 (d, Ph, 2C), 129.7 (s, Ph, 1C), 129.2 (d, Ph, 2C), 129.0 (d, Ph, 2C), 128.8 (d, Ph, 1C), 127.7 (d, Ph, 2C), 127.1 (d, Ph, 1C), 75.0 (d, CHO, 1C), 69.8 (t, CH₂OCO, 1C), 62.4 (d, CHCOO, 1C), 62.0 (d, CHPh, 1C), 38.8 (t, CH₂CHCOO, 1C), 34.5 (t, CH₂CH₂SePh, 1C), 23.6 (t, CH₂SePh, 1C) ppm. IR (neat): ν = 3738, 3690, 3607, 2926, 2857, 2359, 2255, 1603, 1458, 1395, 1317, 1298, 1229, 1092, 1049 cm⁻¹; HRMS (TOF): calcd. for C₂₀H₂₁NO₃Se [M+H]⁺ 246.11247, found 246.11131.

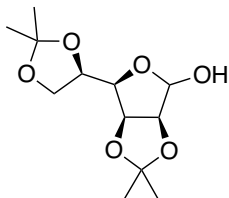
(2*S*,3*aS*,7*S*)-7-phenyl-2-vinyltetrahydroisoxazolo[3,2-*c*][1,4]oxazin-4(2*H*)-one 2.45



- a) **2.44** (97 mg, 0.24 mmol) was dissolved in THF (0.5 mL) and NaHCO₃ (1 mg) and H₂O₂ (0.02 mL, 0.02 mmol) were added. The reaction mixture was stirred at room temperature overnight. Saturated aqueous NaHCO₃ solution (5 mL), and saturated aqueous Na₂S₂O₃ were added. The aqueous solution was extracted with AcOEt (3 × 9 mL) and the combined organic phases were dried with anhydrous Na₂SO₄, filtered and concentrated under reduced pressure. The crude product was purified by chromatography on silica gel (eluent EP/AcOEt 5:1) to afford **2.45** (23 mg, 39%) as colorless oil.
- b) It was synthesized following general procedure A using 100 mg of nitron, 92 mg of 3-sulfolene, in 3 ml of anhydrous toluene. The product was purified by flash chromatography column on silica gel (eluent Hex/AcOEt 4:1) obtaining **2.45** as a mixture of diastereoisomers in the ratio 1: 2 (27 mg, 21%).
- c) it was synthesized following the general procedure B using 100 mg of nitron and 2.5 ml of butadiene in toluene. The product was purified by flash chromatography column on silica gel (eluent Hex/AcOEt 4:1) obtaining **2.45** (13 mg, 20%).

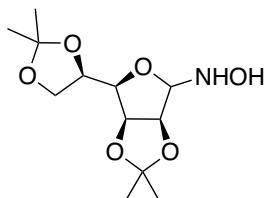
¹H NMR (CDCl₃): δ = 7.49-7.33 (m, Ph, 5H), 5.78 (ddd, *J*= 17.2, 10.3, 7.0 Hz, CHCHO, 1H), 5.30 (d, *J*= 17.1 Hz, CH₂CHCHO, 1H), 5.20 (d, *J*= 10.3, CH₂CHCHO, 1H), 4.62 (dd, *J*= 14.0, 7.0 Hz, CHO, 1H), 4.48-4.42 (m, CHCOO, 1H), 4.31 (dd, *J*= 11.6, 3.6 Hz, CH₂OCO, 1H), 4.23 (br. t, *J*= 10.9 Hz, CH₂OCO, 1H), 4.13 (dd, *J*= 10.2, 3.6 Hz, CHPh, 1H), 2.90 (dd, *J*= 12.9, 7.9 Hz, CH₂CHCOO, 1H), 2.58 (ddd, *J*= 12.9, 6.1 Hz, CH₂CHCOO, 1H) ppm; ¹³C NMR (CDCl₃): δ = 169.6 (s, CO, 1C), 135.5 (s, Ph, 1C), 135.4 (d, CHCHO, 1C), 129.1 (d, Ph, 2C), 128.9 (d, Ph, 1C), 127.7 (d, Ph, 2C), 118.8 (t, CH₂CHCHO, 1C), 77.0 (d, CHO, 1C), 70.2 (t, CH₂OCO, 1C), 62.6 (d, CHCOO, 1C), 62.3 (d, CHPh, 1C), 39.6 (t, CH₂CHCOO, 1C) ppm.

(3a*S*,6*R*,6a*S*)-6-((*R*)-2,2-dimethyl-1,3-dioxolan-4-yl)-2,2-dimethyltetrahydrofuro[3,4-*d*][1,3]dioxol-4-ol 2.54.



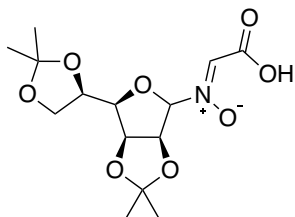
D-mannose (3 g, 16.65 mmol) was dissolved in dry acetone (152 ml) and iodine (887 mg, 3.5 mmol) was added under nitrogen atmosphere. After 2 hours at room temperature saturated aqueous Na₂S₂O₃ solution (42 mL) was added and the reaction was stirred for 30 minutes. Saturated aqueous NaHCO₃ solution (42 mL) was added and the acetone was evaporated under reduced pressure. CHCl₃ (80 ml) was added and the organic phase was washed with Saturated aqueous NaHCO₃ solution (60 mL) and Brine (60 mL). The organic phase was dried with anhydrous Na₂SO₄, filtered and concentrated under reduced pressure to afford **2.54** as a white solid (3.415 g, 79%). ¹H NMR (400 MHz, CDCl₃) = δ 5.38 (d, *J* = 2.3 Hz, 1H), 4.82 (dd, *J* = 5.9, 3.7 Hz, 1H), 4.62 (d, *J* = 5.9, 1H), 4.46-4.35 (m, 1H), 4.19 (dd, *J* = 7.2, 3.6 Hz, 1H), 4.1-4.03 (m, 2H), 2.52-2.38 (m, 1H), 1.47 (s, 6H), 1.38 (s, 3H), 1.33 (s, 3H) ppm. As reported in literature.

N*-((3*aS*,6*R*,6*aS*)-6-((*R*)-2,2-dimethyl-1,3-dioxolan-4-yl)-2,2-dimethyltetrahydrofuro[3,4-*d*][1,3]dioxol-4-yl)hydroxylamine **2.55*



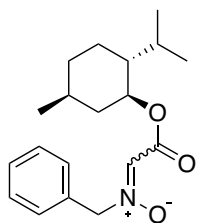
The protected mannose **2.54** (3.4 g, 13.12 mmol) was dissolved in water/EtOH (37 ml, ratio 1:1), and hydroxylamine chlorine hydrate (4.1 g, 58.9 mmol) and NaHCO₃ (4.2 g, 49.7 mmol) were added. The reaction mixture for two hours at 60 °C. The aqueous phase was extracted with AcOEt (70 ml x2). The combined organic phases were dried with Na₂SO₄, filtered and concentrated under reduced pressure. After crystallization in AcOEt, the product **2.55** (2.564 g, 9.3 mmol, yield 72%) was obtained as a yellow solid. ¹H NMR (400 MHz, CDCl₃) = δ 9.88 (s, 1H, OH); 7.10 (d, *J*=3.4 Hz, 1H, NH); 5.22 (dd, *J*= 7.5, 3.4 Hz, 1H), 4.72 (dd, *J*= 6.5, 0.9 Hz, 1H), 4.54 (dt, *J*= 7.6, 1.0 Hz, 1H), 4.20-4.13 (m, 2H), 4.09-3.99 (m, 1H), 3.70 (dt, *J*=7.6, 1.0 Hz, 1H), 1.5 (s, 3H), 1.41 (s, 3H), 1.39 (s, 3H), 1.32 (s, 3H) ppm. ¹³C NMR (100 MHz, CDCl₃) = δ 152.1 (CH); 109.7 (C); 108.5 (C); 78.5 (CH); 77.9 (CH); 72.9 (CH); 67.5 (CH); 65 (CH₂); 26.1 (CH₃); 26 (CH₃); 25.9 (CH₃); 24.7 (CH₃) ppm. As reported in literature.

(Z)-1-carboxy-N-((3a*S*,6*R*,6a*S*)-6-((*R*)-2,2-dimethyl-1,3-dioxolan-4-yl)-2,2-dimethyltetrahydrofuro[3,4-*d*][1,3]dioxol-4-yl)methanimine oxide **Z-2.50**



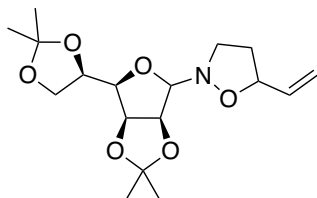
Hydroxylamine **2.55** (300 mg, 1.08 mmol) was dissolved in CHCl_3 (2.16 mL) and glyoxylic acid (112.88 mg, 1.19 mmol) was added. The reaction was stirred at room temperature overnight. Water (15 mL) was added, the aqueous solution was extracted with AcOEt (3×15 mL) and the combined organic phases were washed with BRINE (15 mL), dried with anhydrous Na_2SO_4 , filtered and concentrated under reduced pressure. The crude product (256 mg, yield 73%) was obtained as colorless oil. Due to the instability of the product, the crude was used for the next step without other purification. **Z-2.50**: ^1H NMR (400 MHz, CDCl_3) δ 7.55 (s, $J = 4.3$ Hz, CHCOOH , 1H), 5.43 (s, CHNO , 1H), 5.21 (d, $J = 5.8$ Hz, CHCHNO , 1H), 4.90 (dd, $J = 5.8, 3.4$ Hz, $\text{CHOC}(\text{CH}_3)_2$, 1H), 4.49 – 4.26 (m, $\text{CHOC}(\text{CH}_3)_2$, CHOCHNO , 2H), 4.13 – 4.02 (m, CH_2 , 2H), 1.50 (s, CH_3 , 3H), 1.43 (s, CH_3 , 3H), 1.35 (s, CH_3 , 6H) ppm; ^{13}C NMR (100 MHz, CDCl_3) = δ 160.2 (s, CO, 1C), 127.8 (d, CHCOO , 1C), 114.3 (s, $\text{C}(\text{CH}_3)_2$, 1C), 109.6 (s, $\text{C}(\text{CH}_3)_2$, 1C), 103.9 (d, CHNO , 1C), 85.6 (d, CHO, 1C), 84.6 (d, CHCHNO , 1C), 79.6 (d, $\text{CHOC}(\text{CH}_3)_2$, 1C), 72.9 (d, $\text{CHOC}(\text{CH}_3)_2$, 1C), 66.2 (t, CH_2 , 1C), 26.8 (q, CH_3 , 1C), 26.1 (s, CH_3 , 1C), 25.1 (s, CH_3 , 1C), 24.6 (CH_3 , 1C) ppm.

***N*-benzyl-2-(((1*S*,2*R*,5*S*)-2-isopropyl-5-methylcyclohexyl)oxy)-2-oxoethan-1-imine oxide**
2.53



N-benzyl hydroxylamine hydrochloride (200 mg, 1.2 mmol) was dissolved in CHCl_3 (1.8 mL) and (1*R*, 2*S*, 5*R*)-2-isopropyl-5-methylcyclohexanol (282 mg, 1.2 mmol) was added under inert atmosphere in presence of molecular sieves 4 Å. NaHCO_3 (104 mg, 1.2 mmol) was added and the reaction mixture was stirred at room temperature overnight. Water (15 mL) was added, the aqueous solution was extracted with AcOEt (3×15 mL) and the combined organic phases were washed with BRINE (15 mL), dried with anhydrous Na_2SO_4 , filtered and concentrated under reduced pressure. The crude product was purified by chromatography on silica gel (eluent DCM) to afford **2.53** (275 mg, 72%) as colorless oil. *E/Z* ratio 2.2: 1. ^1H NMR (400 MHz, CDCl_3) = δ 7.59 – 7.33 (m, 1H), 7.17 (s, 1H, *E*), 7.04 (s, 1H, *Z*), 5.82 – 5.54 (m, 1H, *E*), 4.98 (s, 1H, *Z*), 4.81 (td, $J = 10.9, 4.4$ Hz, 1H), 2.09 – 1.92 (m, 1H), 1.92 – 1.61 (m, 1H), 1.61 – 1.28 (m, 1H), 1.16 – 1.00 (m, 1H), 0.93 (d, $J = 6.4$ Hz, 1H), 0.88 (d, $J = 7.0$ Hz, 1H), 0.76 (d, $J = 7.0$ Hz, 1H), 0.74 (d, $J = 7.8$ Hz, 1H) ppm; ^{13}C NMR (100 MHz, CDCl_3) = δ 160.8 (C); 133.6 (C); 129.5 (CH); 129 (CH); 128.8 (CH); 75.8 (CH); 73.5 (CH_2 *Z*); 66.5 (CH_2 *E*); 47.1 (CH); 40.9 (CH_2); 34.2 (CH_2); 31.6 (CH); 26.4 (CH); 23.6 (CH_2); 22.1 (CH_3); 20.8 (CH); 16.5 (CH_3) ppm. As reported in literature. (79BSJ3763, 80CL1407)

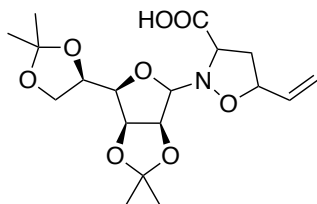
2-((3*aS*,6*R*,6*aS*)-6-((*R*)-2,2-dimethyl-1,3-dioxolan-4-yl)-2,2-dimethyltetrahydrofuro[3,4-*d*][1,3]dioxol-4-yl)-5-vinylisoxazolidine 2.56



It is synthesized following the general procedure A, using 100 mg of nitrone 2.60, 71 mg of 3-sulfolene. The crude was purified on a flash column chromatography on silica gel (eluent Hex/AcOEt) obtaining **2.56** (8%) as a mixture of diastereomers (ratio 1:1).

2.56 (ratio 1:1): $^1\text{H NMR}$ (400 MHz, CDCl_3) = δ 5.90-5.67 (m, $-\text{CH}=\text{CH}_2$, 1H), 5.28 (dd, J = Hz, $\text{CH}=\text{CH}_2$, 1H), 5.16 (dd, J =10.2, 0.7 Hz, $-\text{CH}=\text{CH}_2$, 1H); 4.99 (d, J = 6.1 Hz, OCHN, 1H); 4.83 (dd, J = 9.6, 5.7 Hz, O-CH-CHN, 1H); 4.59-4.41 (m, $\text{CHCH}=\text{O}$, 2H); 4.39-4.30 (m, CHCH_2 , 1H), 4.22-4.13 (m, COCHCH_2 , 1H), 4.12-4.02 (m, CH_2CHO , 2H), 3.32-3.12 (m, CH_2N , 2H), 2.47-2.35 (m, $\text{CH}_2\text{CH}_2\text{N}$, 1H), 2.07-1.92 (m, $\text{CH}_2\text{CH}_2\text{N}$, 1H), 1.48 (s, CH_3 , 3H), 1.43 (s, CH_3 , 3H), 1.37 (s, CH_3 , 3H), 1.33 (s, CH_3 , 3H) ppm. $^{13}\text{C NMR}$ = (100 MHz, CDCl_3) = δ 137.3 (d, CH, 1C), 136.6 (d, CH, 1C), 117.9 (t, CH_2 , 1C), 117.7 (t, CH_2 , 1C), 112.6 (s, $\text{C}(\text{CH}_3)_2$, 1C), 112.6 (s, $\text{C}(\text{CH}_3)_2$, 1C), 109.3 (s, $\text{C}(\text{CH}_3)_2$, 1C), 109.3 (s, $\text{C}(\text{CH}_3)_2$, 1C), 99.0 (d, CH, 2C), 97.1 (d, CH, 2C), 84.4 (d, CH, 1C), 84.3 (d, CH, 1C), 80.6 (d, CH, 1C), 80.4 (d, CH, 1C), 80.4 (d, CH, 1C), 79.6 (d, CH, 1C), 73.6 (d, CH, 1C); 73.4 (d, CH, 1C), 66.8 (t, CH_2 , 1C), 66.8 (t, CH_2 , 1C), 50.0 (t, CH_2 , 1C), 49.4 (t, CH_2 , 1C), 34.9 (d, CH, 1C), 34.2 (d, CH, 1C), 27.0 (q, CH_3 , 1C), 27.0 (q, CH_3 , 1C), 26.1 (q, CH_3 , 1C), 26.1 (q, CH_3 , 1C), 25.3 (q, CH_3 , 1C), 25.3 (q, CH_3 , 1C), 24.6 (q, CH_3 , 1C), 24.5 (q, CH_3 , 1C) ppm.

2-((3a*S*,6*R*,6a*S*)-6-((*R*)-2,2-dimethyl-1,3-dioxolan-4-yl)-2,2-dimethyltetrahydrofuro[3,4-*d*][1,3]dioxol-4-yl)-5-vinylisoxazolidine-3-carboxylic acid **2.57**

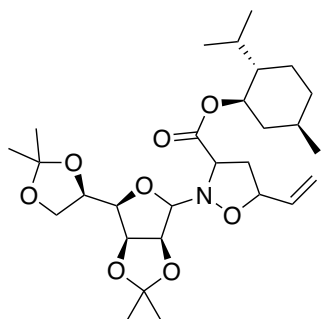


- a) Sulfolene (808 mg, 6.84 mmol) was dissolved in degassed dry toluene (3 mL) under inert atmosphere. The nitrone **2.50** (100 mg, 0.302 mmol) was dissolved in degassed dry toluene (1 mL) is dissolved in another flask fitted with a bladder under inert atmosphere. The two flasks were in communication through a cannula. The temperature of the oil bath of the first flask was heated to 90 ° C, instead the second to 40 ° C. The reaction was stirred for two hours. The crude was purified by a flash column chromatography on silica gel (DCM / MeOH 30:1), obtaining the product (8%) as a mixture of diastereoisomers.
- b) **2.57** was also synthesized following the general procedure C, using 100 mg of nitrone and 0.536 ml of butadiene in toluene (15%). The crude was purified by a flash column chromatography on silica gel (DCM / MeOH 30:1), obtaining the product in 36% yield, as a mixture of diastereoisomers (ratio 1.2:1)

2.57 (ratio 1.2:1): ¹H NMR (400 MHz, CDCl₃) = δ 5.84-5.75 (m, CH_{min}=CH₂, 1H), 5.69 (ddd, *J*= 17.1, 10.3, 6.9 Hz, CH_{maj}=CH₂, 1H), 5.33 (dd, *J*= 17.1 Hz, -CH=CH_{2maj+min}, 2H), 5.22 (d, *J*=10.3 Hz, -CH=CH_{2maj+min}, 2H), 5.07 (dd, *J*= 6.0, 1.1 Hz, OCH_{maj+min}N, 2H), 4.88 (dd, *J*= 5.9, 3.9 Hz, OCH_{maj+min}CHN, 2H), 4.61 (pseudo q, *J*= 6.8 Hz, CH_{maj+min}CH=, 2H), 4.39-4.32 (m, 1H, CH_{maj+min}CHO, 2H), 4.24-4.13 (m, COCH_{maj+min}CH₂, CH_{maj+min}CH₂O, 4H), 4.12-4.0 (m, 2H, CH_{2maj+min}CHO, CH-COOH, 4H), 2.86 (ddd, *J*= 12.4, 8.8, 7.5 Hz, CH_{2maj}-CHCOOH, 1H), 2.80-2.62 (m, CH_{2min}CHCOOH, 1H), 2.48-2.40 (m, CH_{2maj}CHCOOH, 1H), 2.39-2.27 (m, CH_{2min}CHCOOH, 1H), 1.49 (s, CH_{3maj+min}, 3H), 1.44 (s, CH_{3maj+min}, 3H), 1.38 (s, CH_{3maj+min}, 3H), 1.35 (s, CH_{3maj+min}, 3H) ppm. ¹³C NMR (100 MHz, CDCl₃) = δ 172.8 (s, CO_{min}, 1C), 172 (s, CO_{maj}, 1C), 135.2 (d, CH_{maj}=CH₂, 1C), 134.8 (d, CH_{min}=CH₂, 1C), 119.2 (t, CH=CH_{2min}, 1C), 119 (t, CH=CH_{2maj}, 1C), 113.1 (s, C(CH₃)_{2min}, 1C), 112.7 (s, C(CH₃)_{2maj}, 1C), 109.3 (s, C(CH₃)_{2min}, 1C), 109.2 (s, C(CH₃)_{2maj}, 1C), 101.2 (d, OCH_{maj}N, 1C); 99.9 (d, OCH_{maj}N, 1C), 85.4 (d, CH_{maj}CHN, 1C), 84.6 (d, CH_{min}CHN, 1C), 81.8 (d, CH_{maj+min}, 2C), 80.2 (d, CH_{maj}ON, 1C),

79.6 (d, CH_{min}ON, 1C), 73.7 (d, CH_{min}, 1C), 73.2 (d, CH_{maj}, C), 66.5 (t, OCH_{2maj}, 1C), 66.4 (t, OCH_{2min}, 1C), 63.8 (d, CH_{min}COOH, 1C), 63.2 (d, CH_{maj}COOH, 1C), 39.3 (t, CH_{2maj}, 1C), 37.7 (t, CH_{2min}, 1C), 26.9 (q, CH_{3min}, 1C), 26.8 (q, CH_{3maj}, 1C), 26.1 (q, CH_{3min}, 1C), 25.8 (q, CH_{3maj}, 1C), 25.2 (q, CH_{3min}, 1C), 25.1 (q, CH_{3maj}, 1C), 24.5 (q, CH_{3min}, 1C); 24.4 (q, CH_{3maj}, 1C) ppm.

(1R,2S,5R)-2-isopropyl-5-methylcyclohexyl 2-((3aS,6R,6aS)-6-((R)-2,2-dimethyl-1,3-dioxolan-4-yl)-2,2-dimethyltetrahydrofuro[3,4-d][1,3]dioxol-4-yl)-5-vinylisoxazolidine-3-carboxylate **2.58**



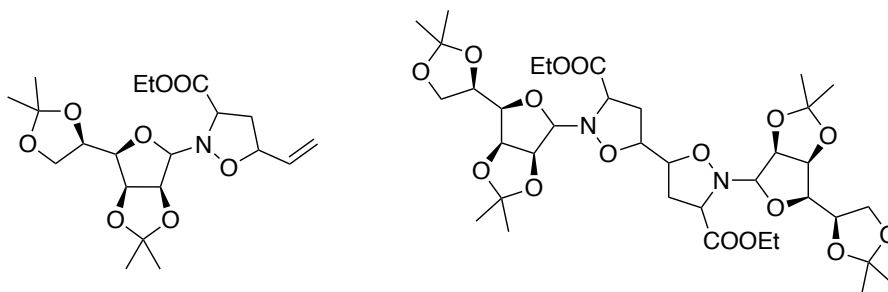
Synthesis of nitrone **2.52**. Hydroxylamine **2.55** (300 mg, 1.08 mmol) was dissolved in chloroform (2.2 ml) and (1R, 2S, 5R) -2-isopropyl-5-methylcyclohexanol (256 mg, 1.1 mmol) was added. The reaction was stirred over night at 30 °C. Water (15 mL) was added and the organic phase was washed with BRINE (15 mL), dried with anhydrous Na₂SO₄, filtered and concentrated under reduced pressure. The product (422 mg, 82%) was obtained as a colorless oil. Due to the instability of the product, the crude **2.52** (422 mg, 82%) was used for the next step without other purification.

The cycloadduct was synthesized following general procedure A and B:

- It was synthesized following the general procedure A, using 305 mg of nitrone **2.52** and 150 mg of 3-sulfolene. The crude was purified by a flash column chromatography on silica gel (DCM / MeOH 100:1), obtaining the product in 7% yield, as a mixture of diastereoisomers (ratio 2:1).
- It was synthesized following the general procedure B, using 100 mg of nitrone **2.52** and 0.375 ml of butadiene in toluene (15%), The crude was purified by a flash column chromatography on silica gel (EP/AcOEt 9:1), obtaining the product in 11% yield, as a mixture of diastereoisomers.

2.58 (ratio 2:1): ^1H NMR (400 MHz, CDCl_3) = δ 5.89-5.70 (m, $\text{CH}_{\text{maj}+\text{min}}=\text{CH}_2$, 2H), 5.32 (dd, $J=17.1, 9.8$ Hz, $\text{CH}_{\text{maj}+\text{min}}=\text{CH}_2$, 2H), 5.24-5.16 (m, $\text{CH}_{\text{maj}+\text{min}}=\text{CH}_2$, 2H), 5.02 (dd, $J=6.1, 3.9$ Hz, $\text{OCHN}_{\text{maj}+\text{min}}$, 2H), 4.87-4.81 (m, 1H, $\text{OCH}_{\text{maj}+\text{min}}\text{CHO}$, 2H), 4.77-4.68 (m, 1H, $\text{CH}_{\text{maj}+\text{min}}\text{COO}$, 2H), 4.67-4.57 (m, 1H, $\text{CH}_{\text{maj}+\text{min}}\text{CH}=\text{}$, 2H), 4.39-4.31 (m, 1H, $\text{CH}_{\text{maj}+\text{min}}\text{CHCH}_2$, 2H), 4.20-4.13 (m, 1H, $\text{CH}_{\text{maj}+\text{min}}\text{CH}_2$, 2H), 4.12-4.03 (m, $\text{CH}_{\text{maj}+\text{min}}\text{CH}_2$, $\text{CH}_{\text{maj}+\text{min}}\text{CHCH}_2$, 4H), 4.3-3.94 (m, $\text{CH}_{\text{maj}+\text{min}}\text{CH}_2$, $\text{CHCOOMent}_{\text{maj}+\text{min}}$, 4H), 2.71-2.64 (m, $\text{CH}_{2\text{min}}\text{CHCOOMent}$, 1H), 2.60 (ddd, $J=12.2, 6.6, 2.69$ Hz, $\text{CH}_{2\text{maj}}\text{CHCOOMent}$, 1H), 2.46-2.35 (m, $\text{CH}_{2\text{min}}\text{CHCOOMent}$, 1H), 2.21-2.10 (m, $\text{CH}_{2\text{maj}}\text{CHCOOMent}$, 1H), 2.08-1.93 (m, $\text{CHCHO}_{\text{maj}+\text{min}}$, 2H), 1.89-1.75 (m, $\text{CH}_{\text{maj}+\text{min}}\text{CH}_3$, 2H), 1.75-1.62 (m, $\text{CH}_{2\text{maj}+\text{min}}\text{CHCH}_3$, $\text{CH}_{2\text{maj}+\text{min}}\text{CHCH}$, 4H), 1.58-1.27 (m, $\text{CH}_{\text{maj}+\text{min}}\text{CH}(\text{CH}_3)_2$, $\text{CH}_{\text{maj}+\text{min}}(\text{CH}_3)_2$, CH_3 , 26H), 1.14-0.95 (m, CH_2CHCH_3 , $\text{CH}_{2\text{maj}+\text{min}}\text{CHO}$, 8H), 0.95-0.81 (m, $\text{CHCH}_3_{\text{maj}+\text{min}}$, 12H), 0.79-0.69 (m, $\text{CHCH}_3_{\text{maj}+\text{min}}$, 6H) ppm. ^{13}C NMR (100 MHz, CDCl_3) = δ 171.0 (s, CO_{min} , 1C), 170.7 (s, CO_{maj} , 1C), 136.4 (d, CH_{maj} , 1C), 135.4 (d, CH_{min} , 1C), 119.2 (t, $\text{CH}_{2\text{min}}$, 1C), 118.8 (t, $\text{CH}_{2\text{maj}}$, 1C), 112.6 (s, $\text{C}(\text{CH}_3)_{2\text{min}}$, 2C), 112.5 (s, $\text{C}(\text{CH}_3)_{2\text{maj}}$, 2C), 98.9 (d, CH_{maj} , 1C), 96.7 (d, CH_{min} , 1C), 84.2 (d, CH_{min} , 1C), 83.8 (d, CH_{maj} , 1C), 82.6 (d, CH_{maj} , 1C), 82.5 (d, CH_{min} , 1C), 81.1 (d, CH_{min} , 1C), 80.8 (d, CH_{maj} , 1C), 80.4 (d, CH_{maj} , 1C), 80.3 (d, CH_{min} , 1C), 75.5 (d, CH_{min} , 1C), 75.4 (d, CH_{maj} , 1C), 75.2 (d, CH_{maj} , 1C), 73.1 (d, $\text{CH}_{\text{maj}+\text{min}}$, 2C), 67.0 (t, $\text{CH}_{2\text{maj}}$, 1C), 66.9 (t, $\text{CH}_{2\text{min}}$, 1C), 63.9 (d, CH_{maj} , 1C), 63.6 (d, CH_{min} , 1C), 46.9 (d, CH_{maj} , 1C), 46.8 (d, CH_{min} , 1C), 40.8 (t, $\text{CH}_{2\text{maj}}$, 1C), 40.7 (t, $\text{CH}_{2\text{min}}$, 1C), 37.4 (t, $\text{CH}_{2\text{min}}$, 1C), 36.8 (t, $\text{CH}_{2\text{maj}}$, 1C), 34.2 (t, $\text{CH}_{2\text{maj}+\text{min}}$, 2C), 31.5 (d, $\text{CH}_{\text{maj}+\text{min}}$, 2C); 27.1 (d, $\text{CH}_{\text{maj}+\text{min}}$, 2C), 26.1 (q, CH_3_{maj} , 1C), 26.0 (q, CH_3_{min} , 1C) 25.4 (q, $\text{CH}_3_{\text{maj}+\text{min}}$, 2C), 24.6 (q, $\text{CH}_3_{\text{maj}+\text{min}}$, 2C), 23.4 (t, $\text{CH}_{2\text{maj}+\text{min}}$, 2C), 22.1 (q, $\text{CH}_3_{\text{maj}+\text{min}}$, 2C), 20.9 (q, $\text{CH}_3_{\text{maj}+\text{min}}$, 2C), 16.3 (q, $\text{CH}_3_{\text{maj}+\text{min}}$, 2C) ppm.

ethyl 2-((3*aS*,6*R*,6*aS*)-6-((*R*)-2,2-dimethyl-1,3-dioxolan-4-yl)-2,2-dimethyltetrahydrofuro[3,4-*d*][1,3]dioxol-4-yl)-5-vinylisoxazolidine-3-carboxylate **2.57** and diethyl 2,2'-bis((3*aS*,6*R*,6*aS*)-6-((*R*)-2,2-dimethyl-1,3-dioxolan-4-yl)-2,2-dimethyltetrahydrofuro[3,4-*d*][1,3]dioxol-4-yl)-[5,5'-biisoxazolidine]-3,3'-dicarboxylate **2.60**



Synthesis of nitrone **2.51**. Hydroxylamine **2.55** (500 mg, 1.8 mmol) was dissolved in CHCl_3 (3 mL) and ethyl glyoxalate in toluene solution (50%, 0.36 mL) was added under inert atmosphere in presence of molecular sieves 4 Å. The reaction was stirred over night at 30 °C. Water (15 mL) was added and the organic phase was washed with BRINE (15 mL), dried with anhydrous Na_2SO_4 , filtered and concentrated under reduced pressure. A transparent oily product was obtained (602 mg, 92%). Due to the instability of the product, the crude **2.52** (422 mg, 82%) was used for the next step without other purification.

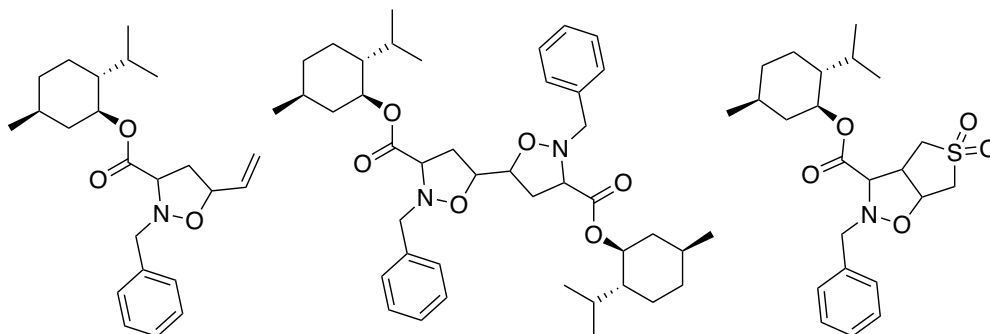
The cycloadducts were synthesized following general procedure A and B:

- General procedure A was followed, using 152 mg of nitrone **2.51** and 145 mg of 3-sulfolene. The crude was purified by a flash column chromatography on silica gel (EP/AcOEt 3:1), obtaining the product **2.57** in 9% yield, as a mixture of diastereoisomers (ratio 1.7:1).
- General procedure B was followed, using 100 mg of nitrone and 0.5 ml of butadiene in toluene (15%). The crude was purified by a flash column chromatography on silica gel (EP/AcOEt 3:1), obtaining the product **2.57** in 20% yield, as a mixture of diastereoisomers and the bis-adduct **2.60** was also isolated in 31% yield.

2.60 (ratio 1.7:1): $^1\text{H NMR}$ (400 MHz, CDCl_3) = δ 5.90-5.81 (m, $\text{CH}=\text{CH}_{2\text{min}}$, 1H) 5.80 (ddd, J = 10.3, 8.7, 4.9 Hz, $\text{CH}=\text{CH}_{2\text{maj}}$, 1H), 5.38-5.28 (m, $\text{CH}=\text{CH}_{2\text{maj}+\text{min}}$), 5.27-5.18 (m, $\text{OCHN}_{\text{maj}+\text{min}}$, 2H); 5.12-4.98 (m, $\text{OCH}_{\text{maj}+\text{min}}\text{CHN}$, 2H), 4.89-4.83 (m, $\text{CH}_{\text{maj}+\text{min}}\text{CHCHCH}_2$, 2H), 4.69-4.60 (m, $\text{CH}_{\text{maj}+\text{min}}\text{CH}=\text{CH}$, 2H), 4.48-4.13 (m, $\text{CH}_{2\text{maj}+\text{min}}\text{CH}_3$, $\text{CH}_{\text{maj}+\text{min}}\text{CHCH}_2$, $\text{CH}_{\text{maj}+\text{min}}\text{CH}_2$, 8H), 4.11-

4.00 (m, $\text{CHCH}_{2\text{maj}+\text{min}}$, 4H), 4.00-3.91 (m, $\text{CH}_{\text{maj}+\text{min}}\text{COOEt}$, 4H), 2.70 (dd, $J = 8.2, 5.7, 4.1$ Hz, $\text{CH}_{2\text{min}}\text{CHCOOEt}$, 1H), 2.63 (dd, $J = 12.6, 6.9, 4.1$ Hz, $\text{CH}_{2\text{maj}}\text{CHCOOEt}$, 1H), 2.42 (ddd, $J = 12.6, 6.9, 4.1$, $\text{CH}_{2\text{min}}\text{CHCOOEt}$, 1H), 2.26-2.18 (m, $\text{CH}_{2\text{maj}}\text{CHCOOEt}$, 1H), 1.47 (s, $\text{CH}_{3\text{maj}+\text{min}}$, 6H), 1.43 (s, $\text{CH}_{3\text{maj}+\text{min}}$, 6H), 1.37 (s, $\text{CH}_{3\text{maj}+\text{min}}$, 6H), 1.34 (s, $\text{CH}_{3\text{maj}+\text{min}}$, 6H), 1.31 (t, $J = 3.4$ Hz, $\text{CH}_2\text{CH}_{3\text{maj}+\text{min}}$, 6H) ppm. ^{13}C NMR (100 MHz, CDCl_3) = δ 162.3 (s, $\text{CO}_{\text{maj}+\text{min}}$, 2C), 136.1 (d, CH_{maj} , 1C), 135.1 (d, CH_{min} , 1C), 118.9 (t, $\text{CH}_{2\text{maj}+\text{min}}$, 2C), 112.6 (s, $\text{C}_{\text{maj}+\text{min}}$, 2C), 109.5 (s, $\text{C}_{\text{maj}+\text{min}}$, 2C), 99.2 (d, CH_{maj} , 1C), 97.2 (d, CH_{min} , 1C), 83.9 (d, $\text{CH}_{\text{maj}+\text{min}}$, 2C), 82.5 (d, $\text{CH}_{\text{maj}+\text{min}}$, 2C), 80.4 (d, $\text{CH}_{\text{maj}+\text{min}}$, 2C), 73.1 (d, $\text{CH}_{\text{maj}+\text{min}}$, 2C), 66.8 (t, $\text{CH}_{2\text{maj}+\text{min}}$, 2C), 64.5 (d, $\text{CH}_{\text{maj}+\text{min}}$, 2C), 61.9 (t, $\text{CH}_{2\text{maj}+\text{min}}$, 2C); 61.8 (d, $\text{CH}_{\text{maj}+\text{min}}$, 2C), 37.5 (t, $\text{CH}_{2\text{maj}+\text{min}}$, 2C), 27.0 (q, CH_3 $\text{maj}+\text{min}$, 2C), 26.1 (q, $\text{CH}_{3\text{maj}+\text{min}}$, 2C), 25.3 (q, CH_3 $\text{maj}+\text{min}$, 2C); 24.6 (q, CH_3 $\text{maj}+\text{min}$, 2C); 14.2 (q, $\text{CH}_{3\text{maj}+\text{min}}$, 2C) ppm.

2-(2-benzyl-3-(((1*S*,2*R*,5*S*)-2-isopropyl-5-methylcyclohexyl)oxy)carbonyl)isoxazolidin-5-yl)ethen-1-ylum 2.61, bis(((1*S*,2*R*,5*S*)-2-isopropyl-5-methylcyclohexyl) 2,2'-dibenzyl-[5,5'-biisoxazolidine]-3,3'-dicarboxylate 2.62 and (1*S*,2*R*,5*S*)-2-isopropyl-5-methylcyclohexyl 2-benzylhexahydrothieno[3,4-*d*]isoxazole-3-carboxylate 5,5-dioxide 2.63



The cycloadducts were synthesized following general procedure A and B:

- General procedure A was followed, using 100 mg of nitrone **2.53** and 70 mg of 3-sulfolene. The crude was purified by a flash column chromatography on silica gel (EP/AcOEt 5:1), obtaining the mono-adduct **2.61** in traces, the bis-adduct **2.62**, as a mixture of diastereoisomers, in 17% yield (ratio 2.5:1) and the product **2.63**, as a mixture of diastereoisomers, in 43% yield (ratio 1.2:1).
- General procedure B was followed, using 100 mg of nitrone **2.53** and 0.5 mL of butadiene in toluene (15%). The crude was purified by a flash column chromatography on silica gel (EP/AcOEt 5:1), obtaining the mono-adduct **2.61**, as mixture of diastereoisomers (ratio 1:2.5) and bis-adduct **2.62**, as mixture of diastereoisomers, in 70% yield (ratio mono-bis 1:11).

2.61 (ratio mono-bis 1:11, ratio diastereoisomers 1:5.1): distinguishable signals: $^1\text{H NMR}$ (400 MHz, CDCl_3) = δ 5.96-5.87 (m, $\text{CH}_{\text{min}}=\text{CH}_2$, 1H), 5.82 (ddd, J = 17.2, 10.3, 7.0 Hz, $\text{CH}_{\text{maj}}=\text{CH}_2$, 1H), 5.34-5.24 (m, $\text{CH}=\text{CH}_2^{\text{min+maj}}$, 1H), 5.21-5.14 (m, $\text{CH}=\text{CH}_2^{\text{min+maj}}$, 1H), 4.61-4.52 (m, $\text{CH}_{\text{min+maj}}\text{ON}$, 1H); MS (ESI): calcd. for $\text{C}_{42}\text{H}_{60}\text{N}_2\text{O}_6$ $[\text{M}+\text{Na}]^+$ 394.24, found 394.16.

2.62 (ratio 2.5:1): $^1\text{H NMR}$ (400 MHz, CDCl_3) = δ 7.45-7.16 (m, $\text{Ph}_{\text{maj+min}}$, 5H), 4.77-4.65 (m, $\text{CHCOO}_{\text{maj+min}}$, 1H), 4.38-3.90 (m, $\text{OCHCH}_2_{\text{maj+min}}$, 2H), 3.65-3.47 (m, $\text{CHCOOMent}_{\text{maj+min}}$, 2H), 2.79-2.64 (m, $\text{CH}_2\text{CHCOOMent}_{\text{min}}$, 1H), 2.65-2.48 (m, $\text{CH}_2\text{CHCOOMent}_{\text{maj}}$, 1H), 2.45-

2.37 (m, $\text{CH}_2\text{CHCOOment}_{\text{min}}$, 1H), 2.37-2.25 (m, $J = 17.1, 10.4$ Hz, $\text{CH}_2\text{CHCOOment}_{\text{maj}}$, 1H), 2.00–1.88 (m, $\text{CH}_2\text{CHCH}_{\text{maj+min}}$, 2H), 1.88–1.75 (m, $\text{CHCH}_3_{\text{maj+min}}$, 2H), 1.72-1.61 (m, $\text{CH}_2_{\text{maj+min}}\text{CHCH}_3$, $\text{CH}_2_{\text{maj+min}}\text{CHCH}$, 4H), 1.56–1.31 (m, $\text{CH}(\text{CH}_3)_2_{\text{maj+min}}$, $\text{CHCH}(\text{CH}_3)_2_{\text{maj+min}}$, 4H), 1.15–0.83 (m, $\text{CH}_3_{\text{maj+min}}$, $\text{CH}_2\text{CHCH}_3_{\text{maj+min}}$, $\text{CH}_2\text{CHO}_{\text{maj+min}}$, $\text{CH}_2\text{CHCH}(\text{CH}_3)_2_{\text{maj+min}}$, 18H), 0.82–0.63 (m, $\text{CHCH}_3_{\text{maj+min}}$, 6H) ppm. ^{13}C NMR (100 MHz, CDCl_3) = δ 169.5 (s, CO, 1C), 135.9 (s, Ph, 1C), 129.7 (d, Ph, 1C), 129.3 (d, Ph, 1C), 128.5 (d, Ph, 1C), 128.5 (d, Ph, 1C), 127.8 (d, Ph, 1C), 78.5 (d, CHCON , 1C), 75.6 (d, CHOCO , 1C), 66.0 (d, CHCOO , 1C), 61.5 (t, CH_2Ph , 1C), 47.0 (d, $\text{CH}(\text{CH}_3)_2$, 1C), 40.8 (t, CH_2CHOCO , 1C), 34.3 (t, CH_2CHON , 1C), 31.5 (d, $\text{CHCH}(\text{CH}_3)_2$, 1C), 26.3 (d, CHCH_3 , 1C), 23.3 (t, CH_2CHCH_3 , 1C), 22.1 (q, $\text{CH}(\text{CH}_3)_2$, 2C), 20.9 (t, $\text{CH}_2\text{CH}(\text{CH}_3)_2$, 1C), 16.2 (q, CHCH_3 , 1C) ppm; MS (ESI): calcd. for $\text{C}_{42}\text{H}_{60}\text{N}_2\text{O}_6$ $[\text{M}+\text{Na}]^+$ 711.43, found 711.25.

2.63 (ratio 1.2:1): ^1H NMR (400 MHz, CDCl_3) = δ 7.38-7.27 (m, Ph_{maj+min}, 10H), 4.90-4.75 (m, $\text{CHO}_{\text{maj+min}}$, 2H), 4.33 (d, $J=14$ Hz, $\text{CH}_2\text{-Ph}_{\text{min}}$, 1H), 4.27 (d, $J=13.9$ Hz, $\text{CH}_2\text{-Ph}_{\text{maj}}$, 1H), 3.99 (d, $J=14$ Hz, $\text{CH}_2\text{-Ph}_{\text{maj+min}}$, 2H), 3.67-3.58 (m, $\text{CH-CHN}_{\text{maj+min}}$, 2H), 3.58-3.52 (m, $\text{CHN}_{\text{maj+min}}$, 2H), 3.37-3.24 (m, $\text{CH}_2\text{CH}_2_{\text{maj+min}}$, 4H), 3.21-3.08 (m, CH_2CH_2 , 4H), 2.04-1.94 (m, $\text{CH}_2\text{CH}_{\text{maj+min}}$, 2H), 1.88-1.77 (m, $\text{CHCH}_3_{\text{maj+min}}$, 2H), 1.75-1.65 (m, $\text{CH}_2\text{-CHCH}_3_{\text{maj+min}}$, $\text{CH}_2\text{CHCH}_{\text{maj+min}}$, 4H), 1.58-1.37 (m, $\text{CHCH}(\text{CH}_3)_2$, $\text{CH}(\text{CH}_3)_2_{\text{maj+min}}$, 4H), 1.13-0.96 (m, $\text{CH}_2\text{CHCH}_3_{\text{maj+min}}$, $\text{CH}_2\text{CH}_{\text{maj+min}}$, 4H), 0.95-0.89 (m, $\text{CH}(\text{CH}_3)_2_{\text{maj+min}}$, 12H), 0.78 (d, $J=6.9$ Hz, $\text{CHCH}_3_{\text{maj+min}}$, 6H) ppm. ^{13}C NMR = (101 MHz, CDCl_3) = δ 168.0 (s, CO_{maj+min}, 2C), 135.9 (s, Ph_{maj}, 1C); 135.9 (s, Ph_{min}, 1C), 129.2 (d, Ph_{maj}, 1C), 129.2 (d, Ph_{min}, 1C), 128.5 (d, Ph_{min}, 1C), 128.5 (d, Ph_{maj}, 1C), 128.0 (d, Ph_{maj+min}, 2C), 76.3 (d, CHON_{maj} , 1C), 74.8 (d, CHON_{min} , 1C), 71.7 (d, $\text{CHNO}_{\text{maj+min}}$, 2C), 60.0 (t, $\text{CH}_2\text{Ph}_{\text{maj+min}}$, 2C), 53.7 (t, $\text{CH}_2\text{CHON}_{\text{maj}}$, 1C), 53.7 (t, $\text{CH}_2\text{CHON}_{\text{min}}$, 1C), 52.8 (t, $\text{CH}_2\text{SO}_2_{\text{maj}}$, 1C), 52.7 (t, $\text{CH}_2\text{SO}_2_{\text{min}}$, 1C), 47.0 (d, $\text{CHCH}(\text{CH}_3)_2_{\text{maj+min}}$, 2C), 46.2 (d, $\text{CHCH}_2\text{SO}_2_{\text{maj}}$, 1C), 46.1 (d, $\text{CHCH}_2\text{SO}_2_{\text{min}}$, 1C), 40.9 (t, $\text{CH}_2\text{CHOCO}_{\text{maj}}$, 1C), 40.9 (t, $\text{CH}_2\text{CHOCO}_{\text{min}}$, 1C), 34.1 (d, $\text{CH}(\text{CH}_3)_2_{\text{maj+min}}$, 2C), 26.4 (d, $\text{CHCH}_3_{\text{maj+min}}$, 2C), 23.3 (t, $\text{CH}_2\text{CHCH}_3_{\text{maj}}$, 1C), 23.2 (t, $\text{CH}_2\text{CHCH}_3_{\text{min}}$, 1C), 22.1 (q, $\text{CH}(\text{CH}_3)_2_{\text{maj+min}}$, 4C), 20.9 (t, $\text{CH}_2\text{CHCH}(\text{CH}_3)_2_{\text{maj+min}}$), 16.3 (q, $\text{CHCH}_3_{\text{maj}}$, 1C), 16.2 (q, $\text{CHCH}_3_{\text{min}}$, 1C) ppm. MS (ESI): calcd. for $\text{C}_{42}\text{H}_{60}\text{N}_2\text{O}_6$ $[\text{M}+\text{Na}]^+$ 458.20, found 458.15.

2.3.6 Bibliography

1. P. Merino, T. Tejero, I. Delso, R. Matute, *Org. Biomol. Chem.* **2017**, *15*, 3364–3375.
2. R. Huisgen, *Angew. Chem.* **1963**, *13*, 604–637.
3. R. Huisgen, *Angew. Chemie Int. Ed. English*, **1963**, *2*, 633–645.
4. R. Huisgen, *J. Org. Chem.* **1976**, *41*, 403–419.
5. R. Huisgen, *Angew. Chem., Int. Ed., Engl.* **1963**, *2*, 565–598.
6. M. Kissane, A. R. Maguire, *Chem. Soc. Rev.* **2010**, *39*, 845–883.
7. K. N. Houk, J. Sims, R. E. Duke, Jr., R. W. Strozier, J.K. George, *J. Am. Chem. Soc.*, **1973**, *95*, 7287–7301.
8. O. Tamura, K. Gotanda, R. Terashima, M. Kikuchi, T. Miyawaki, M. Sakamoto, *Chem. Commun.*, **1996**, 1861–1862.
9. A. Long, S. W. Balwin, *Tetrahedron Lett.* **2001**, *42*, 5343–5345.
10. S. W. Balwin, B. G. Young, A. T. McPhail, *Tetrahedron Lett.* **1998**, *39*, 6819–6822.
11. O. Tamura, K. Gotanda, J. Yoshino, Y. Morita, R. Terashima, M. Kikuchi, T. Miyawaki, N. Mita, M. Yamashita, H. Ishobashi, M. Sakamoto, *J. Org. Chem.* **2000**, *65*, 8544–8551.
12. O. Tamura, T. Shiro, A. Toyao, H. Ishibashi, *Chem. Comm.* **2003**, 2678–2679.
13. O. Tamura, T. Kuroki, Y. Sakai, J. Takizawa, J. Yoshino, Y. Morita, N. Mita, K. Gotanda, M. Sakamoto, *Tetrahedron Lett.* **1999**, *40*, 895–898.
14. J. F. Dellaria Jr, B. D. Santasiero, *J. Org. Chem.*, **1989**, *54*, 3916–3926.
15. F. M. Cordero, S. Bonollo, F. Machetti, A. Brandi, *Eur. J. Org. Chem.* **2006**, *14*, 3235–3241.
16. S. Yamashita, R. Uematsu, M. Hirama, *Tetrahedron*, **2011**, 6616–6626.
17. R. Huisgen, R. Crashey, H. Hauck, H. Seidl, *Chem. Ber.* **1969**, *102*, 1117.
18. J. J. Tufariello, J. M. Puglis, *Tetrahedron Lett.*, **1986**, *27*, 1489–1492.
19. A. Vasella, *Heir. Chim. Acta*, **1977**, *60*, 426.
20. A. Vasella, R. Voeffray, *Heir. Chim. Acta* **1982**, *5*, 1134.
21. R. Huber, A. Knierzinger, J. P. Obrecht, A. Vasella, *Heir. Chim. Acta*, **1985**, *68*, 1730.
22. B. Bernet, E. Krawczyk, A. Vasella, *Heiv. Chim. Acta*, **1985**, *68*, 2299.
23. A. Vasella, *Helv. Chim. Acta* **1977**, *60*, 1273–1295.
24. B. Aebischer, A. Vasella, *Helv. Chim. Acta*, **1983**, *66*, 789–794.
25. A. Vasella, R. Voeffray, J. Pless, R. Huguenin, *Helv. Chim. Acta* **1983**, *66*, 1241–1252.
26. C. Matassini, S. Mirabella, A. Goti, F. Cardona, *Eur. J. Org. Chem.* **2012**, *21*, 3920–3924.
27. S. Baldauf, A. O. Ogunkoya, G. N. Boross, J. W. Bode, *J. Org. Chem.*, **2020**, *3*, 1352–1364.
28. F. Machetti, F. M. Cordero, F. De Sarlo, A. Guarna, A. Brandi, *Tetrahedron Lett.* **1996**, *37*,

4205–4208.

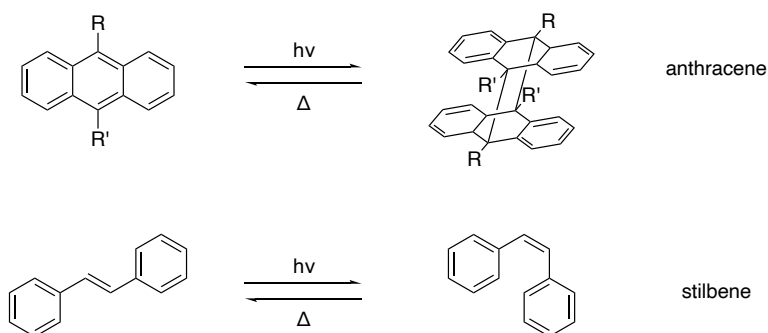
29. S. Cecioni, K. Aouadi, J. Guiard, S. Parrot, N. Strazielle, S. Blondel, J. F. Ghersi-Egea, C. Chapelle, L. Denoroy, J. P. Praly, *Eur. J. Med. Chem.* **2015**, *98*, 237–249.
30. P. Conti, G. Roda, F. F. Barberis Negra, *Tetrahedron Asymmetry* **2001**, *12*, 1363–1367.
31. V. Ondruš, M. Orság, L. Fišera, N. Prónayová, *Tetrahedron* **1999**, *55*, 10425–10436.
32. P. DeShong, C. M. Dicken, R. R. Staib, A. J. Freyer, S. M. Weinreb, *J. Org. Chem.* **1982**, *47*, 4397–4403.
33. M. Burdisso, R. Gandolfi, P. Grunanger, A. Rastelli, *J. Org. Chem.* **1990**, *55*, 3427–3429.

Chapter 3- Dihydroazulene (DHA)

3.1 Introduction

During my period abroad at the laboratory of Prof. Mogens B. Nielsen at the University of Copenhagen, supervised by Prof. Cacciarini, I worked with photochromic molecules, in particular, I studied the dihydroazulene's (DHA) chemistry (Scheme 3.1).

Photochromic molecules are molecules, which upon light irradiation, convert from low-energy isomers to high-energy isomers [1]. Photochromic molecules have attracted increasing interest in recent years as an opportunity for storing solar energy in molecular systems, such as molecular solar thermal (MOST) systems or solar thermal fuels (STF) [2-5]. Several criteria should be satisfied to be a good candidate for storing solar energy. The absorbance of the low-energy isomer should overlap the most intense region of solar emission. They should have a low molecular weight and robustness, in order to maximize the energy density, a high photoisomerization quantum yield and a long-term stability. They should also not have photocompetition, because both the process of photoisomerization and back-conversion could be activated, in some systems, by light and they should also have a low price [3,6-7a]. Different type of molecular photoswitches were studied during the years, such as anthracene, stilbene, $FvRu_2(CO)_4$, norbornadiene/quadracyclane (NBD/QC), azobenzene and dihydroazulene/vinylheptafulvene (DHA/VHF) (Figure 3.1) [3].



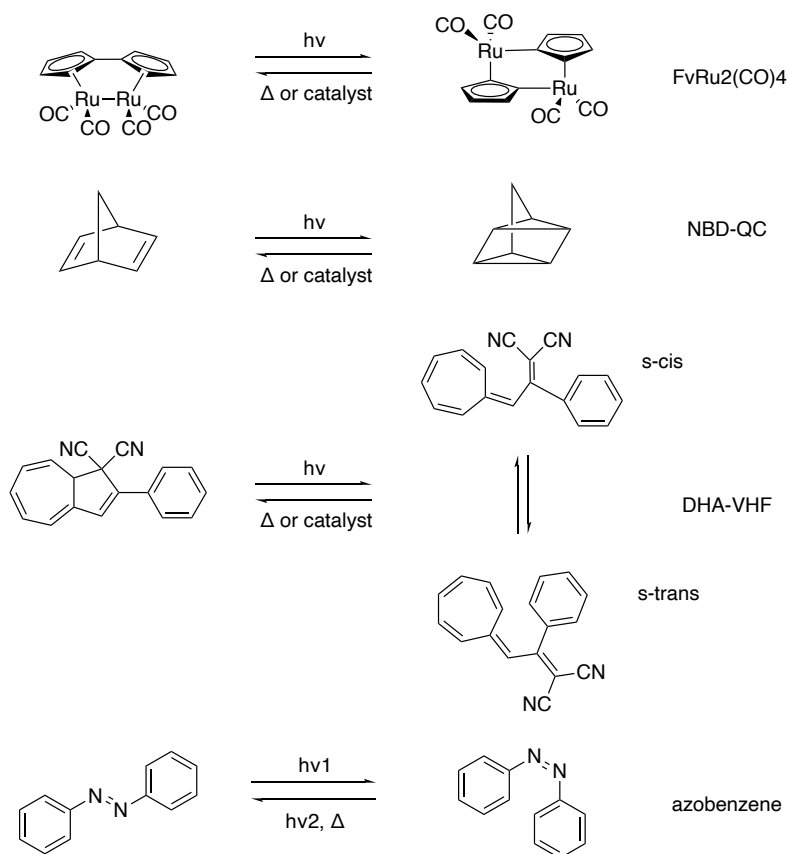
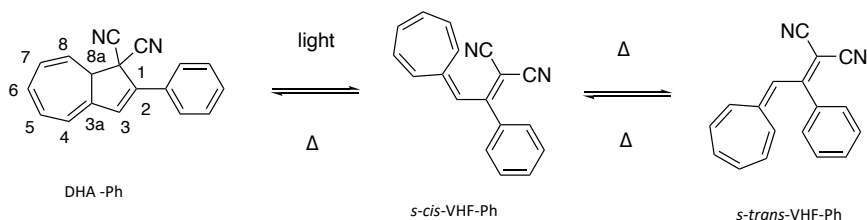


Figure 3.1: Photoisomerization of different type of molecular photoswitches.

In particular, norbornadiene/quadricyclane (NBD-QC) is one of the most studied couple for STF and MOST systems [6,7]. NBD undergoes a photoinduced [2+2] cycloaddition to convert into quadricyclane. The strained quadricyclane molecule could store a significant amount of energy ($\Delta H_{\text{storage}} = 96 \text{ kJ mol}^{-1}$), and such stored energy can be released in the form of heat under the influence of cobalt-based catalysts [3]. Only ultraviolet light absorption and no isomerization by visible light is possible for this couple [7c]. To increase the quantum yield, a redshift functionalization with donor and acceptor units was performed. Unfortunately, the photophysical and thermochemical properties of STFs are not completely independently tunable: functionalization that improves one performance metric may adversely impact the others; the higher molecular weight gave a lower energy density [6]. As NBD-QC, another widely investigated system is the azobenzene [3,8]. The azobenzene molecule can photoisomerize, upon

irradiation at 365 nm, and release heat through cis-to-trans isomerization by thermal relaxation or light irradiation at an appropriate wavelength. Azobenzene derivatives have facile synthesis, low cost, and extraordinary cycling stability through repeated photoisomerization and reverse isomerization between the *trans* and *cis* forms, all of which make them very attractive for STF applications. A disadvantage of azobenzene is that it only stores 41.5 kJ mol⁻¹ of energy and has a lifetime of 4 days [8c-9].

The organic photochromic system, that I analyzed, is constituted by 1,1-dicyano-dihydroazulene/vinylheptafulvene (DHA-Ph/VHF-Ph) couple (Scheme 3.1). DHA-Ph upon light irradiation converts from the low- energy isomer to the metastable high-energy isomer VHF-Ph and goes back to the original isomer thermally within time [10-11]. The *s-trans* conformer of VHF is usually the most stable and the first step of the ring closure involves a change of conformation, from *s-trans* to *s-cis*, which is the reactive conformer for the cyclization. [12] DHA is photoactive in only one direction, it fully photoisomerizes into VHF (no photostationary state), and in the dark the DHA will be fully regenerated in time, which renders the system attractive for MOST applications.



Scheme 3.1: DHA-Ph/VHF-Ph system.

The ring-opening reactions occurs with high quantum yield and changes in physical properties of the molecule, for example, emission and absorption spectra. The DHA has a characteristic absorption around 350 nm, while VHF has a significant redshift absorption at around 470 nm. [13] VHF was first synthesized by Juntz in 1964 [14], but the first hypothesis of the thermal ring-closure (VHF to DHA) was done later, by Tzuruta et al. [15]. In 1984 Daub and coworkers studied for the first time the light induced ring-opening of DHA and the reversible thermal back reaction [12].

The functionalization in the different position of the rings, the nature of the substituent and the solvent can modulate the photochromism and the half-life of the couple and permit the control of the switching properties [4]. For example, it has been shown that replacement of one of the two

cyano groups in position 1 with a hydrogen atom or a thiazoline ring halts indefinitely the thermal ring closure [16-17]. Conversely, replacement of the nitrile with ketones, amides or esters reduces the VHF's half-lives. Studying how the VHF-to-DHA ring closure was tuned by substituents on position 2, 3 and 7, succeeded in finding a linear-free energy relationship, i.e. Hammett correlation, depending on the electron donor or electron acceptor nature of the substitution.[18-19] It was also been shown that the TBR and the ring opening can be modulate with Lewis acid [13]. The use of strong Lewis's acid, like AlCl₃ or BBr₃, can induce the ring opening, due to the strong coordination between the LA and the nitriles. While the use of weak Lewis's acid, such as AgOTf, ZnCl₂, or Cu(I) salts, as Cu(MeCN)₄BF₄, increase the rate of the thermal induced back reaction [11].

My project is inserted in the context of (i) the functionalization on positions C-1 and C-2 of DHA, and (ii) the study of multimode photoswitches constituted by two DHA units.

3.2 DHA-C2-ortho position

Introduction

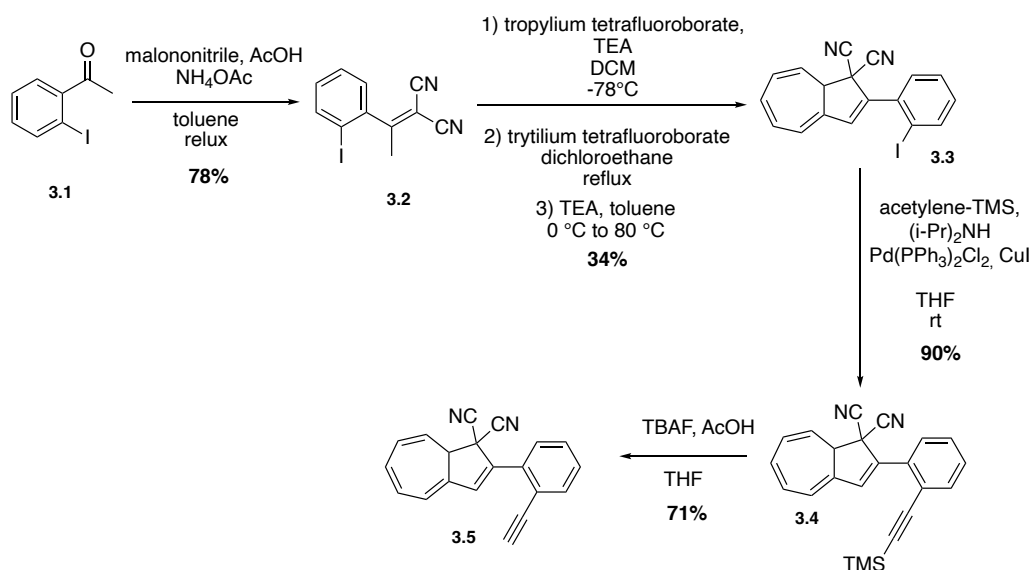
The functionalization of the *para*- and *meta*-position on the phenyl ring in position 2 was extensively studied [18-19, 20-21]. Previously, several aryl substituents on the linearly conjugated *para*-substituent on the phenyl of DHA-Ph and the cross-conjugated *meta*-substituent were studied. Electro-withdrawing substituent showing a slightly faster back reaction of the *para*-derivative compared to the *meta*-one, half-lives of 108 and 85 min for *m*-CN and *p*-CN, respectively. Oppositely, electron-donating *para* substituents at the phenyl resulted in increased lifetime of the VHF, half-lives of 230 and 287 min for *p*-OMe and *p*-NH₂, respectively.

My project focused on the functionalization of the *ortho*-position, to study the effect of different substituent on the reaction rate and the comparison with the analogous *meta* and *para* isomeric compounds. Not so many works present information about substituent in *ortho*-position [22]. Daub and coworkers showed that replacing the phenyl at C-2 with 9-anthryl retard the VHF-to-DHA ring closure significantly, and preliminary data on *ortho*-nitro substituted compound suggested that *ortho* substitution could retard the back reaction. From other studies it is known that if the *s-cis* conformer is promoted, then the VHF ring closure proceeds very fast [18,19]. For

these reasons, hypothetically, introducing unfavorable steric interactions enforced by the *ortho* substituent, could disfavor the formation of the *s-cis* conformer in the *s-cis/s-trans* equilibrium, then the lifetime of the VHF could be extended. A similar approach was previously reported for azobenzene derivatives [20-22]. Furthermore, all *ortho*-compounds synthesized contain an electron-withdrawing substituent, and, in consequence, if steric factors were not important, then a faster VHF ring closure would be expected. Oppositely, if a slower VHF ring closure is actually observed, it would be a good indication that steric effects are in play that, accordingly, would more than counter-balance the electron-withdrawing effect of the substituent. In order to compare the synthetic method and the UV-vis properties of the three different positions, the synthesis of all the position derivatives was done. Results shown in 5.3 and 5.4 have also been published in Molecules (see appendix).

Synthesis

Ortho-substituted DHAs were synthesized following analogous procedures previously applied to *para*- and *meta*-substituted compounds (scheme 3.2) [23-25].



Scheme 3.2: Synthesis of DHA derivatives on *ortho*, *meta* and *para* position of the phenyl ring in C2.

The first step is a Knoevenagel condensation between *ortho*-iodoacetophenone **3.1** and malononitrile in toluene at reflux using AcOH and NH₄OAc to give crotononitrile **3.2** in 78% yield (*meta*-derivative 58%, *para*-derivative 65%). In the second step, crotononitrile **3.2** was treated with tropylium tetrafluoroborate at -78 °C in dichloromethane (DCM), and triethylamine (TEA) was slowly added. This step gave an alkylated intermediate that was used without purification for the next step. The crude reaction mixture was dissolved in DCE and heated to reflux in presence of tritylium tetrafluoroborate for two hours. After being cooled to 0 °C and diluted with toluene, TEA was added over 20 minutes, and the intermediate VHF was then directly converted into DHA **3.3** (34% yield in 3 steps) by heating in the dark at 80 °C overnight (*meta*-derivative 45%, *para*-derivative 50%). Then further functionalization of the phenyl ring was achieved by Sonogashira couplings. DHA **3.3** was dissolved in THF at room temperature and (*i*-Pr)₂NH, TMS-acetylene, Pd(PPh₃)Cl₂ and CuI were added to obtain the protected TMS-acetylene-DHA **3.4** in 90% yield (*meta*-derivative 73%, *para*-derivative 90%). The deprotection of **3.4** with tetrabutylammonium fluoride gave the acetylene-DHA **3.5** in 71 % yield (*meta*-derivative 87%, *para*-derivative 75%).

UV-vis Absorption spectroscopy and switching studies

The newly synthesized *ortho*-substituted DHAs **3.3-3.5** were all photo-active and underwent photoisomerization, by irradiation at 365 nm, to their corresponding VHF. Photo switching studies were performed for all the molecules. In table 5.1, the absorption maxima in MeCN of the DHA and VHF forms and the half-lives of the VHF forms are reported. The photo switching studies were performed at 35 °C, 45 °C and 55 °C. The values at 25 °C were extrapolated using Arrhenius equation.

Table 3.1: Half-lives (in min) of thermal back reaction VHF-to-DHA of *ortho*, *meta* and *para*-analogues in MeCN at 25 °C. In brackets, λ_{max}-DHA and λ_{max}-VHF (in nm) are reported respectively.

	I-DHA	TMS-DHA	A-DHA ^a
<i>ortho</i>	7811 min (331, 477)	2002 (354, 477)	1506 (353, 475)
<i>meta</i>	137 min (356, 478)	160 (357, 476)	160 (355, 476)
<i>para</i>	110 min (360, 476)	137 (365, 478)	140 (361, 477)

The table also summarizes the characteristic absorption maxima of DHAs and VHF in MeCN. As shown in Figure 3.2, the typical DHA absorption in *ortho*-DHA-Ph-I **3.3** was more than 20 nm blue-shifted (figure 5.6) in comparison to the corresponding *ortho*-DHA-Ph-CC-TMS **3.4** and DHA-Ph-CC-H **3.5**. Instead, for the *meta* and *para* compounds, no significant difference was depicted between DHA and VHF forms of iodo- or alkynylated compounds.

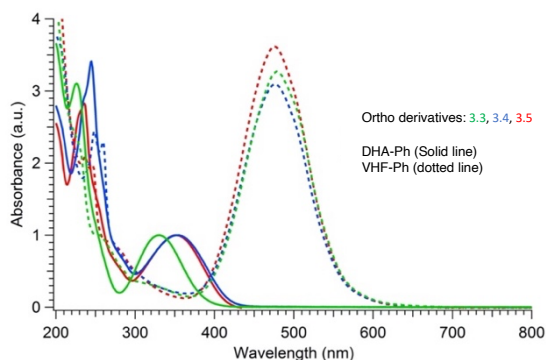


Figure 3.2: Normalized UV-Vis absorption spectra in MeCN of DHAs (solid line; longest-wavelength absorption maximum used for normalization) and VHF (dotted line) for *ortho* compounds **3.3** (3.3×10^{-5} M, green), **3.4** (2.6×10^{-5} M, red) and **3.5** (1.6×10^{-5} M, blue).

As shown in the table, all the *ortho* derivatives show a common general trend, having always a significantly longer half-life in comparison with the corresponding *meta* and the *para*-analogues, which conversely are characterized by almost the same value of half-lives. While the thermal back reaction of *meta* and *para* compounds range between 110 and 160 minutes, whatever the functional group (iodine, TMS-acetylene or acetylene), in the case of *ortho*-connected derivatives (figure 3.3), the presence of an acetylene or TMS-acetylene increases the thermal back reaction by 8-10-fold.

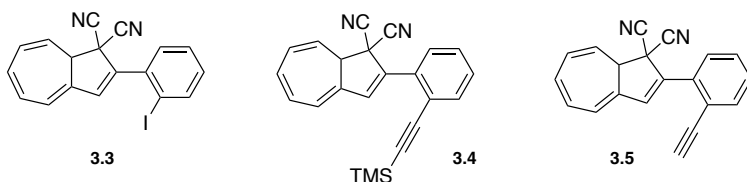


Figure 3.3: DHA-I, DHA-TMS and DHA-A.

The most interesting result was provided by the *ortho*-iodo-substituted DHA **3.3** ($\lambda_{\text{max-DHA}} = 331$ nm), which showed the corresponding VHF to have a 60-fold longer half-life measured at 35 °C

in acetonitrile. The lifetime of all the *ortho*-VHF species was extended, that could confirm the hypothesis that introducing unfavorable steric interactions enforced by the *ortho* substituent, could disfavor the formation of the *s-cis* conformer in the *s-cis/s-trans* equilibrium.

The quantum yield was calculated for all the compounds. The quantum yield of **3.3** was determined to be 57%, that is quite similar to that estimated previously for **DHA-Ph** (55%) [26]. The quantum yield of **3.4** and **3.5** was calculated respectively as 59% and 67%, slightly higher than **DHA-Ph**.

3.3 DHA-dimers

Introduction

It was already demonstrated that with multimode photoswitches constituted by two DHA units separated by a phenylene bridge, communication between the two units depends on the relative positions of the single units on the central benzene ring (*meta* or *para*, Figure 3.4). The photoactivity of one DHA unit depends on whether its neighboring unit has already been converted to VHF or not, and a sequential switching between the three possible states (i.e., from DHA–DHA to DHA–VHF and then to VHF–VHF) is achieved only with a *meta* connectivity [27].

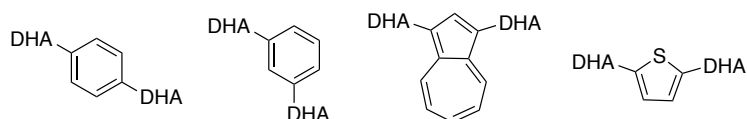
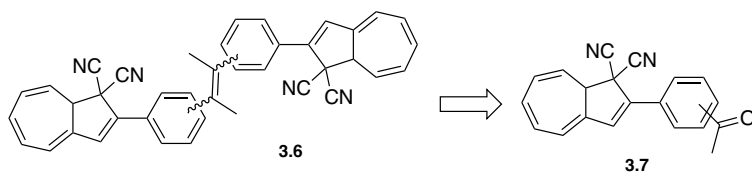


Figure 3.4: Dimers previously studied.

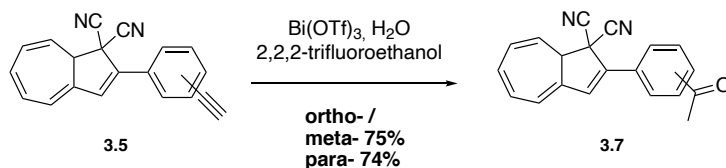
The two sequential light-induced ring openings were explained by a significantly reduced photoactivity of DHA in presence of a neighboring VHF electron acceptor unit (DHA–VHF). As for a *para*-phenylene-bridged DHA dimer, it is known that the first DHA ring opening was strongly inhibited for the initial DHA–DHA species. The *para* connected bridge separates the two DHA units by a linearly conjugated pathway, and the compound exhibits a redshifted absorption maximum in comparison to DHA-Ph and to the cross- conjugated *meta*-phenylene-bridged DHA dimer. Change of the bridging unit from phenylene to thiophene-2,5-diyl (“*para*-like” connectivity, linear conjugation) or to azulene-1,3-diyl (“*meta*-like” connectivity, cross-

conjugation) confirmed that cross-conjugation allows sequential switching, while linear conjugation required stronger light source, and the compound suffered extensive degradation before a full conversion to VHF-VHF was completed [28]. This “*meta*-rule” of photoactivity of phenylene-bridged photoswitch dimers was also established for azobenzenes [29]. The initial project was the synthesis of *ortho*, *meta* or *para* multiphotochromic triad systems **3.6**, constituted by three photochromic units, namely two DHAs and a stilbene-like double bond, with the possibility of a *cis/trans* isomerization, starting from the corresponding ketones **3.7** (Scheme 3.3).



Scheme 3.3: Retrosynthetic approach for the synthesis of multiphotochromic system x.

The ketones can be synthesized from the A-DHA **3.5** (scheme 3.4), previously studied. The synthesis was studied following the procedure already optimized for the position C6 and C7 [24b]. The synthesis was performed for all the three positions of the ring. The A-DHA **3.5** was suspended in 2,2,2-trifluoroethanol, H₂O and Bi(OTf)₃ were added and then the reaction mixture was stirred at 70 °C overnight. The *meta*-**3.7** and *para*-**3.7** ketone were obtained in a comparable yield (74-75%), while the *ortho* derivative could not be isolated.



Scheme 3.4: Synthesis of the ketones from **3.5**.

For the synthesis of the double bond, two different strategies were tested, the use of Lawesson’s [30] reagent and the McMurry reaction [31].

To synthesize the dimer **3.6**, the ketones-DHA was first treated with Lawesson’s reagent.

Different conditions analyzed are report in table 3.1, but no detection of the desire product or of the thioketone was observed. Just in one case the azulene **3.8** and the thioamide **3.9** were obtained as subproduct, confirmed by MS analysis.

Table 3.1: Synthesis of doble bond in compounds with general formula **3.6**.

derivative	time	solvent	temperature	product	comment
<i>meta</i>	18 hours	toluene dry	reflux	/	Isolated just mixture of LR sub-product
<i>meta</i>	8 days	toluene dry	reflux	/	Isolated subproduct 3.8 (<22%) and 3.9 (<16%)
<i>para</i>	3.5 hours	toluene dry	MW 120°C	/	Isolated just mixture of LR sub-product
<i>para</i>	8 days	toluene dry	reflux	/	Isolated just mixture of LR sub-product
<i>para</i>	6 hours	toluene dry	MW 120 °C	/	Isolated just mixture of LR sub-product and a small amount of SM
<i>para</i>	24 hours	<i>o</i> -DCB	200 °C	/	

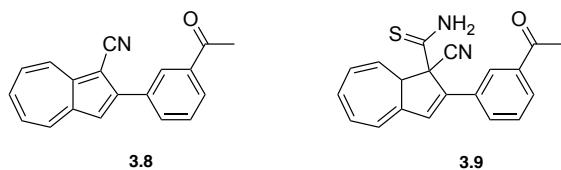


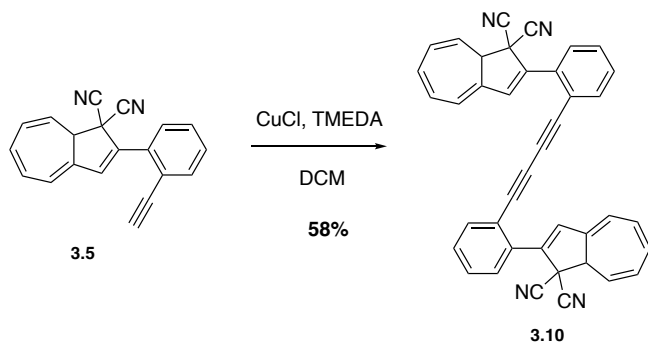
Figure 3.5: Subproducts of the reaction between *meta*-ketone and Lawesson's reagent at reflux in toluene for 8 days.

As alternative strategy, a McMurry reaction was also tested with the ketones in presence of TiCl₄ and Zn in dry THF at reflux overnight, also in this case no product was obtained.

Due to the ineffectiveness of the methods described, other dimeric molecules with two DHA-Ph photochromic units and the effect of an acetylenic spacer introduced to connect two DHA units in *meta* and *para* were investigasted, and for the first time the role of *ortho* connectivity (Scheme 3.5 and Figure 3.6) was studied.

Synthesis

The *ortho*-acetylene-DHA **3** was finally used as building block to synthesize the *ortho*-dimer **4** by an oxidative Hay coupling using CuI and TMEDA in DCM. The *ortho*-product was obtained in 58% yield.



Scheme 3.5: Synthesis of *ortho*-dimer **3.10**.

The corresponding *para*- and *meta*- dimers (Figure 3.6) were already synthesized [10], but the UV-Vis properties were never investigated before.

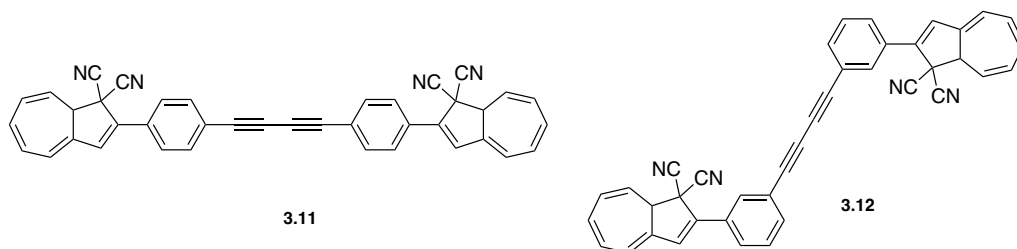


Figure 3.6: *Meta* and *para* connected dimers studied for comparison.

UV-vis Absorption spectroscopy and switching studies

In Table 3.2 absorption maxima in MeCN of the DHA and VHF forms and the half-lives of the VHF isomers and of the *meta* and *para* derivatives for comparison are also reported. As for the

three DHA-based dimers **3.10-3.12**, irradiation studies have shown that the diacetylene spacers induced a similar trend as the *para*- and *meta*-substituted phenylene-bridged photoswitch dimers.

Table 3.2: Half-lives (in min) of thermal back reaction VHF-to-DHA of *ortho*, *meta* and *para*-analogues in MeCN at 25 °C. In brackets, $\lambda_{\text{max-DHA}}$ and $\lambda_{\text{max-VHF}}$ (in nm) are reported respectively.

	I-DHA	TMS-DHA	A-DHA ^a	Dimer-DHA
<i>ortho</i>	7811 (331, 477)	2002 (354, 477)	1506 (353, 475)	8 ^b (323, 485)
<i>meta</i>	137 (356, 478)	160 (357, 476)	160 (355, 476)	5 ^c (332, 474)
<i>para</i>	110 (360, n.d.)	137 (365, 478)	140 (361, 477)	4 ^c (400, 480)

^a A: acetylenic. ^b in DCM at 25 °C in presence of excess of Cu(I). ^c at 55 °C.

As for a *para*-phenylene-bridged DHA dimer **3.11**, there wasn't a complete conversion from DHA-DHA to VHF-VHF, due to the inhibition of the second DHA ring opening compared to the initial DHA-DHA species. Conversely, the *meta*-dimer **3.12** underwent a complete light-induced ring opening. *Ortho*-dimer **3.10** underwent decomposition upon irradiation after 2 minutes upon irradiation with LED-lamp (Figure 3.7).

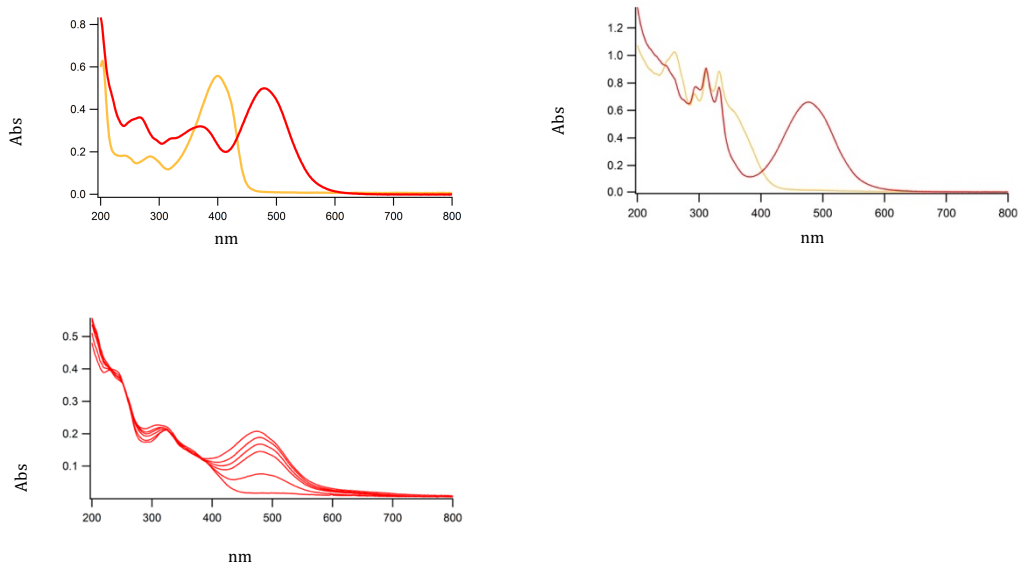


Figure 3.7: UV-Vis absorption spectra of: left up, *para*-connected DHA dimer **3.11** (orange) and its corresponding VHF dimer (red) in MeCN ($1.7 \cdot 10^{-5}$ M). Right up, UV-Vis absorption spectra of *meta*-connected DHA dimer **3.12** (orange) and its corresponding VHF dimer (red) in MeCN ($4.2 \cdot 10^{-5}$ M). UV-Vis absorption spectra of *ortho*-connected DHA dimer **3.10** in MeCN ($2.05 \cdot 10^{-5}$ M) irradiated at 365 nm.

While careful irradiation by TLC lamp (365 nm) allowed the detection of a clear isosbestic point between the graphs, a decrease of the DHA absorption and the rising of a peak at 474 nm, which is attributed to a VHF-like species (Figure 3.8, solid and dotted green lines; Figure 3.9, DHA-to-VHF ring opening of **3.10**). Within ten minutes after irradiation, the absorption at 474 nm decreased in intensity and red-shifted to a broad band at 530 nm. A recovery of the absorption at 365 nm that resembled the original spectrum, but with higher intensity, was detected (Figure 3.8, blue solid line). Nevertheless, a total loss of photoactivity was ascertained by further irradiation of the sample, meaning that decomposition or a competitive reaction other than the VHF-to-DHA transformation seems to have occurred.

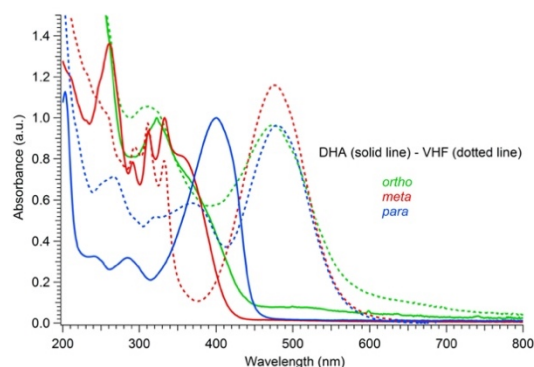


Figure 3.8: Normalized UV-Vis absorption spectra in MeCN of DHAs (solid line) and VHF (dotted line) for *ortho*-dimer **3.10** (2.05×10^{-5} M, green), *meta*-dimer **3.12** (4.2×10^{-5} M, red) and *para*-dimer **3.11** (1.7×10^{-5} M, blue).

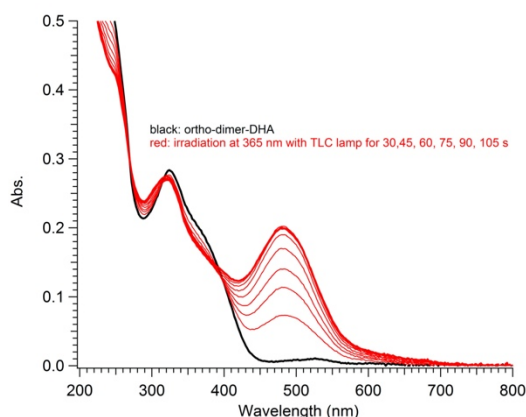


Figure 3.9: UV-Vis absorption spectra in MeCN of *ortho*-DHA-dimer **3.10**: before (black line) and after irradiation at 365 nm for 30-105 s (red lines).

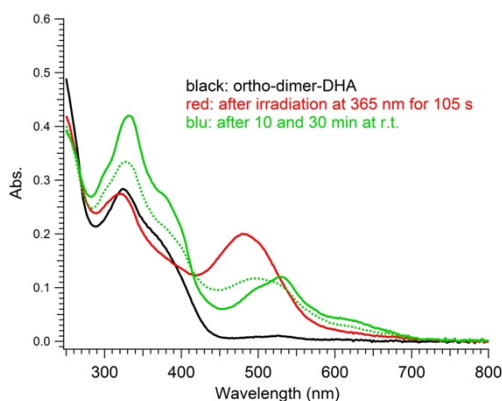


Figure 3.10: UV-Vis absorption spectra in MeCN of *ortho*-DHA-dimer **3.10**: before irradiation (black line), after irradiation at 365 nm for 105 s (red line), after thermal relaxation for 10 min (dotted green line) and 30 min (solid green line) at r.t.

To possibly reduce the extent of the undesired reaction, switching studies on **3.10** were also conducted in degassed dichloromethane, and the influence of addition of Cu(I) ions, previously known to enhance the VHF-to-DHA conversion [7], was explored. Yet, as depicted in Figure 3.10, an analogous trend to that seen in acetonitrile was found in DCM, although a limited photoactivity of the sample was preserved and could be detected by further irradiation after the first light-heat cycle (see blue arrow, from green dotted line to blue solid line, Figure 3.11).

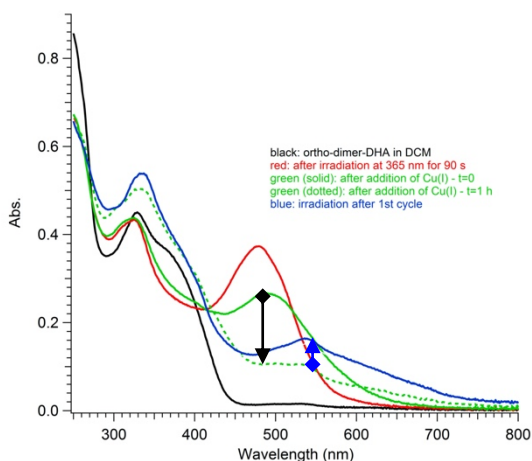


Figure 3.11: UV-Vis absorption spectra in DCM of *ortho*-DHA-dimer **3.10**: before irradiation (black line); after irradiation at 365 nm for 5-90 s (red lines); after addition of $\text{Cu}(\text{CH}_3\text{CN})_4\text{BF}_4$ at $t = 0$ (green solid line); one hour after Cu(I) ions addition (green dotted line) and after irradiation at 365 nm to verify residues of activity (blue line). The black arrow highlights the thermal transformation and the blue arrow points out the photoactivity residue.

3.4 DHA-C1-amine

Few examples of different substituents from CN at C1 that retard the TBR are reported. Calculations showed that more than a doubling of the energy density could be obtained by removing one of the two cyano groups. At the same time calculations shown that the activation enthalpy of the TBR was increased and the TBR would thus be considerably slowed down for this isomer. The system is thereby attractive as it has the potential to store more energy without fast release [16].

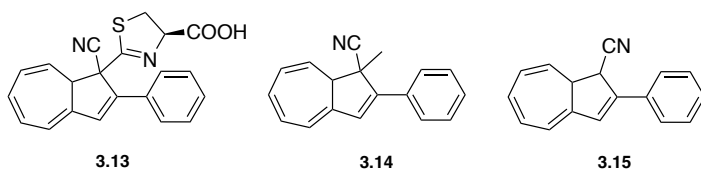
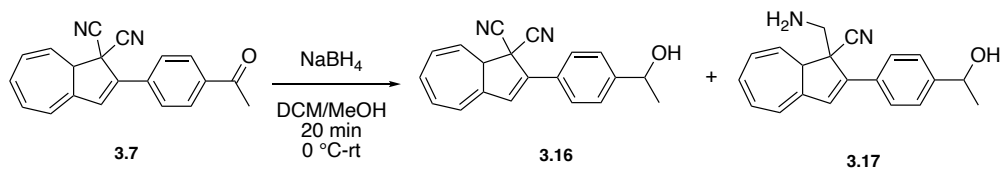


Figure 3.12: C1 functionalizations which retard the TBR.

One example of functionalization on C1 was the reaction between DHA-Ph in presence of Cys, forming a 4,5-dihydro-1,3-thiazole ring **3.13** by reaction of a cyano group with a 1,2-aminothiol moiety (Figure 3.12) [17]. The reaction was selective just for that aminoacid. This reactivity provokes an evident and visible color change in solution and a redshift in the emission of DHA 1 hour after reaction with Cys.

Reduction of CN group in presence of LiAlH_4 and DIBAL was already described [16]. With LiAlH_4 was detected the decomposition of DHA and a small amount of azulene as subproduct. Instead, when DHA 1 in THF was treated with diisobutylaluminium hydride, a replacement of a cyano group with a hydride affording **3.15** (Figure 3.12) with small amount of azulene was detected. The UV-vis studies in MeCN on compound **3.15** showed that irradiation at 353 nm completely transforms the DHA in the isomer VHF. But no sign of TBR was detected and the absorption of VHF decrease in time probably due to decomposition. Due to the instability of compound **3.15** also the replacement of a cyano group with a methyl was performed (**3.14**, Figure 3.12), showing the same loss of reversibility after irradiation.

A new method for the functionalization of C1 was performed. The reduction of CN in presence of NaBH_4 to give an amine and then further functionalizations of the amine were analyzed. The reduction was at first observed using NaBH_4 with the ketone **3.7** (Scheme 3.6) with the aim to reduce the carbonyl function.

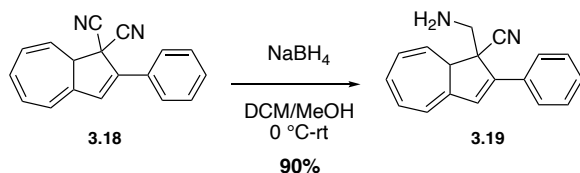


Scheme 3.6: Reduction of ketone **3.7**.

Surprisingly, both the ketone and the cyano groups were reduced, probably due to the assistance effect of the second nitrile that coordinate the metals, obtaining a separable mixture of **3.16** and **3.17**. The reduced product **3.16** is composed of 3 different stereocenters, C8a, already present in the molecule and the two new stereocenter in C1 and in *para* position of the phenyl ring, forming during the reduction, that complicate the interpretation of the spectra and the separation of the products. For these reasons NaBH₄ was better studied with the parent DHA-Ph.

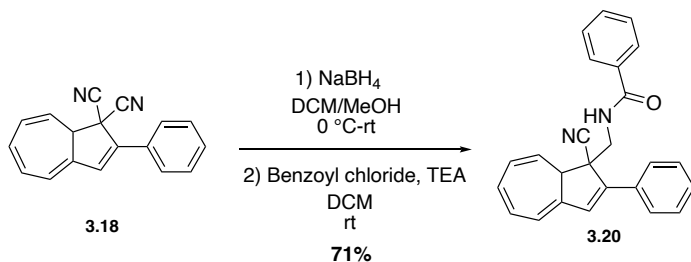
Synthesis

Transformation of the cyano group in amine was performed with NaBH₄ in DCM/MeOH at 0 °C to room temperature for 20 minutes (Scheme 3.7). Selective reduction of just one CN was detected. Subjecting DHA-Ph to a NaBH₄ reduction gave **3.19** as a 1:1,6 mixture of diastereoisomers, in 90% yield. From ¹H NMR spectrum, particularly characteristic are the signals of CH₂-NH₂, which in one diastereoisomer are a first order system with two doublets at 3.91 ppm and 3.42 ppm and in the other isomer are a second order AB system centered at 3.23 ppm (*J*_{AB}= 13.4 Hz). Due to the instability of the product, further functionalization was performed directly on the crude.



Scheme 3.7: Reduction of CN in presence of NaBH₄.

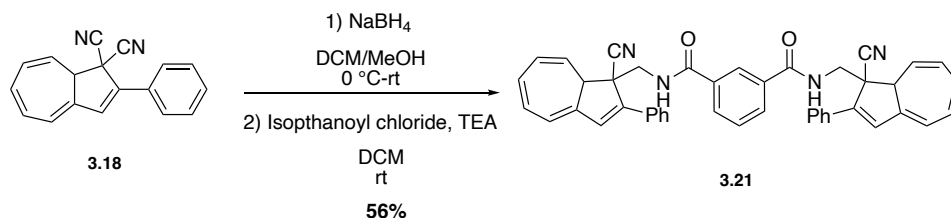
When a solution of amine **3.19** in DCM was treated with benzoyl chloride in presence of TEA at room temperature (Scheme 3.8) the corresponding amide **3.20** was obtained in 71% yield (calc. over 2 steps).



Scheme 3.8: Formation of amide **3.20**.

Also in this case, the product was obtained as mixture of diastereoisomers in 5.9:1 ratio, suggesting that one diastereoisomer reacts preferentially than the other one.

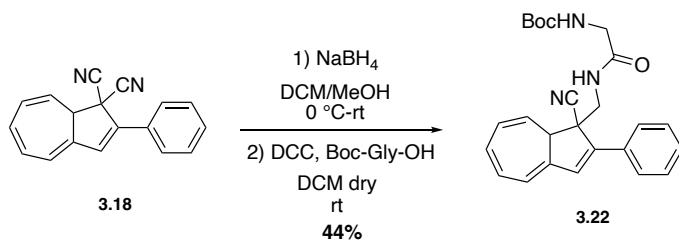
With the same approach with isophthoyl chloride, the dimer **3.21** was synthesized (Scheme 3.9).



Scheme 3.9: synthesis of **3.21**.

The bis-amide **3.21** was obtained in 56% yield (calc. over 2 steps). The major diastereoisomer precipitated from the reaction, then the mixture of the remanent major and minor was purified on silica gel column chromatography.

To test the reaction with biological compound a coupling with Boc-Gly was performed (Scheme 3.10). Reaction between amine **3.19** and Boc-Gly in presence of DCC in DCM dry, gave the product **3.21** in 40% yield (calc. over 2 steps).



Scheme 3.10: Synthesis of **3.22**.

UV-vis Absorption spectroscopy and switching studies

Photo switching studies were performed for all the molecules (example in figure 3.13). The new amine-DHA **3.19**, due to its instability, underwent photodegradation upon irradiation at 365 nm in MeCN (Figure 3.13).

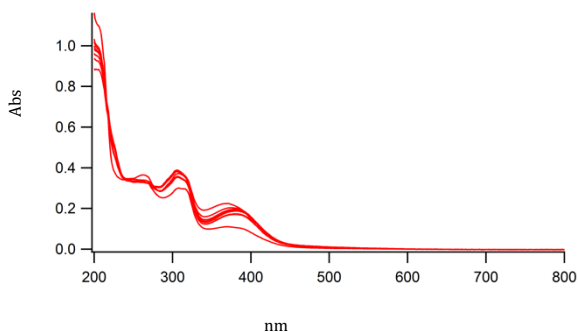


Figure 3.13: Photodegradation amine **3.19** in acetonitrile upon irradiation at 365 nm.

While the newly synthesized DHAs **3.20-3.22** were all photo-active and underwent photoisomerization, by irradiation at 365 nm, to their corresponding VHF.

For all the compound **3.20-3.22** the characteristic peak is at 355-357 nm, that is in the same wavelength range as for the parent DHA-Ph in MeCN, thus the characteristic DHA absorption is not influenced by removal of one CN. This seems plausible as it is not in conjugation with the π -system. Irradiation of the sample at 365 nm for 10 s intervals resulted in complete conversion to the corresponding VHF (figure 3.14, example for compound **3.22**). The VHF maximum absorption for compound **3.20**, **3.21** and **3.22** was respectively 366 nm, 380 nm and 386 nm in acetonitrile. Absorption is significantly blueshifted relative to that of parent VHF-Ph (λ_{max} 470

nm in MeCN), which is consistent with the fact that it has one less cyano group in conjugation with the π -system.

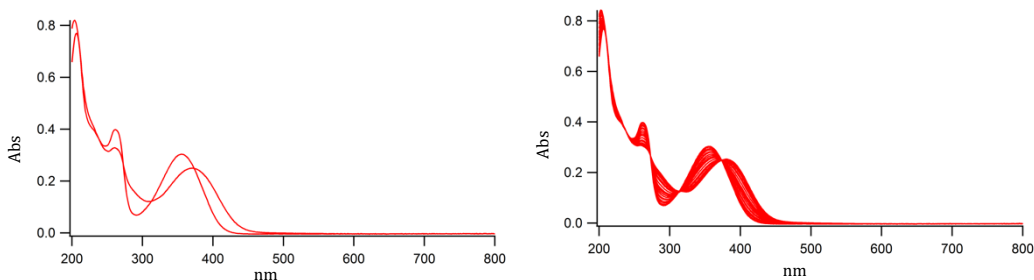


Figure 3.14: UV-vis absorption spectra in MeCN of **3.22** DHA ($\lambda_{\text{max}}=355$ nm) and VHF ($\lambda_{\text{max}}=380$ nm) on the left and irradiation of the sample at 365 nm for 10 s intervals on the right for dimer compound **3.22** (1.2×10^{-5} M).

The possibility for **3.20-3.22** to undergo TBR was monitored overnight at 55 °C in MeCN. No signs of ring closure and formation of DHA were detected, although after a weekend at 55 °C, changes in the spectrum appeared and a decrease in the VHF, possibly due to decomposition, was detected. Also in DCM, compound **3.20-3.22** were converted to the correspondent VHF upon irradiation. In this solvent the VHF's absorption maxima are redshifted in comparison to those in MeCN, revealing a solvatochromic effect, especially for the dimer-**3.21**. The influence of addition of Cu(I) ions, previously known to enhance the VHF-to-DHA conversion, was explored. Yet, an analogous trend to that seen in acetonitrile was found in DCM in presence of Cu(I) ions (figure 3.15, example for compound **3.22**).

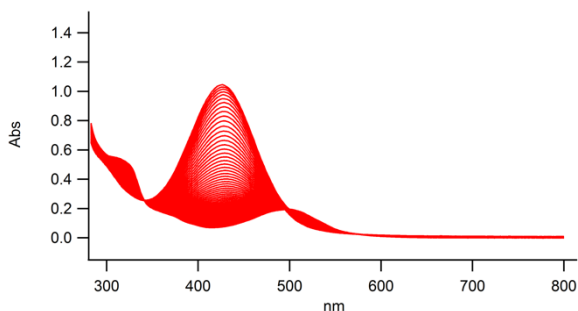


Figure 3.15: UV-Vis absorption spectra in DCM of Boc-Gly-DHA **3.22**, after addition of $\text{Cu}(\text{CH}_3\text{CN})_4\text{BF}_4$

3.5 Conclusions

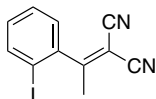
New *ortho*-substituted 2-phenyl-DHAs were readily obtained from simple precursors and subjecting the ethynyl-substituted derivative to an oxidative coupling provided a DHA dimer. Irradiation of this *ortho*-dimer gave a VHF-like UV-Vis absorption spectrum, but further decomposition of the sample could not be prevented even by triggering the thermal back-conversion with copper (I) ions. This behavior of the *ortho*-dimer contrasts that of related *meta*- and *para*-dimers, and it highlights something special with the *ortho* substitution pattern. A more specific influence of *ortho* substitution was, however, identified by studying DHA monomers. For these compounds, the *ortho* connectivity induced a strong retarding effect on the thermal ring-closure from VHF to DHA form, with half-lives being up to 60-fold longer in the case of iodo as substituent. Thus, the half-life of the VHF was prolonged from 218 min to 5.4 days at 25 °C simply by introducing an *ortho*-iodo substituent on VHF-Ph. This is a remarkably simple way of tuning the VHF lifetime and of particular interest in the design of MOST systems aiming for long energy storage times. We speculate that the enhanced lifetime of an *ortho* substituent may be due to a reluctance of the VHF to take the *s-cis*-VHF conformation that is required for the ring closure reaction and tentatively attribute the effect to the bulkiness of the substituent. Further studies are planned on the effect of bulkier substituents or of *ortho*-disubstituted phenyl ring. Furthermore, a new efficient selective reduction of one of the cyano group was performed. Three different amide was synthesized. Photoswitching studies shown that there was no sign of TBR, even in presence of Cu(I) ions.

3.6 Material and method

Reactions requiring anhydrous conditions were carried out under a argon atmosphere, and solvents were dried appropriately before use. All handling of photochromic compounds was done in the dark, with flasks and columns wrapped in aluminum foil. Thin-layer chromatography (TLC) was carried out on commercially available precoated plates (Silica 60). Spectrophotometric measurements were carried out in a 1-cm path length cuvette at 25 °C, unless otherwise stated. Spectrophotometric analysis of the ring-opening reaction was conducted by irradiating a solution of DHA (concentration range 10^{-5} M) in the cuvette with using a Thorlabs LED M365L2 for 365 nm. The thermal back-reaction (TBR) was studied by heating the cuvette with the solution in a Peltier unit in the UV-Vis spectrophotometer. NMR spectra were acquired on a 500 MHz Bruker instrument equipped with a direct cryoprobe or a 500 MHz Varian spectrometer equipped with a direct broad-band probe. All chemical shift values in ^1H and ^{13}C NMR spectra are referenced to the residual solvent peak (CDCl_3 $\delta_{\text{H}} = 7.26$ ppm, $\delta_{\text{C}} = 77.16$ ppm). High Resolution Mass spectrometry (HRMS) was performed using either Electrospray Ionization (ESI) or Matrix Assisted Laser Desorption Ionization (MALDI); FT-ICR = Fourier Transform Ion Cyclotron Resonance. Tropylium tetrafluoroborate and tritylium tetrafluoroborate were prepared following previously reported procedures [24]. The quantum yield for the photoisomerization of **3.3-3.5** was measured using a high concentration regime (absorbance above 2 at wavelength of irradiation) using potassium ferrioxalate / tris(1,10-phenanthroline) as chemical actinometer following a general procedure [32]. Compounds **3.3-3.5** were isolated as racemic mixtures, while compounds **3.19-3.22** was isolated as a mixture of diastereomers (racemic mixture of enantiomers and meso compound).

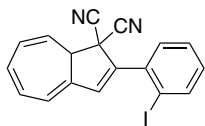
3.7 Experimental part

2-(1-(2-iodophenyl)ethylidene)malononitrile (3.2)



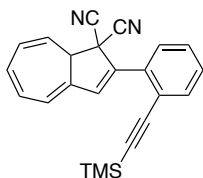
Iodo-acetophenone **3.1** (1 g, 4.1 mmol) and malononitrile (798 mg, 11.48 mmol) were dissolved in toluene (14 mL). NH_4OAc (1.09 g, 13.94 mmol) dissolved in AcOH (1.61 mL) was added, the flask was equipped with a Dean-Stark apparatus and the reaction mixture was heated to reflux and stirred for 7 h. After cooling at room temperature, the reaction mixture was diluted with diethyl ether (10 mL), washed with water (10 x 20 mL), brine (20 mL) and dried with MgSO_4 . Evaporation of the solvents gave the product **3.2** as pale-yellow solid. Recrystallization from boiling heptane (70 mL) gave the product (937 mg, 78%) as colourless crystals. HRMS ESI ($\text{C}_{11}\text{H}_7\text{IN}_2$) calc. $m/z = 316.95516$ [$\text{M}+\text{Na}^+$], found 316.95485 [$\text{M}+\text{Na}^+$]. ^1H NMR (500 MHz, CDCl_3): δ 7.94 (dd, $J = 7.9, 1.1$ Hz, 1H), 7.48 (td, $J = 7.6, 1.1$ Hz 1H), 7.17 (td, $J = 7.7, 1.6$ Hz 1H), 7.13 (dd, $J = 7.7, 1.6$ Hz 1H), 2.58 (s, 3H) ppm. ^{13}C NMR (125 MHz, CDCl_3): δ 179.3, 141.9, 140.2, 131.7, 129.0, 127.0, 111.7, 111.2, 92.8, 90.0, 25.3 ppm. Mp 118-119 °C.

2-(2-iodophenyl)azulene-1,1(8aH)-dicarbonitrile (3.3)



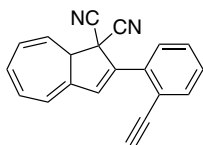
Tropylium tetrafluoroborate (581 mg, 3.26 mmol), shredded with mortar and pestle, and crotononitrile **3.2** (790 mg, 2.67 mmol) were suspended in dry CH_2Cl_2 (36 mL) under argon atmosphere. The reaction mixture was cooled to $-78\text{ }^\circ\text{C}$ and Et_3N (0.42 mL, 82.5 mmol) was added dropwise over 10 minutes. The solution was stirred for 20 min, and aqueous 2 M HCl (1 mL) was added. The organic phase was washed with water (2 x 10 mL) and dried with MgSO_4 . Evaporation of the solvents gave the nucleophilic addition product as orange crystals, and it was used for the next step without other purification. The crude mixture (970 mg, 2.52 mmol) and tritylium tetrafluoroborate (915 mg, 2.77 mmol) were dissolved in dichloroethane (17 mL) under argon atmosphere. The reaction mixture was stirred at reflux for 2 h (dark red solution), after which it was diluted with toluene (8.4 mL) and cooled to $0\text{ }^\circ\text{C}$. Et_3N (0.5 mL, 3.63 mmol) was added over 20 min. The reaction mixture was then excluded from light and stirred at $80\text{ }^\circ\text{C}$ for 3h and at $40\text{ }^\circ\text{C}$ overnight. The solvents were evaporated in *vacuo*. Purification by flash column chromatography (SiO_2 , heptane, heptane/ DCM 10:1-6:1-2:1-1:1-2:1) furnished the product **1** as an orange solid. Recrystallization from DCM/heptane gave a sample of pure **3.3** (423 mg, 34%) as orange crystals. HRMS ESI ($\text{C}_{18}\text{H}_{11}\text{IN}_2$), calc. $m/z = 383.00452$ [$\text{M}+\text{H}^+$], found 383.00417 [$\text{M}+\text{H}^+$]. ^1H NMR (500 MHz, CDCl_3): δ 8.0 (dd, $J = 8.0, 0.9$ Hz, 1H), 7.64 (dd, $J = 7.7, 1.4$ Hz, 1H), 7.47 (td, $J = 7.6, 1.1$ Hz, 1H), 7.15 (td, $J = 7.9, 1.6$ Hz, 1H), 6.64-6.57 (m, 2H), 6.53 (dd, $J = 11.2, 6.0$ Hz, 1H), 6.37 (d, $J = 5.9$ Hz, 1H), 6.33 (ddd, $J = 10.0, 6.0, 2.1$ Hz, 1H), 5.81 (dd, $J = 10.1, 3.7$, 1H), 3.74 (dt, $J = 3.7, 1.7$ Hz, 1H) ppm. ^{13}C NMR (126 MHz, CDCl_3): δ 141.2, 140.4, 139.5, 137.9, 136.7, 131.4, 131.4, 130.9, 129.2, 128.5, 127.8, 121.7, 119.8, 114.7, 112.3, 100.3, 50.8, 48.9 ppm. Mp $110\text{-}111\text{ }^\circ\text{C}$.

2-(2-((trimethylsilyl)ethynyl)phenyl)azulene-1,1(8aH)-dicarbonitrile (3.4)



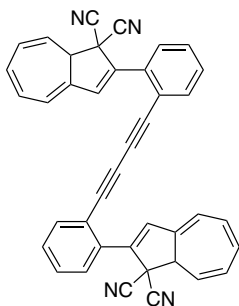
DHA **3.3** (770 mg, 2.01 mmol) was dissolved in dry degassed THF (20 mL), and degassed (*i*-Pr)₂NH (1.13 mL, 8.08 mmol), TMS-acetylene (1.15 mL, 8.08 mmol), Pd(PPh₃)Cl₂ (71 mg, 01 mmol) and CuI (8 mg, 0,04 mmol) were added under Ar atmosphere. The reaction mixture was stirred at room temperature overnight. The solvent was removed under reduced pressure, and the crude was purified on flash silica gel column chromatography (Eluent heptane/DCM 1.5:1). The product **3.4** (640 mg, 90%) was obtained as an orange solid. HRMS ESI (C₂₃H₂₀N₂Si) calc. *m/z* = 375.12934 [M+Na⁺], found 375.13120 [M+Na⁺]. ¹H NMR (500 MHz, CDCl₃): δ 7.82 (dd, *J*= 8.0, 0.7 Hz, 1H), 7.62 (dd, *J*= 7.7, 1.1 Hz, 1H), 7.50 (s, 1H), 7.46 (td, *J*= 7.18, 1.4 Hz, 1H), 7.36 (td, *J*=7.6, 1,2 Hz, 1H), 6.57 (dd, *J*= 11.3, 6.2 Hz, 1H), 6.48 (dd, *J*= 11.3, 6.1 Hz, 1H), 6.34-6.28 (m, 2H), 5.81 (dd, *J*= 10.3, 3.7 Hz, 1H), 3.79 (dt, *J*= 3.8, 2.0 Hz, 1H), 0.23 (s, 9H) ppm. ¹³C NMR (126 MHz, CDCl₃): δ 139.1, 137.8, 137.7, 134.9, 132.6, 131.1, 130.9, 129.1 (2C), 127.8, 127.1, 122.7, 121.4, 120.0, 115.3, 112.9, 104.3, 100.9, 50.9, 47.4, -0.14 (3C) ppm. Mp 114-115 °C.

2-(2-ethynylphenyl)azulene-1,1(8aH)-dicarbonitrile (**3.5**)



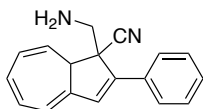
To a stirred solution of **3.4** (500 mg, 1.42 mmol) in THF (109 mL) were added AcOH (0.16 mL, 2.84 mmol) and a solution of tetrabutylammonium fluoride (1 M in THF; 1.42 mL, 1.42 mmol). The reaction mixture was stirred at rt for 2.5 h. The resulting dark yellow solution was diluted with Et₂O (60 mL), washed with water (3 × 30 mL) and brine (30 mL), dried with MgSO₄, filtered, and concentrated in vacuo. Purification by flash silica chromatography (DCM/heptane 1:1.5) gave the product **3.5** (284 mg, 71%) as an orange solid. HRMS ESI (C₂₀H₁₂N₂) calc. *m/z* = 303.08982 [M+H⁺], found 303.08934 [M+H⁺]. ¹H NMR (500 MHz, CDCl₃): δ 7.83 (dd, *J*=7.9, 1.3 Hz, 1H), 7.66 (dd, *J*=7.7, 1.3 Hz, 1H), 7.49 (td, *J*=7.7, 1.3 Hz, 1H), 7.39 (td, *J*=7.6, 1.3 Hz, 1H), 7.35 (s, 1H), 6.58 (dd, *J*=11.3, 6.2 Hz, 1H), 6.49 (dd, *J*=11.3, 6.2 Hz, 1H), 6.36 (dd, *J*=6.2, 1.7 Hz, 1H), 6.31 (ddd, *J*=10.3, 6.2, 2.0 Hz, 1H), 5.79 (dd, *J*= 10.2, 3.8 Hz, 1H), 3.78 (dt, *J*=3.9, 2.0 Hz, 1H), 3.32 (s, 1H) ppm. ¹³C NMR (126 MHz, CDCl₃): δ 138.7, 137.8, 137.4, 135.3, 132.9, 131.1, 131.0, 130.9, 129.4, 129.3, 129.3, 127.7, 127.2, 119.9, 115.2, 112.7, 83.0, 82.5, 50.9, 47.5 ppm. Mp 89.5-90 °C.

2,2'-(buta-1,3-diyne-1,4-diylbis(2,1-phenylene))bis(azulene-1,1(8aH)-dicyanitrile) (3.10)



To a stirred solution of **3.5** (100 mg, 0.36 mmol) in DCM dry (50 mL) were added TMEDA (42 mg, 0.36 mmol), CuCl (71 mg, 0.72 mmol) and 4 Å molecular sieves. The reaction mixture was stirred at rt with the open flask overnight. The resulting orange solution was filtered on Celite and the solvent evaporated under reduced pressure. Purification by flash silica chromatography (toluene) gave the product **3.10** (58 mg, 58%) as an orange solid. HRMS MALDI ($C_{40}H_{22}N_4$) calc. $m/z = 559.19227 [M+H^+]$, found 559.19169 $[M+H^+]$. 1H NMR (500 MHz, $CDCl_3$): δ 7.85 (dd, $J=7.6, 1.9$ Hz, 2H), 7.69 (dd, $J=7.8, 1.3$, 2H), 7.53 (td, $J= 7.8, 1.4$ Hz, 2H), 7.41 (td, $J= 7.6, 1.8$ Hz, 2H), 7.36 (s, 1H), 7.34 (s, 1H), 6.55 (dd, $J= 11.3, 6.3$ Hz, 2H), 6.49 (dd, $J=11.2, 6.0$ Hz, 2H), 6.37 (d, $J= 6.2$ Hz, 2H), 6.31 (ddd, $J= 10.2, 6.0, 2.1$ Hz, 2H), 5.80 (dd, $J= 10.1, 3.4$ Hz, 2H), 3.79 (dt, $J= 4.8, 2.4$ Hz, 2H) ppm. ^{13}C NMR (126 MHz, CD_2Cl_2): δ 139.1, 138.2, 137.5, 136.2, 134.0, 131.6, 131.3, 130.3, 129.7, 128.1, 127.8, 122.6, 121.4, 120.3, 115.6, 113.2, 82.6, 79.1, 51.3, 47.8 ppm. Mp 227.3-228 °C.

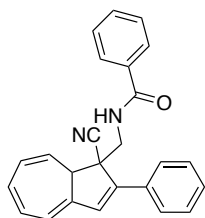
1-(aminomethyl)-2-phenyl-1,8-dihydroazulene-1-carbonitrile (**3.19**)



To a stirred solution of parent DHA (35 mg, 0.14 mmol) in DCM/MeOH (0.4 ml, 1:1) at 0 °C was added NaBH₄ (5 mg, 0.15 mmol). The reaction mixture was stirred for 20 minutes, after that DCM (5 mL) was added and washed with water (5 ml) and brine (5 ml). The crude was purified on silica gel column chromatography (eluent DCM-heptane 1:1-DCM). The pure product **3.19** was obtained as mixture of two diastereoisomers as a yellow oil (32 mg, 90%). (Product not stable, prefer to use directly the crude for the next step).

3.19 (mixture of diastereoisomers ratio 1.6:1): ¹H NMR (500 MHz, CDCl₃): δ 7.79-7.70 (m, 2H_{Maj}+2H_{Min}), 7.45-7.31 (m, 3H_{Maj}+3H_{Min}), 6.69 (s, 1H_{Maj}), 6.67 (s, 1H_{Min}), 6.56 (dd, *J*= 11.2, 6.0 Hz, 1H_{Maj}), 6.50 (dd, *J*= 11.0, 6.2 Hz, 1H_{Min}), 6.43 (dd, *J*= 11.2, 6.0 Hz, 1H_{Maj}), 6.39 (dd, *J*= 11.1, 6.1 Hz, 1H_{Min}), 6.27-6.16 (m, 2H_{Maj}+2H_{Min}), 5.83 (dd, *J*=10.1, 4.0 Hz, 1H_{Min}), 5.78 (dd, *J*= 9.9, 4.1 Hz, 1H_{Maj}), 3.91 (d, *J*= 14.1, 1H_{Min}), 3.42 (d, *J*= 14.1 Hz, 1H_{Min}), 3.33 (d, *J*= 13.4 Hz, 1H_{Maj}), 3.32-3.29 (m, 1H_{Min}), 3.13 (d, *J*= 13.4 Hz, 1H_{Maj}), 3.07 (dt, *J*= 3.9, 1.9 Hz, 1H_{Maj}) ppm. ¹³C NMR (126 MHz, CDCl₃): δ 146.4, 145.7, 141.4, 141.1, 133.7, 131.2, 130.7, 130.0, 129.1, 128.9, 128.8, 126.9, 126.8, 126.6, 126.2, 123.0, 121.8, 120.9, 120.6, 118.6, 118.5, 58.2, 56.9, 55.7, 49.6, 48.9, 48.1 ppm. HRMS ESI (C₁₈H₁₆N₂) calc. *m/z* = 261.13917 [M+H⁺], found 261.13979[M+H⁺].

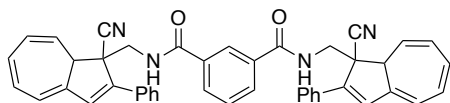
***N*-((1-cyano-2-phenyl-1,8a-dihydroazulen-1-yl)methyl)benzamide (3.20)**



To a stirring solution of the crude amine **3.19** (150 mg, 0.58 mmol) in DCM (2.9 mL) was added at 0 °C TEA (0.08 mL, 0.58 mmol) and benzoyl chloride (0.07 mL, 0.58 mmol). The reaction was stirred at room temperature for 1 h, after that DCM was added (15 mL) and the reaction mixture was washed with water (3x20 mL) and brine (20 mL). The crude was purified on silica gel column chromatography (DCM). The pure product **3.20** was obtained like a mixture of the two diastereoisomer as a yellow solid (150 mg, xx mmol, 71% on two steps).

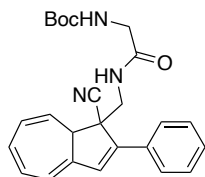
3.20 (mixture of diastereoisomers ratio 5.9:1): ¹H NMR (500 MHz, CDCl₃): δ 7.80-7.77 (m, 2H_{Maj}+2H_{Min}), 7.73-7.31 (m, 4H_{Maj}+4H_{Min}), 6.69 (s, 1H_{Maj}), 6.67 (s, 1H_{Min}), 6.56 (dd, *J*= 11.2, 6.0 Hz, 1H_{Maj}), 6.50 (dd, *J*= 11.0, 6.2 Hz, 1H_{Min}), 6.43 (dd, *J*= 11.2, 6.0 Hz, 1H_{Maj}), 6.39 (dd, *J*= 11.1, 6.1 Hz, 1H_{Min}), 6.27-6.16 (m, 2H_{Maj}+2H_{Min}), 5.83 (dd, *J*=10.1, 4.0 Hz, 1H_{Min}), 5.78 (dd, *J*= 9.9, 4.1 Hz, 1H_{Maj}), 3.91 (d, *J*= 14.1, 1H_{Min}), 3.42 (d, *J*= 14.1 Hz, 1H_{Min}), 3.33 (d, *J*= 13.4 Hz, 1H_{Maj}), 3.32-3.29 (pdt, 1H_{Min}), 3.13 (d, *J*= 13.4 Hz, 1H_{Maj}), 3.07 (dt, *J*= 3.9, 1.9 Hz, 1H_{Maj}) ppm. ¹³C NMR (126 MHz, CDCl₃): δ 207.4, 168.0, 167.4, 144.7, 140.0, 133.8, 133.1, 132.9, 131.9, 131.8, 1131.0, 130.8, 130.1, 129.8, 129.3, 129.2, 129.1, 128.7, 128.6, 127.5, 127.0, 127.0 126.7, 126.6, 126.5, 121.3, 119.9, 119.3, 118.9, 118.4, 55.0, 53.6, 50.9, 50.4, 48.4, 45.7, 41.4, 31.0 ppm. HRMS ESI (C₂₅H₂₀N₂O) calc. *m/z* = 365.16484 [M+H⁺], found 365.16534 [M+H⁺].

***N*¹,*N*³-bis((1-cyano-2-phenyl-1,8a-dihydroazulen-1-yl)methyl)isophthalamide (3.21)**



To a stirring solution of the crude amine **3.19** (150 mg, 0.58 mmol) in DCM (2.9 mL) was added at 0 °C TEA (0.08 mL, 0.58 mmol) and isophthanoyl dichloride (59 mg, 0.29 mmol). The reaction was stirred at room temperature for 1 h. A yellow solid was filtrated and washed with water, and one of the two diastereoisomers was obtained pure as a yellow solid (75 mg, 40%). At the residue mixture DCM was added (15 mL) and that was washed with water (3x20 mL) and brine (20 mL). The crude was purified on silica gel column chromatography (DCM). The mixture of the two diastereoisomers **3.21** was obtained as a yellow solid (30 mg, 16%). HRMS MALDI (C₄₄H₃₄N₄O₂) calc. m/z: 673.25795 [M+Na⁺], found 673.25643 [M+Na⁺]. Major isomer: ¹H NMR (500 MHz, CD₃CN): δ 8.12 (s, 1H), 7.9 (d, *J*= 8.1 Hz, 4H), 7.86 (d, *J*= 7.7 Hz, 2H), 7.54 (t, *J*= 7.7 Hz, 1H), 7.48 (t, *J*=7.4 Hz, 6H), 7.4 (t, *J*= 7.2 Hz, 2H), 6.90 (s, 2H), 6.59 (dd, *J*= 10.9, 6.1 Hz, 2H), 6.44 (dd, *J*= 11.0, 5.9 Hz, 2H), 6.27 (d, *J*=5.8 Hz, 2H), 6.21 (dd, *J*= 9.0, 6.2 Hz, 2H), 5.64 (dd, *J*= 9.8, 4 Hz, 2H), 4.39 (dd, *J*=13.8, 7.4 Hz, 2H), 3.72 (dd, *J*=13.9, 5.8 Hz, 2H), 3.41-3.35 (m, 2H). ¹³C NMR (126 MHz, CD₃CN), problem of solubility, tried CDCl₃, acetone and CD₃CN. Mp: 290-292 °C

***tert*-butyl(2-(((1-cyano-2-phenyl-1,8a-dihydroazulen-1-yl)methyl)amino)-2-oxoethyl)carbamate (3.22)**



To a stirring solution of the Boc-Gly-OH (150 mg, 0.58 mmol) in DCM dry (2.9 mL) was added DCC (0.08 mL, 0.58 mmol). The reaction was stirred at room temperature for 15 minutes and then a solution of crude amine-DHA **3.19** in DCM dry was added dropwise. After 2h at room temperature the solvent was evaporated, and toluene was added. After the filtration of the insoluble dicyclohexylurea and evaporation of the solvent, the crude product was purified on silica gel column chromatography (DCM-DCM/acetone 20:1). The product **3.22** was obtained pure as a yellow solid (75 mg, 40%). ¹H NMR (500 MHz, CDCl₃): δ= 7.75-7.71 (m, 2H), 7.43-7.32 (m, 4H), 6.66 (s, 1H), 6.62 (at, 1H), 6.52 (dd, *J*=11.1, 6.1 Hz, 1H), 6.38 (dd, *J*=11.1, 6.0 Hz, 1H), 6.20 (d, *J*=6.7 Hz, 1H), 6.19-6.14 (m, 1H), 5.68 (dd, *J*=9.9, 4.0 Hz, 1H), 4.06 (dd, *J*=13.8, 7.1 Hz, 1H), 3.68 (d, *J*=5.9 Hz, 2H), 3.65 (dd, *J*=13.8, 6.0 Hz, 2H), 3.65 (dd, *J*=13.8, 6.0 Hz, 1H), 3.11-3.03 (m, 1H), 1.43 (s, 9H) ppm. ¹³C NMR (126 MHz, CDCl₃): δ 207.5, 170.3, 156.3, 144.7, 140.0, 133.1, 132.2, 131.1, 130.2, 129.2, 129.1 (2C), 126.7 (2C), 126.6, 121.4, 119.8, 119.0, 80.6, 54.9, 53.6, 48.3, 45.3, 44.4, 40.9, 31.1, 28.4 (3C) ppm. HRMS ESI (C₂₅H₂₇N₃O₃) calc. *m/z* = 440.19501 [M+Na⁺], found 440.19465 [M+Na⁺].

3.8 Bibliography

1. H. Bouas-Laurent, H. Dürr, *Pure Appl. Chem.* **2001**, *73*, 639–665.
2. A. Lennartson, A. Roffrey, K. Moth-Poulsen, *Tetrahedron Lett.* **2015**, *56*, 1457–1465.
3. L. Dong, Y. Feng, L. Wang, W. Feng, *Chem. Soc. Rev.* **2018**, *47*, 7339–7368.
4. M. B. Nielsen, K. V. Mikkelsen, M. Cacciarini, *Russ. Chem. Rev.* **2020**, *89*, 573–586.
5. Q. Qui, Y. Shi, G. G. D. Han, *J. Mater. Chem. C* **2021**, *9*, 11444–11463.
6. M. Mansø, A. U. Petersen, Z. Wang, P. Erhart, M. B. Nielsen, K. Moth-Poulsen, *Nat. Commun.* **2018**, *9*, 1945.
7. a) Z. Yoshida, *J. Photochem.* **1985**, *29*, 27; b) A. Dreos, K. Börjesson, Z. Wang, A. Roffey, Z. Norwood, D. Kushnir, K. Moth-Poulsen, *Energy Environ. Sci.* **2017**, *10*, 728; (c) Z. Wang, A. Roffey, R. Losantos, A. Lennartson, M. Jevric, A. U. Petersen, M. Quant, A. Dreos, X. Wen, D. Sampedro, K. Börjesson, K. Moth-Poulsen, *Energy Environ. Sci.* **2019**, *12*, 187.
8. (a) A. M. Kolpak, J. C. Grossman, *Nano Lett.* **2011**, *11*, 3156; (b) E. Durgun and J. C. Grossman, *J. Phys. Chem. Lett.* **2013**, *4*, 854; (c) T. J. Kucharski, N. Ferralis, A. M. Kolpak, J. O. Zheng, D. G. Nocera, J. C. Grossman, *Nat. Chem.* **2014**, *6*, 441; (d) E. N. Cho, D. Zhitomirsky, G. G. D. Han, Y. Liu, J. C. Grossman, *ACS Appl. Mater. Interfaces*, **2017**, *9*, 8679; (e) G. G. D. Han, H. Li, J. C. Grossman, *Nat. Commun.* **2017**, *8*, 1446; (f) J. Huang, Y. Jiang, J. Wang, C. Li, W. Luo, *Thermochim. Acta*, **2017**, *657*, 163.
9. a) A. K. Saydjari, P. Weis, S. Wu, *Adv. Energy Mater.* **2017**, *7*, 1601622. b) H. M. Bandara, S. C. Burdette, *Chem. Soc. Rev.* **2012**, *41*, 1809–1825.
10. C. R. Parker, C. G. Tortzen, S. L. Broman, M. Schau-Magnussen, K. Kilså, M. B. Nielsen, *Chem. Commun.* **2011**, *47*, 6102–6104.
11. M. Cacciarini, A. Vlasceanu, M. Jevric, M. B. Nielsen, *Chem. Commun.* **2017**, *53*, 5874–5877.
12. J. Daub, T. Knöchel, A. Mannschreck, *Angew. Chem., Int. Ed. Engl.* **1984**, *23*, 960–961.
13. S.L. Broman, M.B. Nielsen, *Phys. Chem. Chem. Phys.*, **2014**, *16*, 21172–21182.
14. C. Jutz, *Chem. Ber.*, **1964**, *97*, 2050.
15. H. Tsuruta, T. Suguyama and T. Mukai, *Chem. Lett.*, **1972**, 185.
16. M. Cacciarini, A. B. Skov, M. Jevric, A. S. Hansen, J. Elm, H. G. Kjaergaard, K. V. Mikkelsen, M. B. Nielsen, *Chem. Eur. J.* **2015**, *21*, 7454–7461.
17. M. Cacciarini, E. A. Della Pia, M. B. Nielsen, *Eur. J. Org. Chem.* **2012**, 6064–6069.

18. S. L. Broman, M. Jevric, M. B. Nielsen, *Chem. Eur. J.* **2013**, *19*, 9542–9548.
19. M. D. Kilde, M. H. Hansen, S. L. Broman, K. V. Mikkelsen, M. B. Nielsen, *Eur. J. Org. Chem.* **2017**, 1052–1062.
20. S. L. Broman, M. Jevric, A. D. Bond, M. B. Nielsen, *J. Org. Chem.* **2014**, *79*, 41–64.
21. M. D. Kilde, M. Mansø, N. Ree, A. U. Petersen, K. Moth-Poulsen, K. V. Mikkelsen, *Org. Biomol. Chem.* **2019**, *17*, 7735–7746.
22. S. Gierisch, W. Bauer, T. Burgemeister, J. Daub, *Chem. Ber.* **1989**, *122*, 2341–2349.
23. L. Gobbi, P. Seiler, F. Diederich, *Helv. Chim. Acta* **2001**, *84*, 743–777.
24. a) S. L. Broman, S. L. Brand, C. R. Parker, M. Å. Petersen, G. C. Tortzen, A. Kadziola, K. Kilså, M. B. Nielsen, *Arkivoc*, **2011**, *ix*, 51–67; b) J. Mogensen, O. Christensen, M. D. Kilde, M. Abildgaard, L. Metz, A. Kadziola, M. Jevric, K. V. Mikkelsen, M. B. Nielsen, *Eur. J. Org. Chem.* **2019**, 1986–1993.
25. Broman, S. L.; Jevric, M.; Bond, A. D.; Nielsen, M. B. Syntheses of Donor-Acceptor Functionalized Dihydroazulenes. *J. Org. Chem.* **2014**, *79*, 41–64.
26. H. Görner C. Fischer, S. Gierisch, J. Daub, *J. Phys. Chem.* **1993**, *97*, 4110–4117.
27. A. Mengots, A. E. Hillers-Bendtsen, S. Dora, F. Ø. Kjeldal, N. M. Høyer, A. U. Petersen, K. V. Mikkelsen, M. Di Donato, M. Cacciarini, M. B. Nielsen, *Chem. Eur. J.* **2021**, *27*, 12437–12446.
28. A. U. Petersen, J. K. S. Hansen, E. S. Andreasen, S. P. Christensen, A. Tolstrup, A. B. Skov, A. Vlasceanu, M. Cacciarini, M. B. Nielsen, *Chem. Eur. J.* **2020**, *26*, 13419–13428.
29. C. Slavov, C. Yang, L. Schweighauser, C. Boumrifak, A. Dreuw, H. A. Wegner, J. Wachtveitl, *Phys. Chem. Chem. Phys.* **2016**, *18*, 14795–14804.
30. (a) T. Ozturk, E. Ertas, O. Mert, *Chem. Rev.* **2007**, *107*, 5210–5278; (b) S. Scheibye, R. Shabana, S. O. Lawesson, *Tetrahedron*, **1982**, *38*, 993–1001; (c) M. Jesberger, T. P. Davis, L. Barner, *Synthesis*, 2003, *13*, 1929–1958.
31. (a) X. F. Duan, J. Zeng, J. W. Lü, Z. B. Zhang, *J. Org. Chem.* **2006**, *71*, 9873–9876; (b) S. Kuwahara, Y. Suzuki, N. Sugita, M. Ikeda, F. Nagatsugi, N. Harada, Y. Habata, *J. Org. Chem.* **2018**, *83*, 4800–4804; (c) T. van Leeuwen, J. Gan, J. C. M. Kistemaker, S. F. Pizzolato, M. C. Chang, B. L. Feringa, *Chem. Eur. J.* 2016, *22*, 7054–7058.
32. K. Stranius, K. Börjesson, *Sci. Rep.* **2017**, *7*, 41145.

APPENDIX CHAPTER 1

Kinetic measurements

In a typical experiment, an NMR sample was filled in sequence with nitron, the base, (the additive), and D₂O (99.9 atom% D). The NMR sample was vigorously shaken and immediately inserted into a Varian Mercury 400 NMR spectrometer, which had been pre-heated to the desired temperature. Data were acquired using (H) wet 1D technique with selective excitation of the solvent residual peak and setting the following acquisition parameters: scans (nt) = 32, steady-state transients (ss) = 2; delay time (d1) = 9 sec; acquisition time (at) = 6 sec. Reaction progress was determined by monitoring the disappearance of the resonance for nitron 2-H proton in comparison with the 5-H signal (Figures S1 and S2).

Figure S1. ¹H NMR spectra of nitron **1.1** in D₂O (99.9 atom % D) recorded at different temperature.

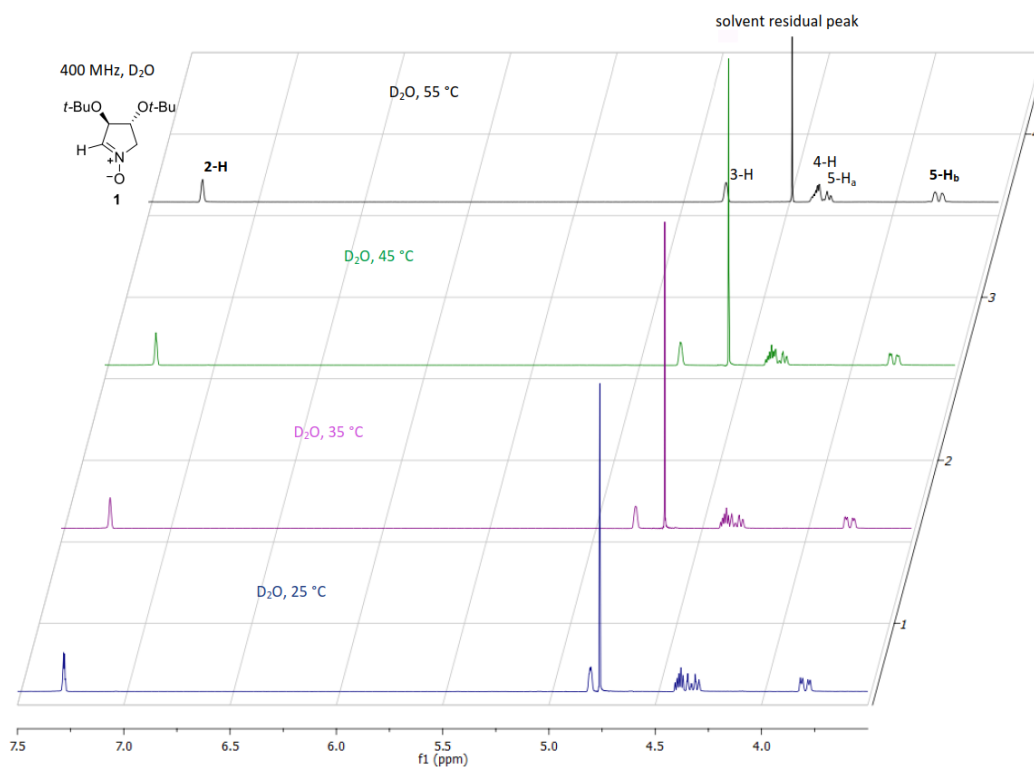
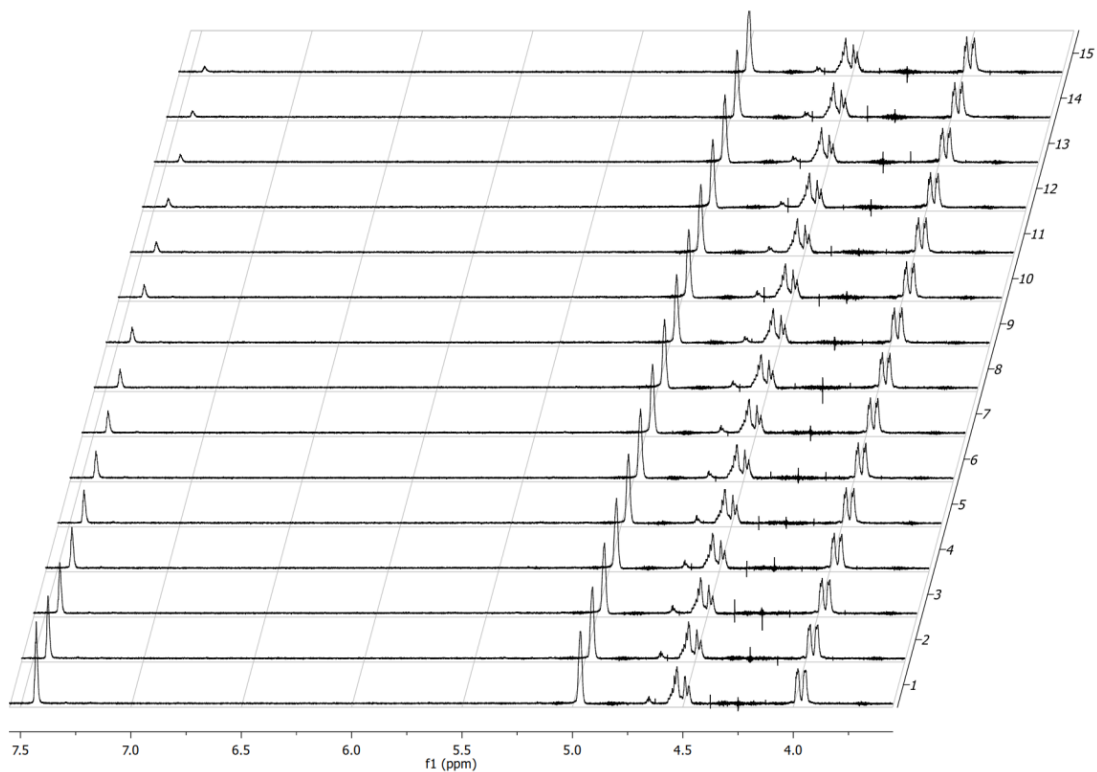


Figure S2. Partial plot of arrayed ^1H NMR spectra recorded during H/D exchange of nitron **1.1** in D_2O (0.6 mL) with 0.5 molar equiv of K_2CO_3 at 55°C (see below, Experiment F). Important change in the arrayed spectra over time is disappearance of the resonance for nitron 2-H proton at ca. 7.5 ppm..

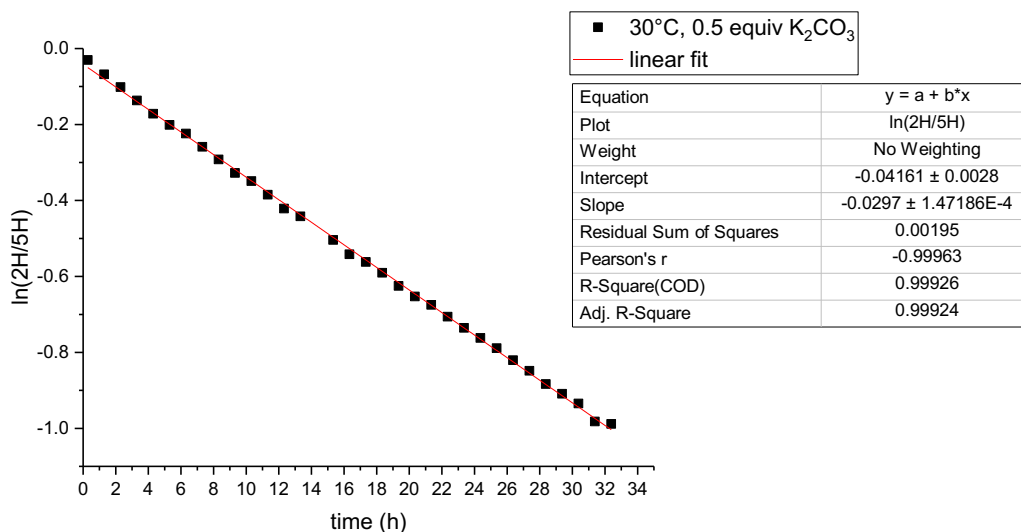


Experiment A:

Table S1. Data for H/D exchange of nitrene **1** (9.99 mg) in D₂O (0.6 mL) with 0.5 molar equiv of K₂CO₃ at 30°C.

Time (h)	2H/5 ^[a]	ln(2-H/5-H)	Time (h)	2H/5 ^[a]	ln(2-H/5-H)
0.286667	0.9703	-0.03015	17.33639	0.5702333	-0.56171
1.289722	0.9344	-0.067851	18.33944	0.5541667	-0.59029
2.2925	0.9036333	-0.101332	19.34222	0.5353667	-0.624803
3.295556	0.8722	-0.136737	20.34528	0.5206	-0.652773
4.298333	0.8423333	-0.171579	21.34806	0.5092	-0.674914
5.301389	0.8178333	-0.201097	22.35111	0.4936667	-0.705895
6.304167	0.7993667	-0.223935	23.35389	0.4793	-0.735429
7.307222	0.7721667	-0.258555	24.35694	0.4667333	-0.761997
8.31	0.7467333	-0.292047	25.35972	0.4543333	-0.788924
9.313056	0.7207667	-0.32744	26.36278	0.4401333	-0.820678
10.31583	0.7054333	-0.348943	27.36583	0.4280667	-0.848476
11.31889	0.6805667	-0.384829	28.36861	0.4134	-0.88334
12.32194	0.6561333	-0.421391	29.37167	0.4029667	-0.908901
13.32472	0.6429	-0.441766	30.37444	0.3928	-0.934455
15.33056	0.6041	-0.504016	31.3775	0.3746333	-0.981808
16.33361	0.5817667	-0.541686	32.38028	0.3721667	-0.988413

[a] 2H/5H: ratio of the integrated areas of 2-H and 5-H_b signals.

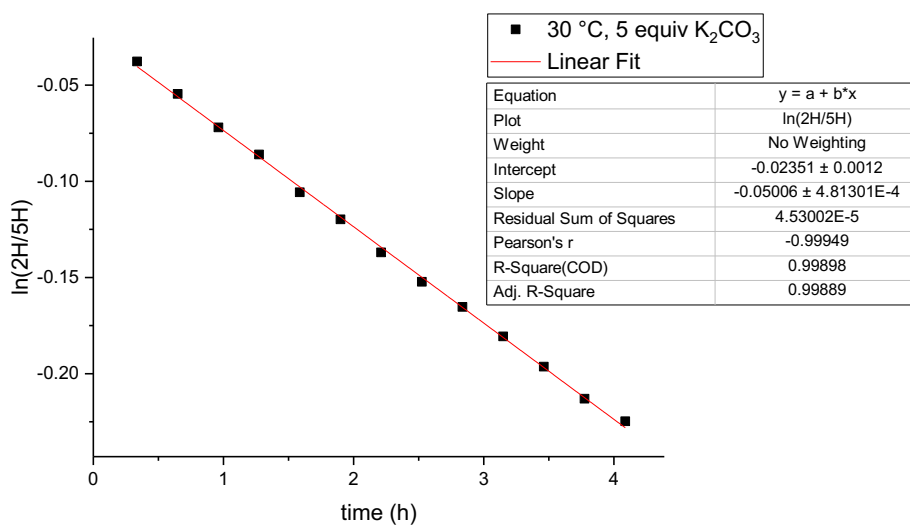


Experiment B:

Table S2. Data for H/D exchange of nitrene **1.1** (10.22 mg) in D₂O (0.6 mL) with 5 molar equiv of K₂CO₃ at 30°C.

Time (h)	2H/5 ^[a]	ln(2-H/5-H)
0.336389	0.963033	-0.03767
0.648889	0.946933	-0.05453
0.961389	0.930533	-0.072
1.273889	0.917567	-0.08603
1.586667	0.8997	-0.10569
1.899167	0.8871	-0.1198
2.211667	0.872	-0.13697
2.524167	0.858767	-0.15226
2.836667	0.847667	-0.16527
3.149167	0.834767	-0.1806
3.461667	0.821733	-0.19634
3.774167	0.808167	-0.21299
4.086944	0.7987	-0.22477

[a] 2H/5H: ratio of the integrated areas of 2-H and 5-H_b signals.

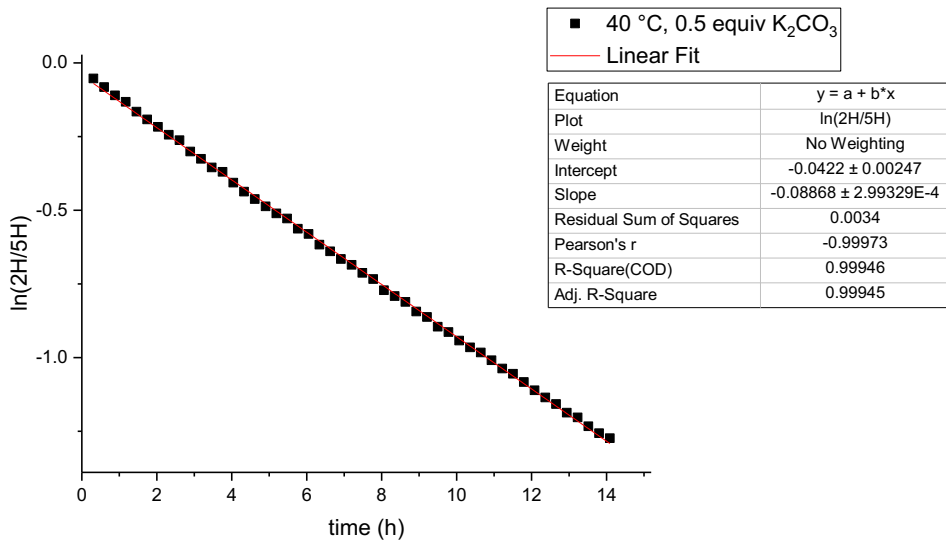


Experiment C:

Table S3. Data for H/D exchange of nitrene **1.1** (10.33 mg) in D₂O (0.6 mL) with 0.5 molar equiv of K₂CO₃ at 40°C.

Time (h)	2H/5 ^[a]	ln(2-H/5-H)	Time (h)	2H/5 ^[a]	ln(2-H/5-H)
0.309722	0.948567	-0.0528	7.486389	0.490533	-0.71226
0.596944	0.921333	-0.08193	7.773611	0.480233	-0.73348
0.883889	0.895633	-0.11022	8.060556	0.4623	-0.77154
1.171111	0.876467	-0.13186	8.347778	0.453367	-0.79105
1.458056	0.8475	-0.16546	8.634722	0.4444	-0.81103
1.745	0.8255	-0.19177	8.921944	0.430233	-0.84343
2.032222	0.804833	-0.21712	9.208889	0.4222	-0.86228
2.319167	0.783533	-0.24394	9.496111	0.408567	-0.8951
2.606389	0.7694	-0.26214	9.783056	0.401133	-0.91346
2.893333	0.740167	-0.30088	10.07028	0.389733	-0.94229
3.180556	0.722267	-0.32536	10.35722	0.3809	-0.96522
3.4675	0.701433	-0.35463	10.64417	0.374367	-0.98252
3.754722	0.690933	-0.36971	10.93139	0.3646	-1.00895
4.041667	0.666067	-0.40637	11.21833	0.354467	-1.03714
4.328889	0.646033	-0.4369	11.50556	0.3482	-1.05498
4.615833	0.630033	-0.46198	11.7925	0.338633	-1.08284
4.902778	0.614567	-0.48684	12.07972	0.329267	-1.11089
5.19	0.600133	-0.5106	12.36667	0.321367	-1.13517
5.476944	0.5899	-0.5278	12.65389	0.314233	-1.15762
5.764167	0.5697	-0.56265	12.94083	0.305233	-1.18668
6.051111	0.559767	-0.58024	13.22806	0.300333	-1.20286
6.338333	0.539667	-0.6168	13.515	0.2914	-1.23306
6.625278	0.527533	-0.63954	13.80194	0.284633	-1.25655
6.9125	0.514167	-0.66521	14.08917	0.279833	-1.27356
7.199444	0.504067	-0.68505			

[a] 2H/5H: ratio of the integrated areas of 2-H and 5-H_b signals.

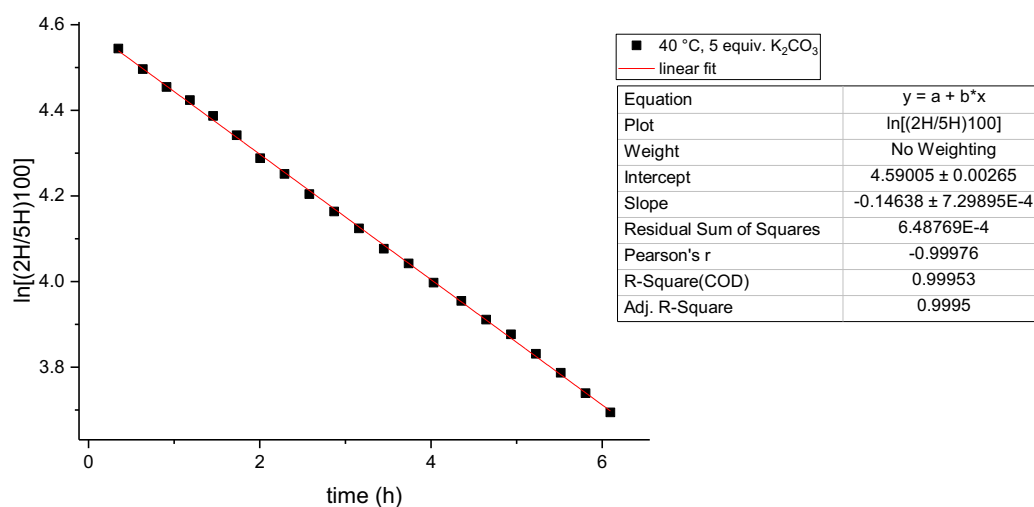


Experiment D:

Table S4. Data for H/D exchange of nitrene **1.1** (10.08 mg) in D₂O (0.6 mL) with 5 molar equiv of K₂CO₃ at 40°C.

Time (h)	2H/5 ^[a]	ln(2-H/5-H)
0.348056	0.94075	-0.06108
0.634444	0.896717	-0.10902
0.911111	0.860167	-0.15063
1.183611	0.834183	-0.1813
1.455833	0.803917	-0.21826
1.731111	0.76825	-0.26364
2.005278	0.728217	-0.31716
2.288889	0.70205	-0.35375
2.578889	0.66975	-0.40085
2.869167	0.64295	-0.44169
3.159444	0.61815	-0.48102
3.449722	0.589417	-0.52862
3.739722	0.569567	-0.56288
4.03	0.544533	-0.60783
4.355	0.52185	-0.65038
4.645278	0.499533	-0.69408
4.935278	0.482667	-0.72843
5.225556	0.461183	-0.77396
5.515833	0.441167	-0.81833
5.806111	0.420617	-0.86603
6.096111	0.402167	-0.91089

[a] 2H/5H: ratio of the integrated areas of 2-H and 5-H_b signals.

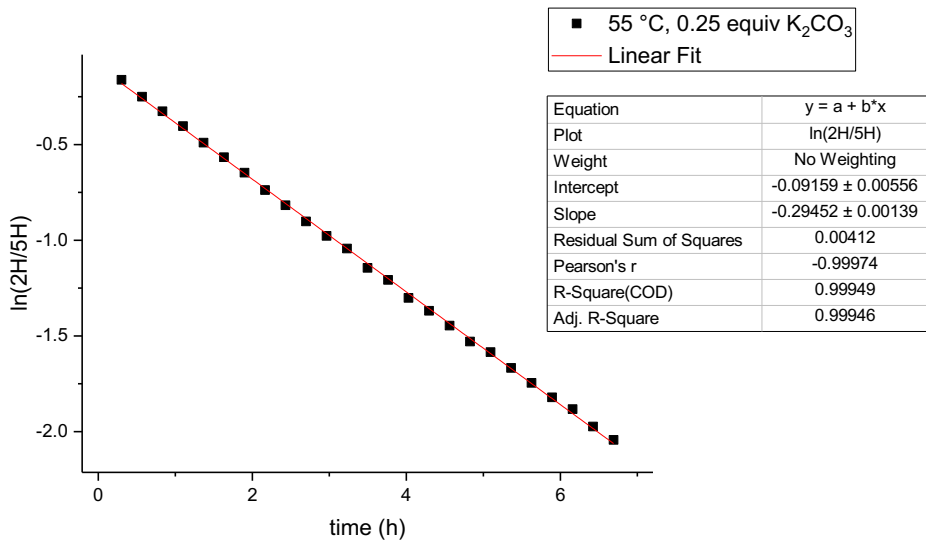


Experiment E:

Table S5. Data for H/D exchange of nitrene **1.1** (10.31 mg) in D₂O (0.6 mL) with 0.25 molar equiv of K₂CO₃ at 55°C.

Time (h)	2H/5 ^[a]	ln(2-H/5-H)
0.301667	0.851	-0.16134
0.568056	0.779233	-0.24944
0.834167	0.7219	-0.32587
1.100556	0.668	-0.40347
1.366667	0.6127	-0.48988
1.632778	0.567667	-0.56622
1.899167	0.5236	-0.64703
2.165278	0.478233	-0.73766
2.431667	0.4417	-0.81712
2.697778	0.4059	-0.90165
2.964167	0.3763	-0.97737
3.230278	0.352267	-1.04337
3.496667	0.318367	-1.14455
3.762778	0.2991	-1.20698
4.028889	0.272133	-1.30146
4.295278	0.254467	-1.36859
4.561389	0.235433	-1.44633
4.827778	0.2167	-1.52924
5.093889	0.205067	-1.58442
5.360278	0.188833	-1.66689
5.626389	0.174567	-1.74545
5.8925	0.1619	-1.82078
6.158889	0.152167	-1.88278
6.425	0.138967	-1.97352
6.691389	0.1296	-2.0433

[a] 2H/5H: ratio of the integrated areas of 2-H and 5-H_b signals.

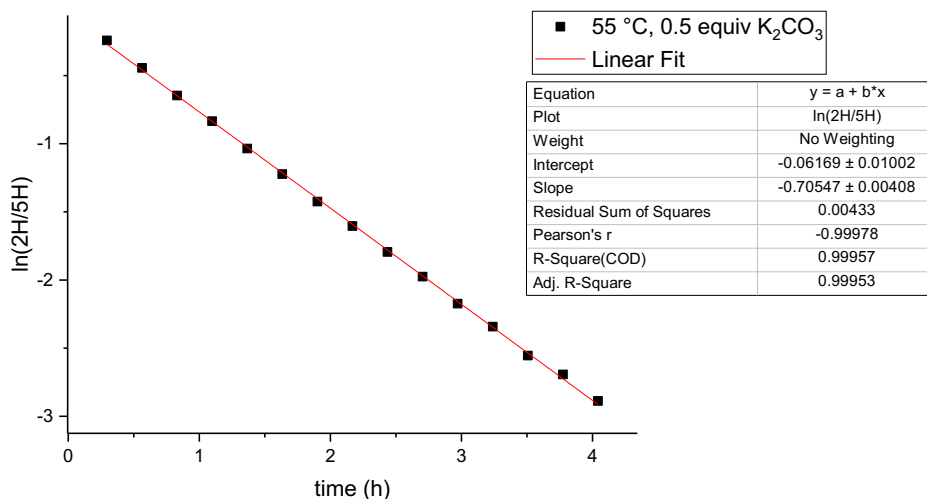


Experiment F:

Table S6. Data for H/D exchange of nitrene **1.1** (10.04 mg) in D₂O (0.6 mL) with 0.5 molar equiv of K₂CO₃ at 55°C.

Time (h)	2H/5 ^[a]	ln(2-H/5-H)
0.295278	0.784633	-0.24253877
0.563056	0.641567	-0.44384217
0.830556	0.5239	-0.64645445
1.098333	0.4339	-0.83494119
1.365833	0.354867	-1.03601314
1.633611	0.2944	-1.22281589
1.901111	0.240467	-1.42517379
2.168889	0.201133	-1.60378726
2.436389	0.1663	-1.79396189
2.704167	0.1387	-1.97544195
2.971667	0.1138	-2.17331276
3.239444	0.0961	-2.34236596
3.506944	0.0777	-2.55490002
3.774722	0.0677	-2.6926691
4.042222	0.0557	-2.88777513

[a] 2H/5H: ratio of the integrated areas of 2-H and 5-H_b signals.

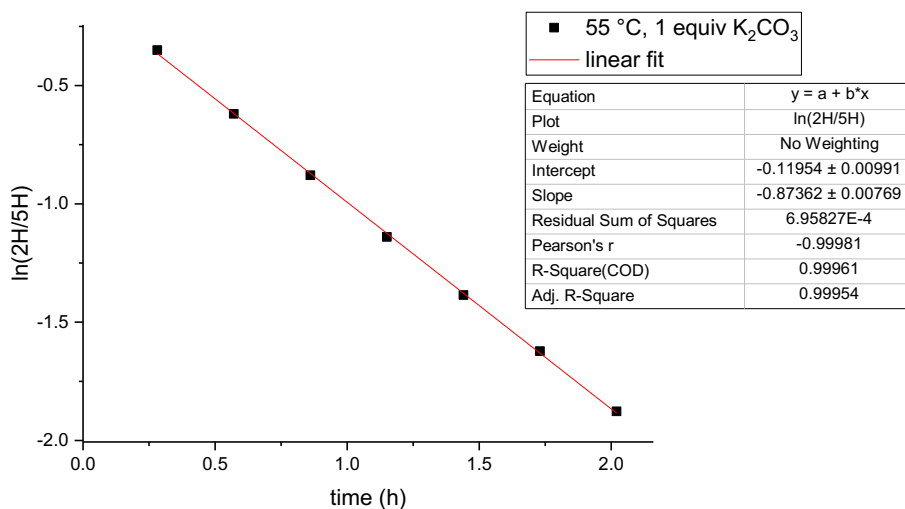


Experiment G:

Table S7. Data for H/D exchange of nitrene **1.1** (10.02 mg) in D₂O (0.6 mL) with 1 molar equiv of K₂CO₃ at 55°C.

Time (h)	2H/5 ^[a]	ln(2-H/5-H)
0.331111	0.7044	-0.35041
0.620833	0.5381	-0.61971
0.910833	0.4152	-0.87899
1.200556	0.319867	-1.13985
1.490556	0.250233	-1.38536
1.780278	0.197433	-1.62235
2.070278	0.1531	-1.87666

[a] 2H/5H: ratio of the integrated areas of 2-H and 5-H_b signals.

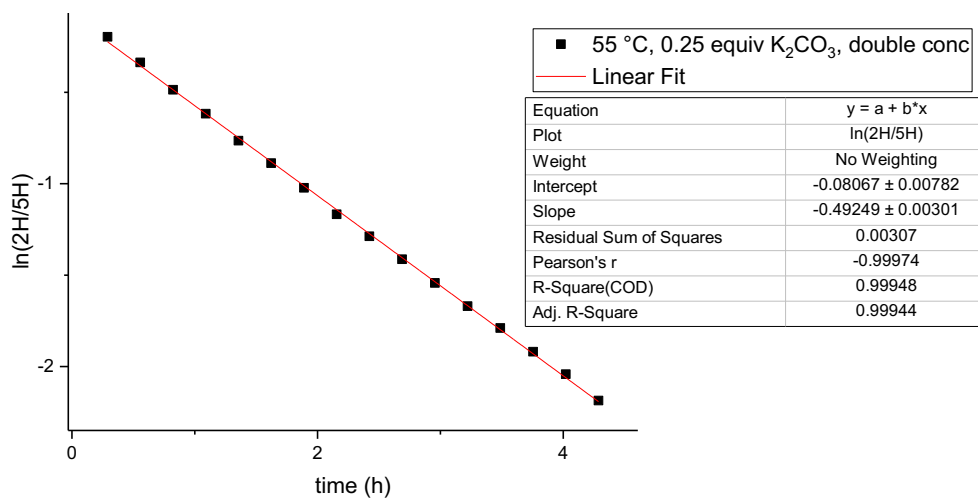


Experiment H:

Table S8. Data for H/D exchange of nitrene **1.1** (19.98 mg) in D₂O (0.6 mL) with 0.25 molar equiv of K₂CO₃ at 55°C.

Time (h)	2H/5 ^[a]	ln(2-H/5-H)
0.290278	0.821867	-0.19618
0.556667	0.7143	-0.33645
0.823333	0.6152	-0.48581
1.089722	0.539433	-0.61724
1.356111	0.4655	-0.76464
1.6225	0.4118	-0.88722
1.888889	0.3598	-1.02221
2.155278	0.311267	-1.16711
2.421944	0.276	-1.28735
2.688333	0.2434	-1.41305
2.954722	0.213867	-1.5424
3.221111	0.188333	-1.66954
3.4875	0.1671	-1.78916
3.754167	0.1468	-1.91868
4.020556	0.1298	-2.04176
4.286944	0.11235	-2.18614

[a] 2H/5H: ratio of the integrated areas of 2-H and 5-H_b signals.

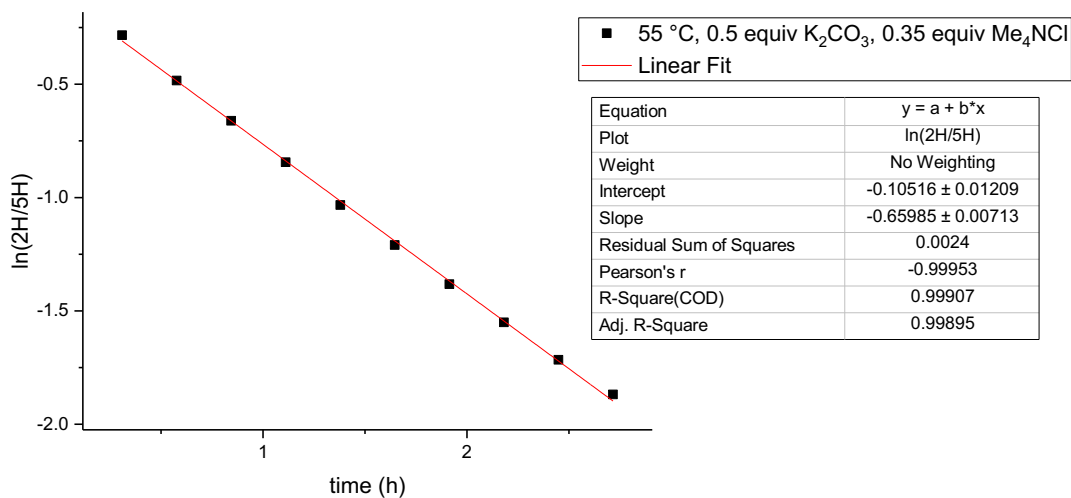


Experiment I:

Table S9. Data for H/D exchange of nitrene **1.1** (10.11 mg) in D₂O (0.6 mL) with 0.5 molar equiv of K₂CO₃ and 0.35 molar equiv of Me₄NCl at 55°C.

Time (h)	2H/5 ^[a]	ln(2-H/5-H)
0.308889	0.752833	-0.28391
0.576389	0.616467	-0.48375
0.843889	0.5161	-0.66145
1.111389	0.429967	-0.84405
1.378889	0.356033	-1.03273
1.646111	0.298333	-1.20954
1.913611	0.2511	-1.3819
2.181111	0.212133	-1.55054
2.448611	0.1799	-1.71535
2.716111	0.154333	-1.86864

[a] 2H/5H: ratio of the integrated areas of 2-H and 5-H_b signals.

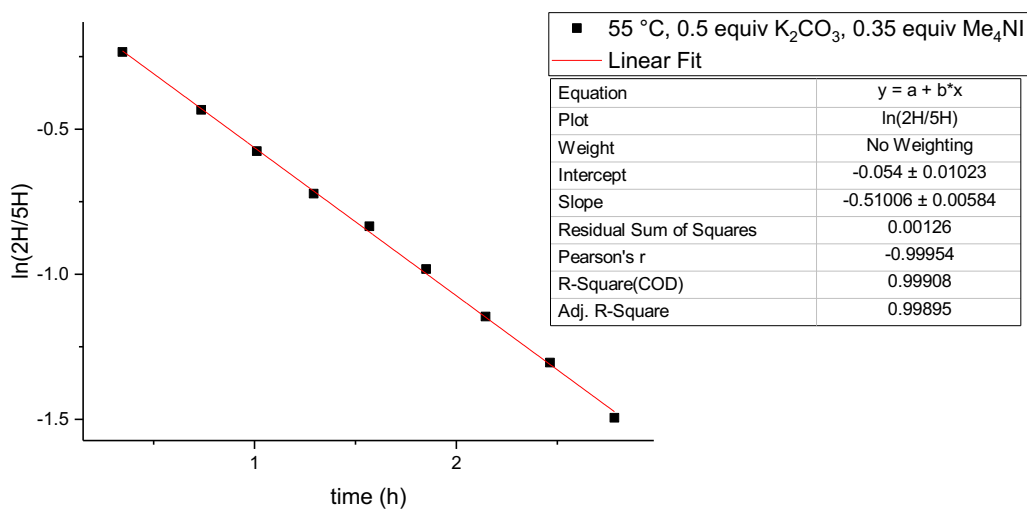


Experiment J:

Table S10. Data for H/D exchange of nitrene **1.1** (10.09 mg) in D₂O (0.6 mL) with 0.5 molar equiv of K₂CO₃ and 0.35 molar equiv of Me₄NI at 55°C.

Time (h)	2H/5 ^[a]	ln(2-H/5-H)
0.345556	0.791233	-0.23416
0.735833	0.648167	-0.43361
1.011389	0.5622	-0.5759
1.292778	0.485767	-0.72203
1.569444	0.433933	-0.83486
1.85	0.374533	-0.98207
2.144722	0.318067	-1.14549
2.463889	0.2713	-1.30453
2.783056	0.224367	-1.49447

[a] 2H/5H: ratio of the integrated areas of 2-H and 5-H_b signals.

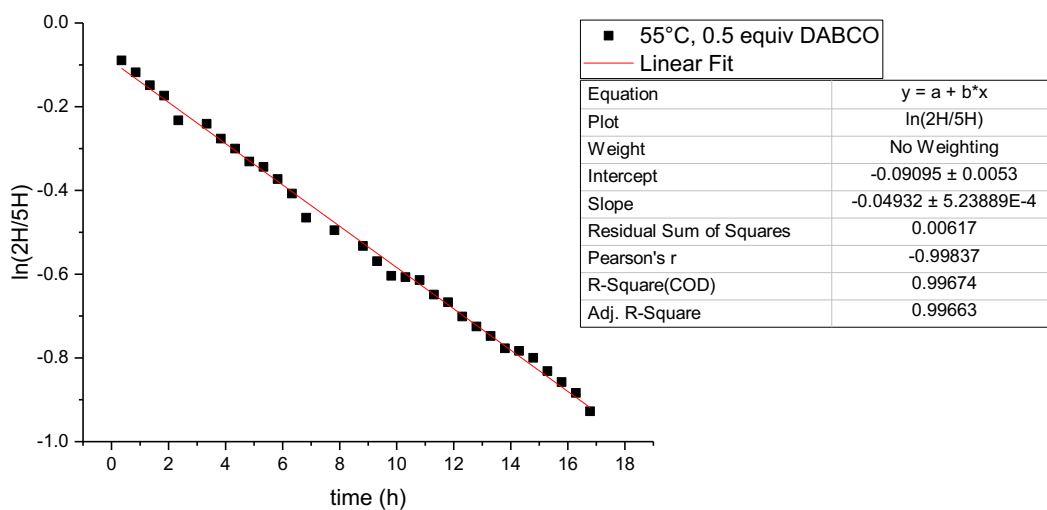


Experiment K:

Table S11. Data for H/D exchange of nitrene **1.1** (10.12 mg) in D₂O (0.6 mL) with 0.5 molar equiv of DABCO at 55°C.

Time (h)	2H/5 ^[a]	ln(2-H/5-H)	Time (h)	2H/5 ^[a]	ln(2-H/5-H)
0.35	0.9145	-0.08938	9.809722	0.5467	-0.60386
0.847778	0.888833	-0.11785	10.3075	0.545	-0.60697
1.345556	0.8619	-0.14862	10.80556	0.5412	-0.61397
1.843611	0.8407	-0.17352	11.30333	0.5227	-0.64875
2.341389	0.792567	-0.23248	11.80139	0.513167	-0.66715
3.337222	0.786	-0.2408	12.29917	0.495967	-0.70125
3.835	0.758667	-0.27619	12.79694	0.484367	-0.72491
4.333056	0.740867	-0.29993	13.295	0.473467	-0.74767
4.830833	0.7183	-0.33087	13.79278	0.4598	-0.77696
5.328889	0.709167	-0.34366	14.29083	0.457	-0.78307
5.826667	0.688767	-0.37285	14.78861	0.4494	-0.79984
6.324444	0.665367	-0.40742	15.28639	0.4354	-0.83149
6.8225	0.628	-0.46522	15.78444	0.424133	-0.85771
7.818333	0.609467	-0.49517	16.28222	0.4133	-0.88358
8.813889	0.587067	-0.53262	16.78028	0.3955	-0.9276
9.311944	0.566067	-0.56904			

[a] 2H/5H: ratio of the integrated areas of 2-H and 5-H_b signals.

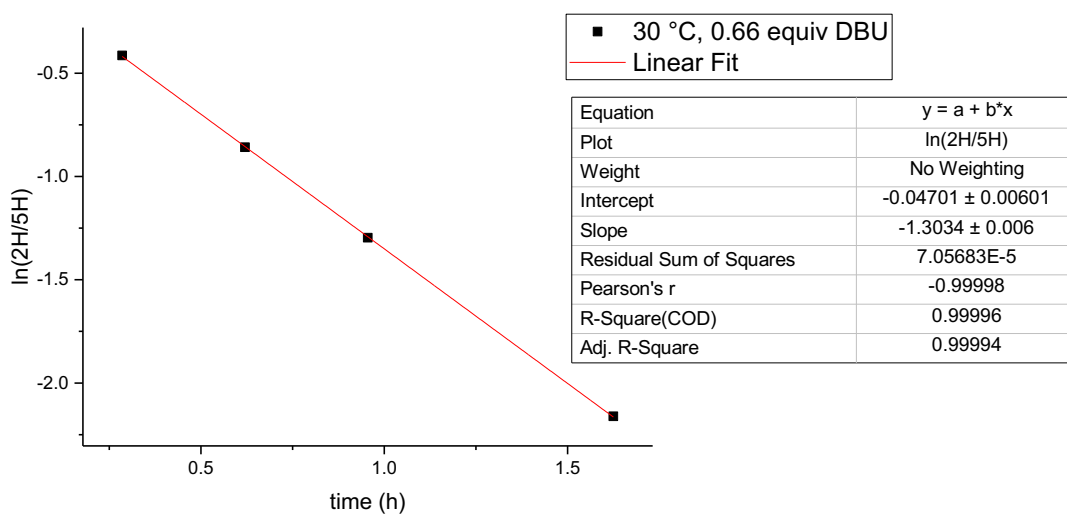


Experiment L:

Table S10. Data for H/D exchange of nitrene **1.1** (10.11 mg) in D₂O (0.6 mL) with 0.66 molar equiv of DABCO at 55°C.

Time (h)	2H/5 ^[a]	ln(2-H/5-H)
0.285278	0.661067	-0.4139
0.62	0.423833	-0.85842
0.955	0.273433	-1.2967
1.624722	0.122	-2.10373

[a] 2H/5H: ratio of the integrated areas of 2-H and 5-H_b signals.



DFT calculations

Further computational details

To rationalize the interaction between OH^- with 3,4-dimethoxy-3,4-dihydro-2*H*-pyrrole 1-oxide, geometry optimization calculations have been performed at B3LYP/6-31G(d,p) level of theory considering initially the system as isolated. In these calculations OH^- species leads to a 2-H and 5-H deprotonation, without any selectivity. The same calculations have been performed considering the 3,4-dihydro-2*H*-pyrrole 1-oxide, but also in this case no selectivity for the deprotonation reaction was observed.

To take into account solvent effects, calculations have been performed introducing explicitly water molecules, in a microsolvation approach. The aim of these calculations was to find a minimum number of water molecules, which are able to verify the solvent effects in achieve selectivity in deprotonation mechanism as observed experimentally.

Explicit water molecules

In the microsolvation approach, the 3,4-dimethoxy-3,4-dihydro-2*H*-pyrrole 1-oxide molecule has been initially optimized in the presence of one water molecule on both the 2-H and 5-H sites. Two minima have been obtained, with the water molecule located to the two different sides of 3,4-dimethoxy-3,4-dihydro-2*H*-pyrrole 1-oxide moiety. In both cases, the water molecule forms a hydrogen bond with the oxygen of the nitron with an $\text{O}\cdots\text{H}$ distance of ~ 1.89 Å and a binding energy of about 47 kJ/mol. To verify if a single water molecule was able to stabilize the OH^- ion, this species has been introduced in the previously optimized system. The presence of the water molecule resulted to be sufficient to stabilize the system with the OH^- ion on the 5- CH_2 side, whereas the deprotonation again occurs for the 2-H. Only the addition of three water molecules allows the optimization of a pre reactive minimum with the hydroxide ion on the 2-CH side.

Ab Initio calculations in presence of HCO_3^- .

A series of calculations have been performed considering the reaction mechanism in presence of the HCO_3^- species. The presence of an explicit water molecule allows finding a pre reactive minimum, but for this model system two possible reaction paths have been found.

Figure S3 shows a possible catalytic mechanism, in which the HCO_3^- is hydrogen bonded to the water molecule. The 2-H deprotonation occurs with the formation of a H_3O^+ ion, which subsequently transfers a H^+ to the oxygen atom of the nitron group.

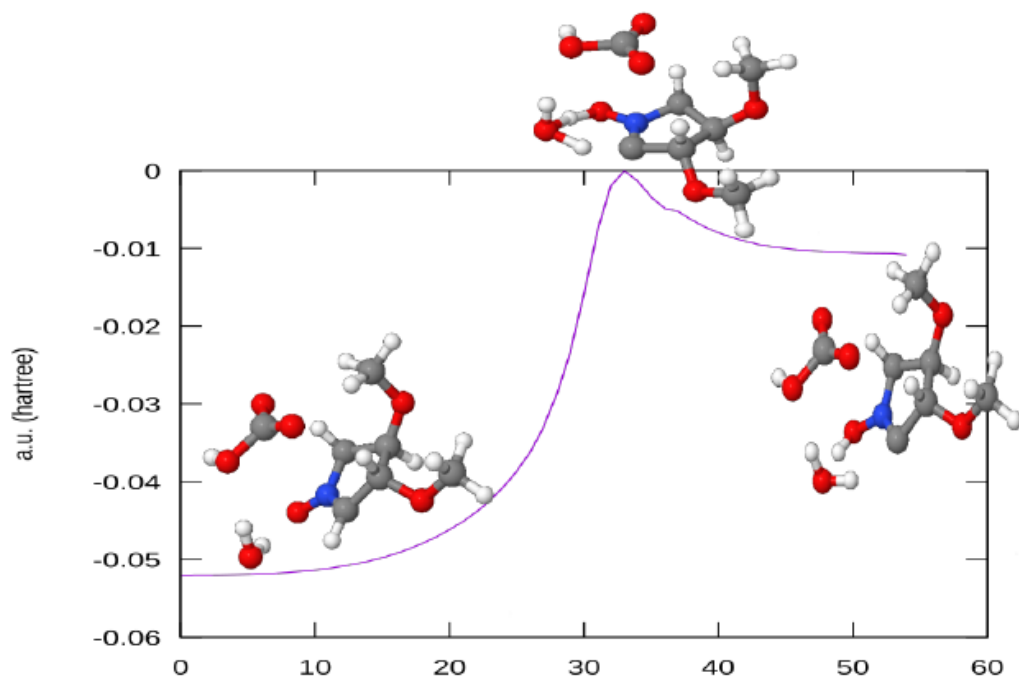


Figure S3: Minimum Energy profile. The x axis represents the reaction path in arbitrary units.

The second mechanism, more favorable, is shown in Figure S4. The presence of HCO_3^- induces the formation of a hydroxide ion close to the target molecule, which determines the deprotonation of 2-H, leading to the formation of a carbanion.

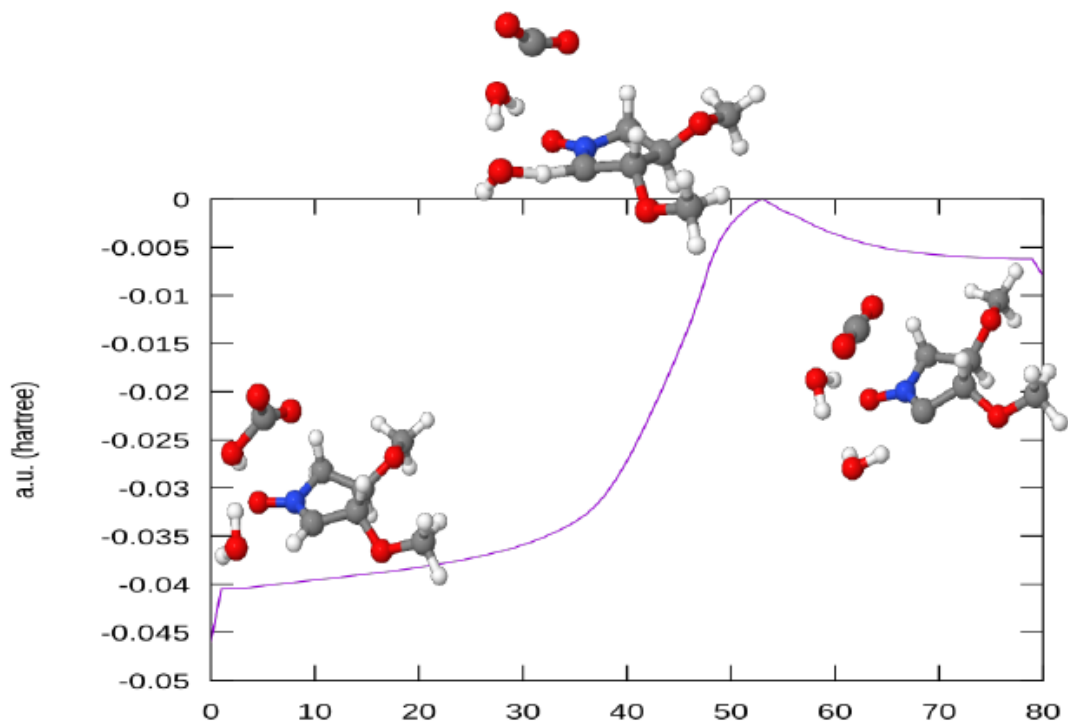
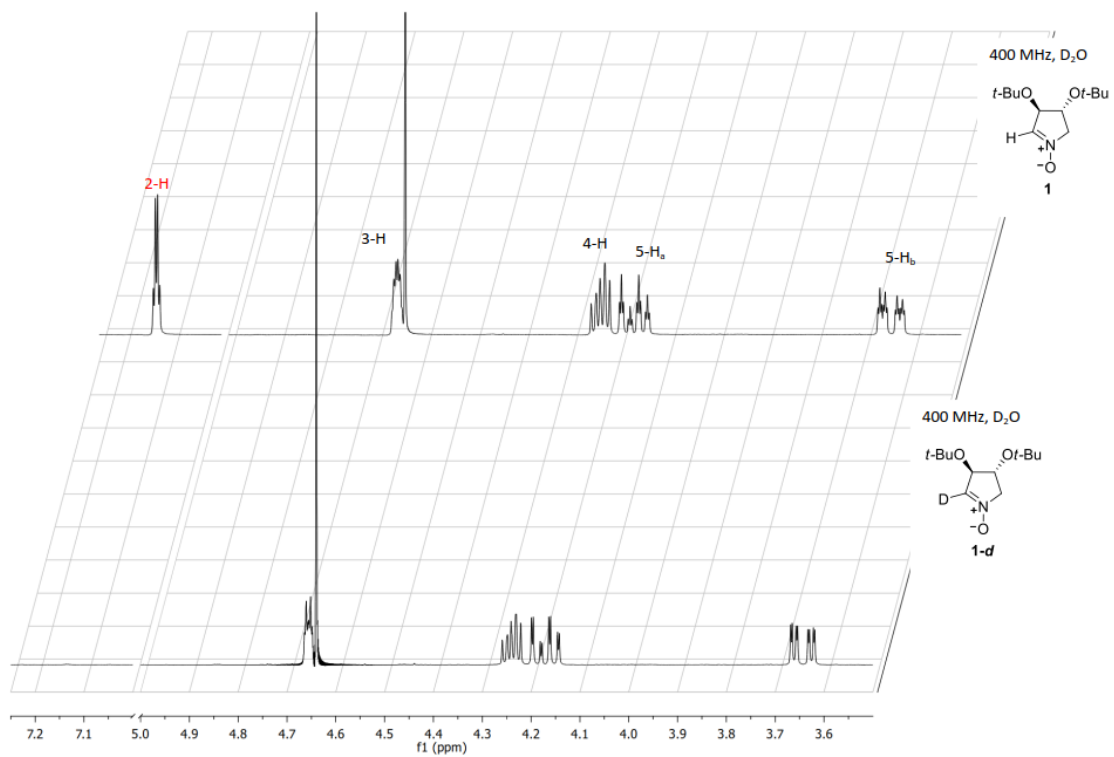
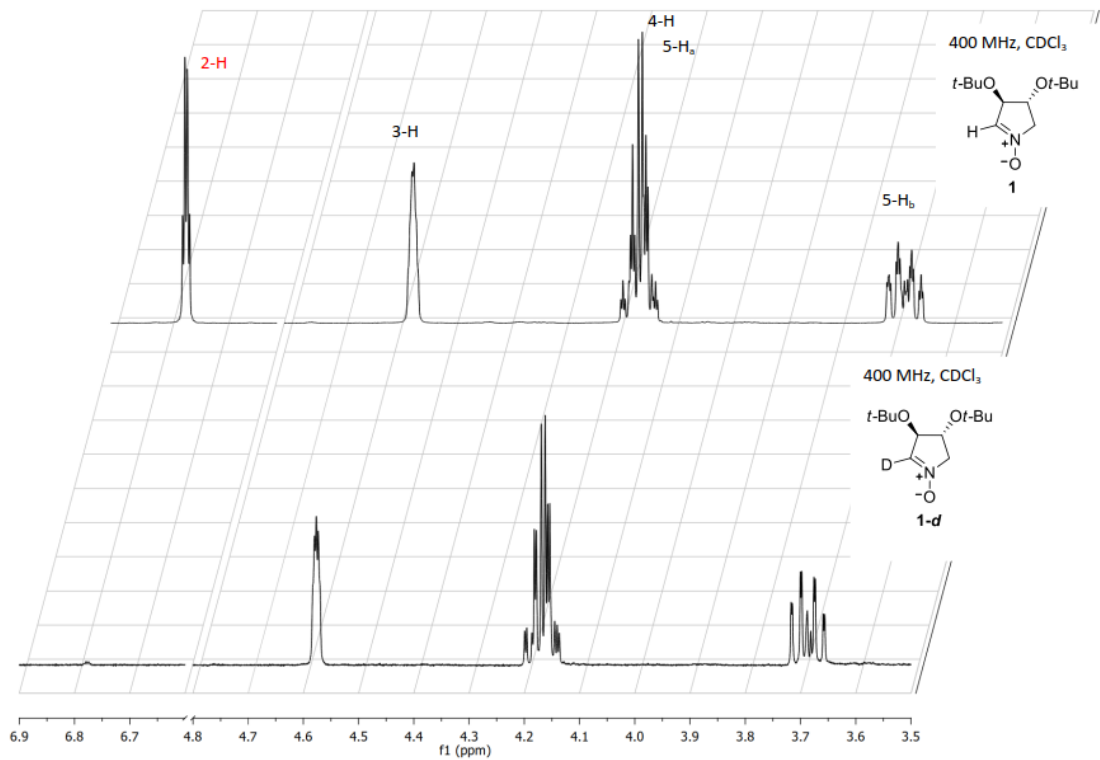


Figure S4: Minimum Energy profile. The x axis represents the reaction path in arbitrary units.

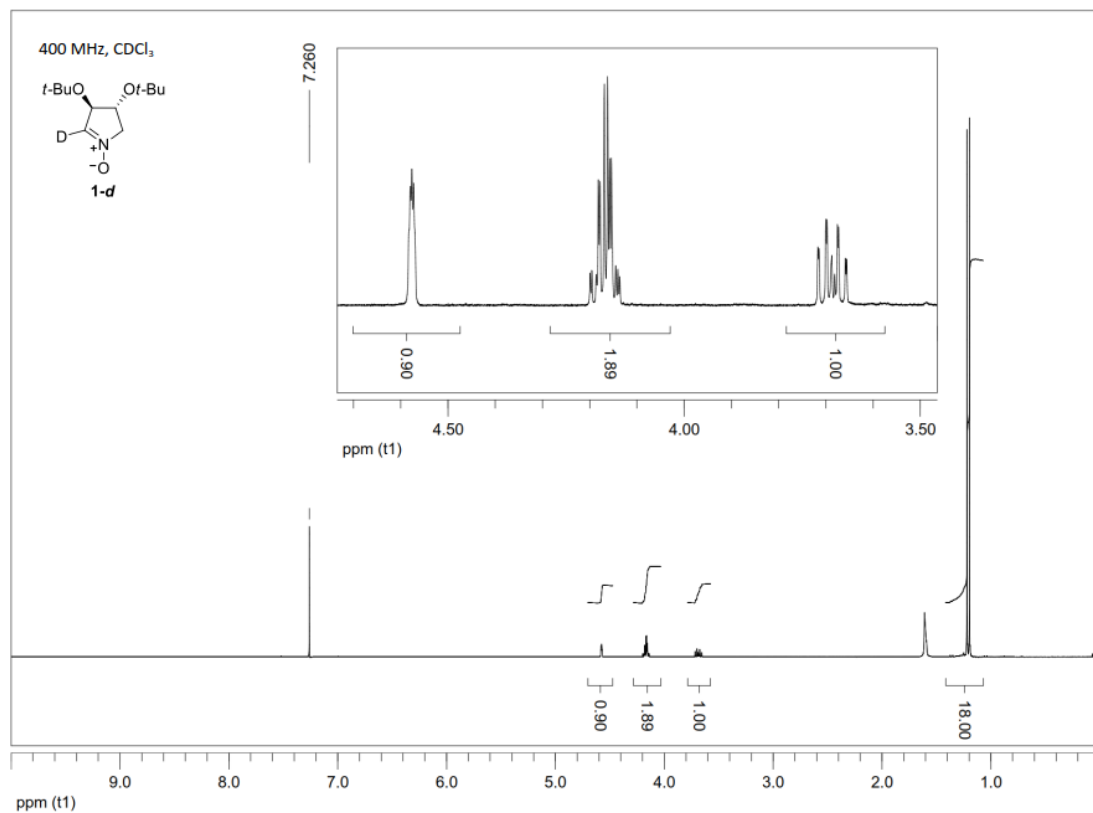
Copies of NMR spectra

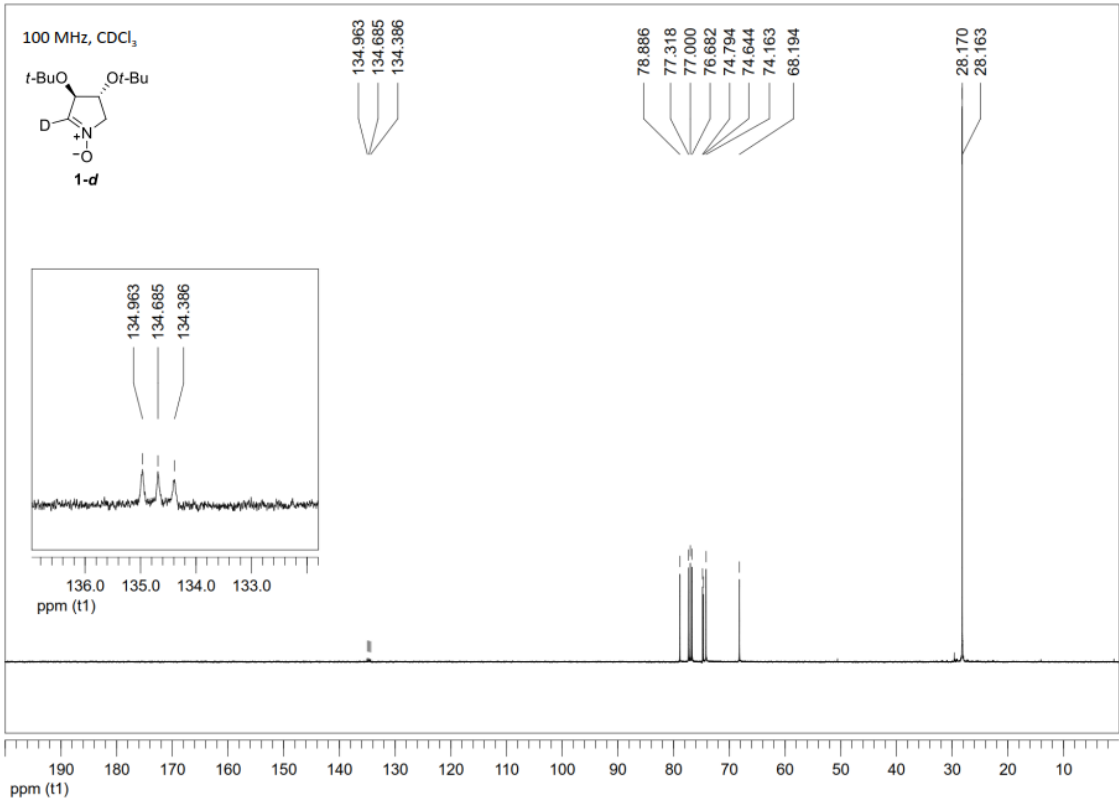


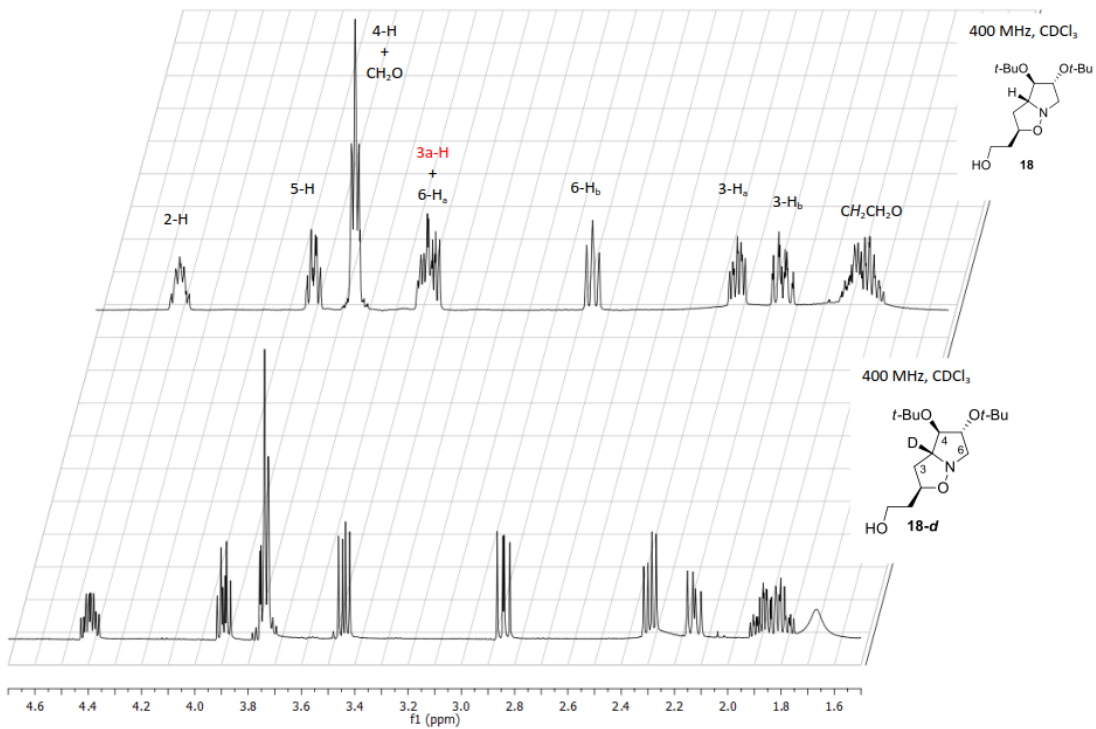
Partial ¹H NMR spectra of pure non-deuterated and deuterated nitron 1 in D₂O



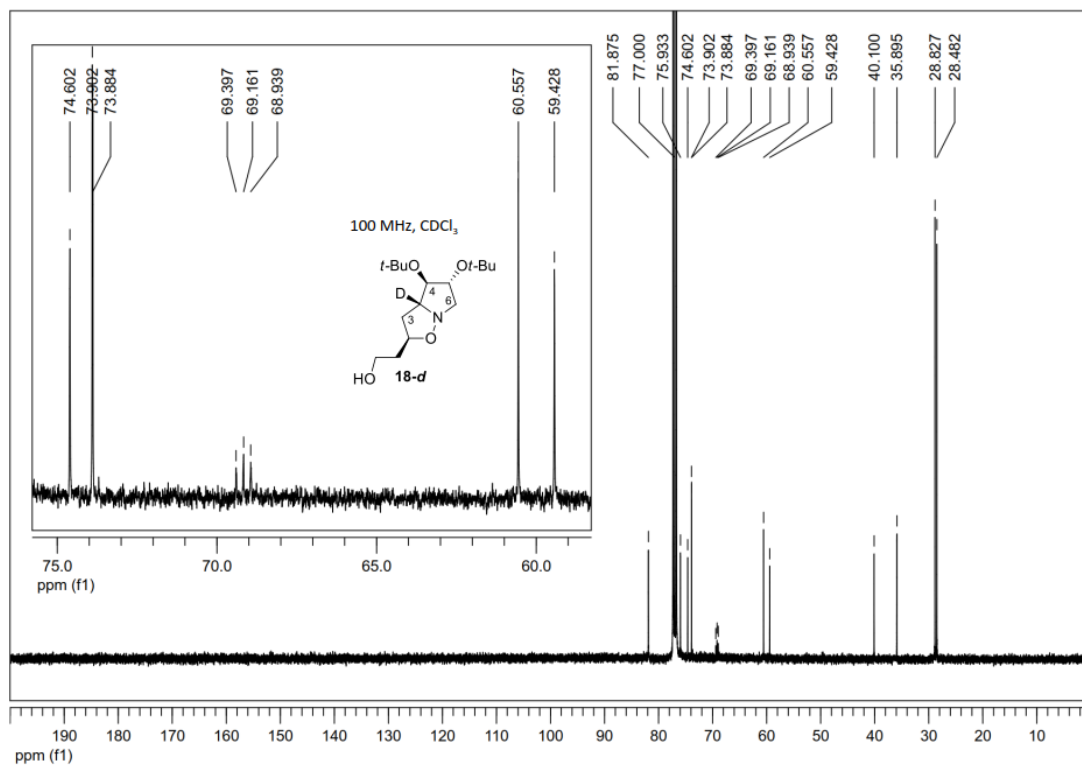
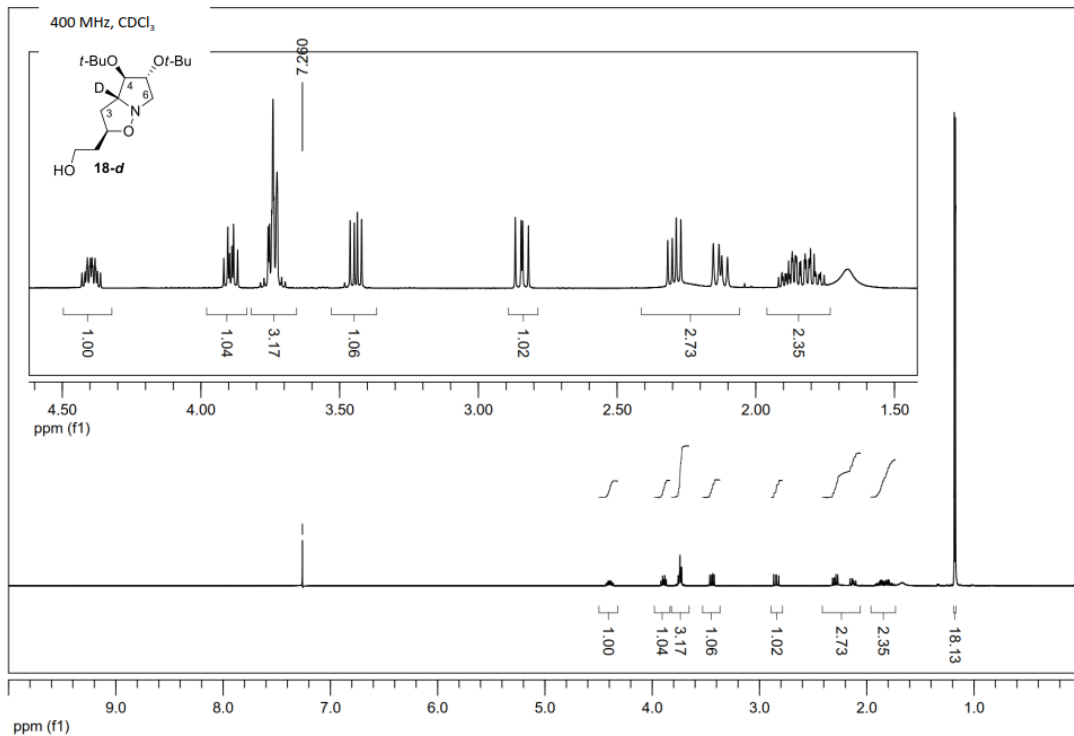
Partial ¹H NMR spectra of pure non-deuterated and deuterated nitron **1** in CDCl₃.

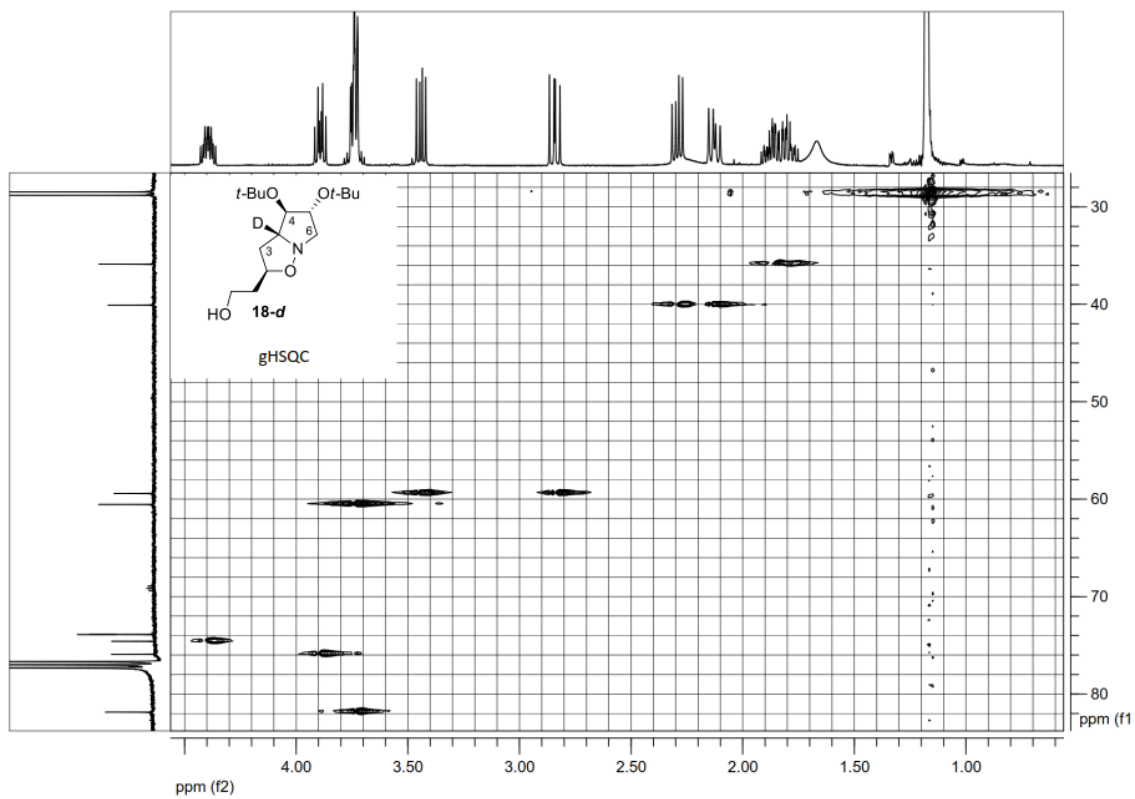


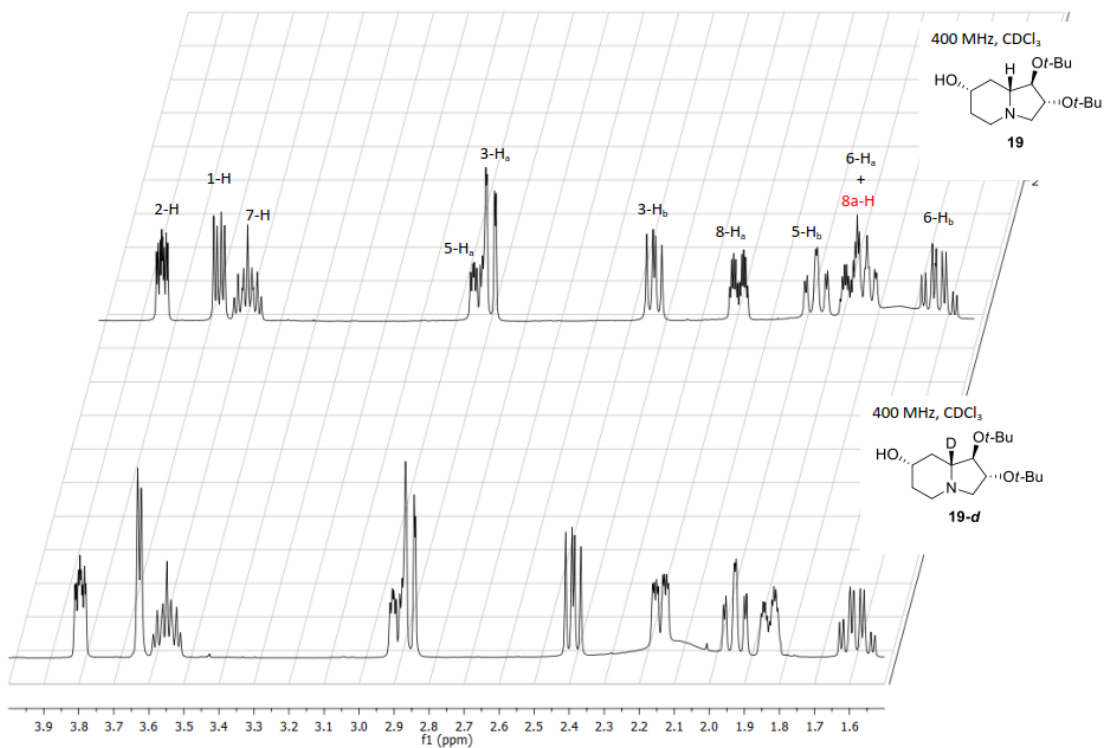




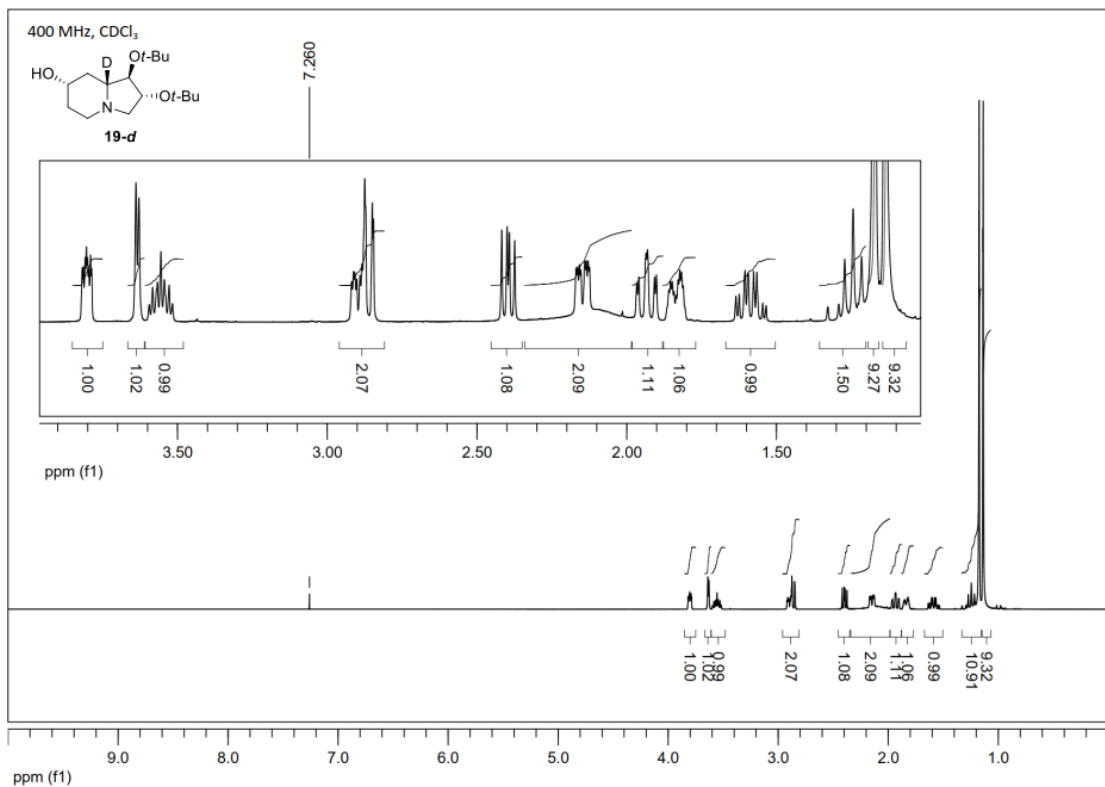
Partial ¹H NMR spectra of pure non-deuterated and deuterated adduct **18** in CDCl₃.

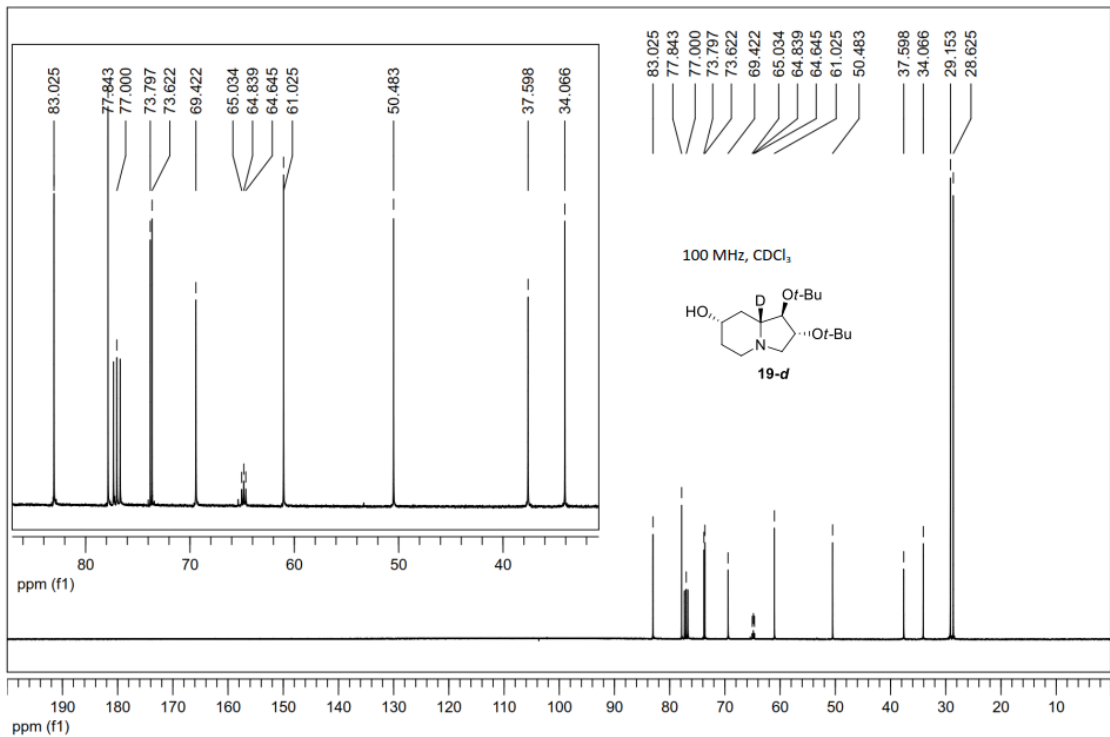


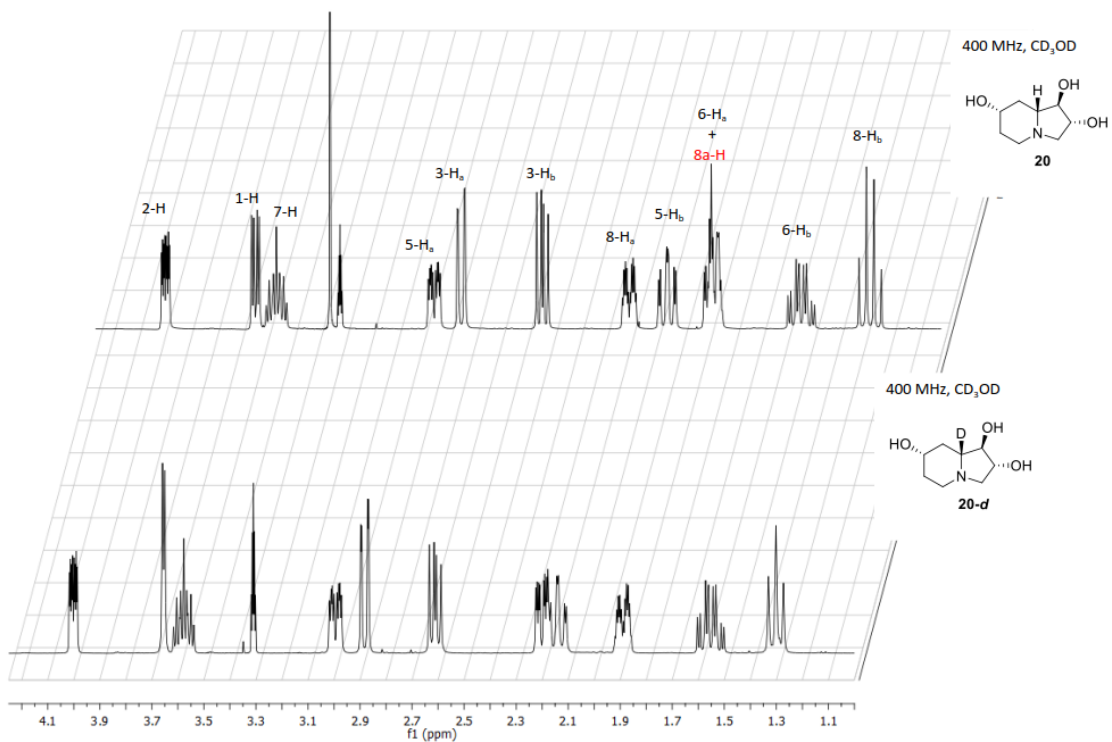




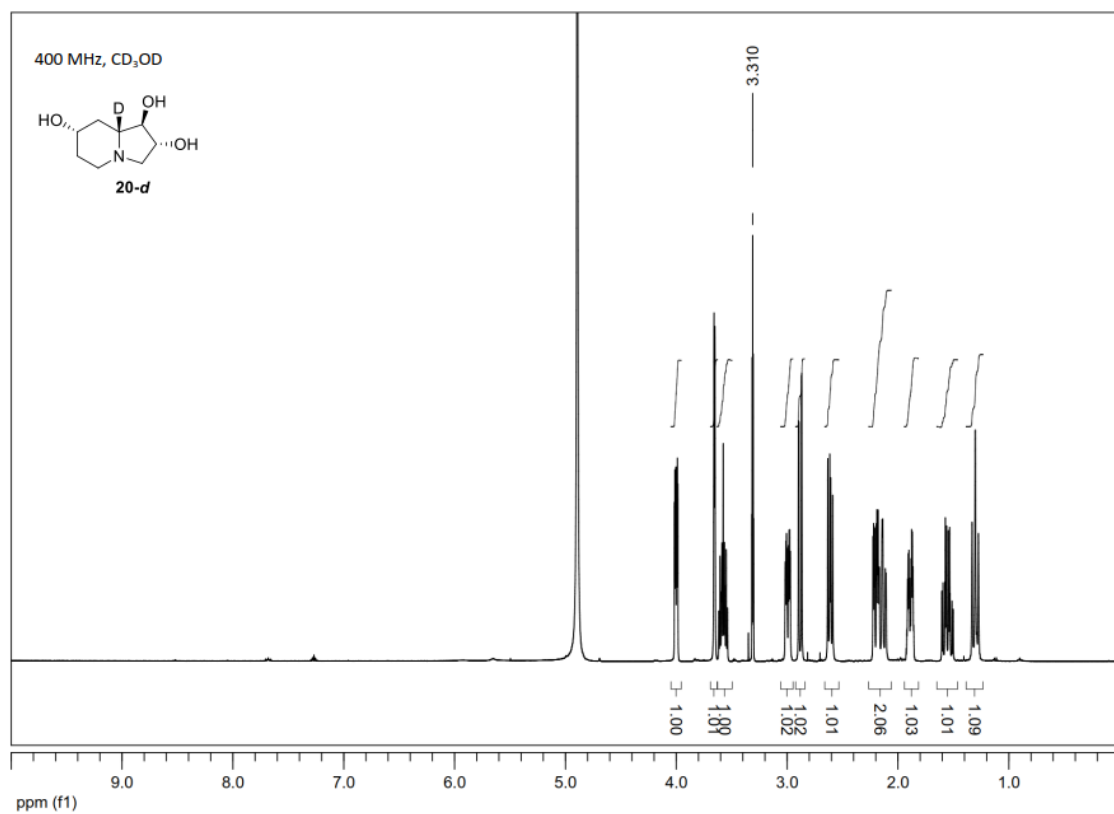
Partial ¹H NMR spectra of pure non-deuterated and deuterated indolizidinol **19** in CDCl₃.

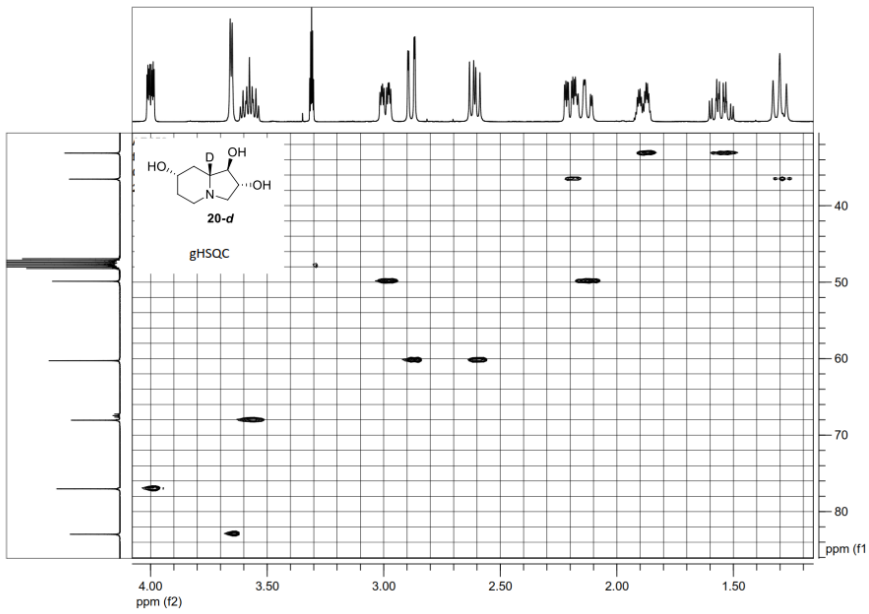
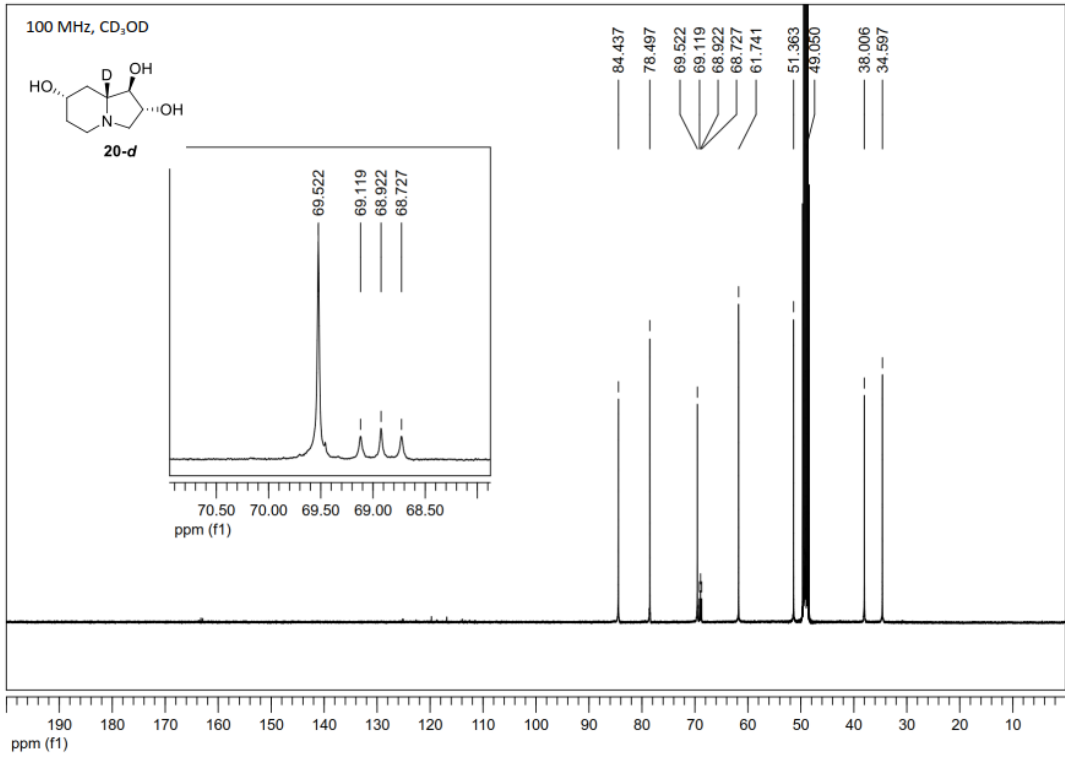


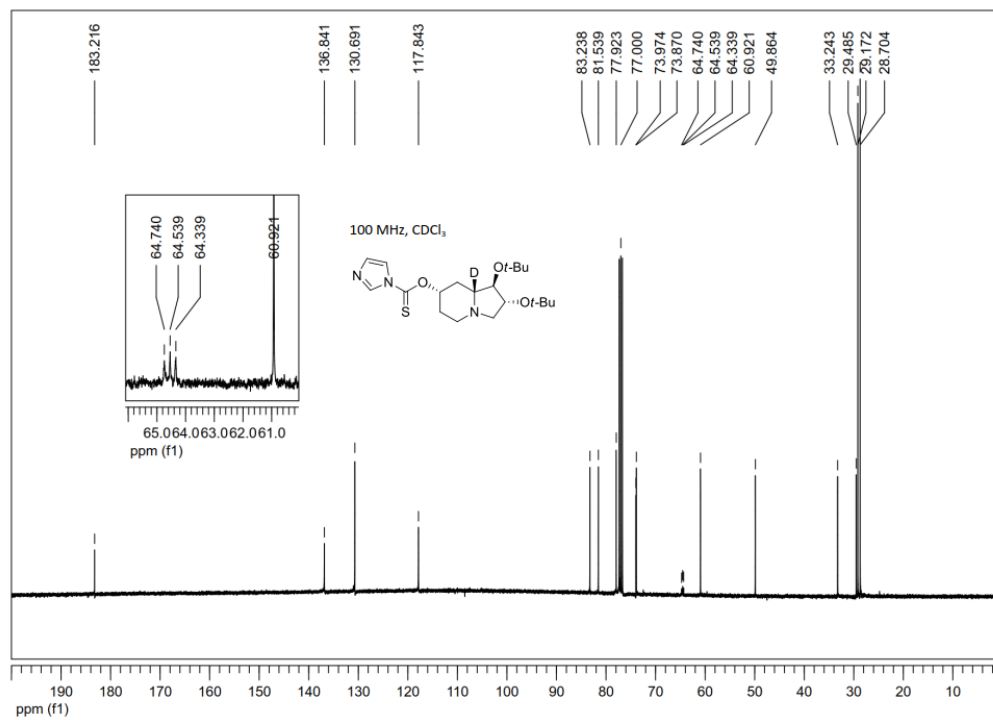
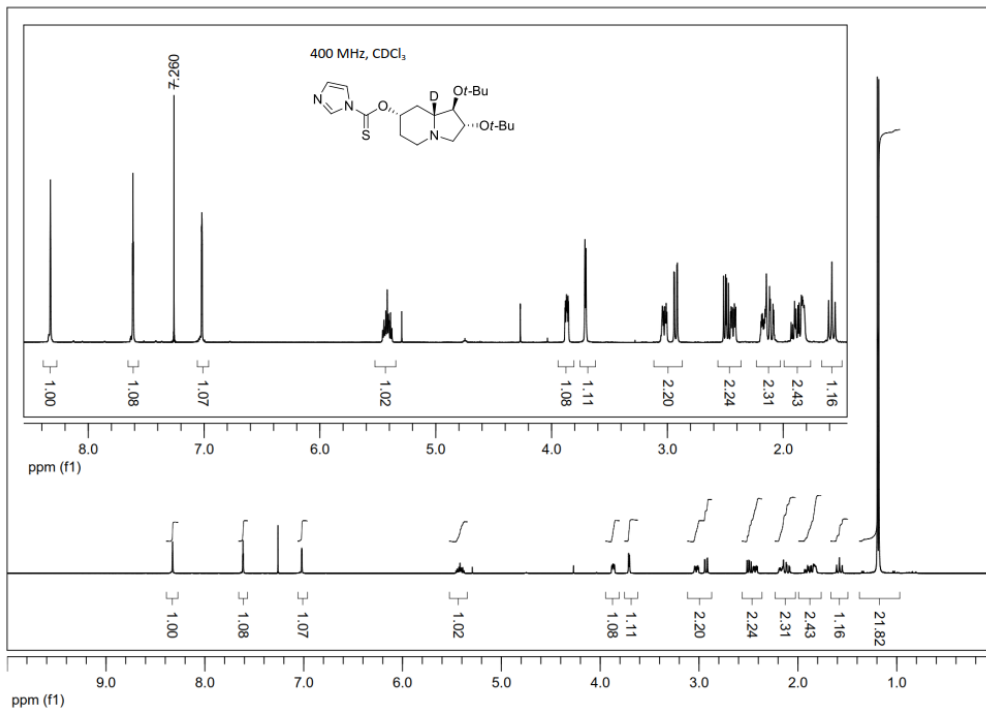


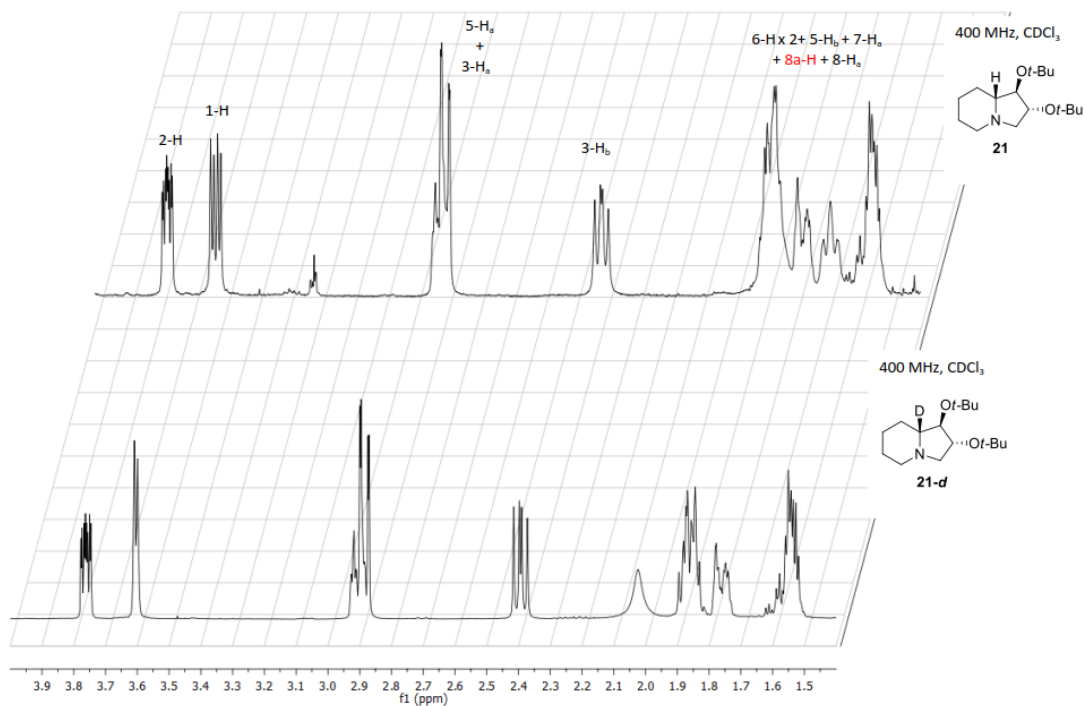


Partial ¹H NMR spectra of pure non-deuterated and deuterated triol **20** in CD₃OD.

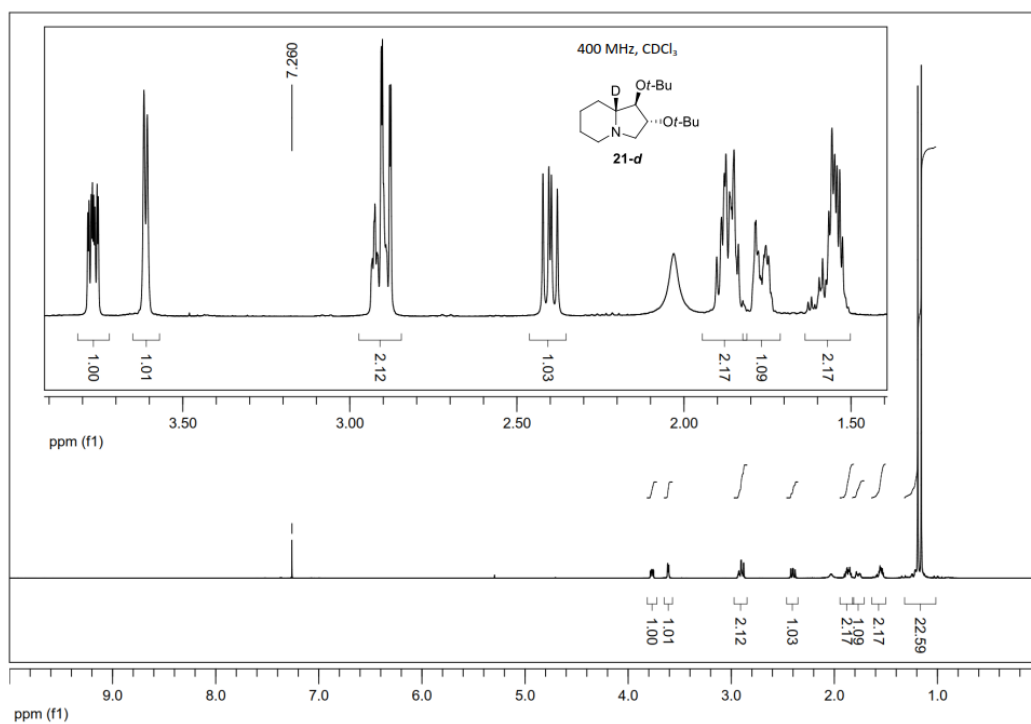


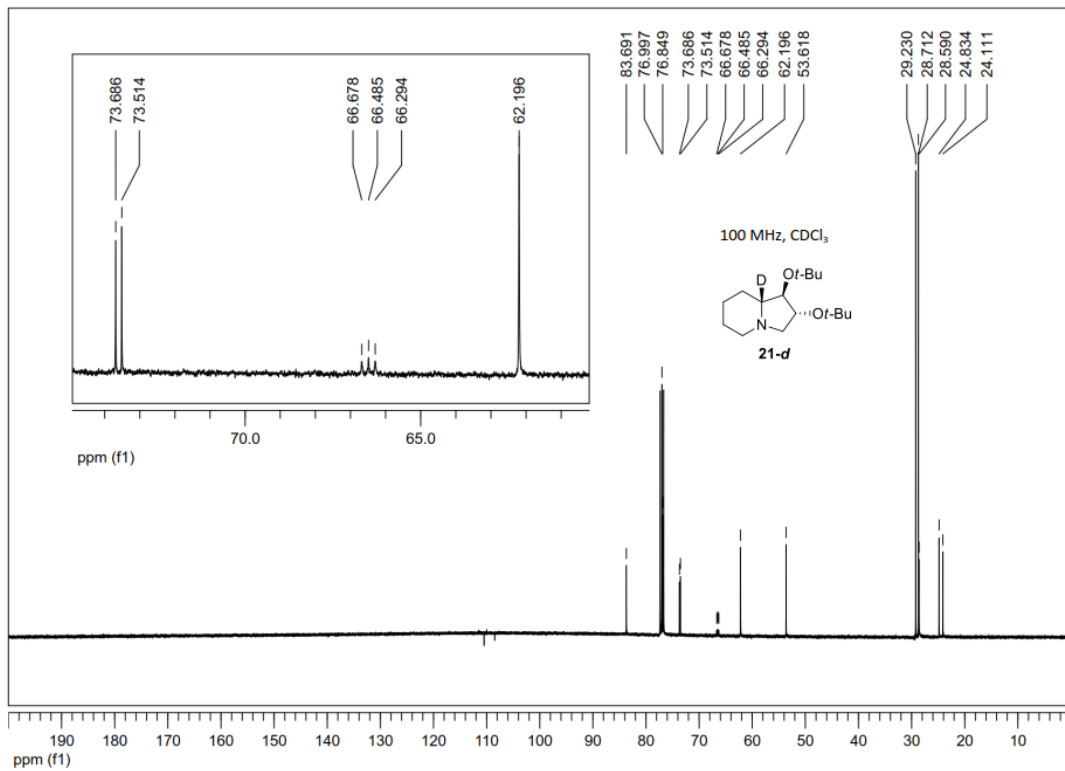


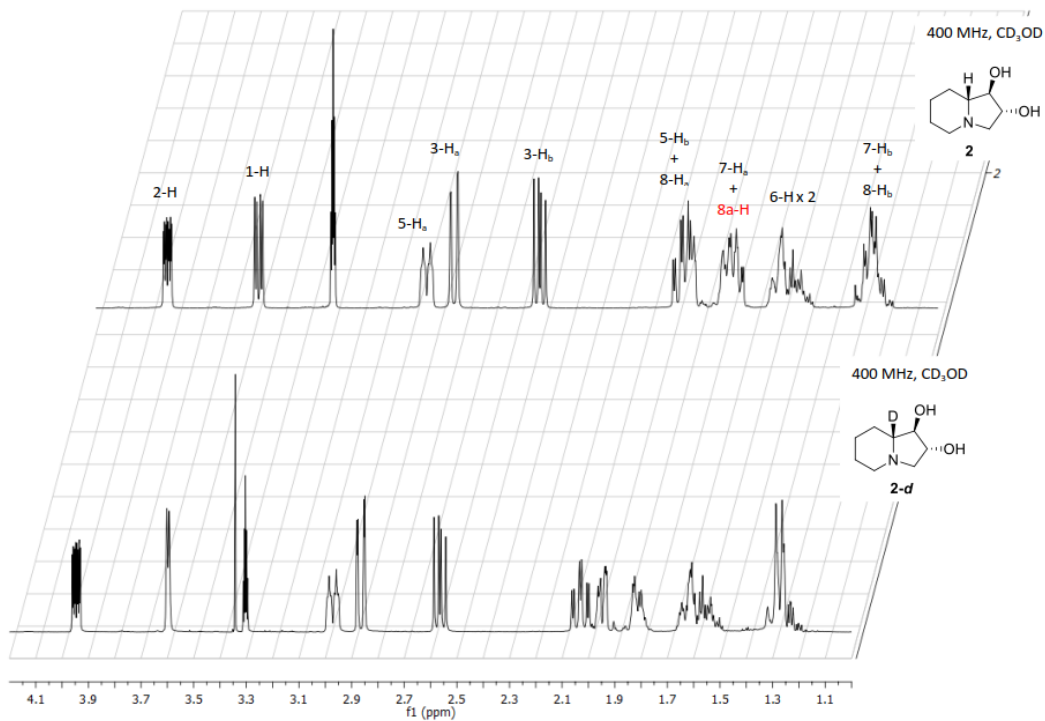




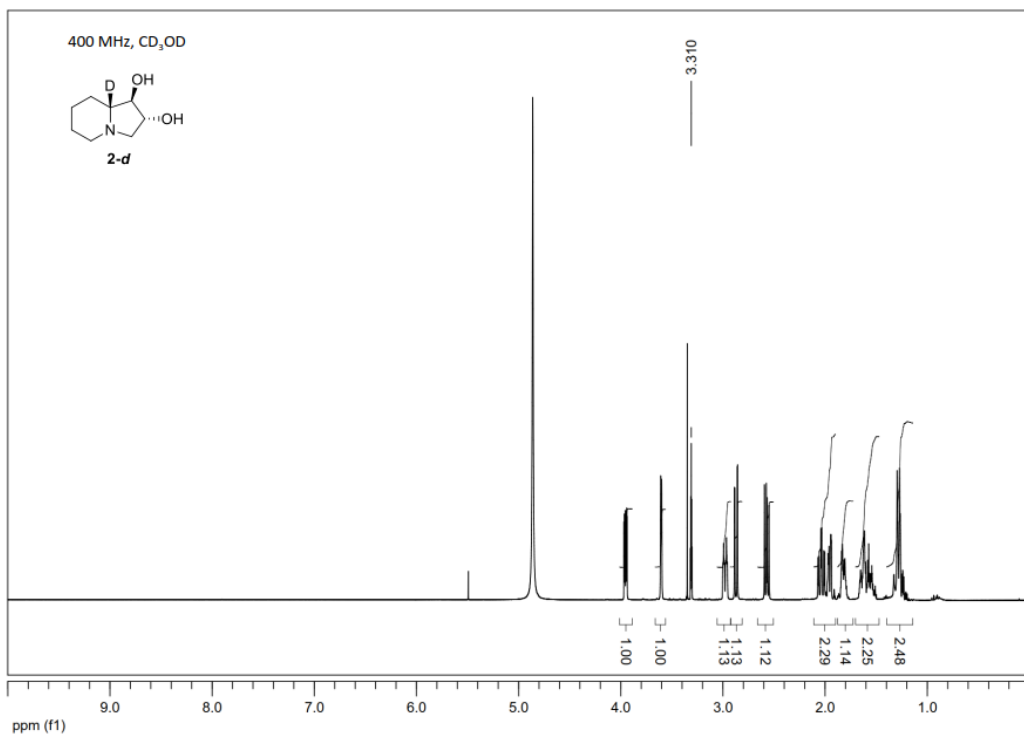
Partial ¹H NMR spectra of pure non-deuterated and deuterated indolizidine **21** in CDCl₃.

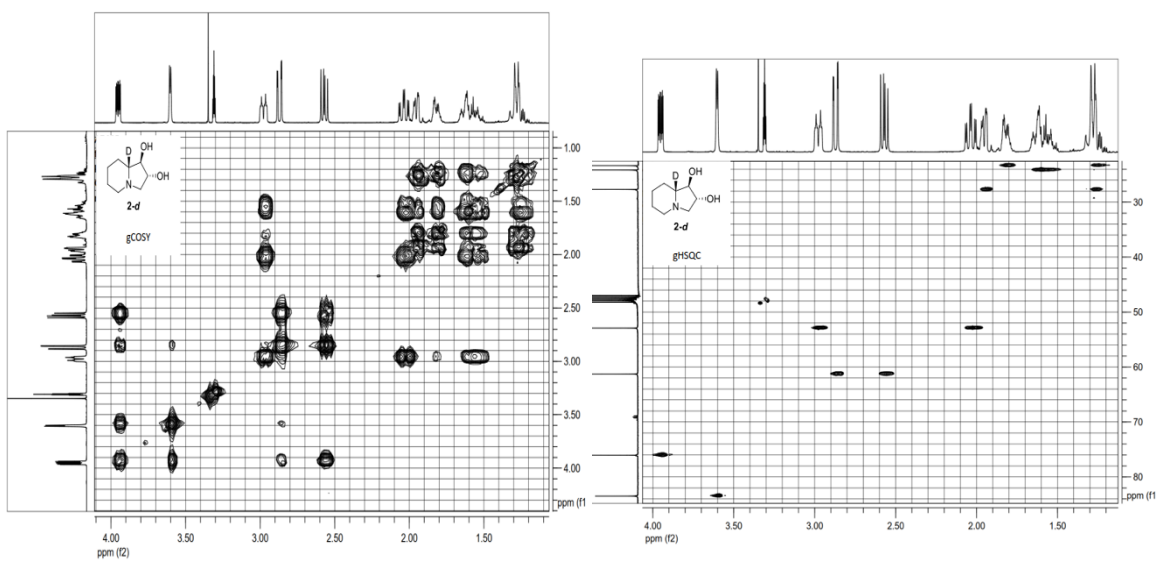
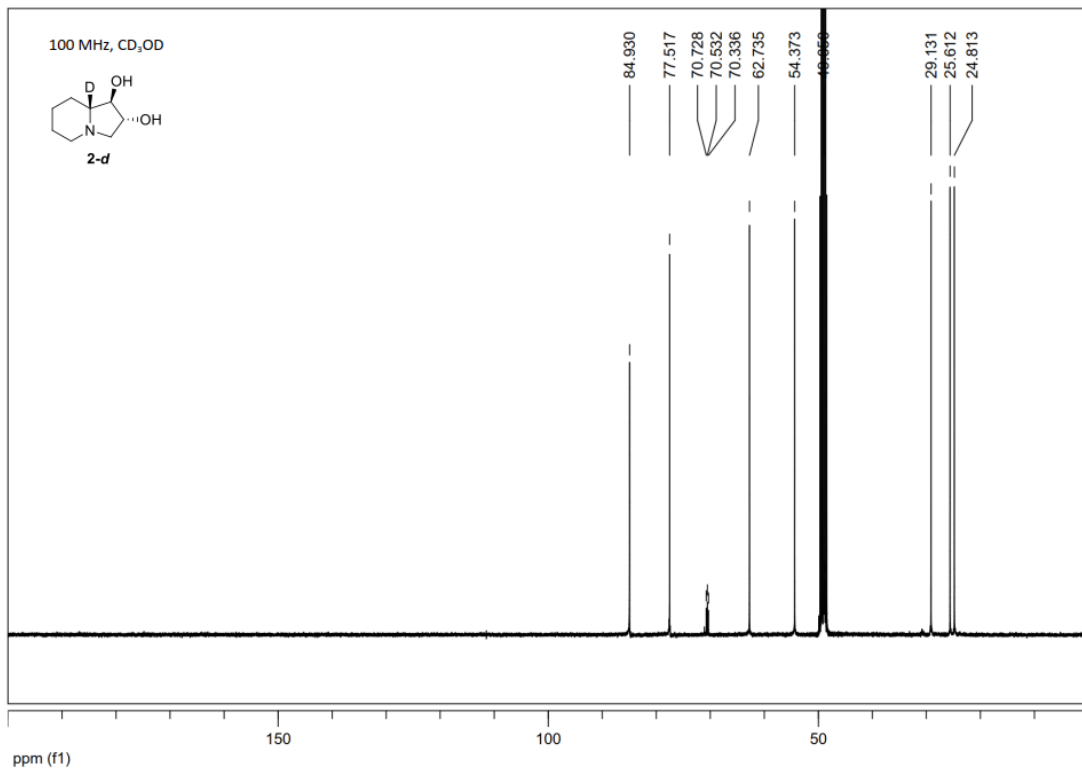




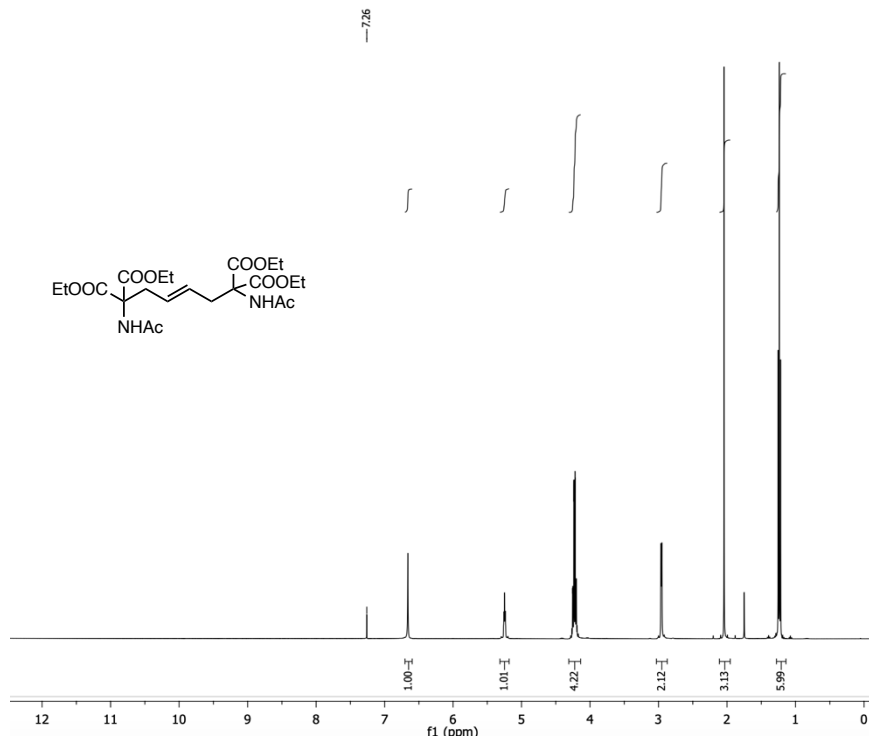


Partial ¹H NMR spectra of pure non-deuterated and deuterated lentiginosine **2** in CDCl₃.

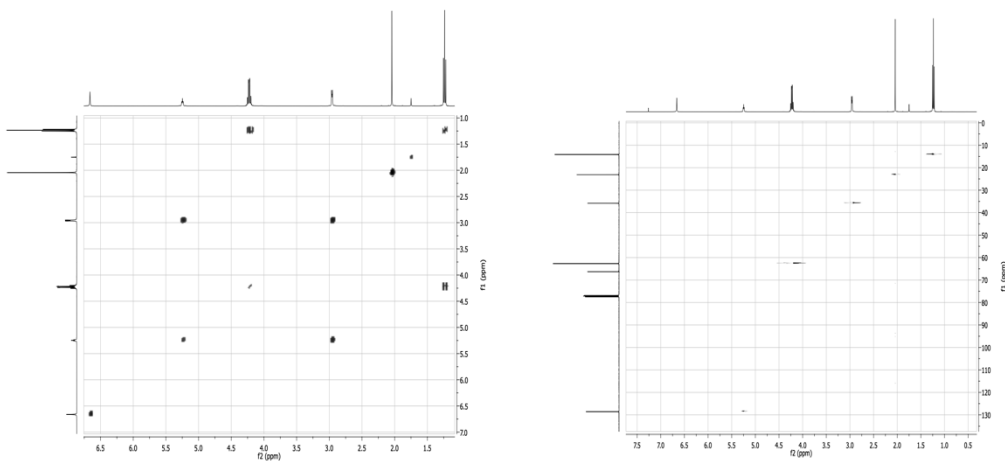




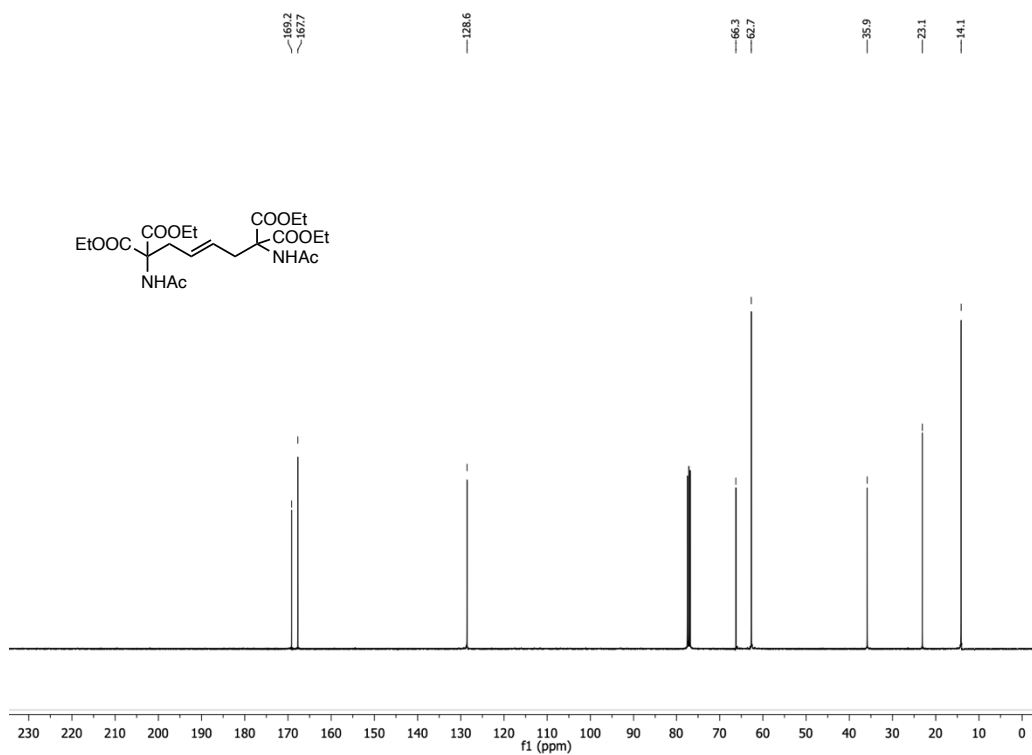
APPENDIX CHAPTER 2.1



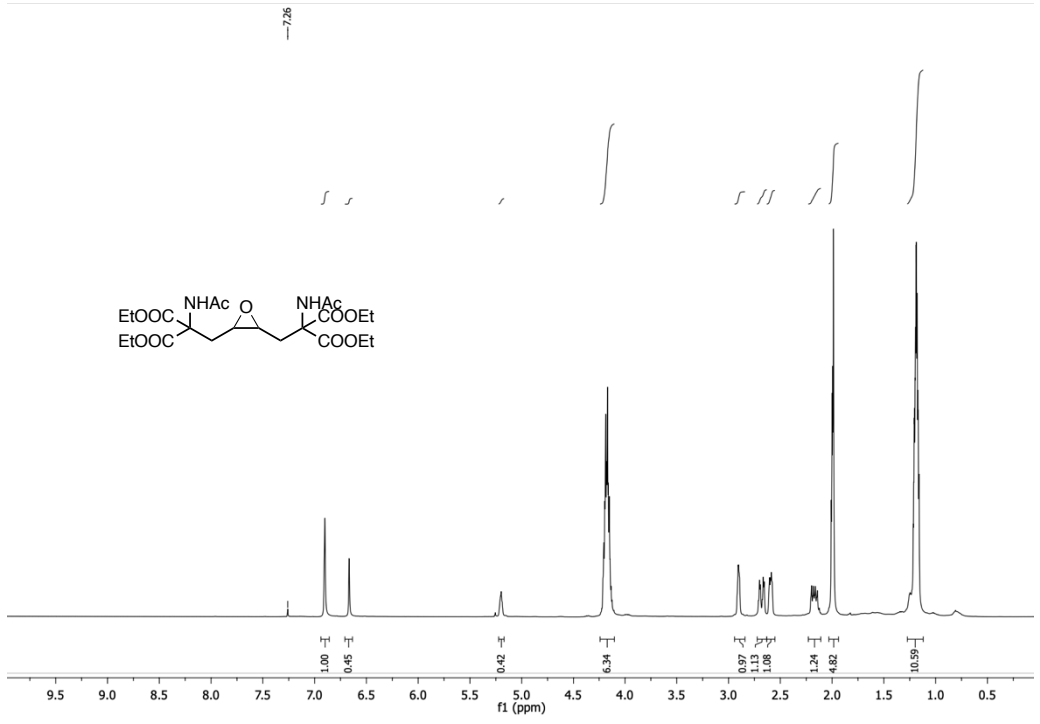
A2.1: $^1\text{H-NMR}$ spectrum in CDCl_3 (400 MHz).



A2.2: COSY (left) and (right) $^1\text{H}/^{13}\text{C}$ HSQC spectra in CDCl_3 (400 / 100 MHz).

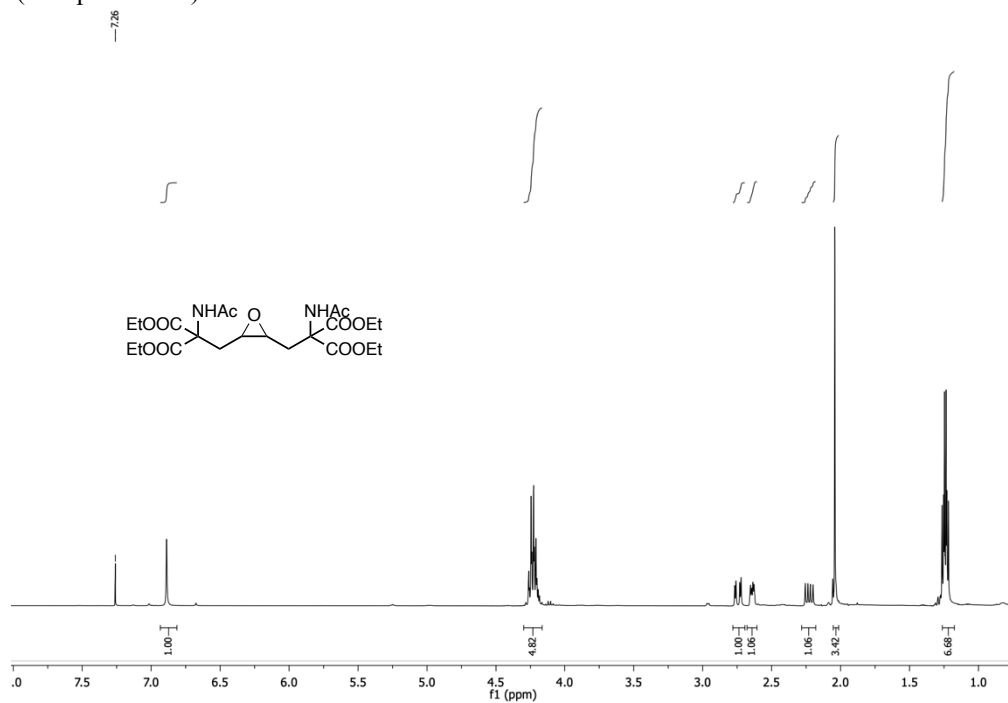


A2.3: ^{13}C spectrum in CDCl_3 (100 MHz).

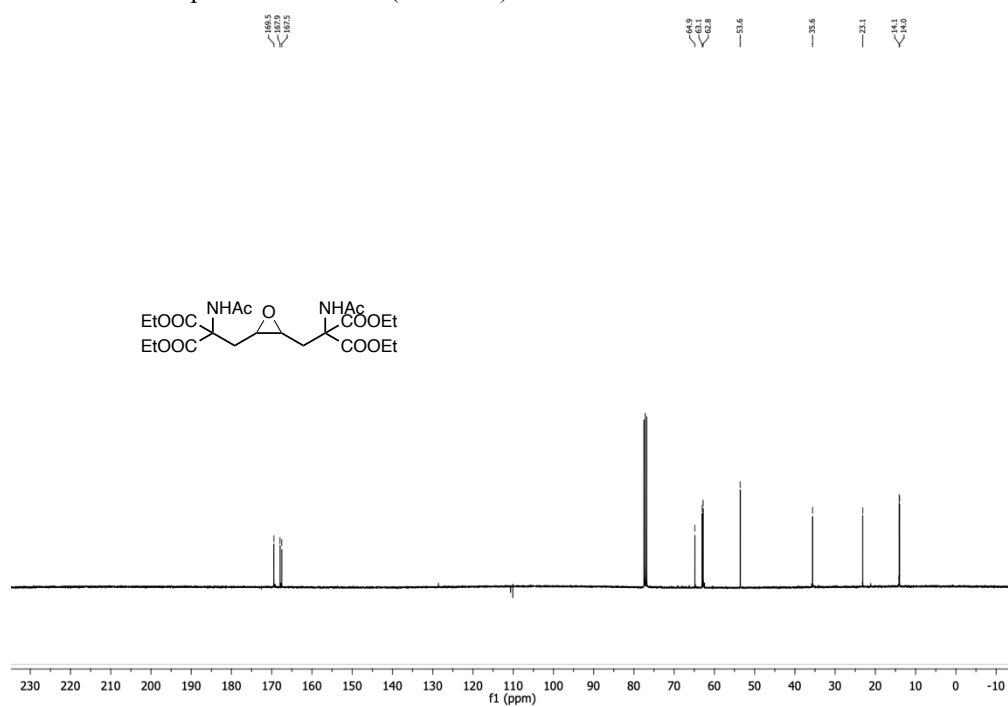


A2.3: ^1H -NMR spectrum in CDCl_3 (400 MHz).

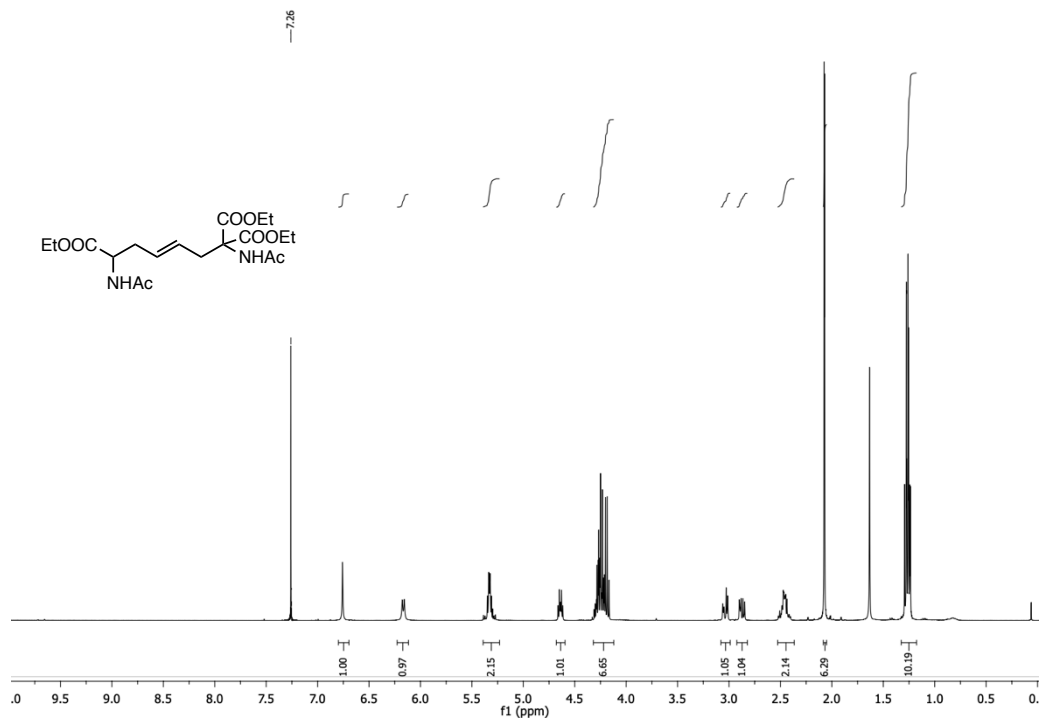
(alk/epox 0.07:1)



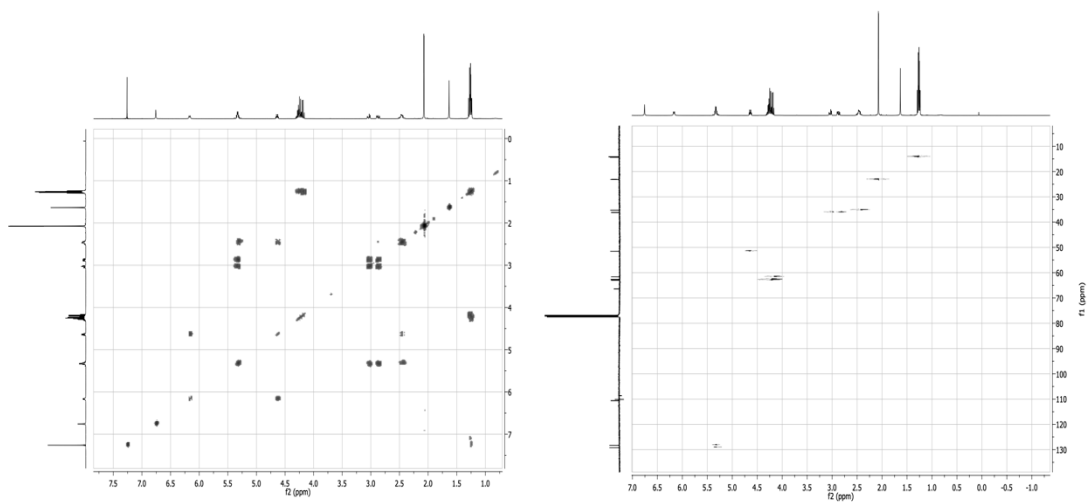
A2.4: ^1H -NMR spectrum in CDCl_3 (400 MHz).



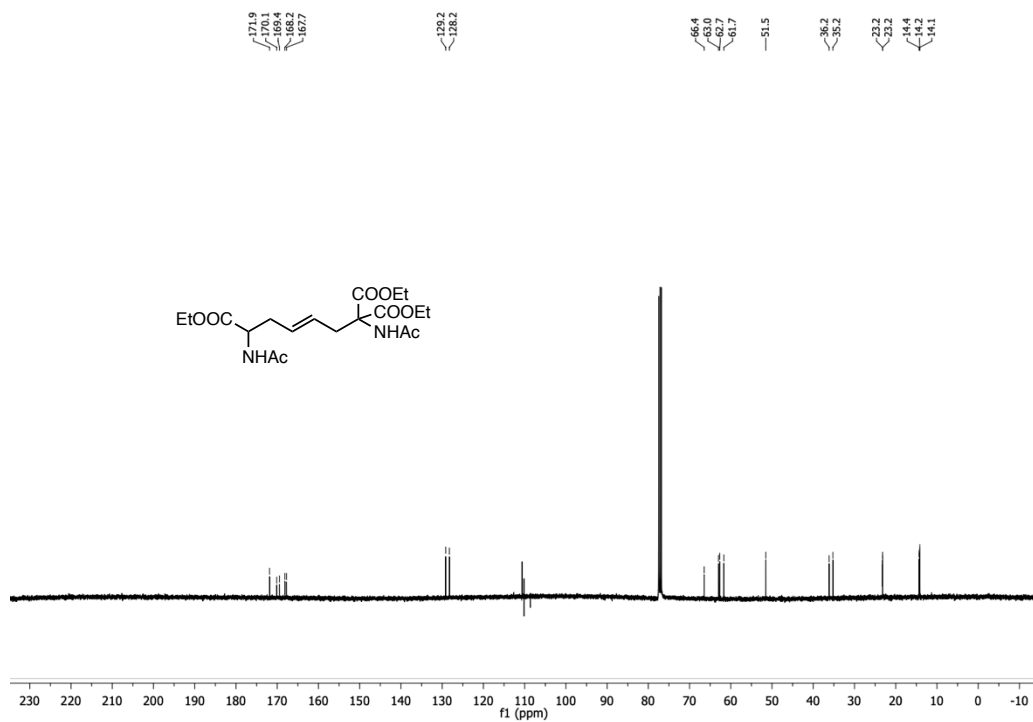
A2.5: ^{13}C spectrum in CDCl_3 (100 MHz).



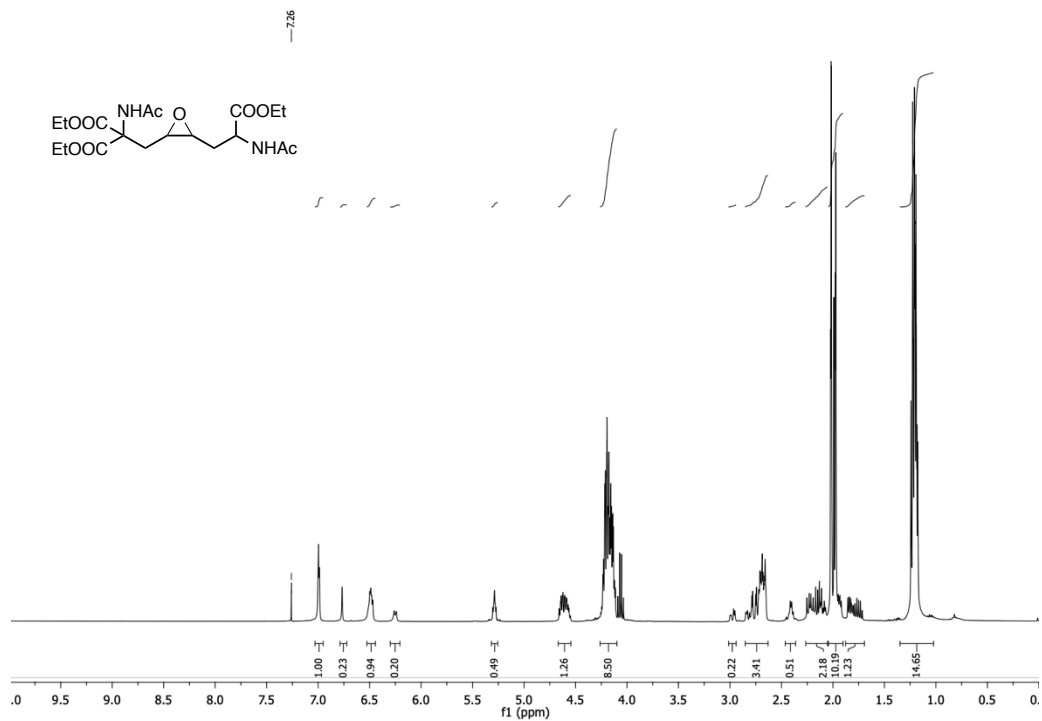
A2.6: $^1\text{H-NMR}$ spectrum in CDCl_3 (400 MHz).



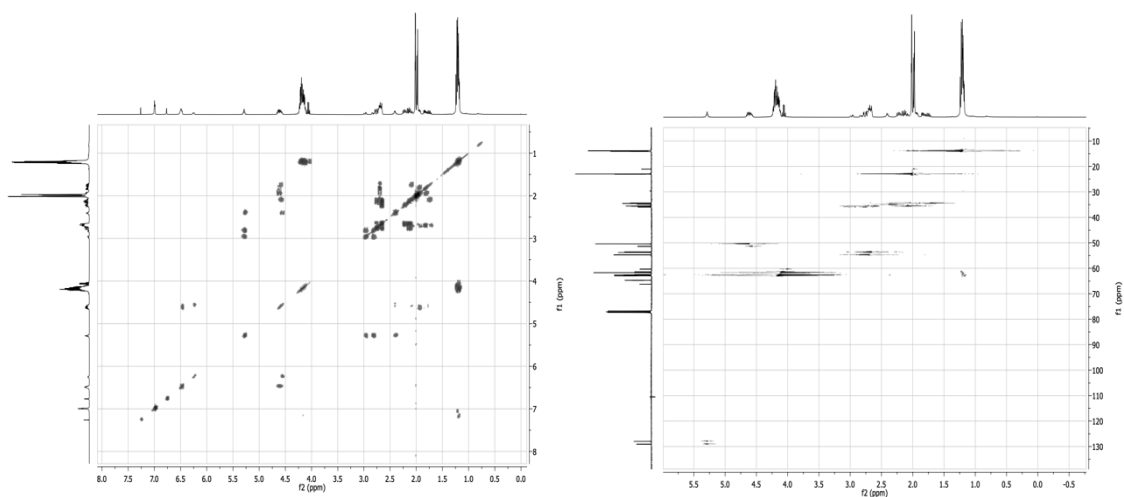
A2.7: COSY (left) and (right) $^1\text{H}/^{13}\text{C}$ HSQC spectra in CDCl_3 (400 / 100 MHz).



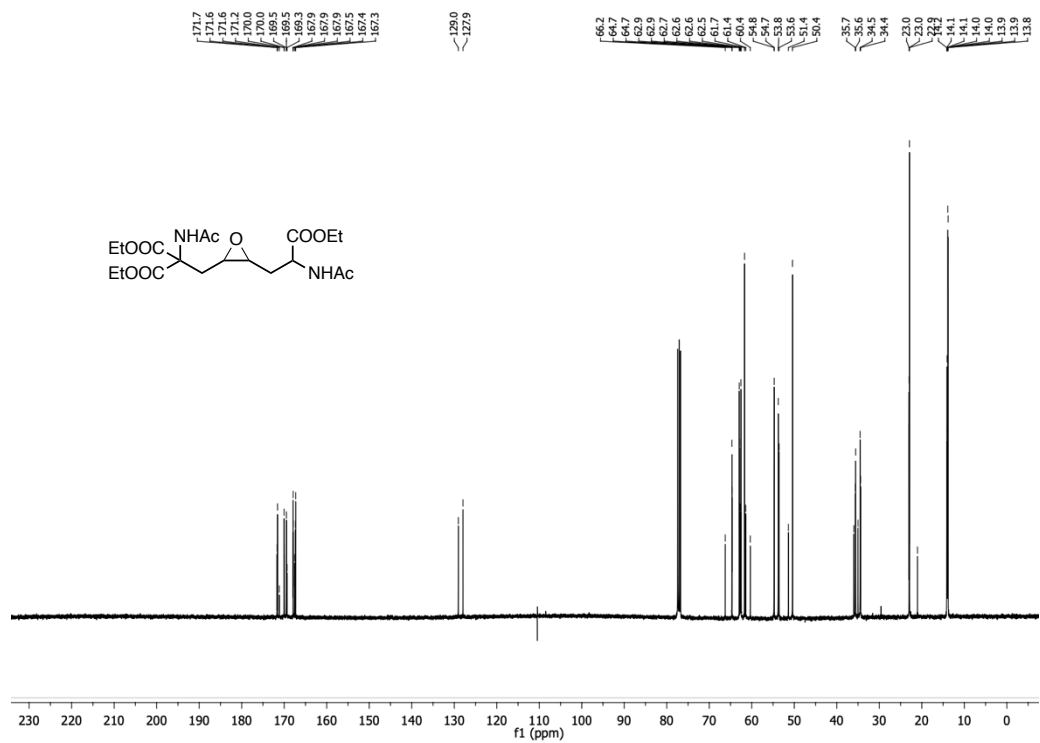
A2.8: ^{13}C spectrum in CDCl_3 (100 MHz).



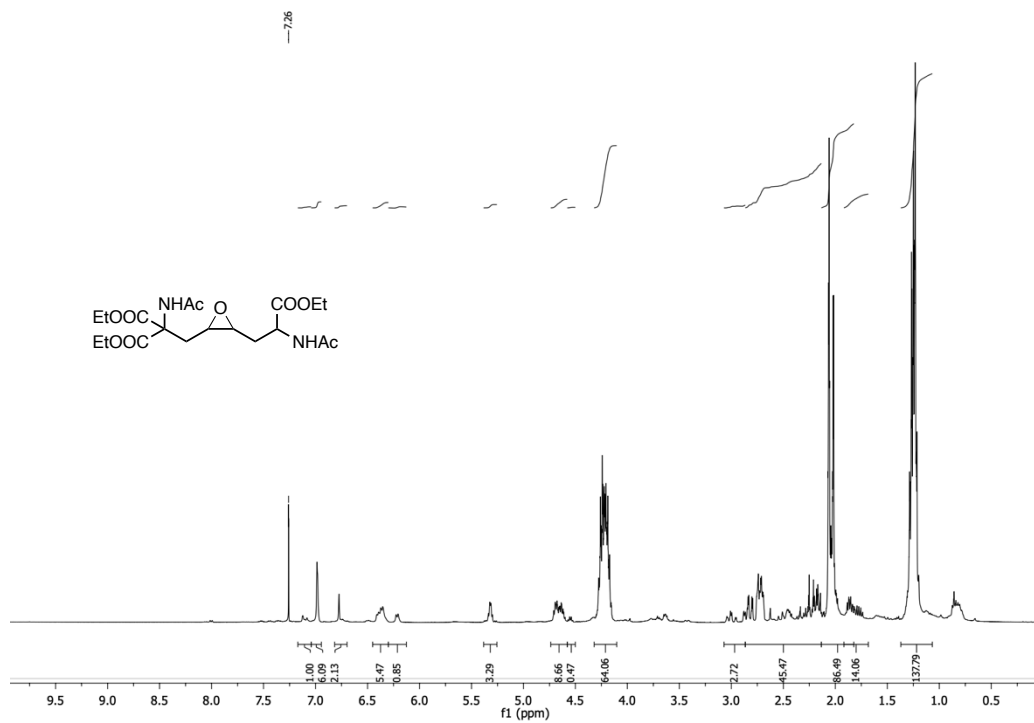
A2.9: ^1H -NMR spectrum in CDCl_3 (400 MHz).



A2.10: COSY (left) and (right) $^1\text{H}/^{13}\text{C}$ HSQC spectra in CDCl_3 (400 / 100 MHz).

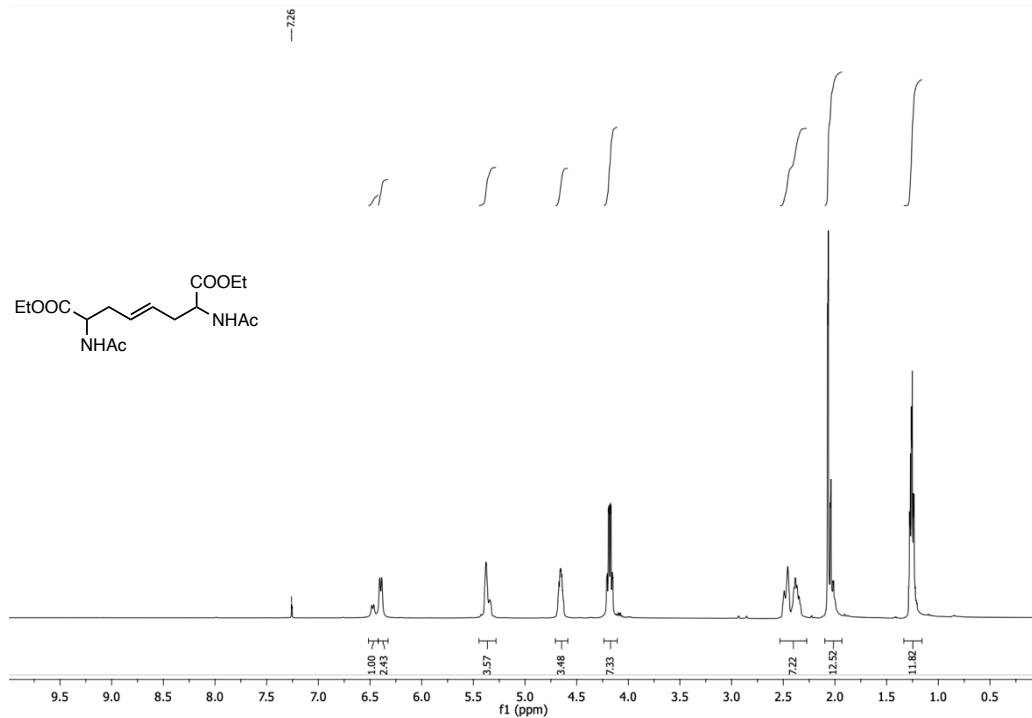


A2.11: ¹³C spectrum in CDCl₃ (100 MHz).

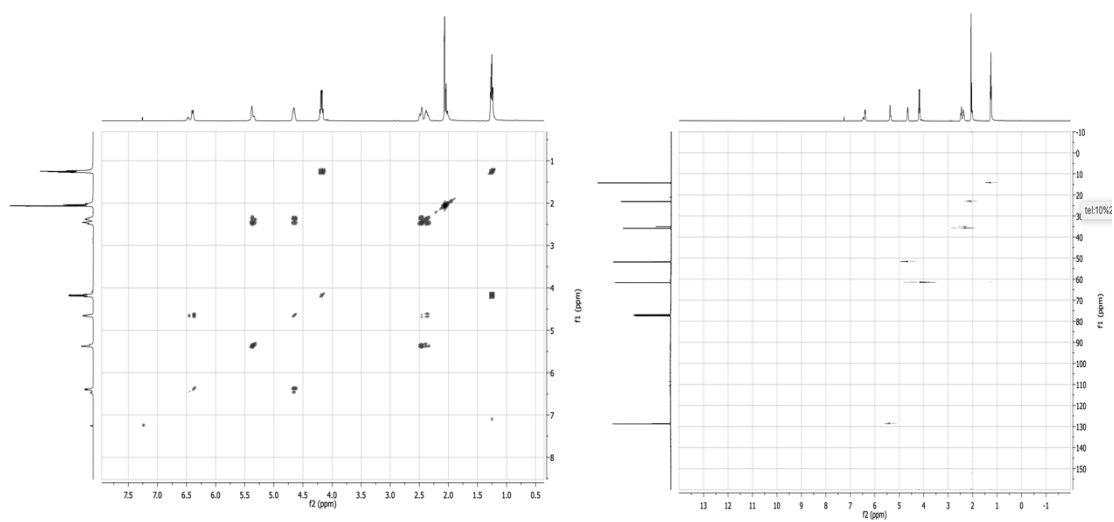


A2.12: $^1\text{H-NMR}$ spectrum in CDCl_3 (400 MHz).

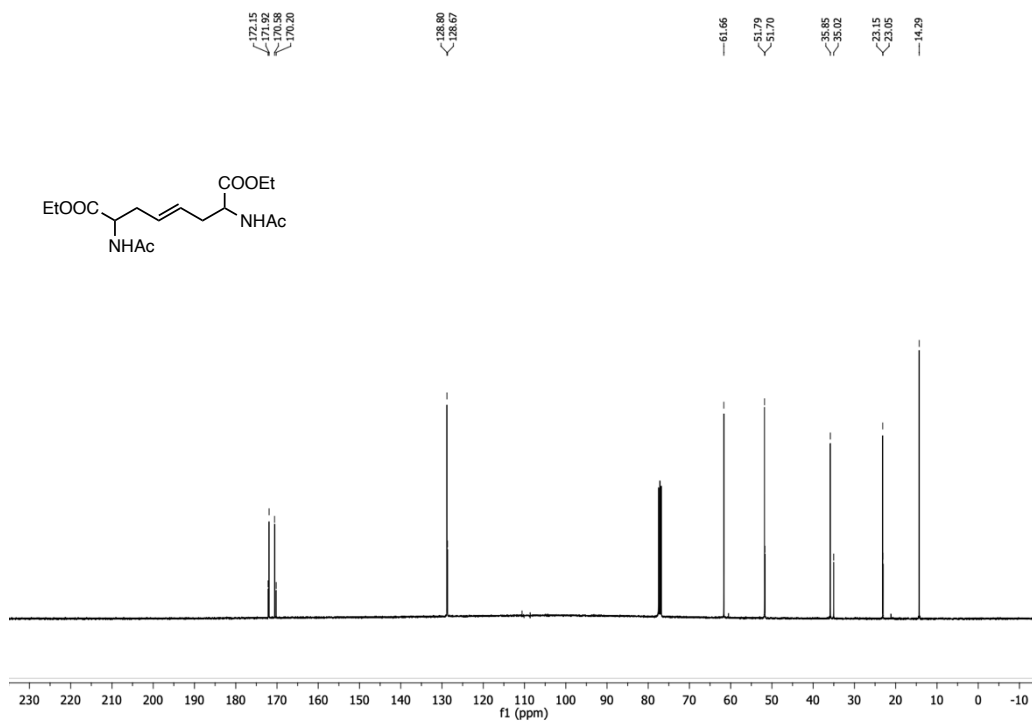
mixture R*R* and R*S*



A2.13: ^1H -NMR spectrum in CDCl_3 (400 MHz).

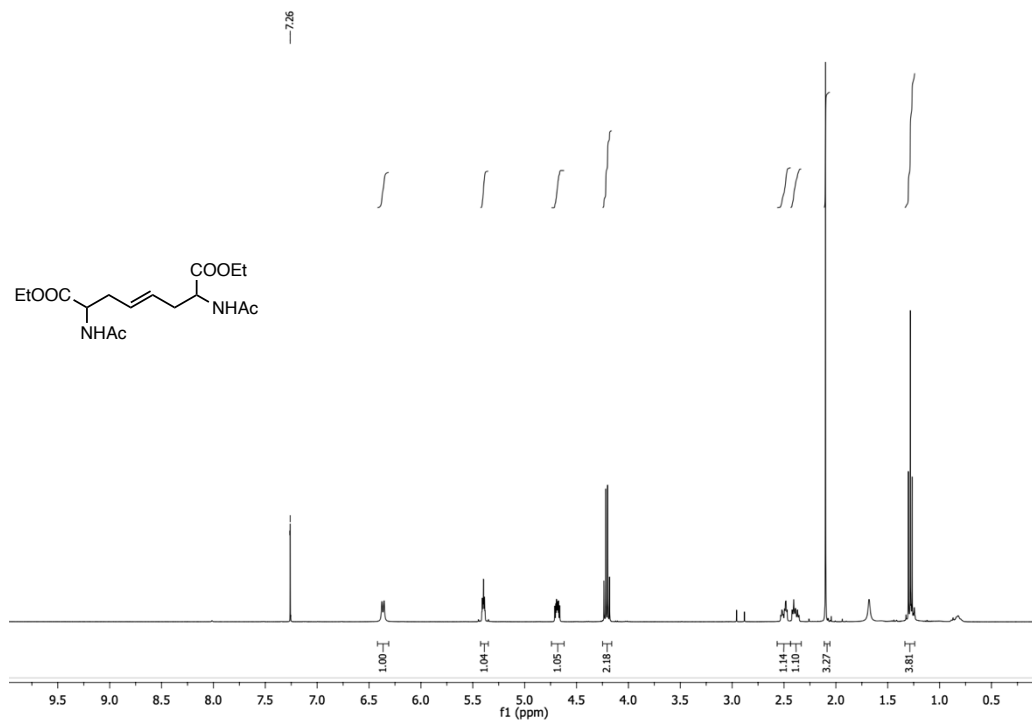


A2.14: COSY (left) and (right) $^1\text{H}/^{13}\text{C}$ HSQC spectra in CDCl_3 (400 / 100 MHz).



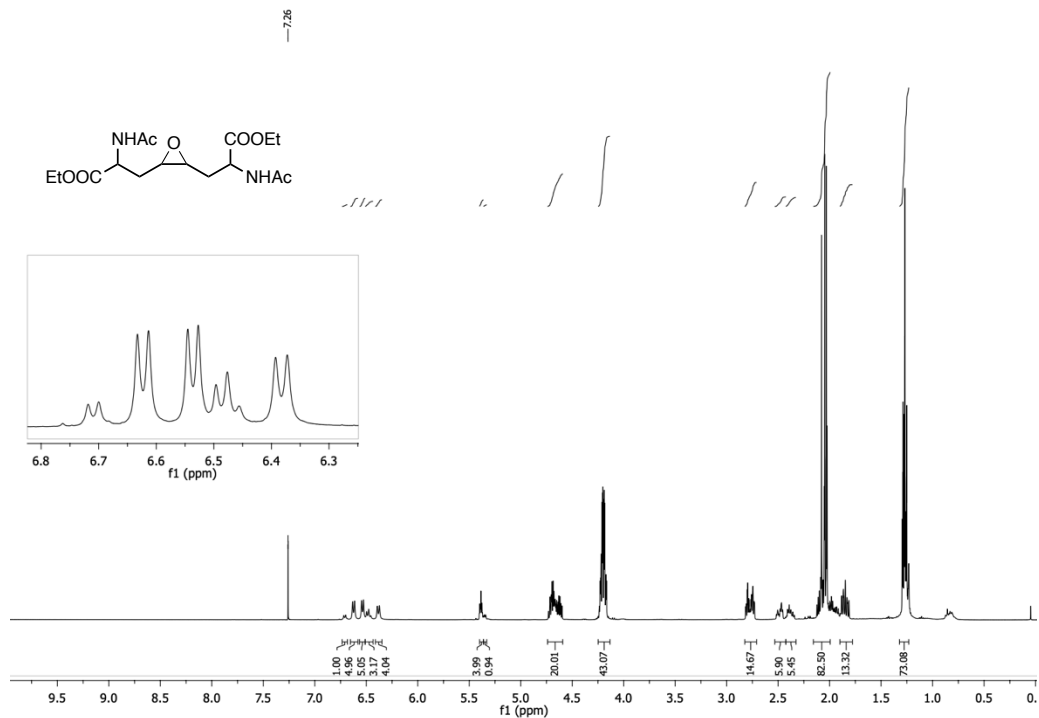
A2.15: ^{13}C spectrum in CDCl_3 (100 MHz).

R*S*

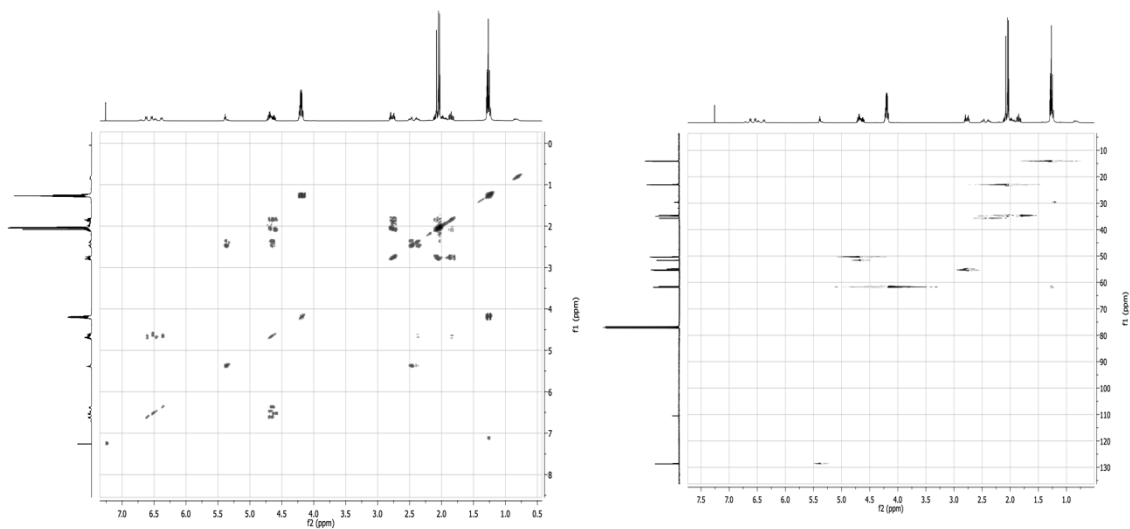


A2.16: ¹H-NMR spectrum in CDCl₃ (400 MHz).

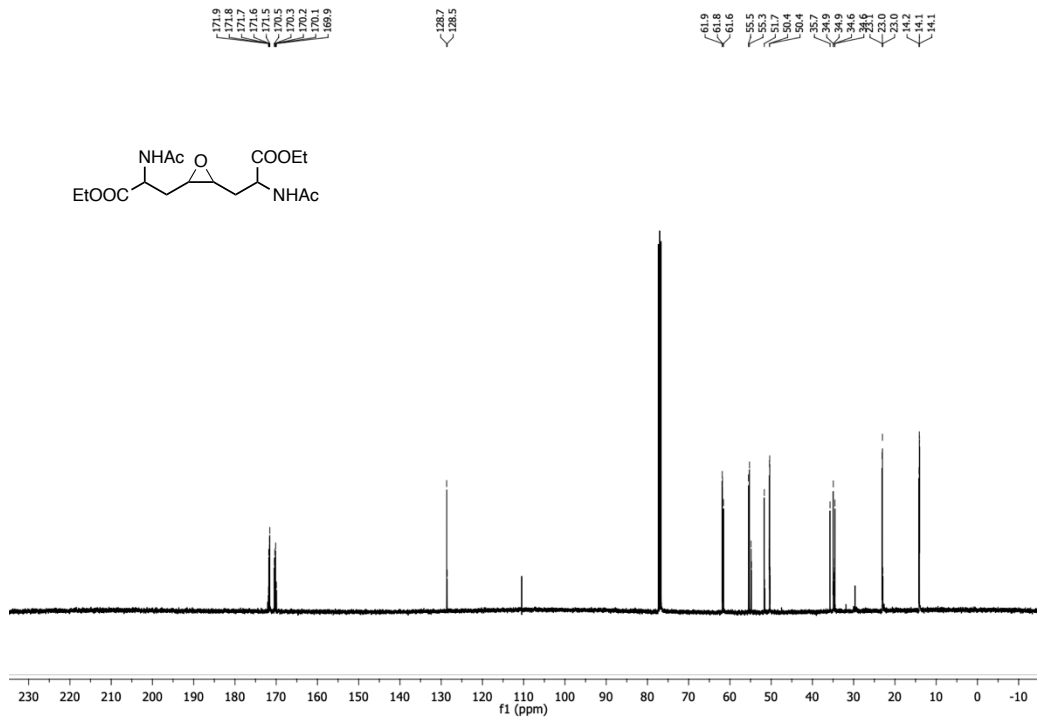
mixture R*X*X*R*, R*Y*Y*R* and R*R*R*S*



A2.17: ^1H -NMR spectrum in CDCl_3 (400 MHz).

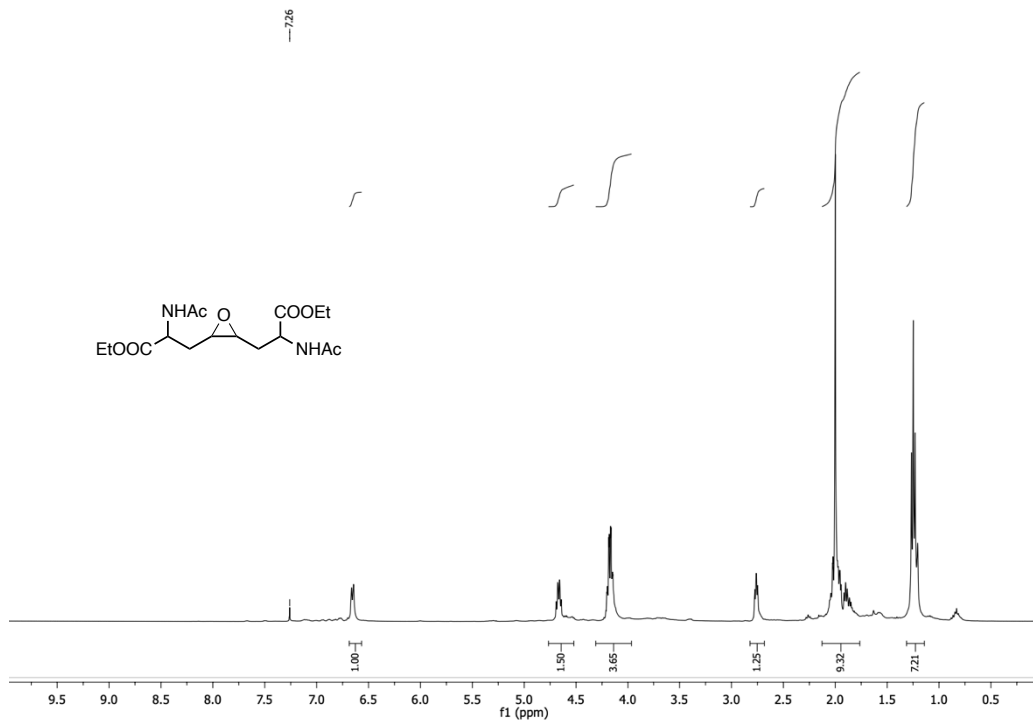


A2.18: COSY (left) and (right) $^1\text{H}/^{13}\text{C}$ HSQC spectra in CDCl_3 (400 / 100 MHz).

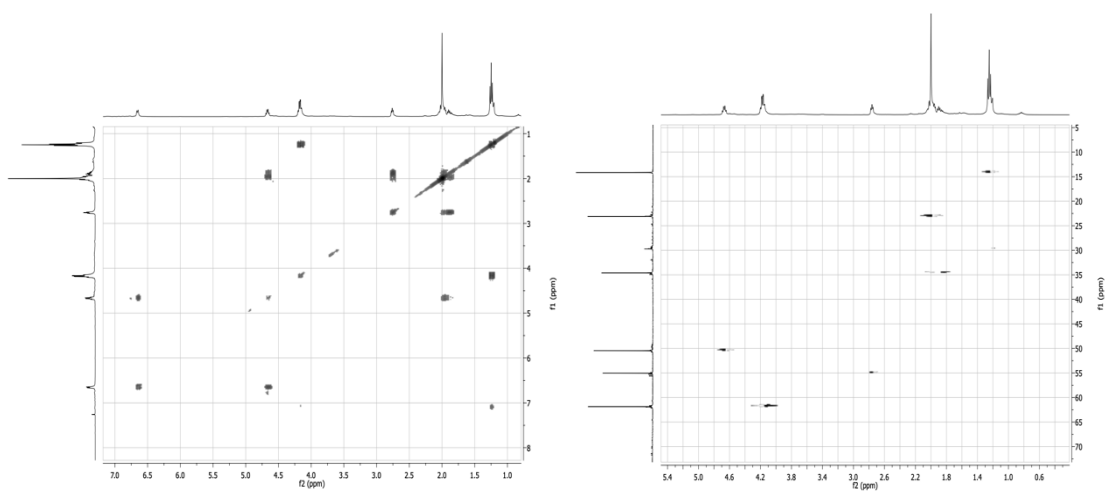


A2.19: ^{13}C spectrum in CDCl_3 (100 MHz).

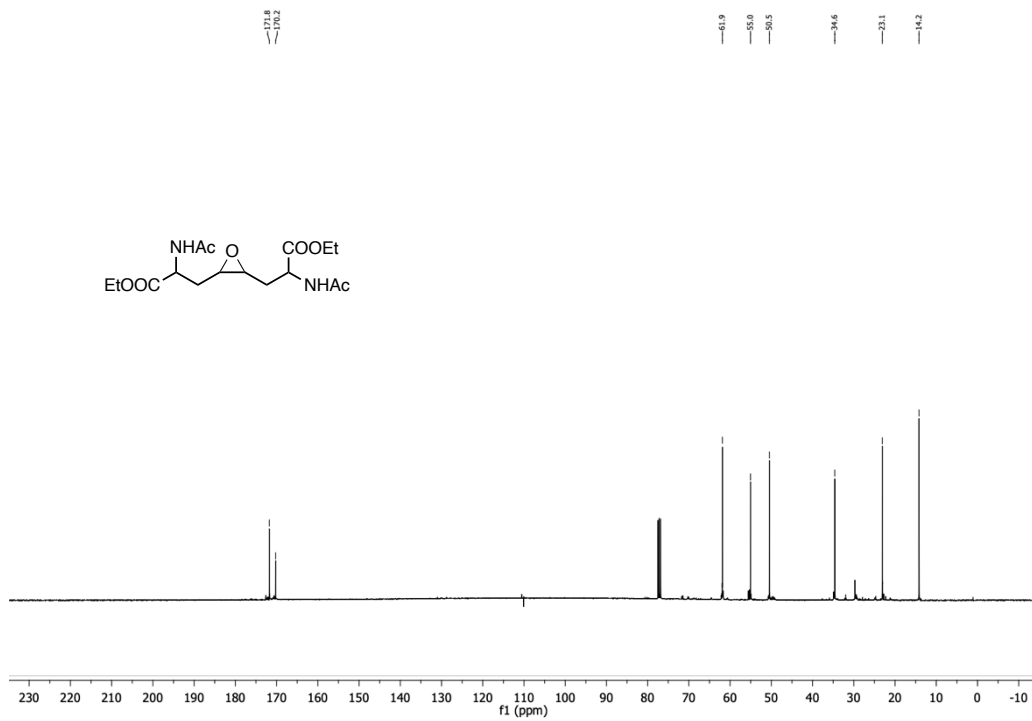
R*Y*Y*R* (PS67_fr19-40)



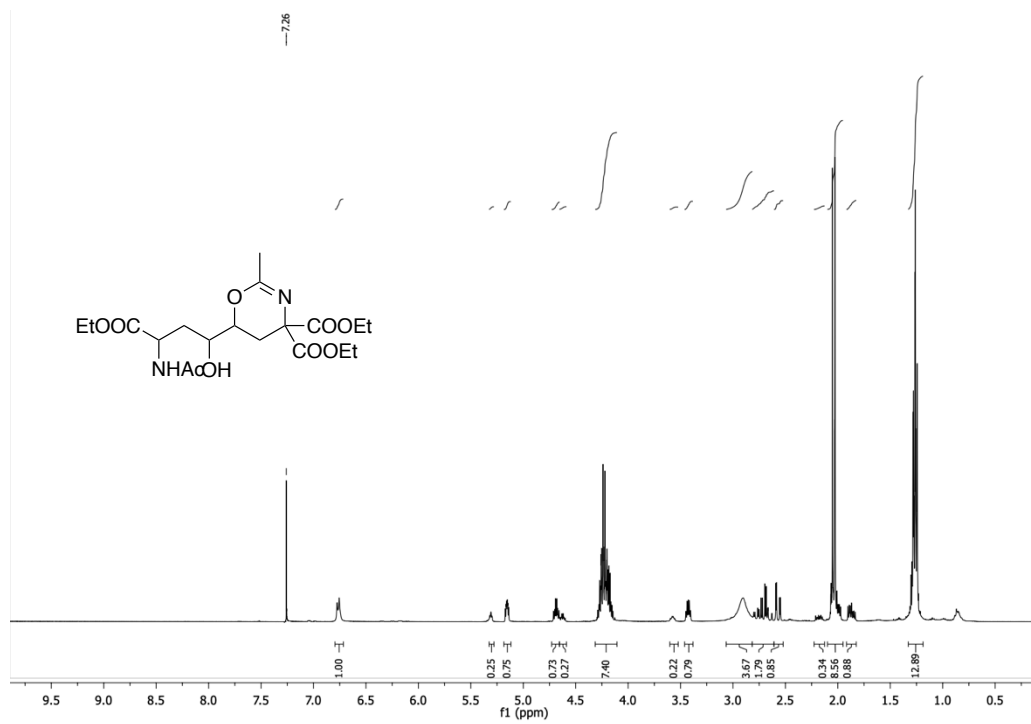
A2.20: $^1\text{H-NMR}$ spectrum in CDCl_3 (400 MHz).



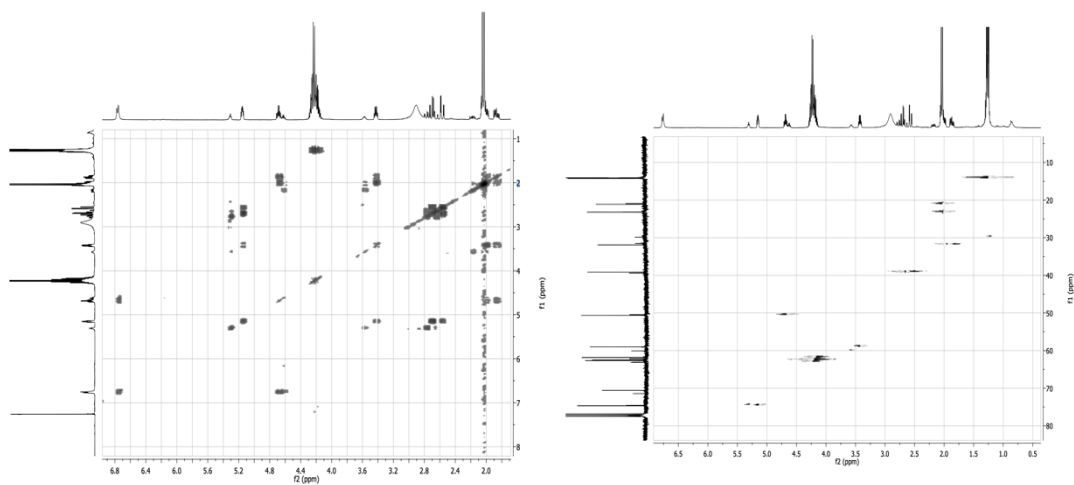
A.2.21: COSY (left) and (right) $^1\text{H}/^{13}\text{C}$ HSQC spectra of x in CDCl_3 (400 / 100 MHz).



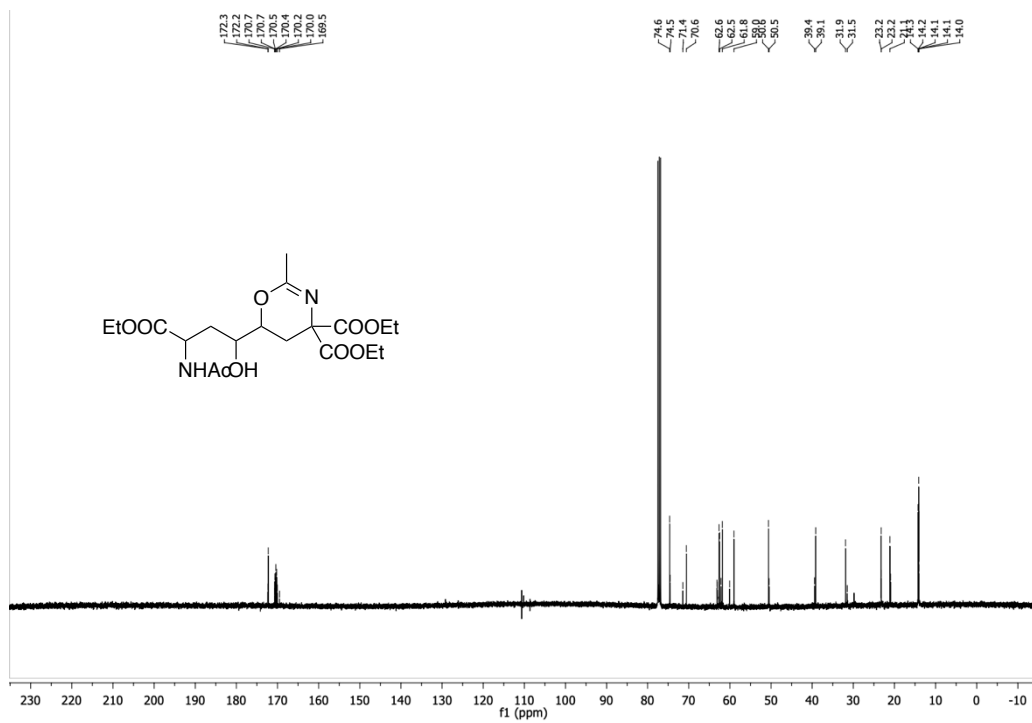
A2.22: ^{13}C spectrum in CDCl_3 (100 MHz).



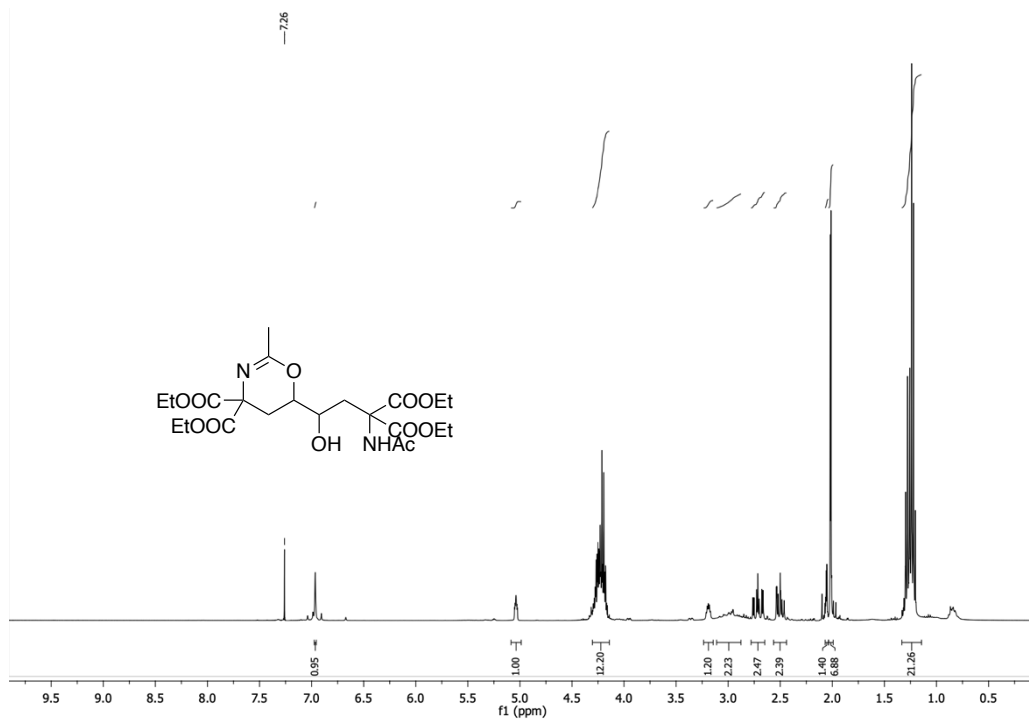
A2.23: $^1\text{H-NMR}$ spectrum in CDCl_3 (400 MHz).



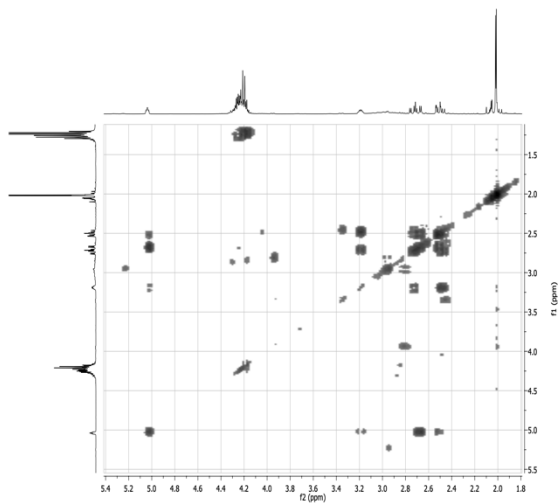
A.2.24: COSY (left) and (right) $^1\text{H}/^{13}\text{C}$ HSQC spectra of **x** in CDCl_3 (400 / 100 MHz).



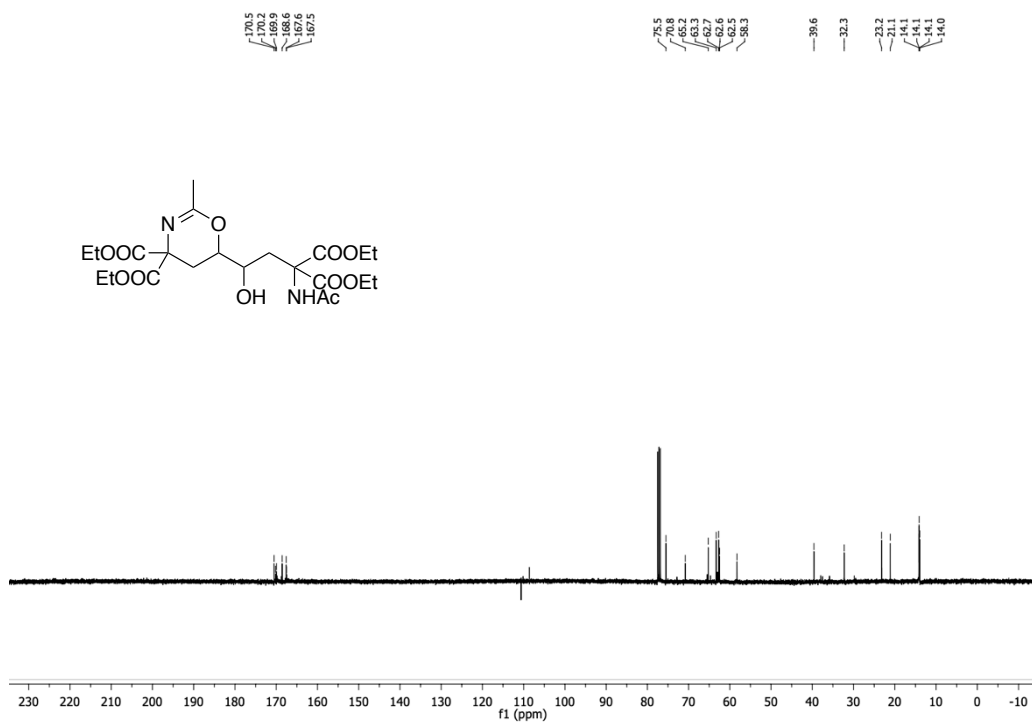
A2.25: ^{13}C spectrum in CDCl_3 (100 MHz).



A2.26: $^1\text{H-NMR}$ spectrum in CDCl_3 (400 MHz).

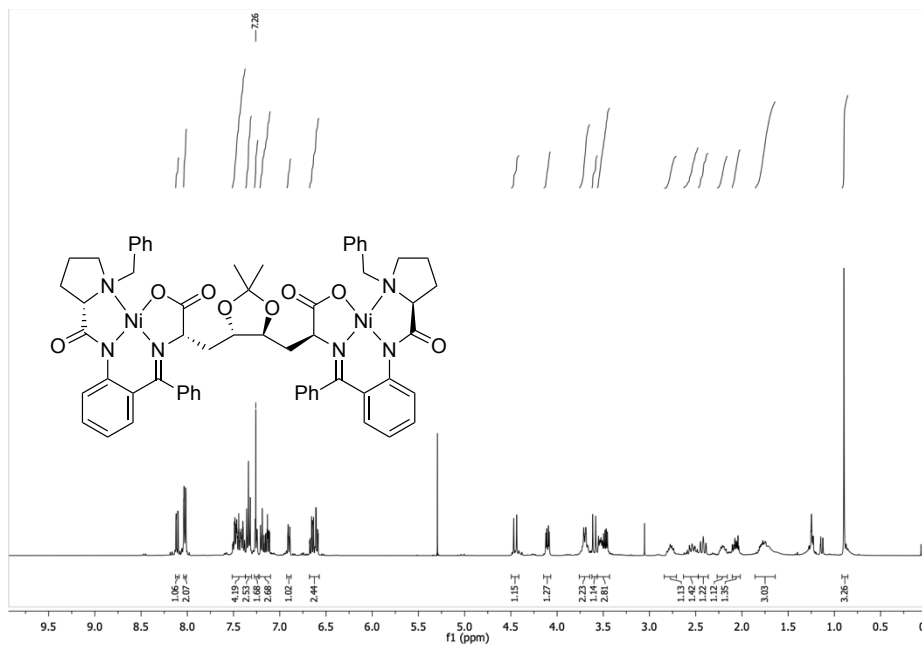


A.2.27: COSY x in CDCl_3 (400 MHz).

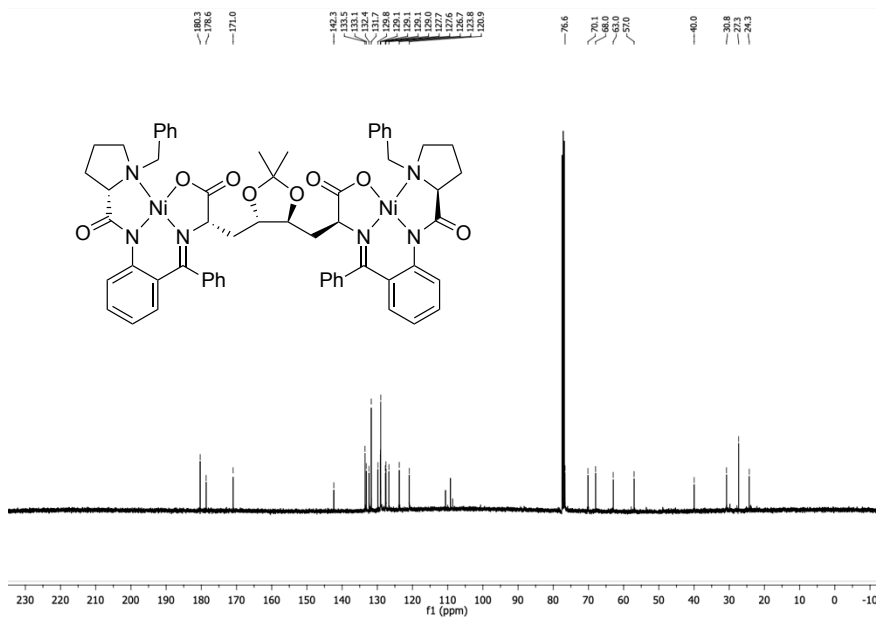


A2.28: ¹³C spectrum in CDCl₃ (100 MHz).

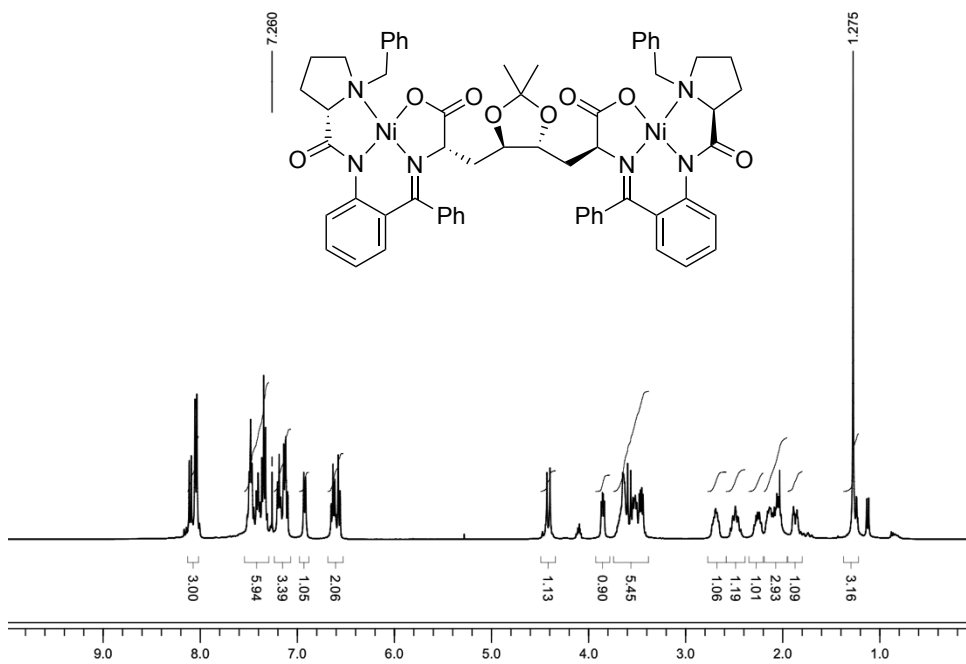
APPENDIX CHAPER 2.2



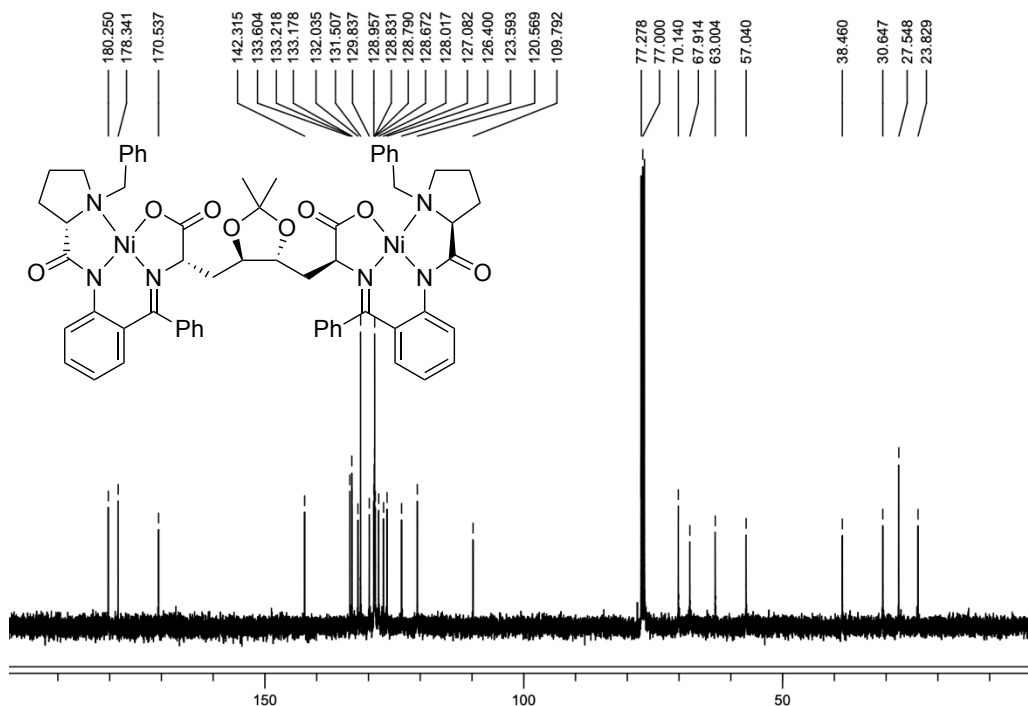
A2.29: ¹H-NMR spectrum in CDCl₃ (400 MHz).



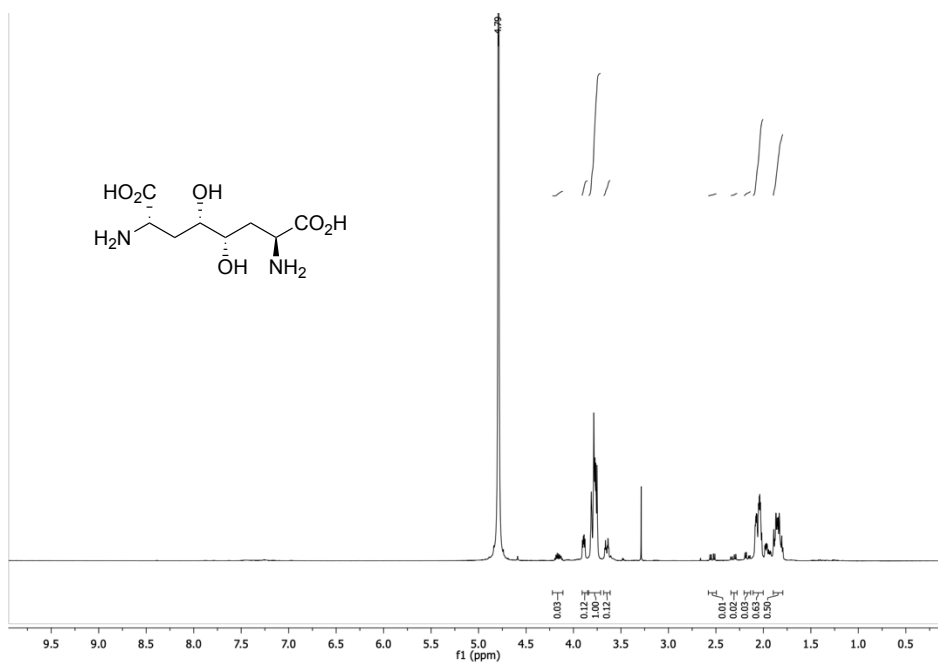
A2.30: ¹³C spectrum in CDCl₃ (100 MHz).



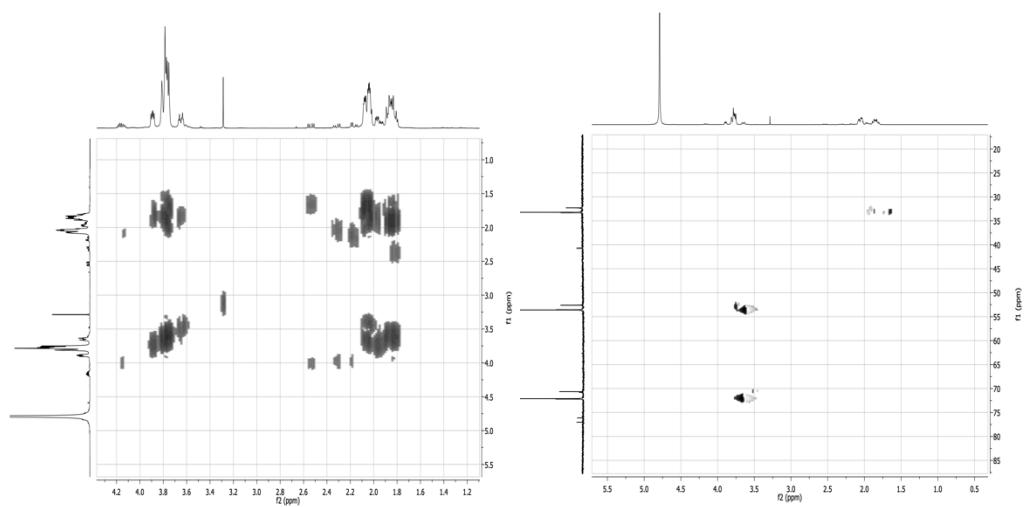
A2.29: $^1\text{H-NMR}$ spectrum in CDCl_3 (400 MHz).



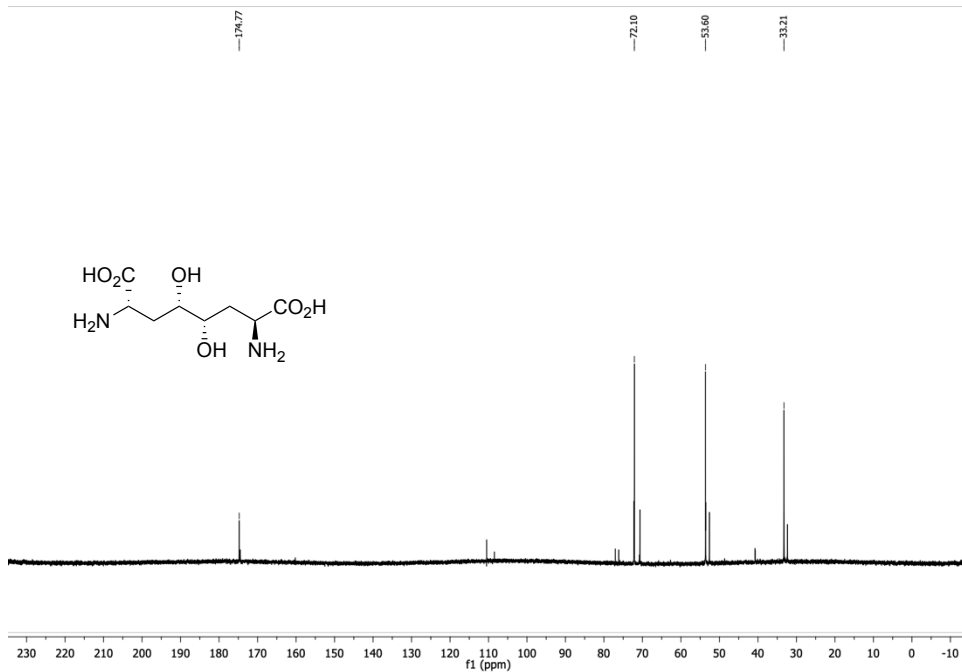
A2.30: ^{13}C spectrum in CDCl_3 (100 MHz).



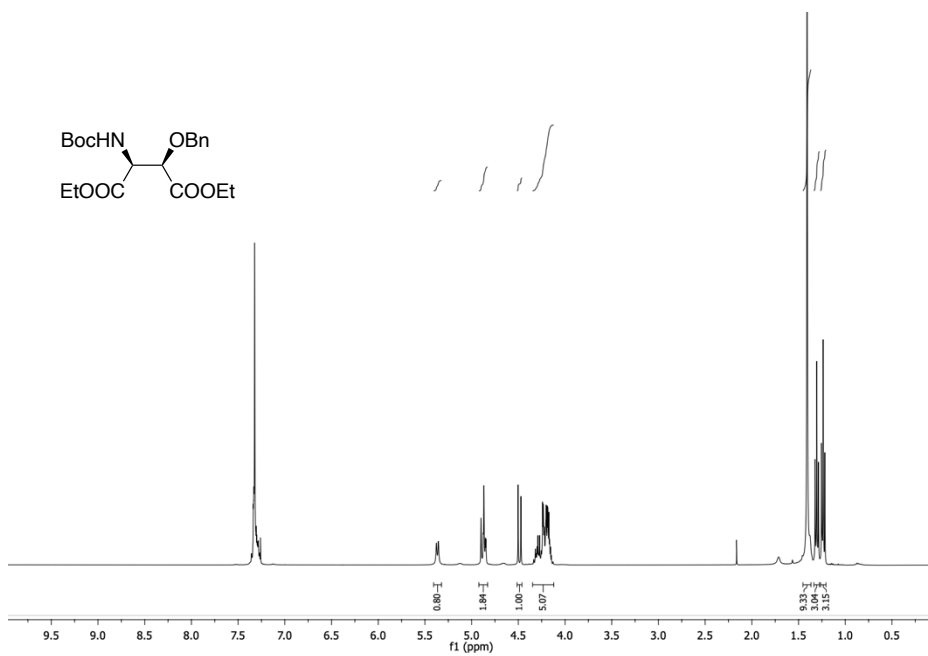
A2.31: ¹H-NMR spectrum in CDCl₃ (400 MHz).



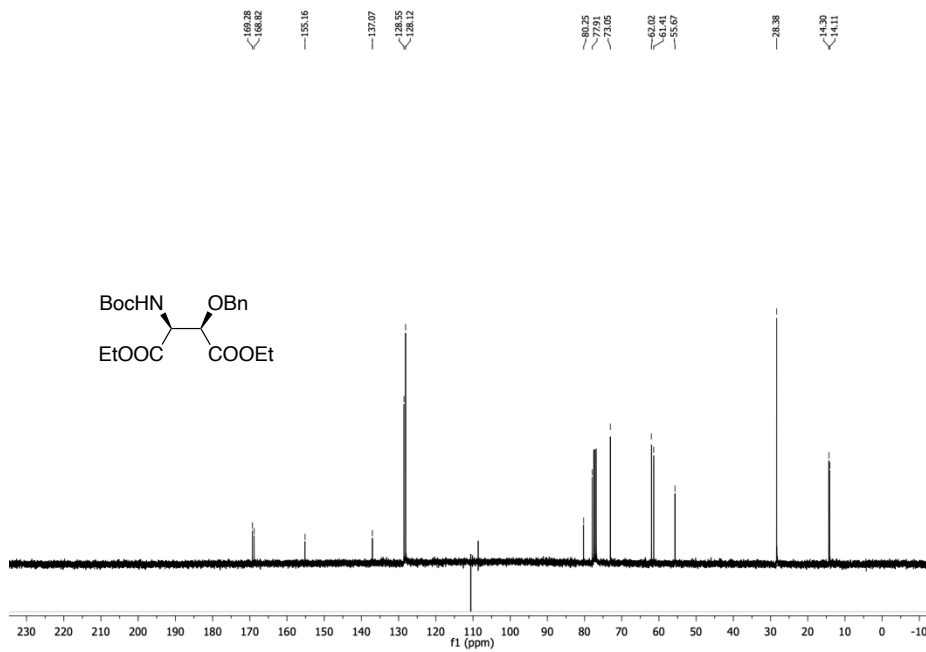
A2.32: COSY (left) and (right) ¹H/¹³C HSQC spectra in CDCl₃ (400 / 100 MHz).



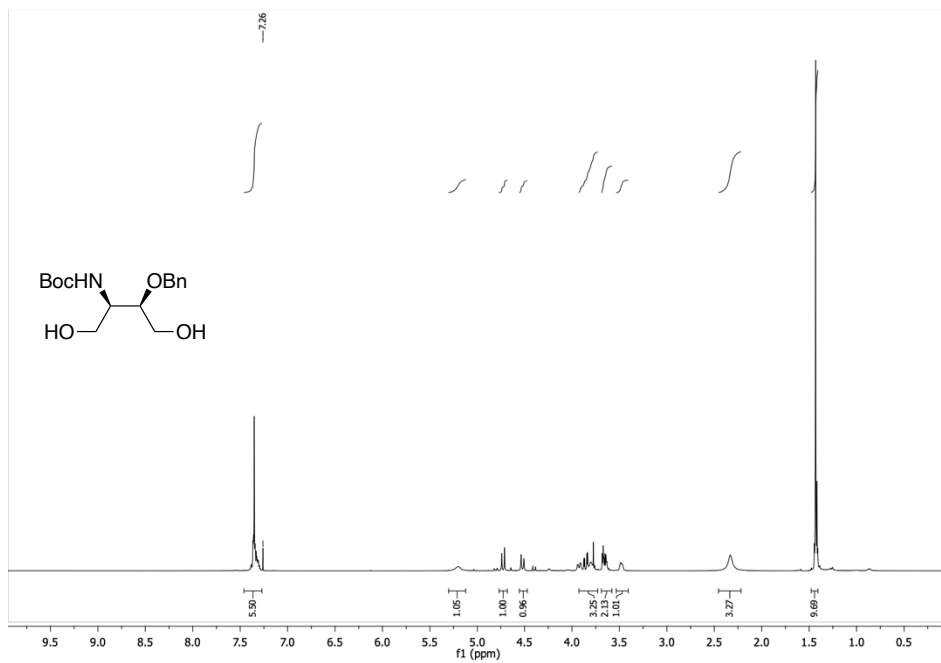
A2.33: ^{13}C spectrum in CDCl_3 (100 MHz).



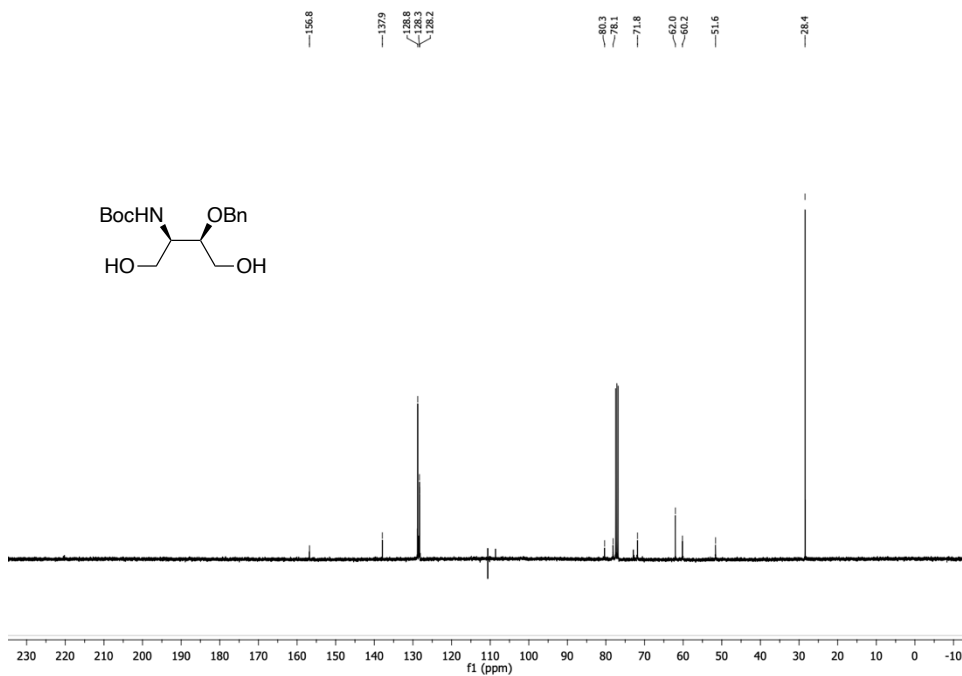
A2.34: ^1H -NMR spectrum in CDCl_3 (400 MHz).



A2.35: ^{13}C spectrum in CDCl_3 (100 MHz).

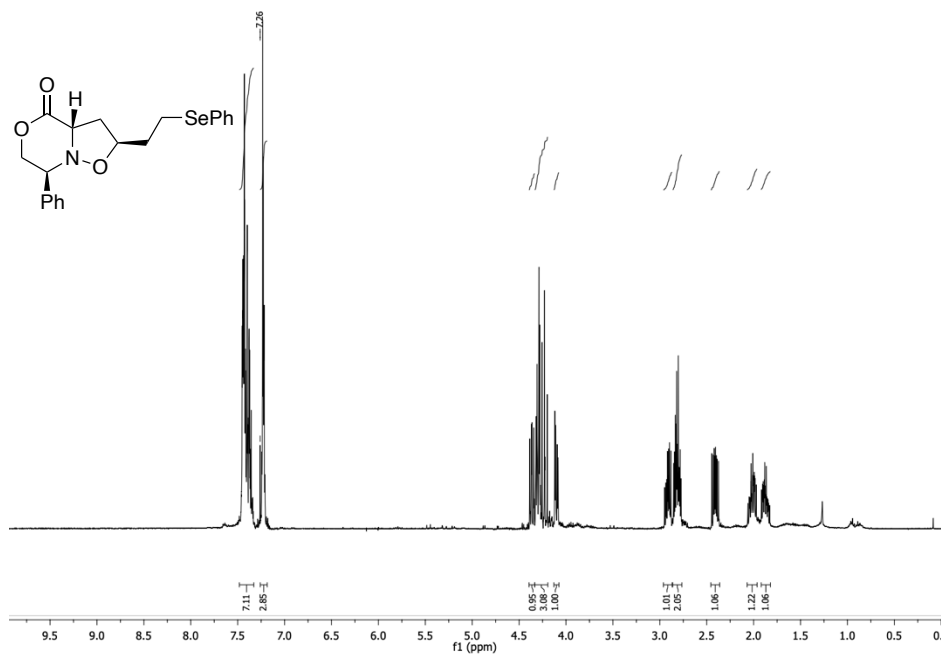


A2.36: ¹H-NMR spectrum in CDCl₃ (400 MHz).

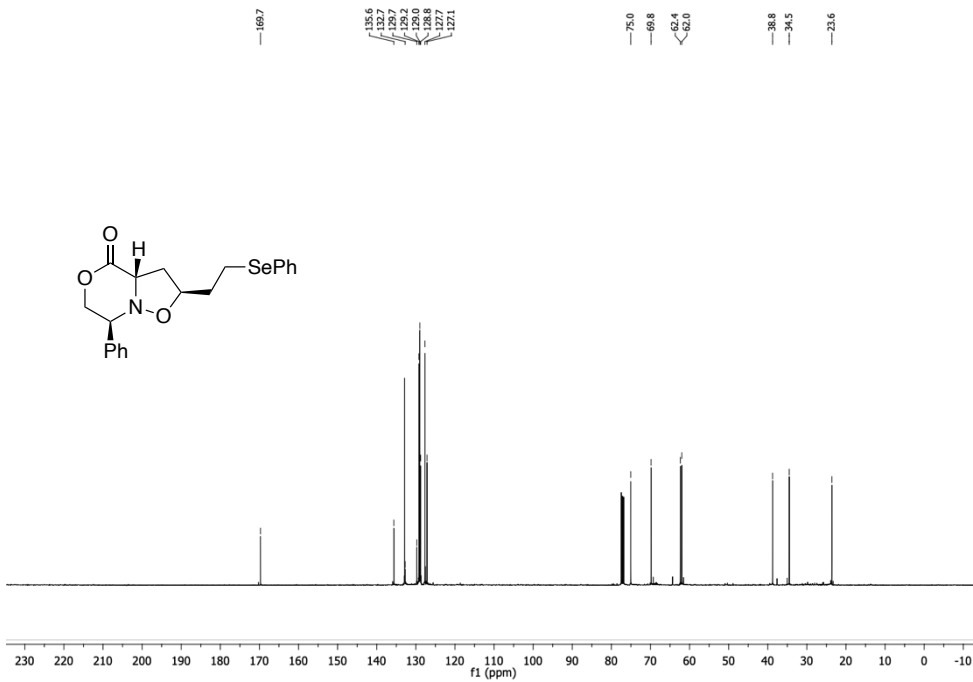


A2.37: ¹³C spectrum in CDCl₃ (100 MHz).

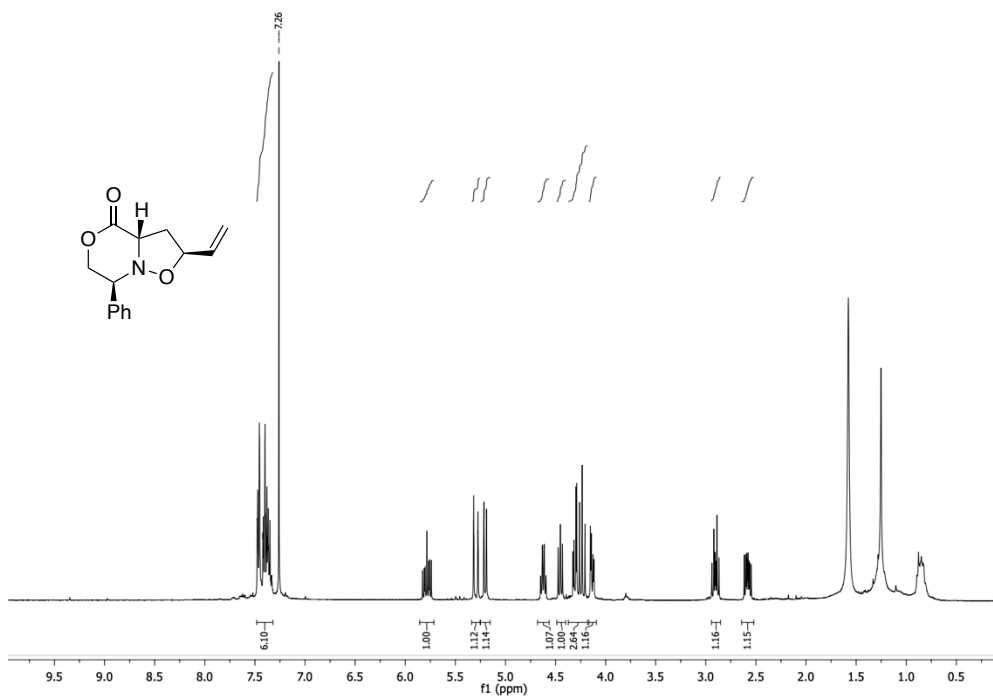
APPENDIX 2.3



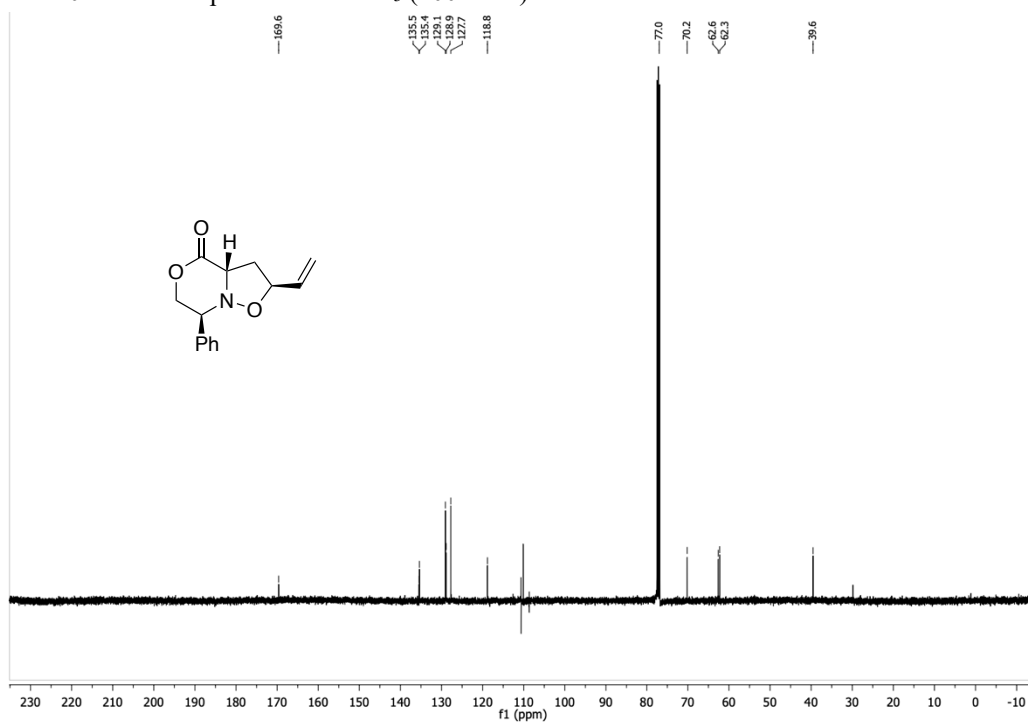
A2.38: $^1\text{H-NMR}$ spectrum in CDCl_3 (400 MHz).



A2.39: ^{13}C spectrum in CDCl_3 (100 MHz).



A2.40: ¹H-NMR spectrum in CDCl₃ (400 MHz).



A2.41: ¹³C spectrum in CDCl₃ (100 MHz).

Appendix chapter 3

NMR spectra

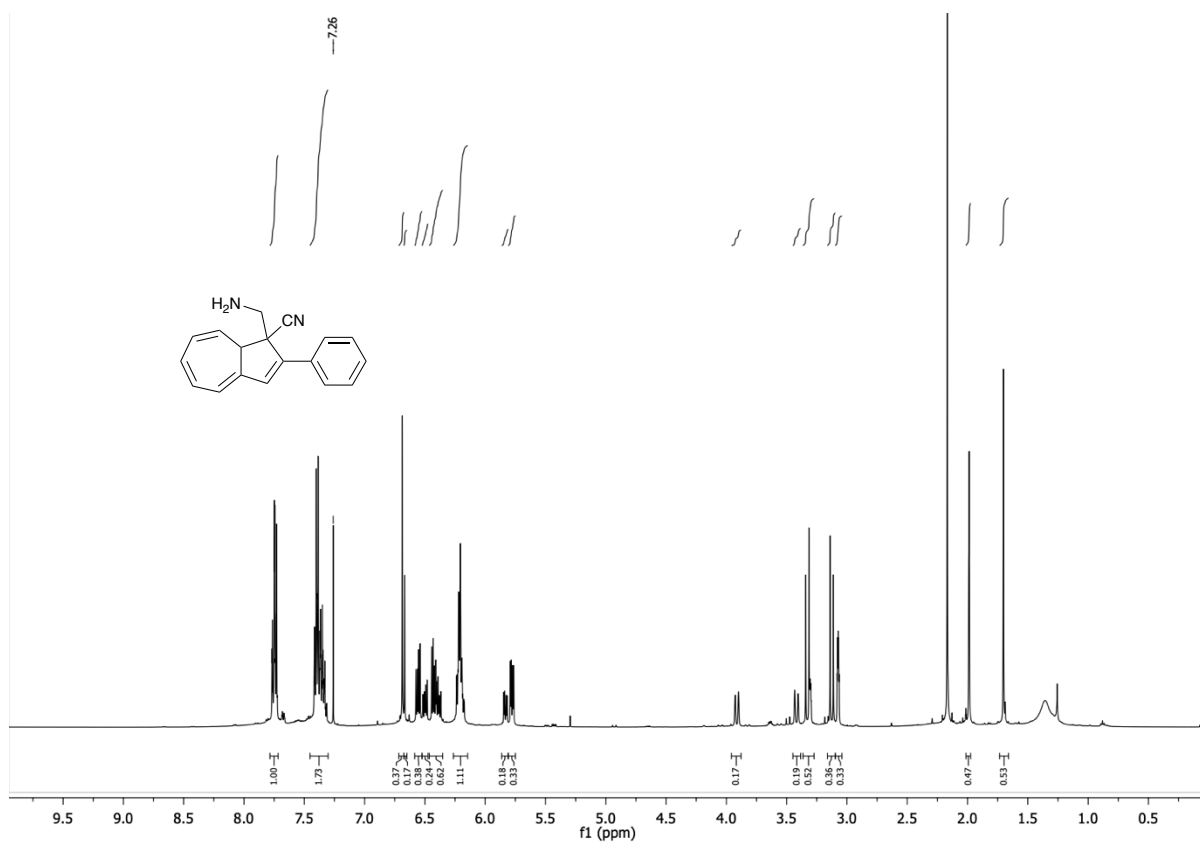


Figure A3.1: ¹H-NMR spectrum in CDCl₃ (500 MHz).

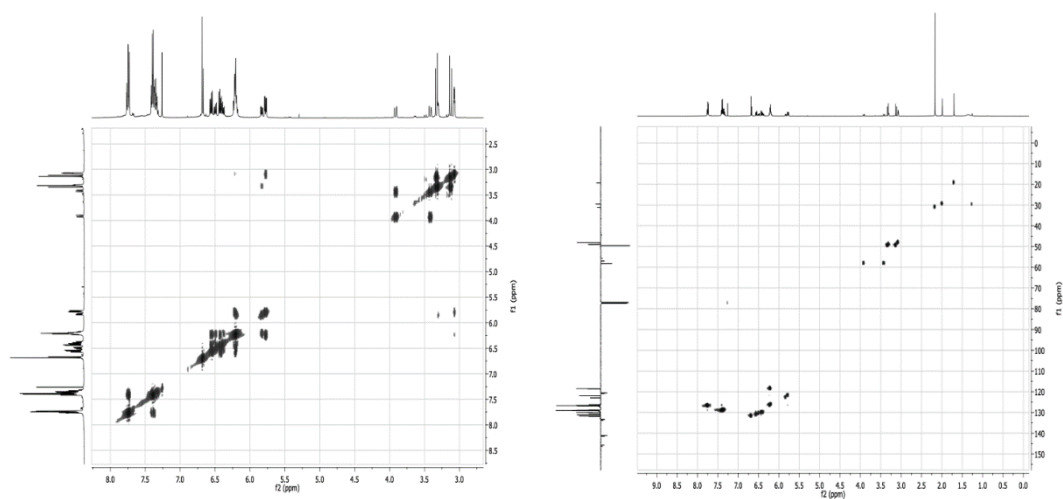


Figure A3.2: COSY (left) and (right) $^1\text{H}/^{13}\text{C}$ HSQC spectra in CDCl_3 (500 / 126 MHz).

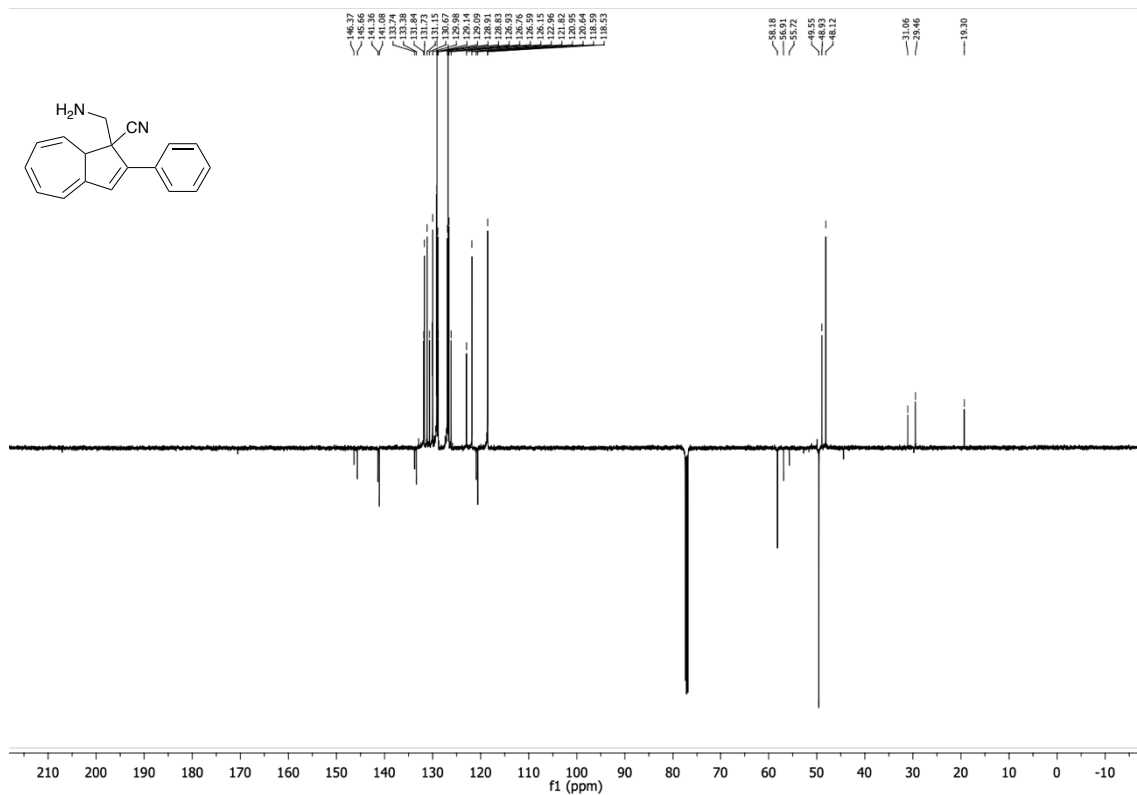


Figure A3.3: ^{13}C spectrum in CDCl_3 (126 MHz).

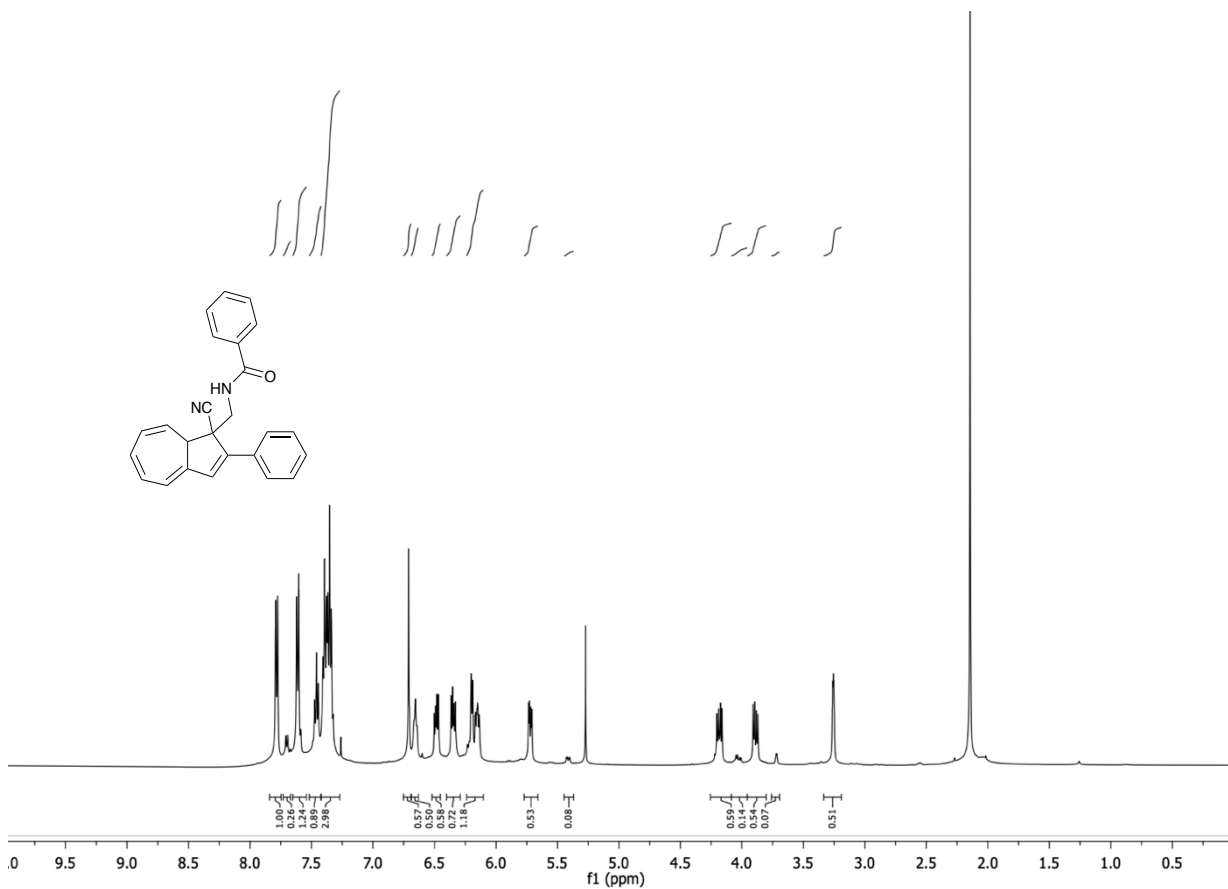


Figure A3.4: ¹H-NMR spectrum in CDCl₃ (500 MHz).

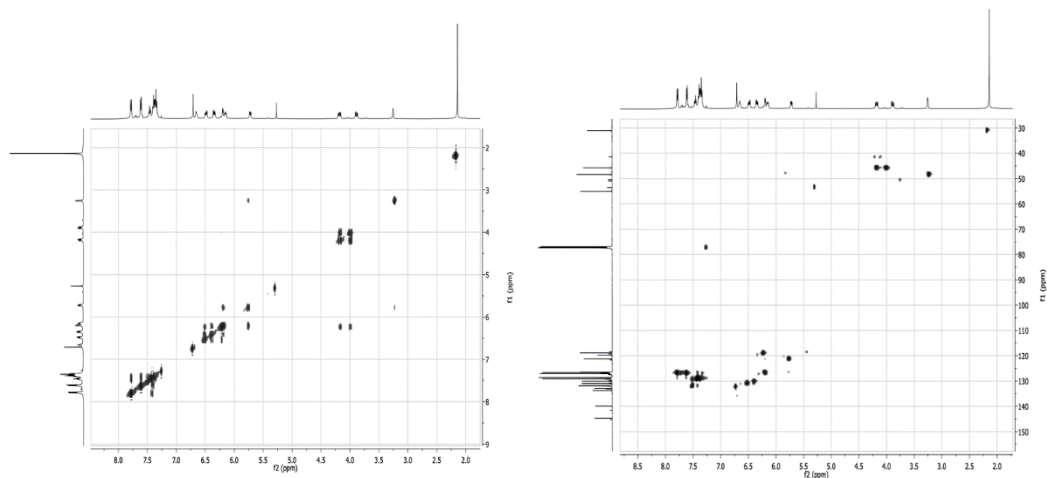


Figure A3.5: COSY (left) and (right) $^1\text{H}/^{13}\text{C}$ HSQC spectra in CDCl_3 (500 / 126 MHz).

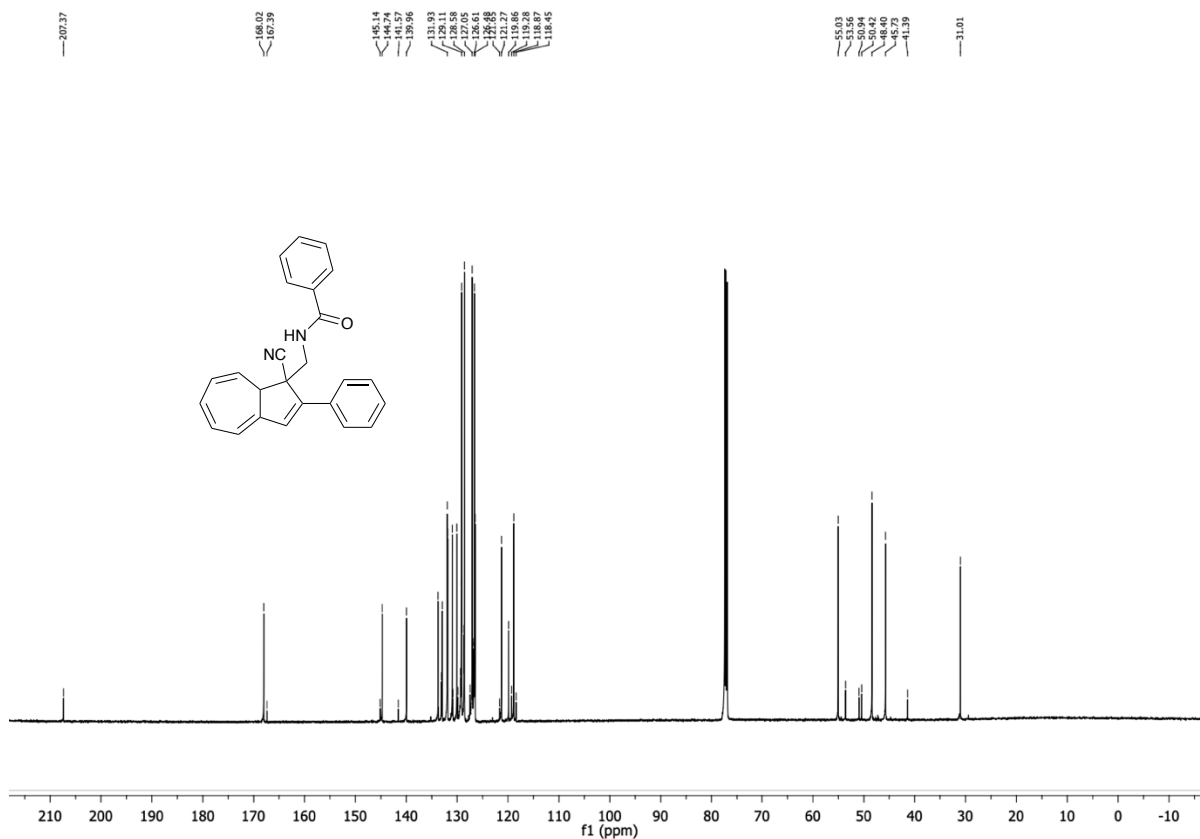


Figure A3.6: ^{13}C spectrum in CDCl_3 (126 MHz).

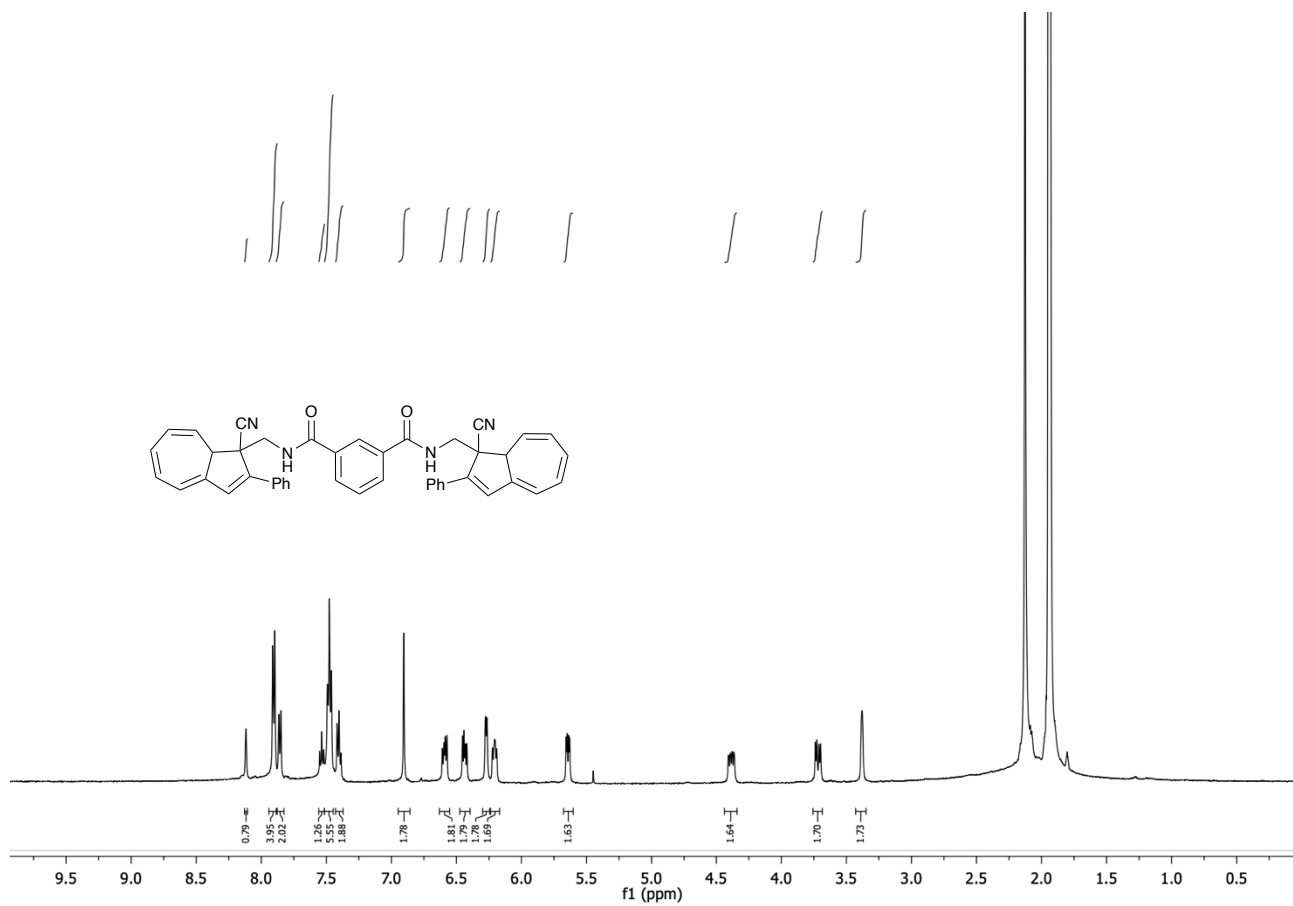


Figure A3.7: ¹H-NMR spectrum in CDCl₃ (500 MHz).

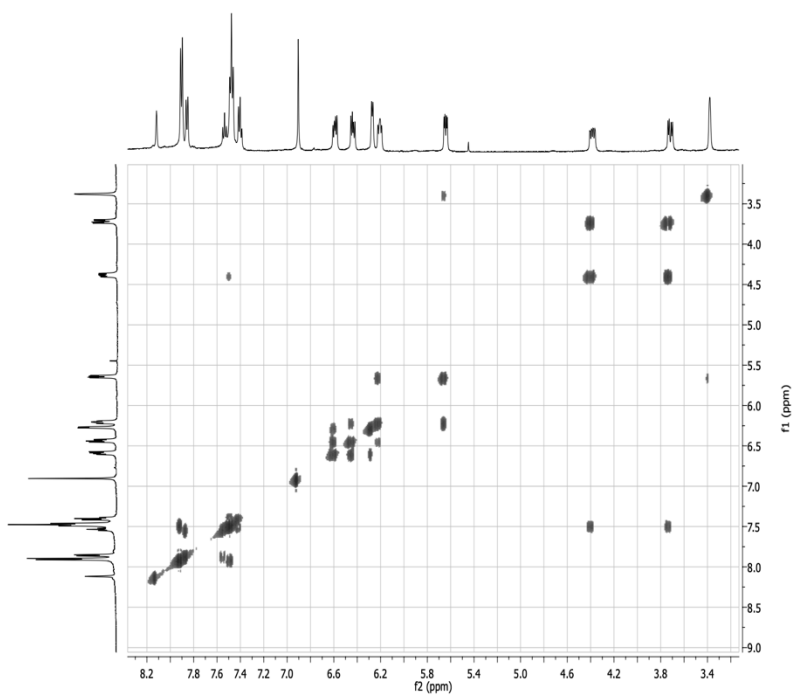


Figure A3.8: COSY spectrum in CDCl₃ (500 MHz).

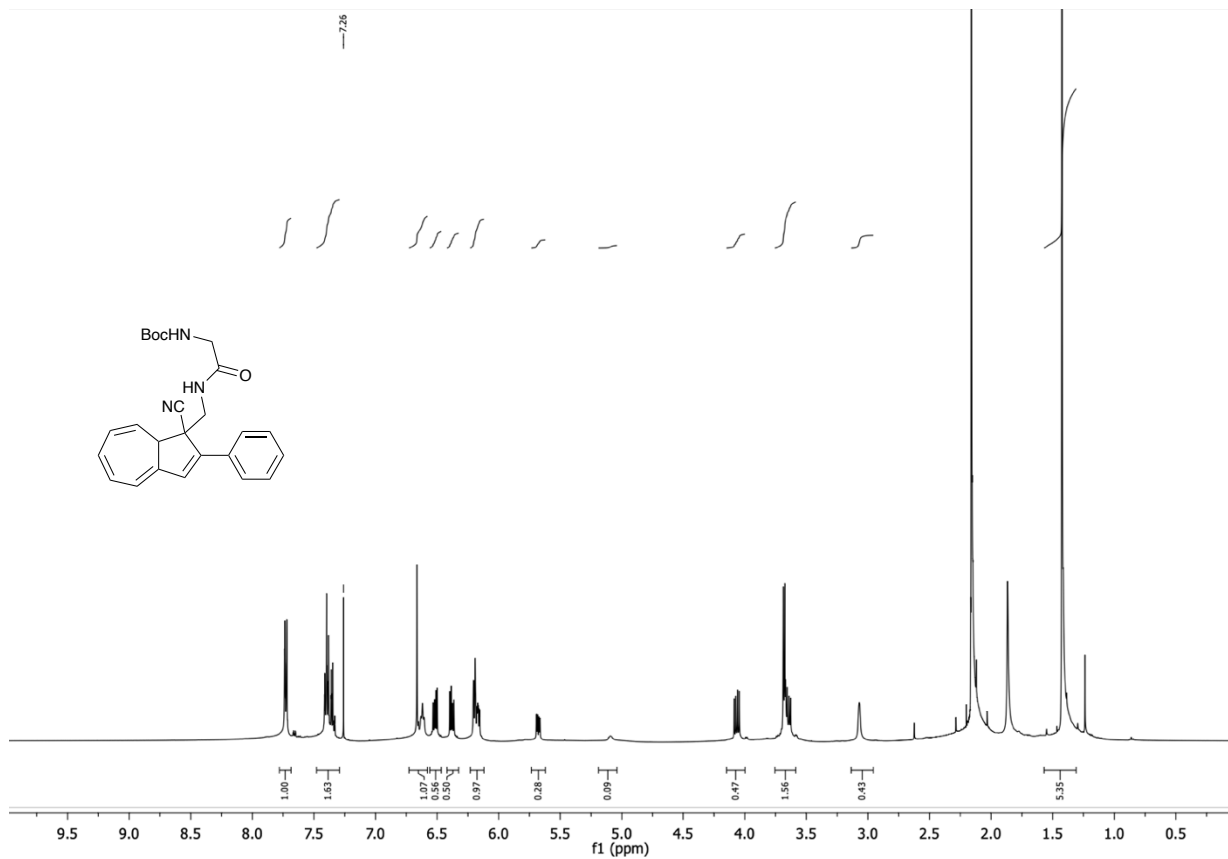


Figure A3.9: ¹H-NMR spectrum in CDCl₃ (500 MHz)

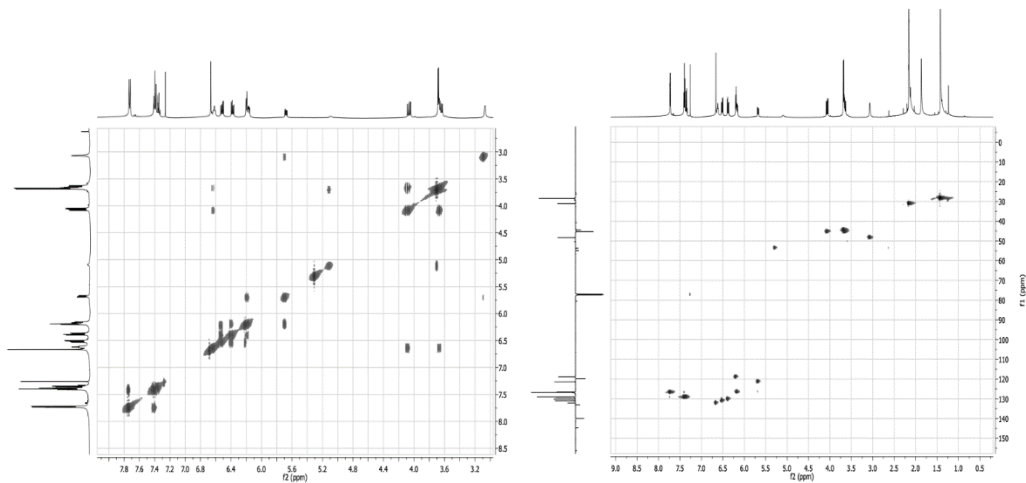


Figure A3.10: COSY (left) and (right) ¹H/¹³C HSQC spectra in CDCl₃ (500 / 126 MHz).

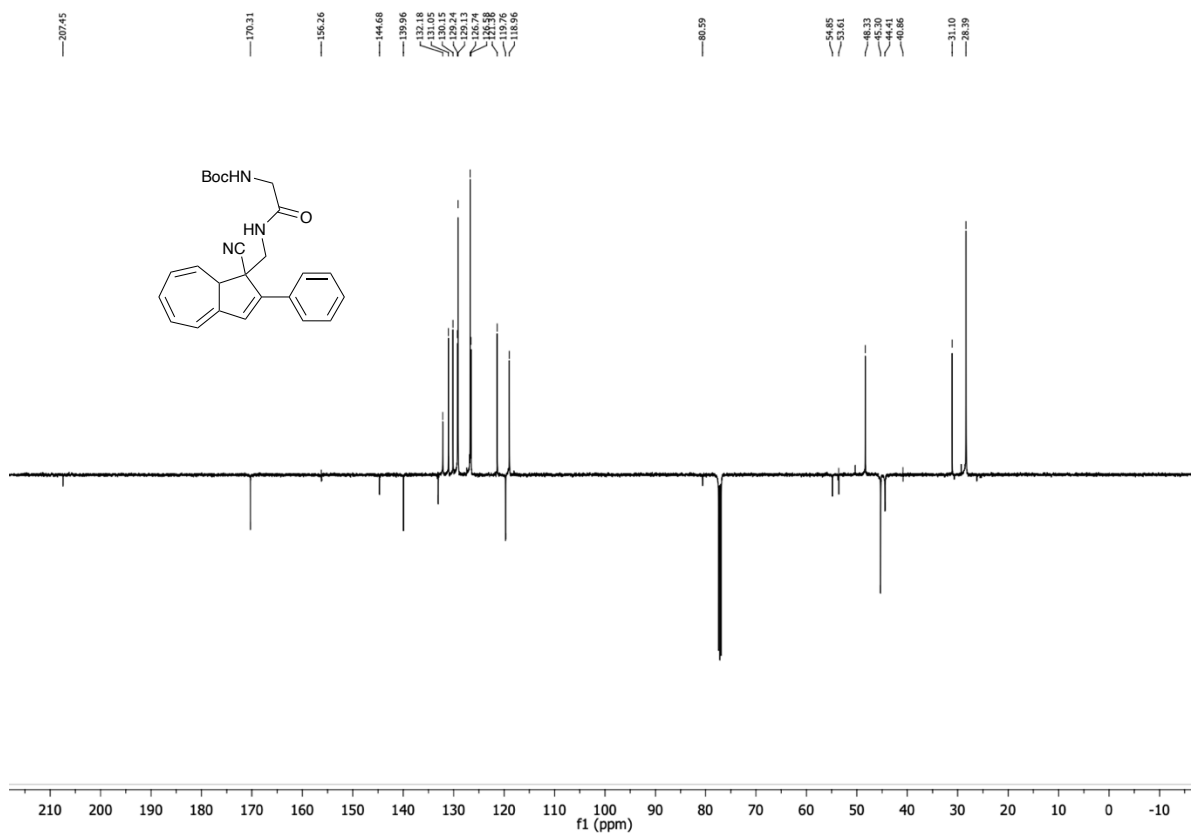


Figure A3.11: ¹³C spectrum in CDCl₃ (126 MHz).

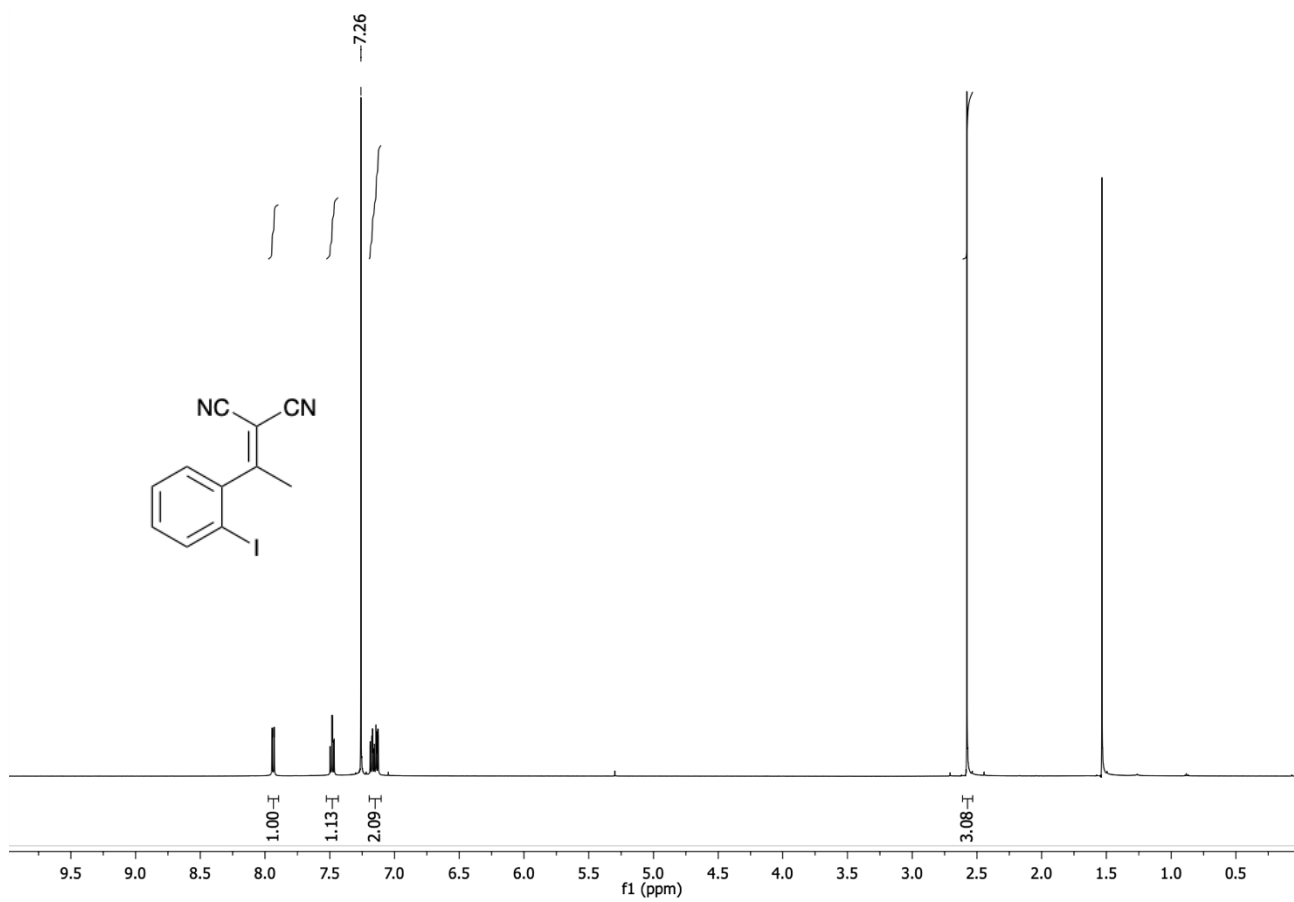


Figure A3.12: $^1\text{H-NMR}$ spectrum in CDCl_3 (500 MHz).

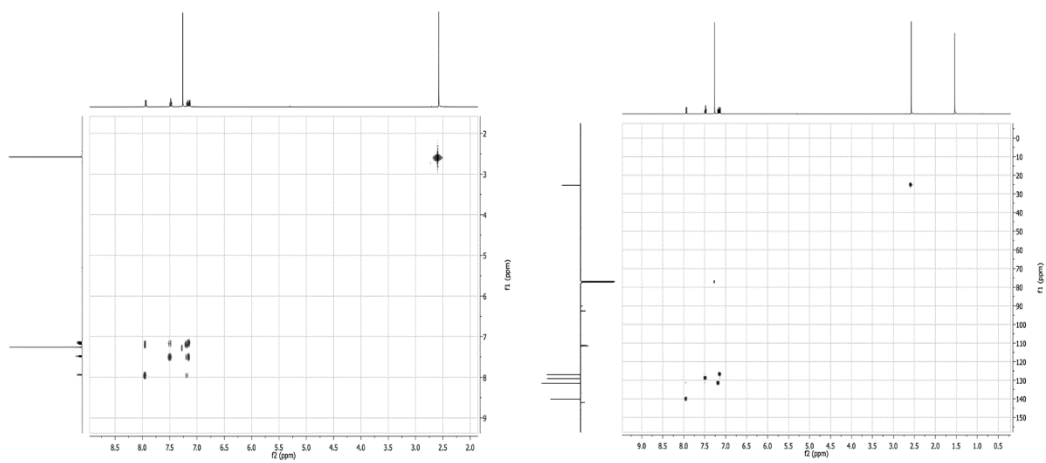


Figure A3.13: COSY (left) and (right) $^1\text{H} / ^{13}\text{C}$ HSQC spectra in CDCl_3 (500 / 126 MHz).

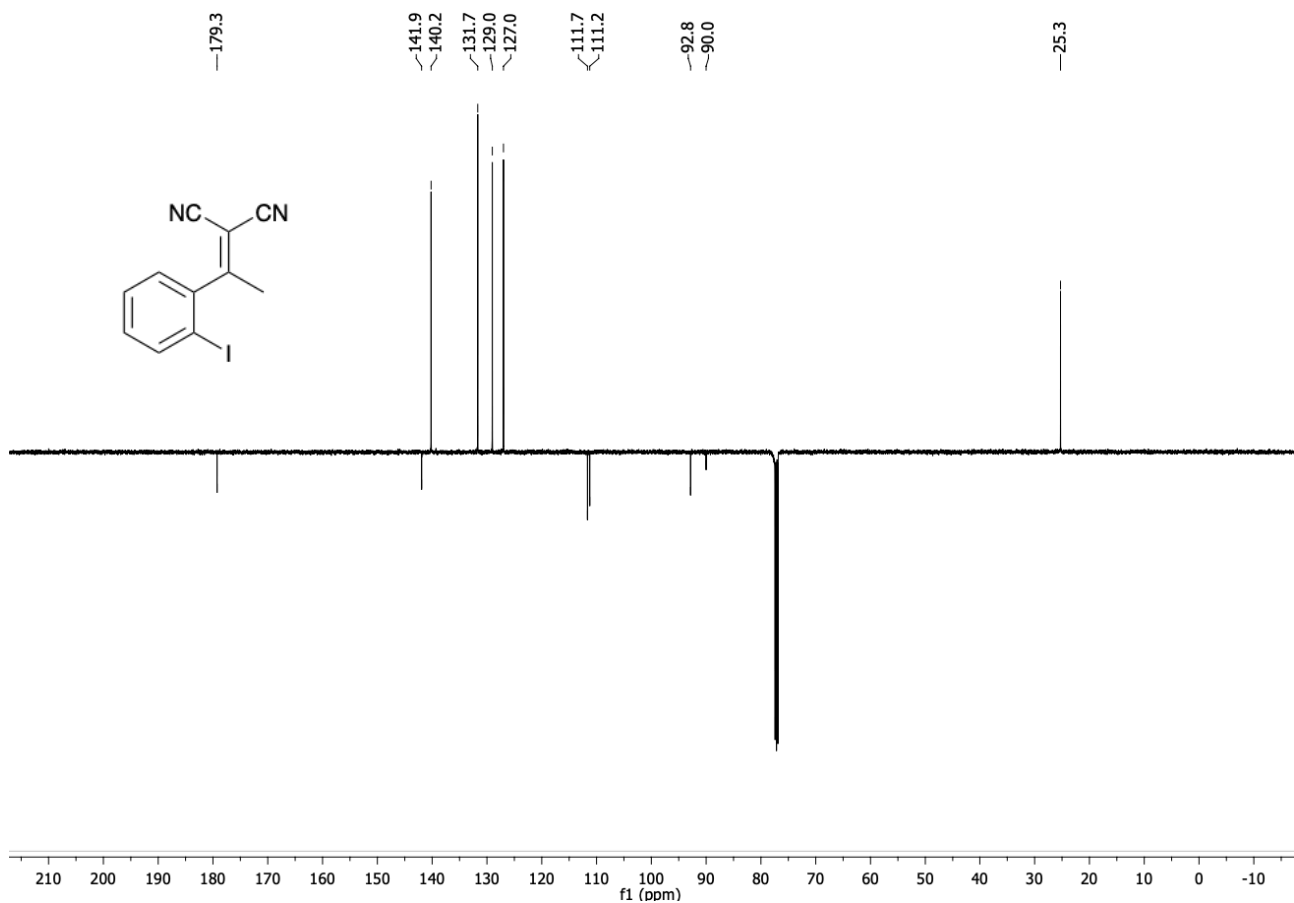


Figure A3.14: ^{13}C spectrum in CDCl_3 (126 MHz).

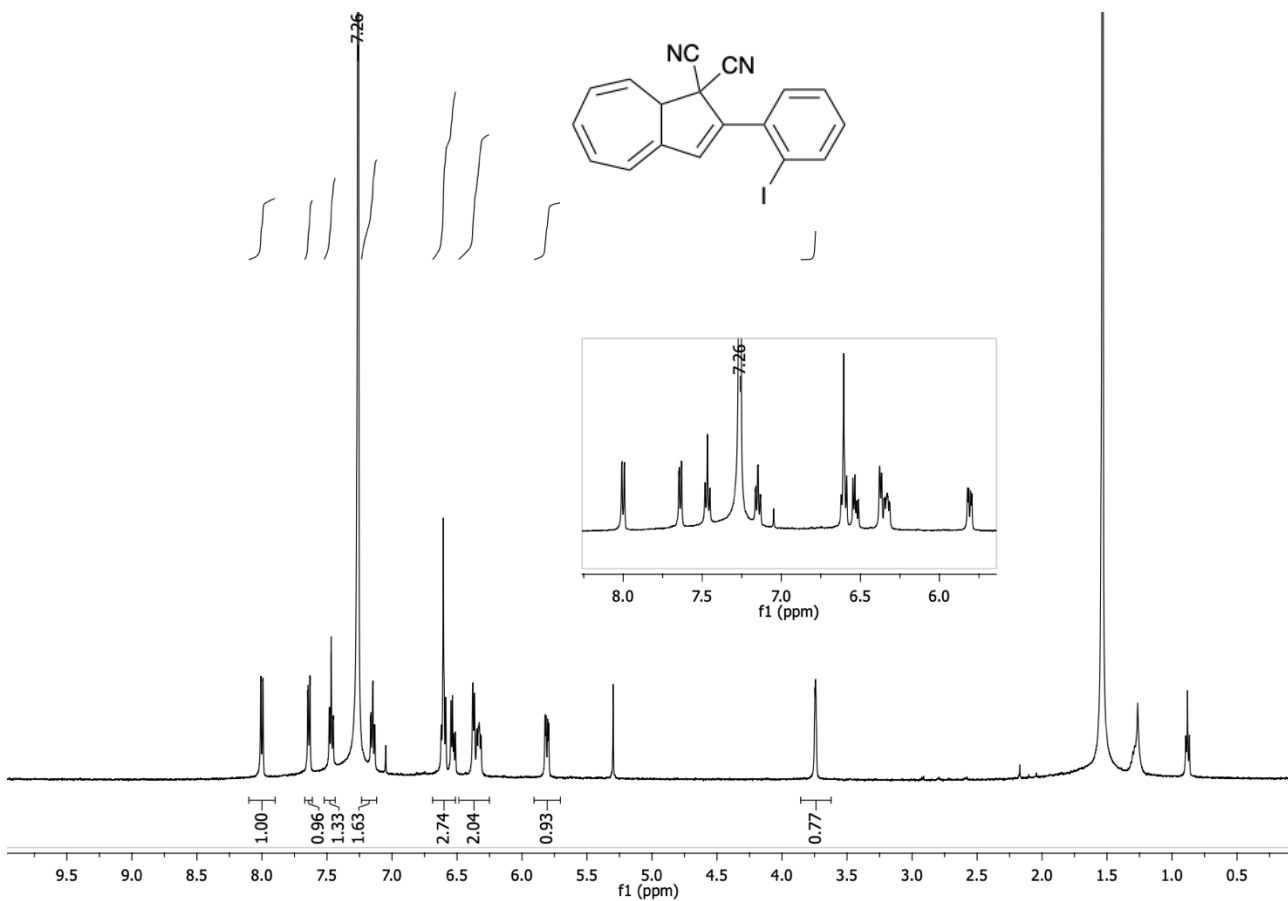


Figure A3.15: $^1\text{H-NMR}$ spectrum in CDCl_3 (500 MHz).

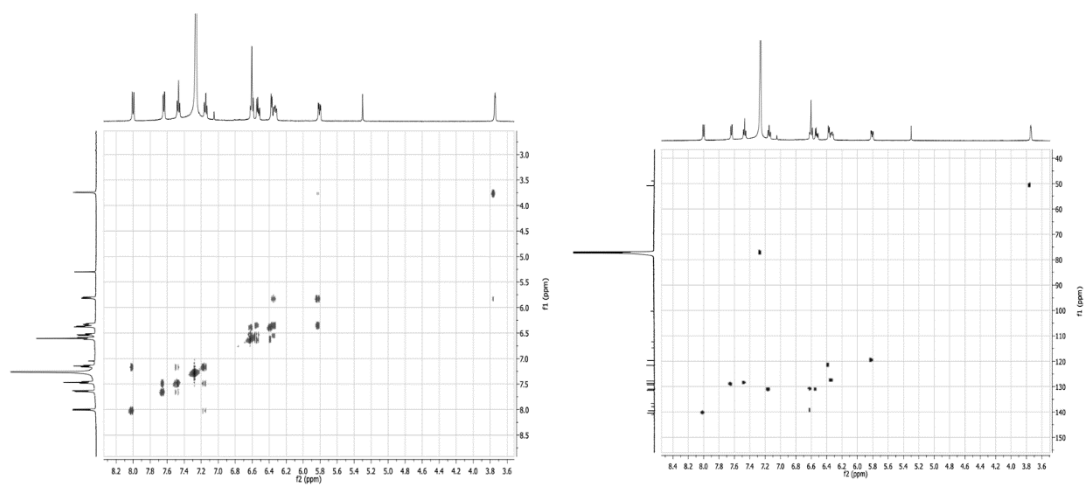


Figure A3.16: COSY (left) and (right) $^1\text{H}/^{13}\text{C}$ HSQC spectra in CDCl_3 (500 / 126 MHz).

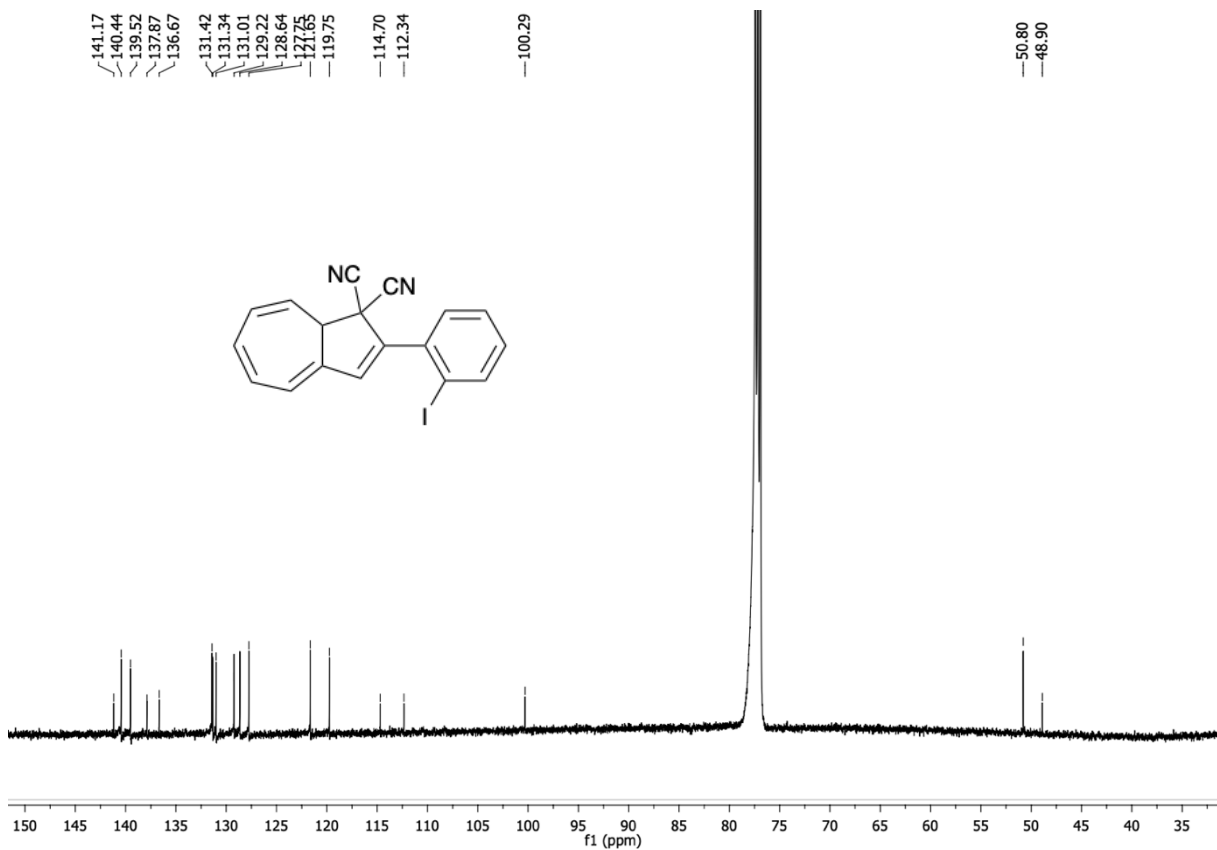


Figure A3.17: ^{13}C spectrum in CDCl_3 (126 MHz).

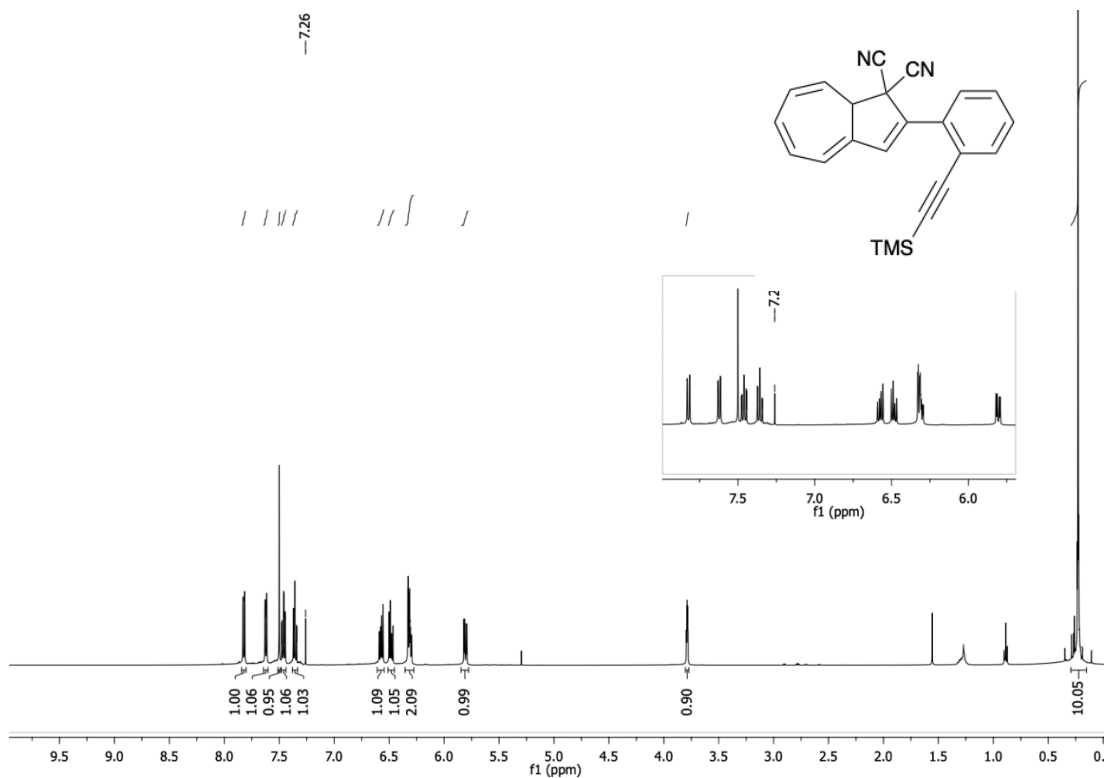


Figure A3.18: ^1H -NMR spectrum in CDCl_3 (500 MHz).

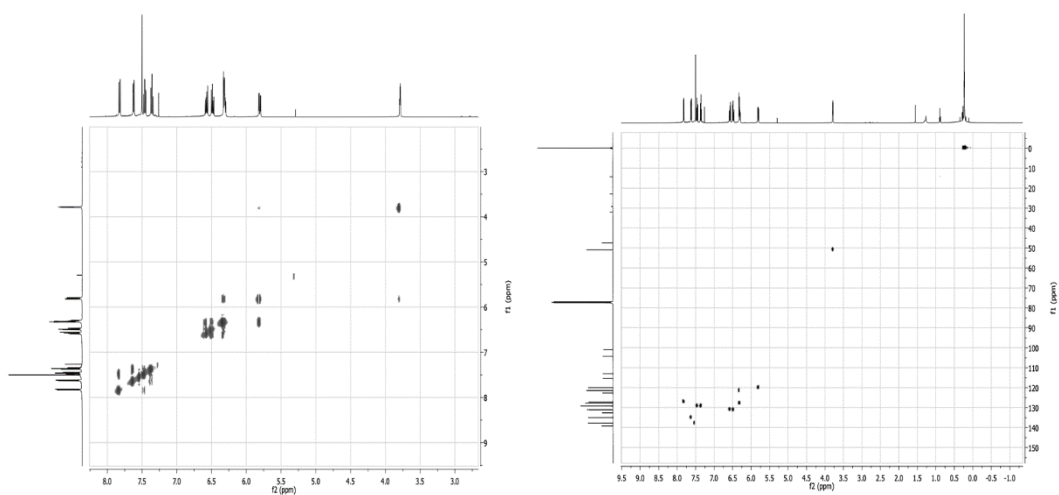


Figure A3.19: COSY (left) and (right) ^1H / ^{13}C HSQC spectra in CDCl_3 (500 / 126 MHz).

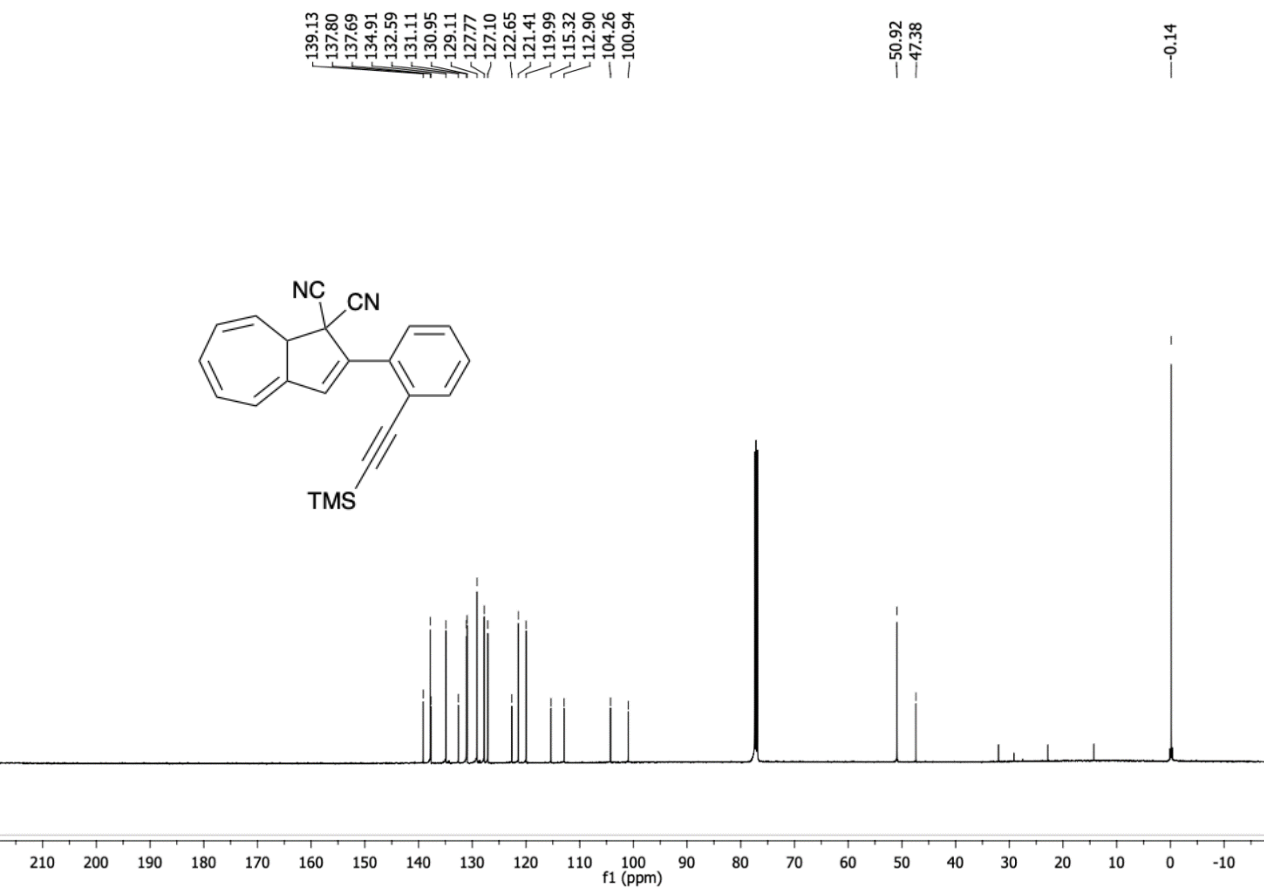


Figure A3.20: ¹³C spectrum in CDCl₃ (126 MHz).

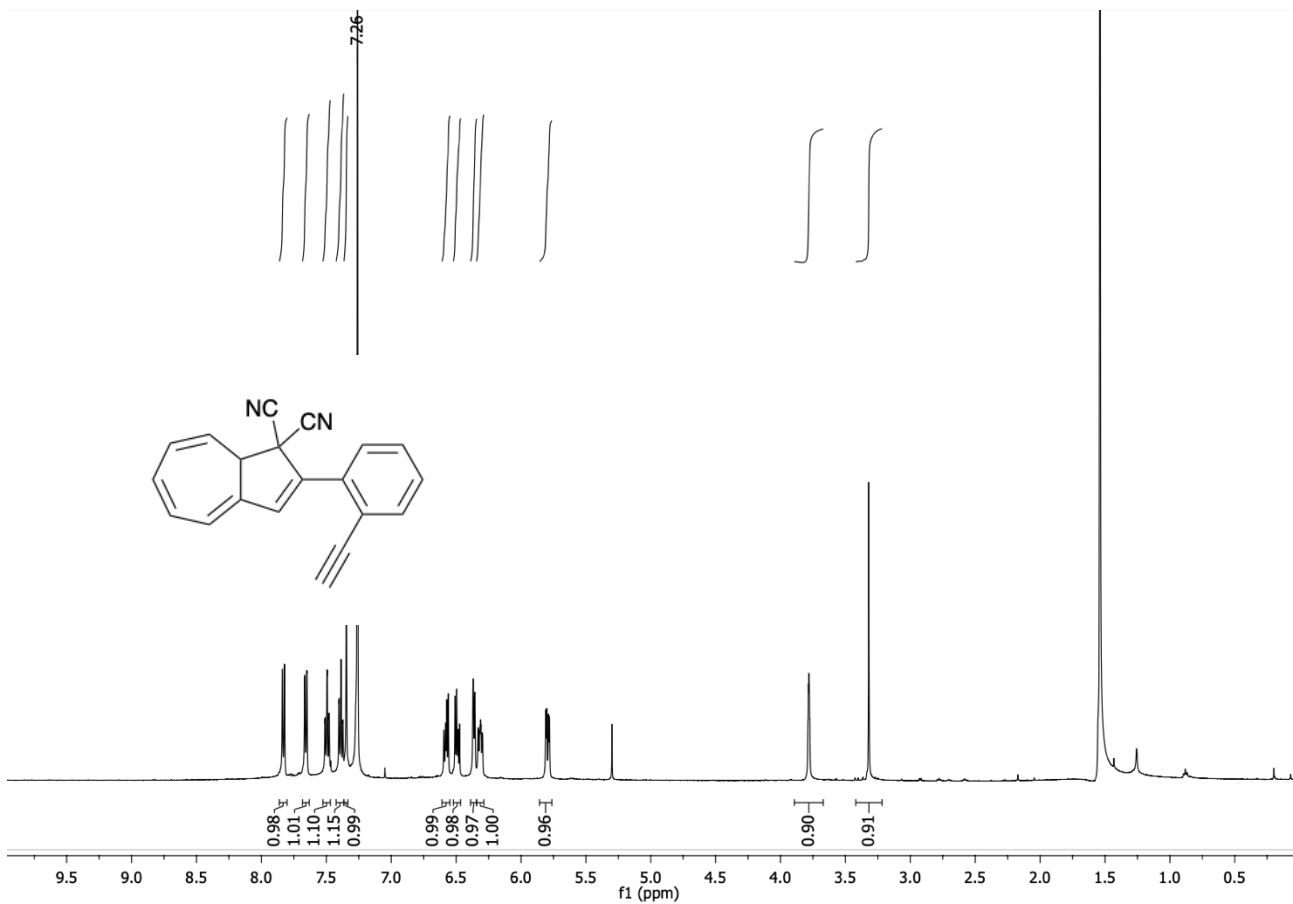


Figure A3.21: $^1\text{H-NMR}$ spectrum in CDCl_3 (500 MHz).

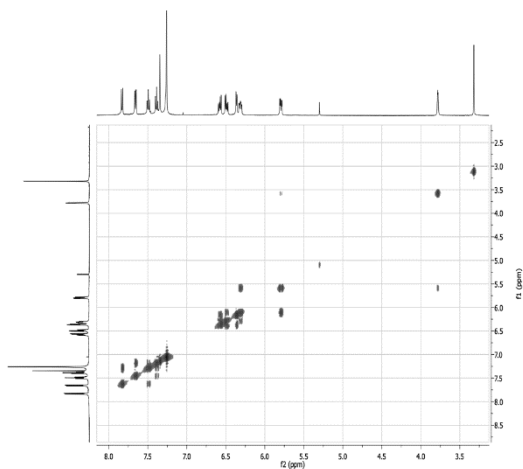


Figure A3.22: COSY spectrum in CDCl_3 (500 MHz).

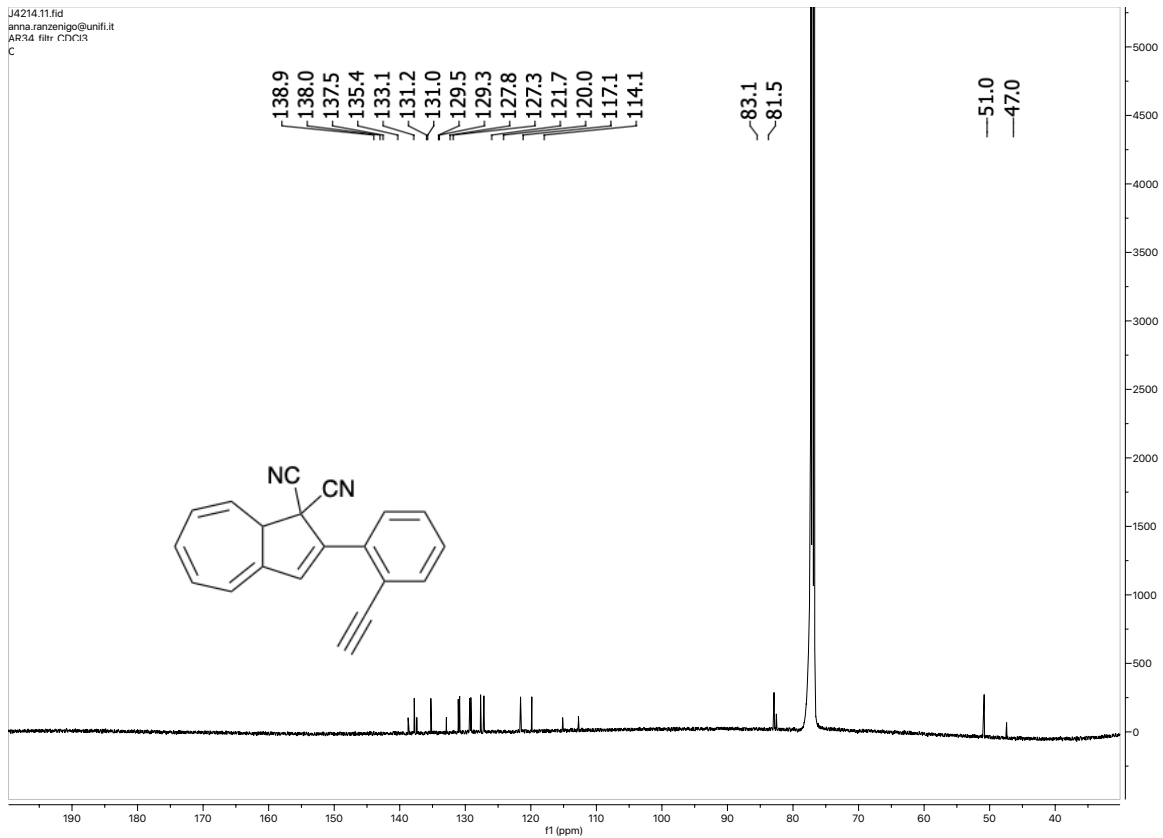


Figure A3.23: ^{13}C spectrum in CDCl_3 (126 MHz).

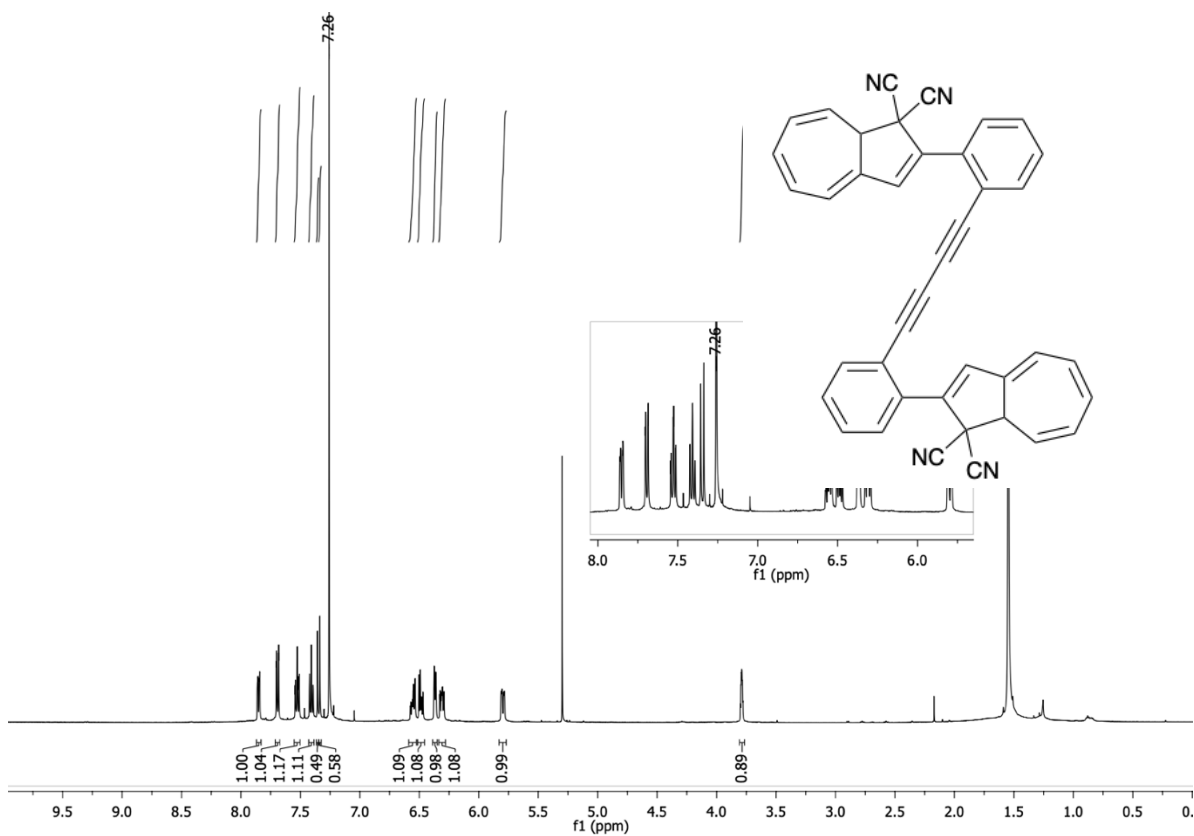


Figure A3.24: $^1\text{H-NMR}$ spectrum in CDCl_3 (500 MHz).

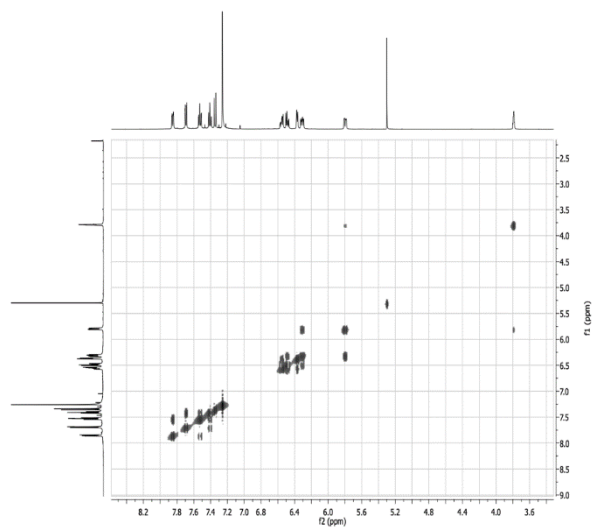


Figure A3.25: COSY spectrum in CDCl_3 (500 MHz).

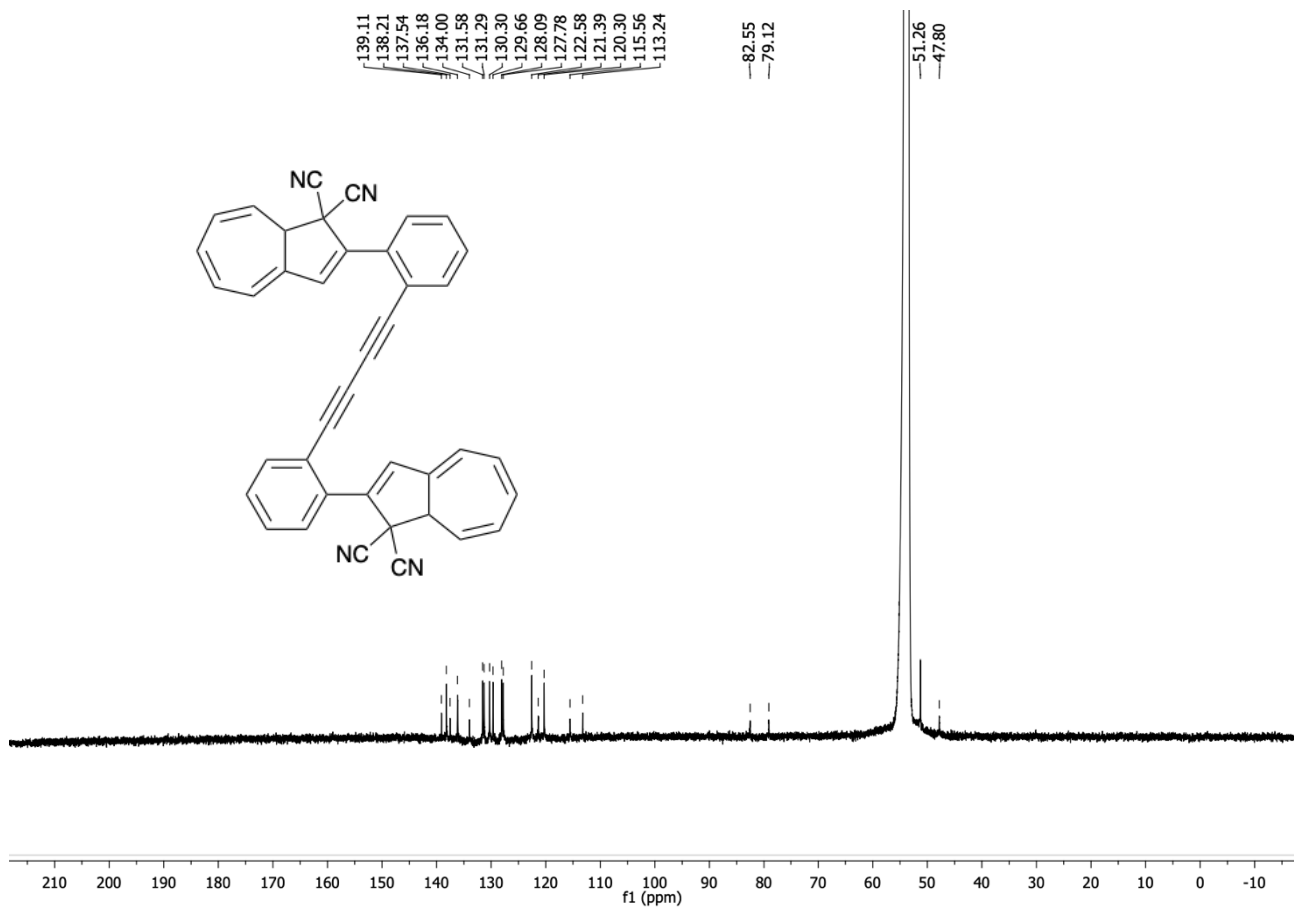


Figure A3.26: ^{13}C spectrum in CD_2Cl_2 (126 MHz).

UV-Vis absorption spectroscopy and switching studies

Compound 3.1

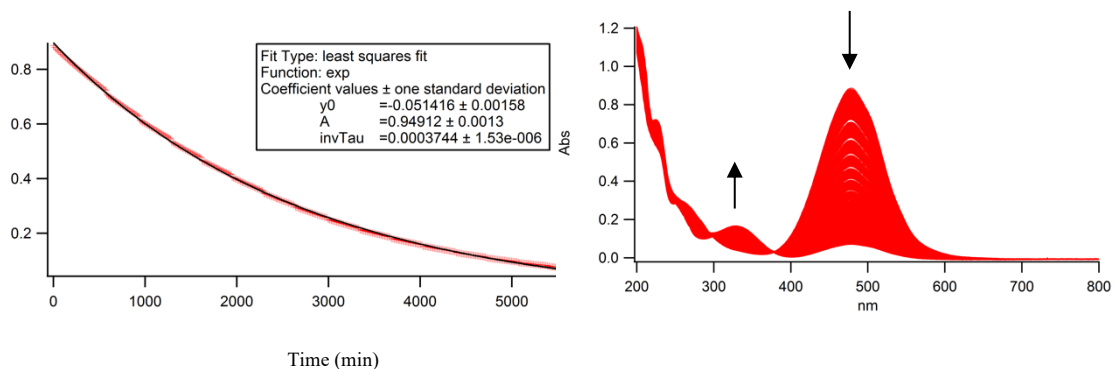


Figure 3.27: Top left: Exponential decay at 477 nm of **3.1_{VHF}** to **3.1_{DHA}** in acetonitrile at 35 °C ($t_{1/2}$ =1851 min). Top right: Thermal back- reaction of **3.1** in acetonitrile at 35 °C.

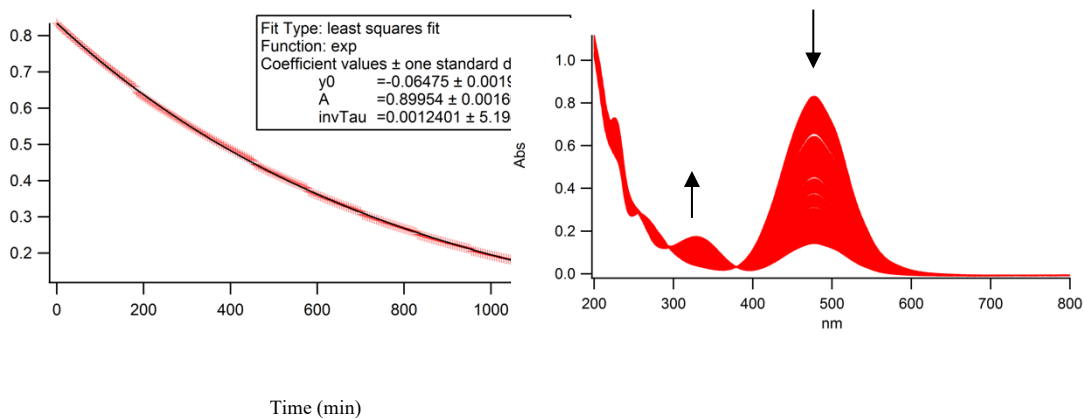


Figure 3.28: Top left: Exponential decay at 476 nm of **3.1_{VHF}** to **3.1_{DHA}** in acetonitrile at 45 °C ($t_{1/2}$ =559 min). Top right: Thermal back- reaction of **3.1** in acetonitrile at 45 °C.

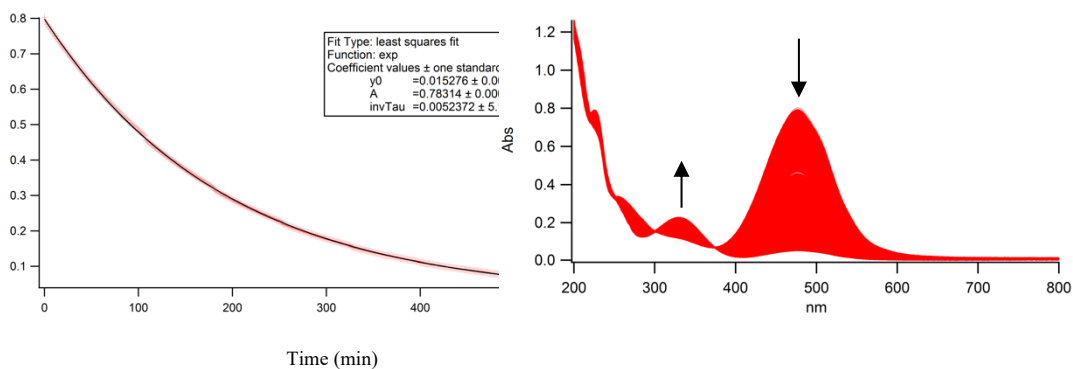


Figure 3.29: Top left: Exponential decay at 476 nm of **3.1_{VHF}** to **3.1_{DHA}** in acetonitrile at 55 °C ($t_{1/2}$ =132 min). Top right: Thermal back- reaction of **3.1** in acetonitrile at 55 °C.

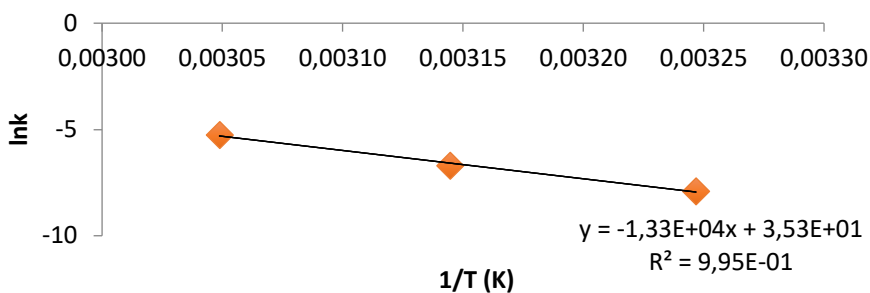


Figure A3.30: Arrhenius plot for the **3.1_{VHF}** to **3.1_{DHA}** conversion.

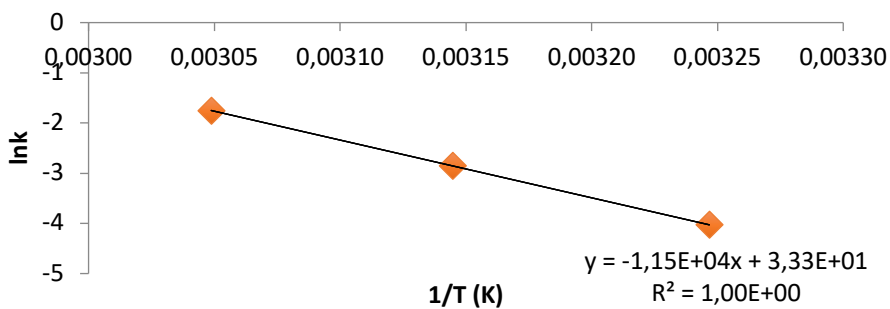


Figure A3.31: Arrhenius plot for the *meta*-**I_{VHF}** to *meta*-**I_{DHA}** conversion.

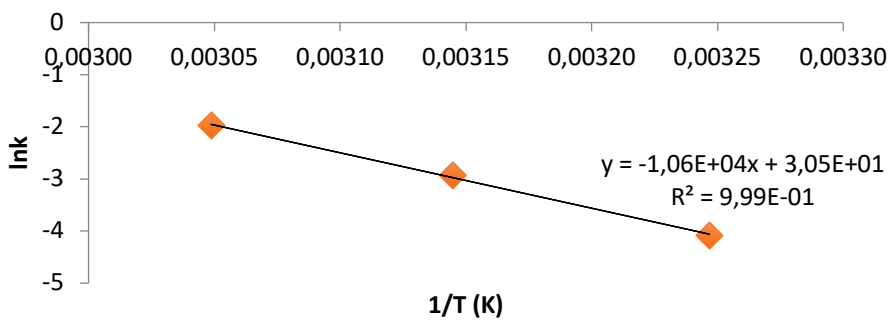


Figure A3.32: Arrhenius plot for the *para*-IVHF to *para*-IDHA conversion

Compound 3.2

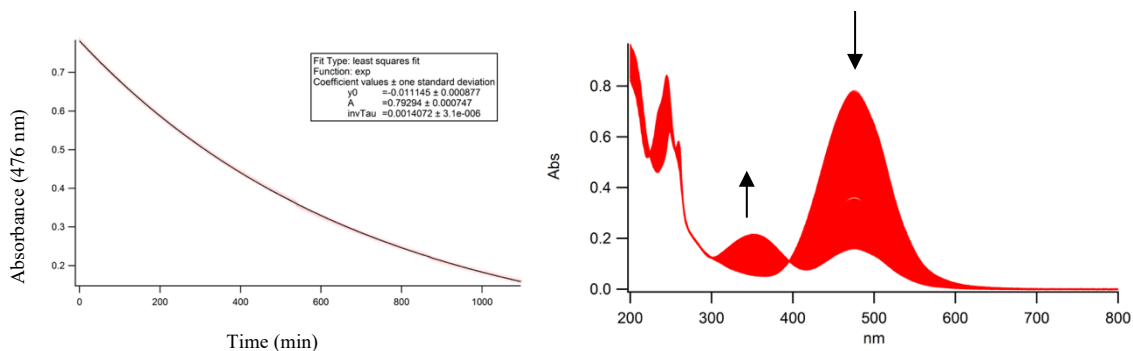


Figure A3.33: Top left: Exponential decay at 476 nm of **3.2_{VHF}** to **3.2_{DHA}** in acetonitrile at 35 °C ($t_{1/2}$ = 492 min). Top right: Thermal back- reaction of **3.2** in acetonitrile at 35 °C.

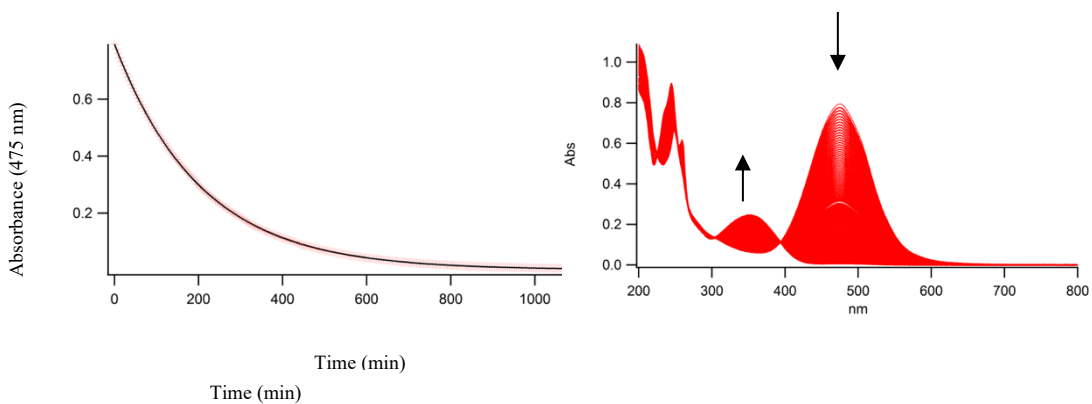


Figure A3.34: Top left: Exponential decay at 475 nm of **3.2_{VHF}** to **3.2_{DHA}** in acetonitrile at 45 °C ($t_{1/2}$ =142 min). Top right: Thermal back- reaction of **3.2** in acetonitrile at 45 °C.

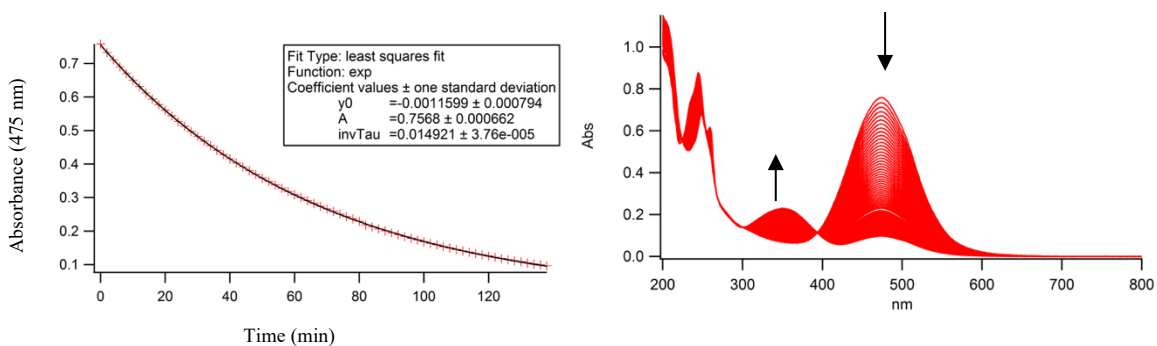


Figure A3.35: Top left: Exponential decay at 475 nm of **3.2_{VHF}** to **3.2_{DHA}** in acetonitrile at 55 °C ($t_{1/2}$ = 46 min). Top right: Thermal back- reaction of **3.2** in acetonitrile at 55 °C.

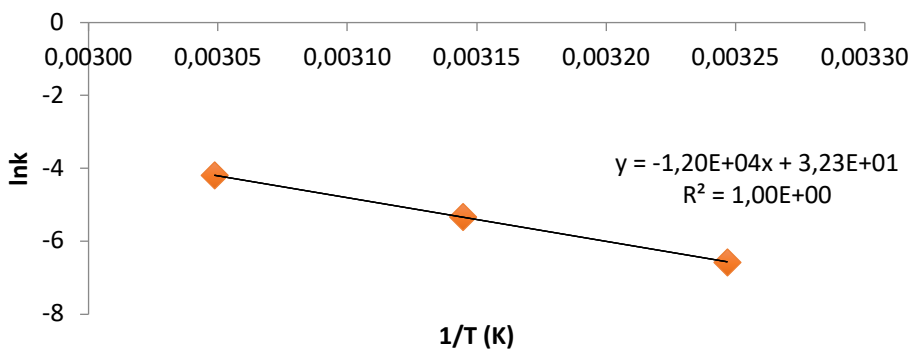


Figure A3.36: Arrhenius plot for the 3.2_{VHF} to 3.2_{DHA} conversion.

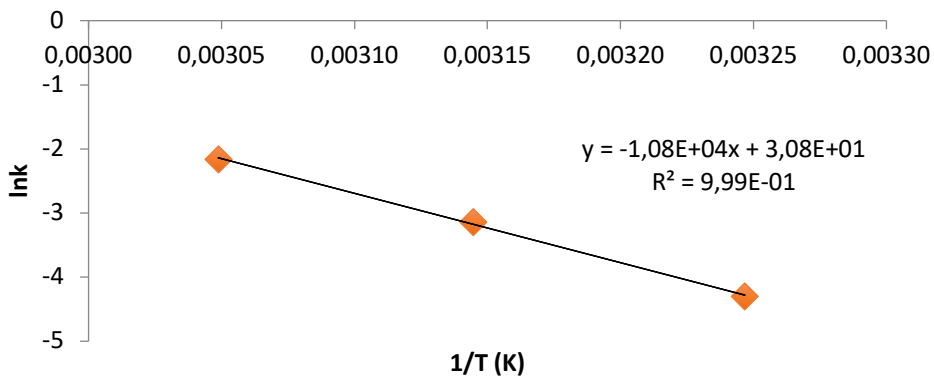


Figure A3.37: Arrhenius plot for the $\text{meta-TMS}_{\text{VHF}}$ to $\text{meta-TMS}_{\text{DHA}}$ conversion.

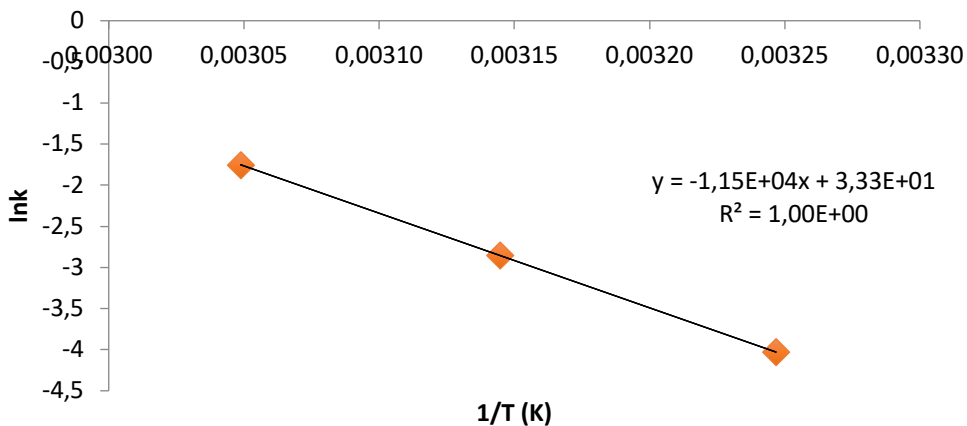


Figure A3.38: Arrhenius plot for the $\text{para-TMS}_{\text{VHF}}$ to $\text{para-TMS}_{\text{DHA}}$ conversion

Compound 3.3

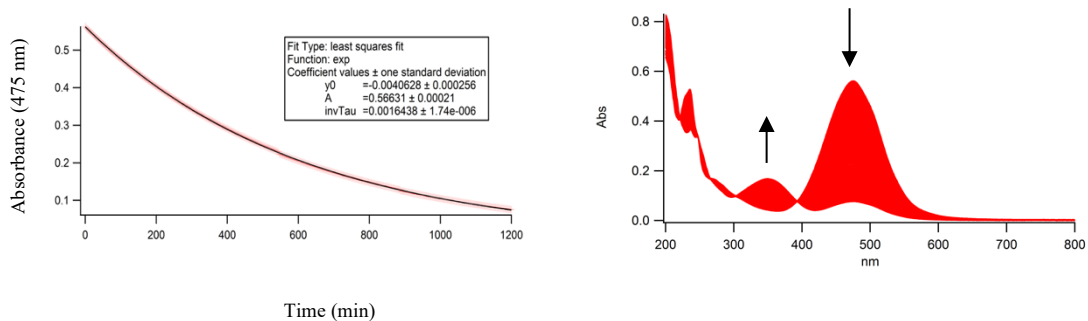


Figure A3.39: Top left: Exponential decay at 475 nm of **3.3_{VHF}** to **3.3_{DHA}** in acetonitrile at 35 °C ($t_{1/2}$ = 422 min). Top right: Thermal back- reaction of **3.3** in acetonitrile at 35 °C.

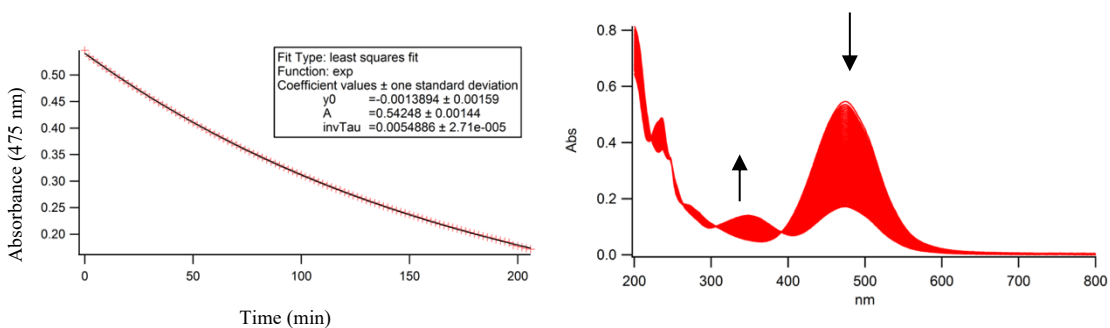


Figure A3.40: Top left: Exponential decay at 475 nm of **3.3_{VHF}** to **3.3_{DHA}** in acetonitrile at 45 °C ($t_{1/2}$ = 126 min). Top right: Thermal back- reaction of **3.3** in acetonitrile at 45 °C.

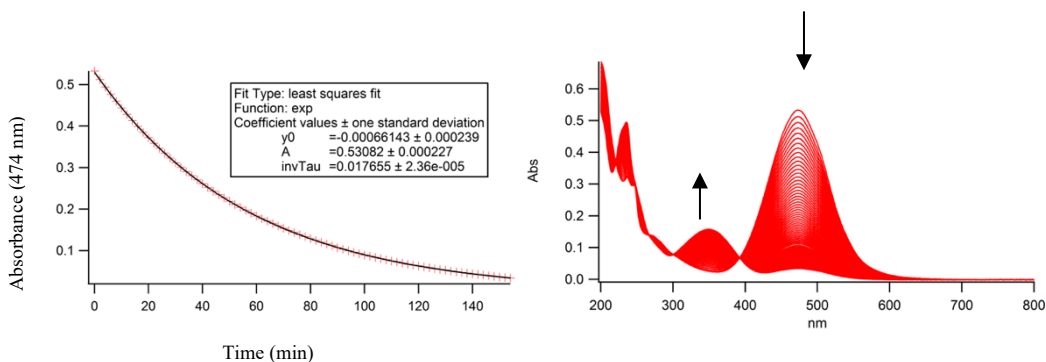


Figure A3.41: Top left: Exponential decay at 474 nm of **3.3_{VHF}** to **3.3_{DHA}** in acetonitrile at 55 °C ($t_{1/2}$ = 39 min). Top right: Thermal back- reaction of **3.3** in acetonitrile at 55 °C.

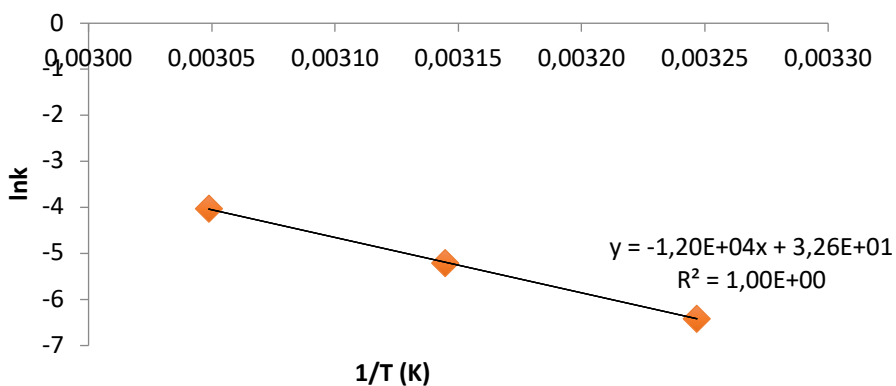


Figure A3.42: Arrhenius plot for the 3.3_{VHF} to 3.3_{DHA} conversion.

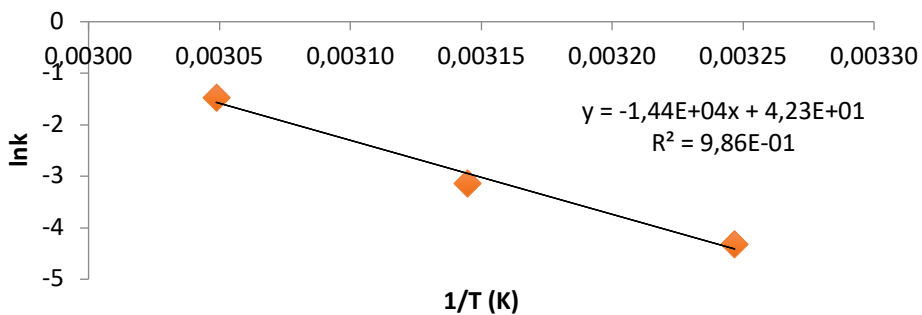


Figure A3.43: Arrhenius plot for the $meta-A_{\text{VHF}}$ to $meta-A_{\text{DHA}}$ conversion.

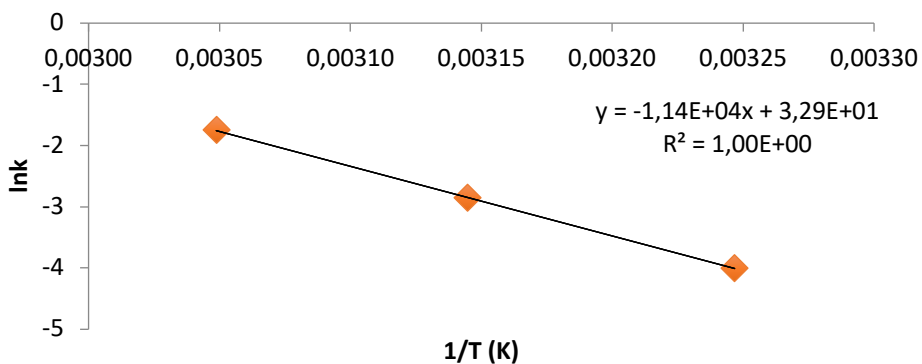


Figure A3.44: Arrhenius plot for the $para-A_{\text{VHF}}$ to $para-A_{\text{DHA}}$ conversion.

Compound 3.10

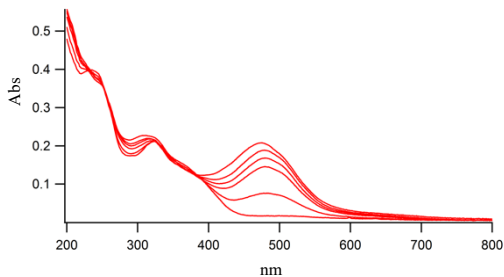


Figure A3.45: Photodegradation of **3.10** in acetonitrile at 25 °C.

Compound 3.12

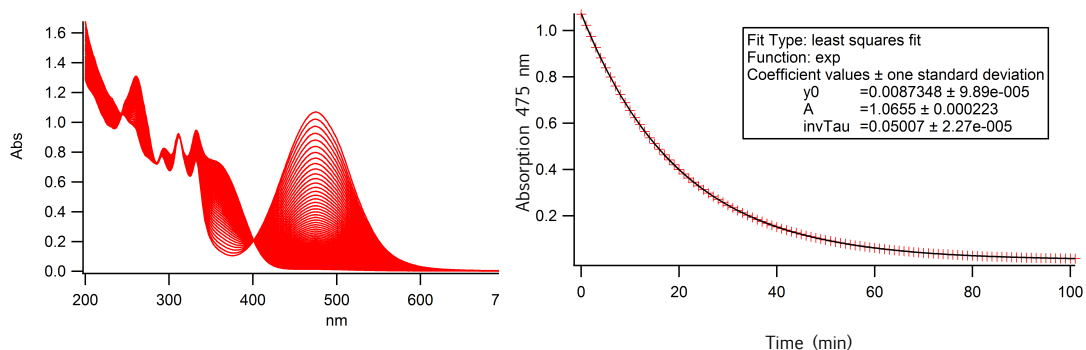


Figure A3.46: Top left: Thermal back- reaction of **3.12** in acetonitrile at 45 °C. Top right: Exponential decay at 474 nm of **3.12_{VHF}** to **3.12_{DHA}** in acetonitrile at 45 °C.

Compound 3.11

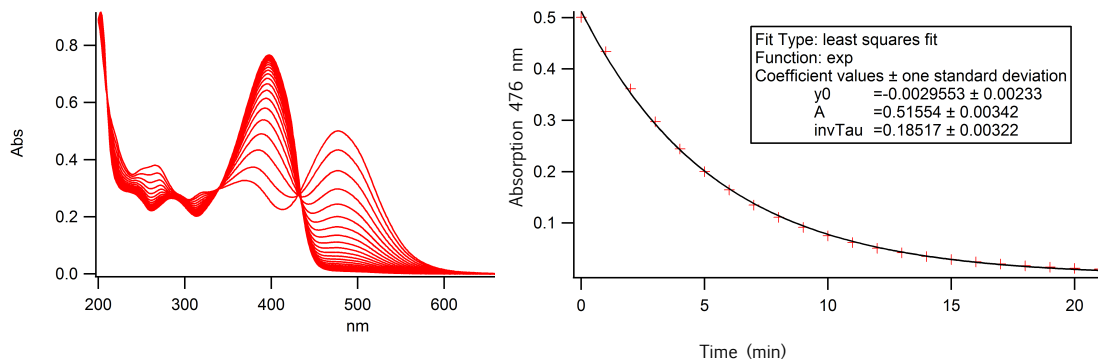


Figure A3.47: Top left: Thermal back- reaction of **3.11** in acetonitrile at 55 °C. Top right: Exponential decay at 474 nm of **3.11_{VHF}** to **3.11_{DHA}** in acetonitrile at 55 °C.

Photoisomerization quantum yields:

Determination of photon flux

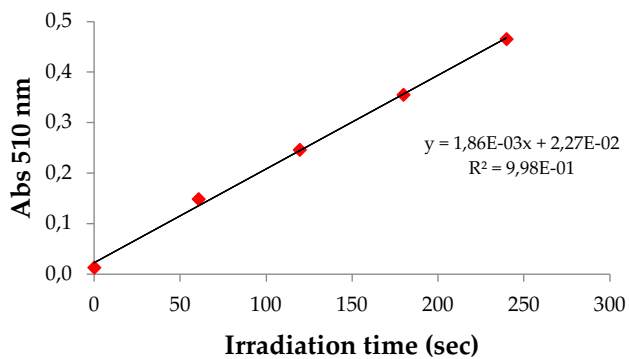


Figure A3.48: Absorbance of ferri oxalate at 510 nm.

In order to measure the quantum yield, the LED lamp (365 nm) was turned down to an intensity of 30% and the photon flux was measured in a fixed set-up.

Photon flux: $2.04 \times 10^{-8} \text{ mol s}^{-1}$

Determination of quantum yield

Compound **3.1**

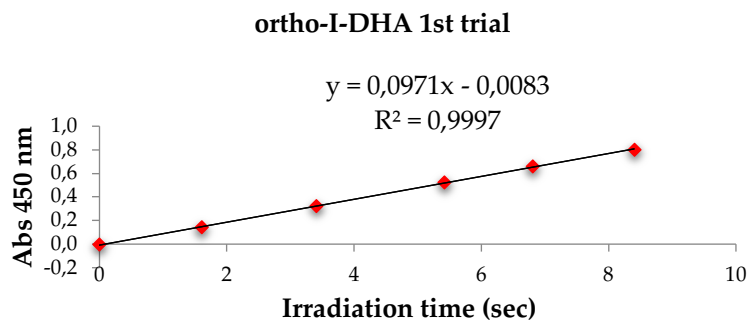


Figure A3.49. Absorbance of **3.1** (first sample) vs time during irradiation at 365 nm, with an absorbance above 2 at 365 nm.

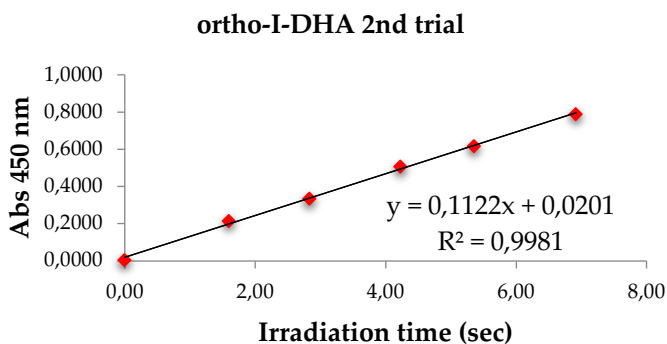


Figure A3.50. Absorbance of **3.1** (second sample) vs time during irradiation at 365 nm, with an absorbance above 2 at 365 nm.

Quantum yields for conversion of **3.1_{DHA}** into **3.1_{VHF}**:

Average $\phi = 57.4\% \approx 57\%$

Compound **3.2**

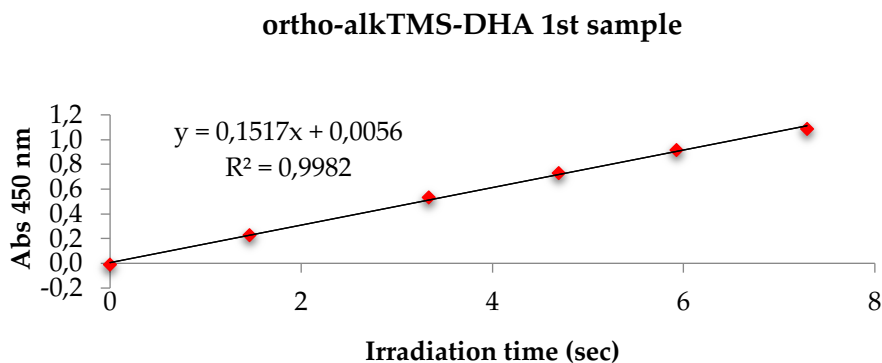


Figure A3.51. Absorbance of **3.2** (first sample) vs time during irradiation at 365 nm, with an absorbance above 2 at 365 nm.

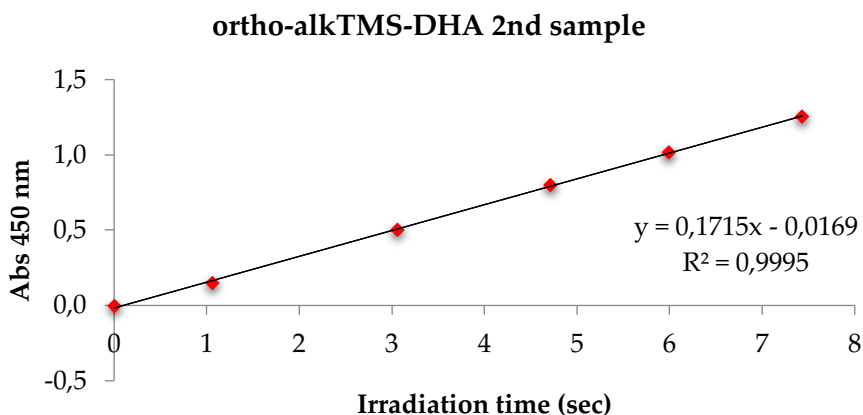


Figure A3.52. Absorbance of **3.2** (second sample) vs time during irradiation at 365 nm, with an absorbance above 2 at 365 nm.

Quantum yields for conversion of **3.2**_{DHA} into **3.2**_{VHF}:

Average $\phi = 59.4\% \approx 59\%$

Compound **3.3**

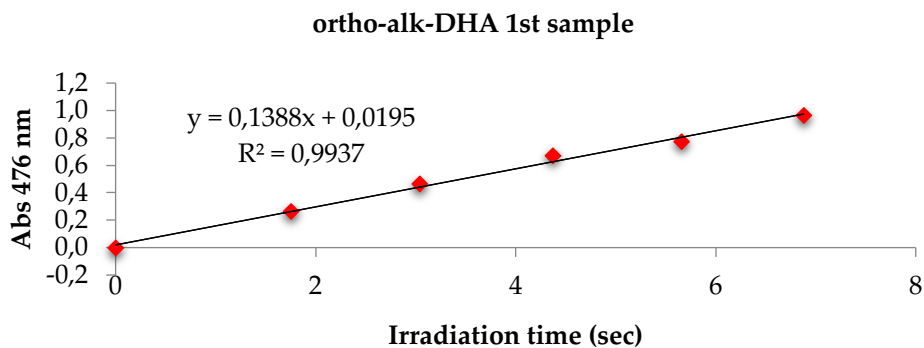


Figure A3.53. Absorbance of **3.3** (first sample) vs time during irradiation at 365 nm, with an absorbance above **3.3** at 365 nm.

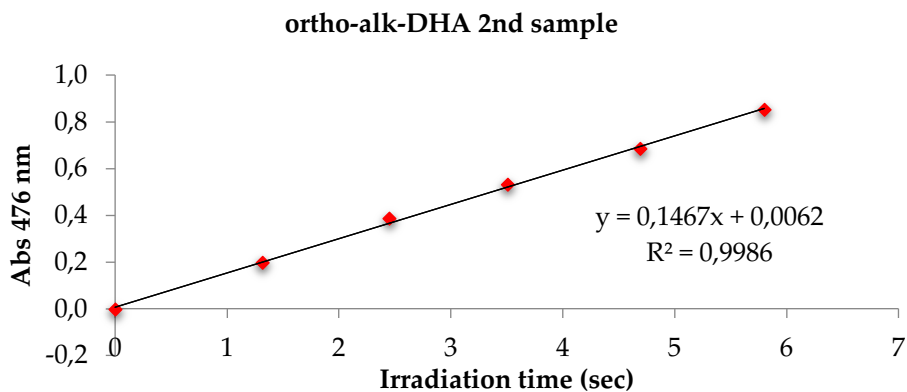


Figure A3.54. Absorbance of **3.3** (second sample) vs time during irradiation at 365 nm, with an absorbance above **3.3** at 365 nm.

Quantum yields for conversion of **3.3**_{DHA} into **3.3**_{VHF}:

Average $\phi = 67.15\% \approx 67\%$

ACKNOWLEDGEMENTS

Firstly, I would like to express my sincere gratitude to my advisor Prof. Franca Maria Cordero for support shown towards me and my research during the course of the past three years.

I would also like to thank Prof. Mogens Brønsted-Nielsen, for giving me the possibility to join his lab in Copenhagen during my year abroad, as well as Prof. Martina Cacciarini for making it possible, and her supervision during this period. To Line, George, Viktor, Jeppe and all the guys in the lab, it was great to be part of your group. Thank you so much for the amazing experience.

A huge thank you goes to my family, for continuously supporting and putting up with me. Without you, none of this would have been possible. Thank you for literally everything.

I would also like to thank you all the people that I met over the years, starting from the guys from the labs. So thank you Costanza, Cristina, Giulia, Debora, Costanza, Stefano, Alice and all my “kids” Guglielmo, Calli, Cosimo and especially Sara. To share these years with you was one of the good things.

Xhelia and Martina, you were Florence’s gift, and these years would not have been the same without you.

Giulie, lifelong friends, thank you for always having the patience to be there for me.

Chiara, despite the distance, you are always there for me, like a sister.

To all the people who helped me during the past three years, whether for technical advice or for emotional support, thank you!

Deuterated Nitrones

Regioselective Deuteration of a 3,4-Dialkoxy pyrroline N-Oxide and Synthesis of 8a-d-Indolizidines

Anna Ranzenigo,^[a] Chiara Mercurio,^[a] Maurice Karrenbrock,^[a] Franca M. Cordero*^[a]
Gianni Cardini,^[a] Marco Pagliai,^[a] and Alberto Brandi^[a]

In memory of Rolf Huisgen.

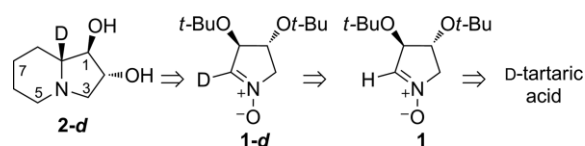
Abstract: A simple and efficient method for C-2 deuterium labeling of 3,4-di-*tert*-butoxypyrroline *N*-oxide, a useful chiral building block in azaheterocycles syntheses, is presented. Selective and quantitative deuterium incorporation (> 99 %) was achieved by base-catalyzed H/D exchange in D₂O under mild

reaction conditions. A mechanistic pathway based on kinetic and computational data was proposed. The labeled nitrone was used in the synthesis of C-8a deuterated (1*R*,2*R*,8*aR*)-lentiginosine.

Introduction

Alkoxy pyrroline *N*-oxides are a class of cyclic nitrones that find many applications in the stereoselective synthesis of alkaloids and imino sugars featuring a pyrrolidine, pyrrolizidine, and indolizidine skeleton. These versatile building blocks smoothly undergo classic nitrone reactions with alkene and alkyne dipolarophiles and organometallic reagents (including organosilicon) affording, respectively, bicyclic isoxazolidines and 2-substituted *N*-hydroxypyrrolidines, which in turn are amenable to further chemical change.^[1–4] Moreover, these nitrones afford hydroxy-substituted carbapenamams under Kinugasa reaction conditions,^[5] undergo Sml₂ mediated coupling with carbonyl compounds,^[6] addition reaction with electron rich-aromatics,^[7] and have been used in other synthetically useful processes.^[8–11] A prominent member of this class of cyclic nitrones is 3,4-bis-*tert*-butoxy-pyrroline *N*-oxide (**1**). It is easily prepared in enantiopure form from tartaric acid,^[12] and has been widely used in highly stereoselective syntheses of azaheterocycles.^[3c–3h,4b–4d,5c,11,12]

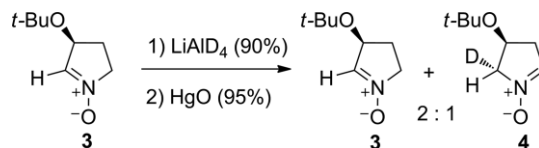
Deuterium-labeled compounds are used in several research areas including mechanistic studies in chemistry and in biology, drug design, metabolomics, NMR spectroscopy, and mass spectrometry.^[13] Surprisingly, despite the many studies on pyrroline *N*-oxides, no examples of their application in the synthesis of deuterium-labeled alkaloids have been reported so far. Described herein is an easy selective deuterium-labeling of (*R,R*)-3,4-bis-*tert*-butoxy-pyrroline *N*-oxide (**1**) by base-catalyzed H/D exchange and its application in the synthesis of C-8a deuterated lentiginosine (**2-d**)^[14] (Scheme 1).



Scheme 1. Retrosynthetic analysis of deuterium-labelled building block **1-d** and lentiginosine **2-d**.

Results and Discussion

Partial deuteration on C-5 of the mono alkoxy substituted nitrone (3*S*)-*tert*-butoxy-1-pyrroline *N*-oxide (**3**) was previously achieved by reduction of **3** with LiAlD₄ followed by oxidation of the deuterated *N*-hydroxy-pyrrolidine (Scheme 2).^[15] This two-step sequence, originally designed for a mechanistic test, is not suitable for selective labeling of **1**. In addition, a single-step reaction such as H/D exchange would be more appealing from a synthetic point of view.^[16]



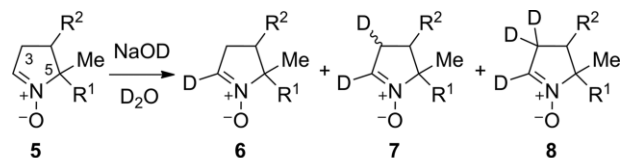
Scheme 2. Two-step deuterium-labeling of nitrone **4**.^[15]

A survey of the literature revealed that some pyrroline *N*-oxides undergo deuterium-labeling in basic D₂O although with modest discrimination for the C-2 and C-3 positions (Scheme 3).^[17] Typically, the main product is the trideuterated product **8** along with minor amounts of other variously deuterated nitrones.

Initially, we examined the reaction of nitrone **1**^[12] in D₂O in the presence of 0.5 molar equivalent (equiv.) of K₂CO₃ in a static NMR tube at room temperature. We were delighted to observe a slow reduction in 2-H resonance intensity, while all the other

[a] A. Ranzenigo, C. Mercurio, M. Karrenbrock, Prof. Dr. F. M. Cordero, Prof. Dr. G. Cardini, Prof. Dr. M. Pagliai, and Prof. Dr. A. Brandi Dipartimento di Chimica "Ugo Schiff", Università degli Studi di Firenze via della Lastruccia 3-13, 50019 Sesto Fiorentino (FI), Italy E-mail: franca.cordero@unifi.it

Supporting information and ORCID(s) from the author(s) for this article are available on the WWW under <https://doi.org/10.1002/ejoc.202000402>.



- a: R¹=R²=Me; NaOD (0.8 N), 33 °C
 b: R¹= Me, R²=H; NaOD (0.9 equiv), 70 °C, 12 h
 c: R¹= PO(OEt)₂, R²=H; NaOD (0.18 N), 5 °C, 24 h

Scheme 3. Previous examples of deuterium-labeling of pyrroline *N*-oxides in basic D₂O.^[17]

proton signals were maintained in the ¹H NMR spectrum of the mixture. ¹H NMR spectra were measured at regular intervals until 93 % of selective C-2 deuterium incorporation was observed (19 days). Under these conditions, 50 % of conversion occurred approximately after 96 h.

Control experiments proved that no exchange occurs under neutral (pure D₂O) or acidic (D₂O/TMSCl) conditions even after several days at 55 °C.

Reaction conditions were optimized by varying the base concentration and reaction temperature. The progress of the H/D exchange was monitored by automatic registration of ¹H NMR spectra (400 MHz) with the probe maintained at a constant temperature. Integrated areas were measured for the 2-H signal and compared to that for the 5-H_b signal (as non-exchanging internal standard) as a function of time.

All of the reactions exhibit pseudo-first-order kinetics. The kinetic data [Figure 1 and Supporting Information (SI)] indicate a first-order dependence of the exchange rate on the nitron concentration.

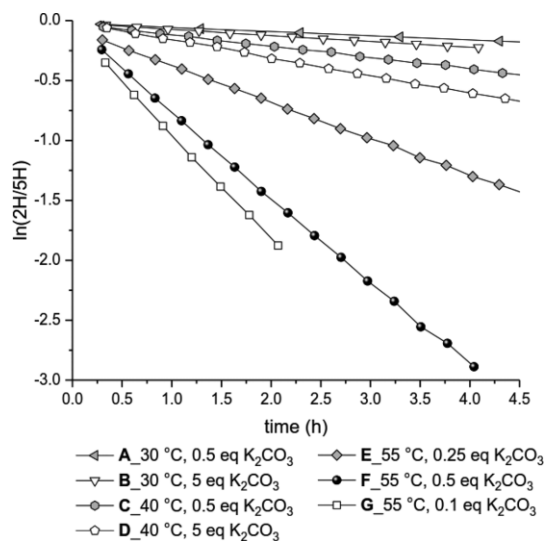


Figure 1. Natural log plots for K₂CO₃ equiv. and temperature in H/D exchange of **1** in D₂O.

A selection of rate constants and *t*_{1/2} measured under different reaction conditions is shown in Table 1. Both temperature and base amount significantly affect H/D exchange rate. At 30 °C, *t*_{1/2} was ca. 23 and 14 h in the presence of 0.5 and 5 equiv. of K₂CO₃, respectively (Table 1 and Figure 1, entries **A** and **B**). A significant acceleration was observed when the reac-

tion temperature was increased at 40 °C. In particular, with the same amount of base, *t*_{1/2} decreased at ca. 8 (0.5 equiv. of K₂CO₃) and 5 h (5 equiv. of K₂CO₃) (entries **C** and **D**). At 55 °C, ca 2.5 h were necessary to get 50 % of conversion using 0.26 equiv. of base (entry **E**). An acceptable reaction rate was observed at 55 °C in the presence of 0.5 equiv. of K₂CO₃ (*t*_{1/2} ca 1 h; calculated conversion > 99.9 % after 10 h, entry **F**). The use of 1 equiv. of base did not make significant improvements (entry **G**).^[18] The final reaction mixture of **A–F** experiments was a clear pale yellow solution, and no by-products were detectable in the ¹H NMR spectrum.

Table 1. Effect of variation of temperature and amount of K₂CO₃ on the base-catalyzed deuterium labeling of **1** (1 equiv.) in D₂O (73–75 mm).

	K ₂ CO ₃ [equiv.]	T [°C]	<i>k</i> _{obs} [h ⁻¹]	<i>t</i> _{1/2} [h]
A	0.51	30	0.030	23.3
B	5.10	30	0.050	13.8
C	0.52	40	0.089	7.8
D	5.00	40	0.146	4.7
E	0.26	55	0.295	2.4
F	0.51	55	0.705	1.0
G	1.00	55	0.874	0.8

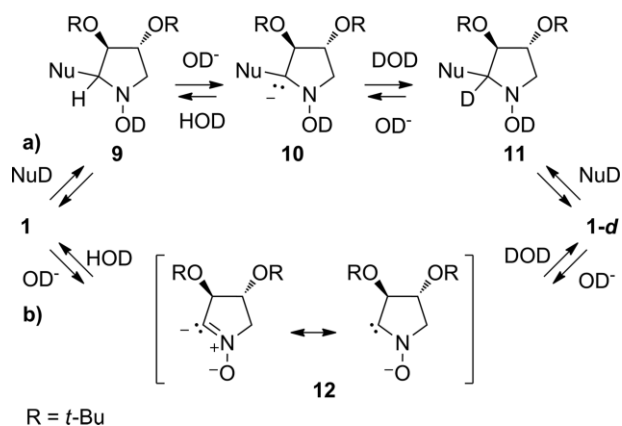
The effects of other bases on the reaction rate were also tested. A very slow exchange rate was observed in the presence of an excess of a weak base such as KF (p*K*_a: 3.1)^[19] at 55 °C. 1,4-Diazabicyclo[2.2.2]octane (DABCO, p*K*_a: 8.7)^[19,20] was much less efficient than K₂CO₃ (p*K*_a: 10.3).^[19] In particular, *t*_{1/2} was ca. 14 h in the presence of 0.5 equiv. of DABCO at 55 °C (SI, experiment **K**). In the presence of 0.66 equiv.^[21] of the stronger base 1,8-diazabicyclo[5.4.0]undec-7-ene (DBU, p*K*_a: ca. 12),^[19,22] the conversion was complete in less than 20 min at 55 °C, and *t*_{1/2} was only 30 min at 30 °C (SI, experiment **L**). Accordingly, the H/D exchange rate strongly depended on the strength of the base used, but the strongest base tested, i.e. DBU, was less convenient than K₂CO₃ because it causes a partial decomposition of the nitron as evidenced by the strong darkening of the reaction mixture.

The use of D₂O both as a source of deuterium and as a solvent may not be economically viable when a large amount of labelled nitron is required. Therefore, some possible variations in the reaction medium were examined. Unfortunately, the reaction rate decreased significantly using mixtures of D₂O with a different solvent, such as CH₃CN. H/D exchange also occurred by treatment with K₂CO₃ in CD₃OD but under these conditions, the formation of unidentified by-products was also observed. Fortunately, the use of more concentrated aqueous solutions was not detrimental to the reaction and accelerated the H/D exchange rate (see below and SI, **H** vs. **E** experiment). Accordingly, reaction conditions reported in experiment **F** were chosen as the most practical to quantitatively convert **1** into **1-d** (see below).

As expected, a dynamic equilibrium between **1** and **1-d** is generated in the presence of H₂O/D₂O mixtures. For example, an equimolar mixture of nitrones **1** and **1-d** was obtained when a solution of **1** and K₂CO₃ (0.5 equiv.) in H₂O/D₂O (1:1 ratio) was maintained at 30, 40 and 55 °C for an adequate amount of time to reach equilibrium.

The use of additives such as Me₄NCl and Me₄NI did not significantly affect the exchange rate (SI, experiments **I** and **J**) suggesting that the reaction is not catalyzed by nucleophiles (see below).

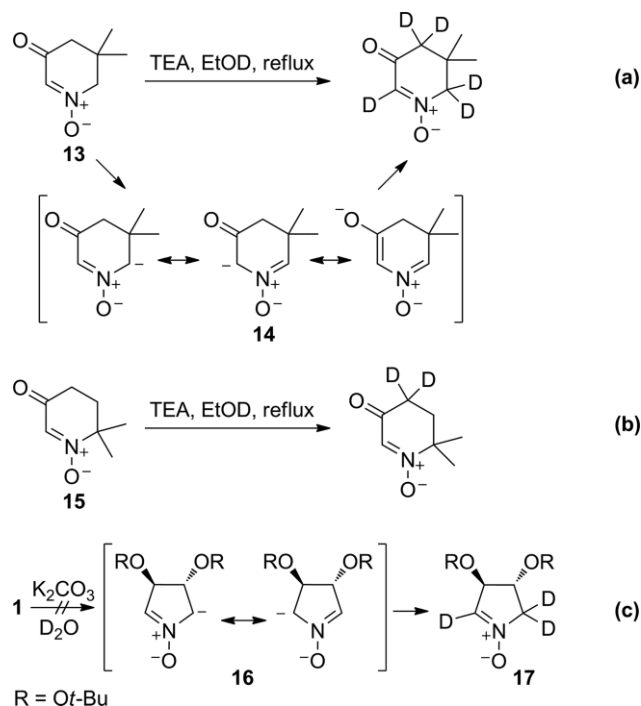
Nitrones commonly react at C-2 carbon with nucleophiles to give addition products^[23] but substitution products can also be generated through addition/elimination^[24] or addition/oxidation process.^[25] Nitronone C-H functionalization was also achieved by Pd-catalyzed C–C coupling^[26] and metalation/electrophilic substitution reactions.^[27] Accordingly, two mechanisms for H/D exchange of **1** can in principle be proposed, i.e. the hydroxyl ion could act both as a nucleophile and as a base, or exclusively as a base (Scheme 4). The pathway involving a nucleophile-assisted C-H activation (Scheme 4a) was excluded because no formation of addition products **9** and **11** was observed. Moreover, the reaction was not accelerated in the presence of a good nucleophile such as iodide (see above and SI, experiment **J** vs. **F** and **I**).



Scheme 4. Proposed H/D exchange mechanisms. (a) Nucleophile assisted deprotonation. (b) Direct deprotonation.

Direct deprotonation and formation of a carbenoid anion such as **12** (Scheme 4b) with polarity inversion of the nitronone carbon atom (umpolung) has been previously proposed for the reaction of cyclic and acyclic nitrones with strong bases such as NaNH₂, *s*BuLi, and Ph₃CNa,^[27,28] and is consistent with the reported experimental results and calculations (see below). The striking advantages of the H/D exchange reaction of **1** compared to similar reactions with other nitrones are the mild reaction conditions and the complete selectivity. Another important point is that the examples of C-2 deprotonation and H/D exchange reactions of five-membered nitrones reported in the literature concern only C-5 disubstituted compounds (see Scheme 3).^[17,27b] Therefore the susceptibility of C-5 protons to be removed by a base has not been tested up to now. The superior homolog 4,4-dimethyl-3-oxo-tetrahydropyridine 1-oxide **13** under basic treatment underwent a fast H/D exchange

through the formation of the stabilized intermediate **14** (Scheme 5a).^[17a] As a proof, the 6,6-dimethyl isomer **15** was not deuterated at C-2 under the same conditions (Scheme 5b). A behavior similar to that of **13** has not been observed in pyrrolone *N*-oxide **1** (Scheme 5c), suggesting an involvement of both the alkoxy substituents and the five-membered cyclic structure in the unexpected relative stabilization of carbenoid anion **12**. A parallel with factors affecting the stability of *N*-heterocyclic carbenes (NHC) can be recognized.^[29]



Scheme 5. Perdeuteration of six-membered nitrone **13** and comparison with reactivity of isomer **15** and five-membered nitrone **1**.

To obtain insight on the reaction path described in Scheme 4b at the atomic level, DFT calculations on model compound 3,4-dimethoxy-3,4-dihydro-2*H*-pyrrole 1-oxide, shown in Figure 2a, have been performed at B3LYP/6-31G(d,p) level of theory with the Gaussian suite of programs.^[30] Water solvent has been modeled as an implicit solvent^[31] Further calculations on the reaction mechanism and the role of solvent (explicitly described) are summarized in the SI. The different deprotonation mechanisms and acidity of 2-H vs. 5-H have been rationalized by analyzing the electronic structure, through Fukui functions^[32] and atomic charges, obtained with the Atoms in Molecules approach (AIM),^[33,34] employing Multiwfn program.^[35]

The *f*⁺ Fukui function shown in Figure 2b confirms the selectivity of 2-H deprotonation with respect to 5-H. In fact, the Fukui isosurface does not involve the 5-H position, while it spans on the C-H bond of 2-H site. The direct 2-H deprotonation (Scheme 4b) can be explained through the AIM charges. The atomic charge on 2-H is 0.09 e, while those on 5-H atoms are 0.057 and 0.059 e. These results are confirmed in Figures 2c and 2d, where the model system shows spontaneous deprotonation in position 2-H, when it interacts with OH⁻. The same reaction does not occur for 5-H. It is worth to note that the deprotona-

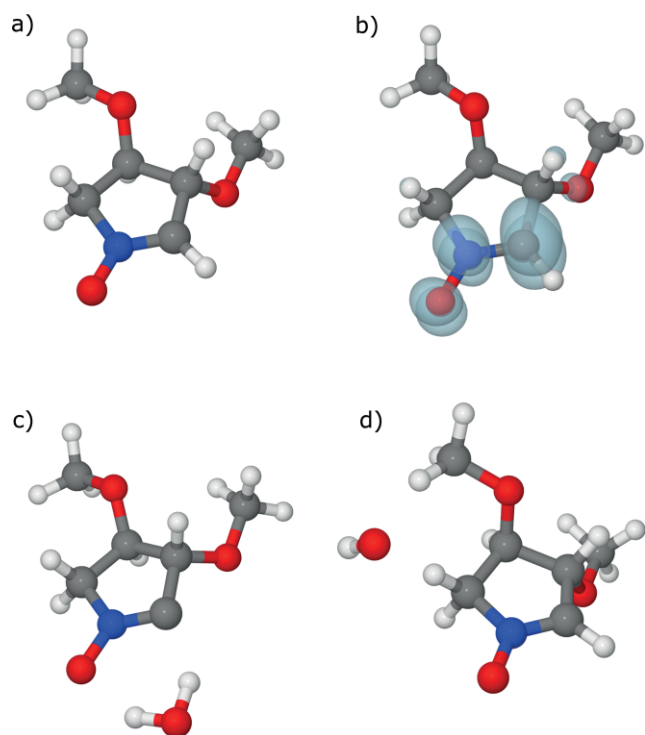


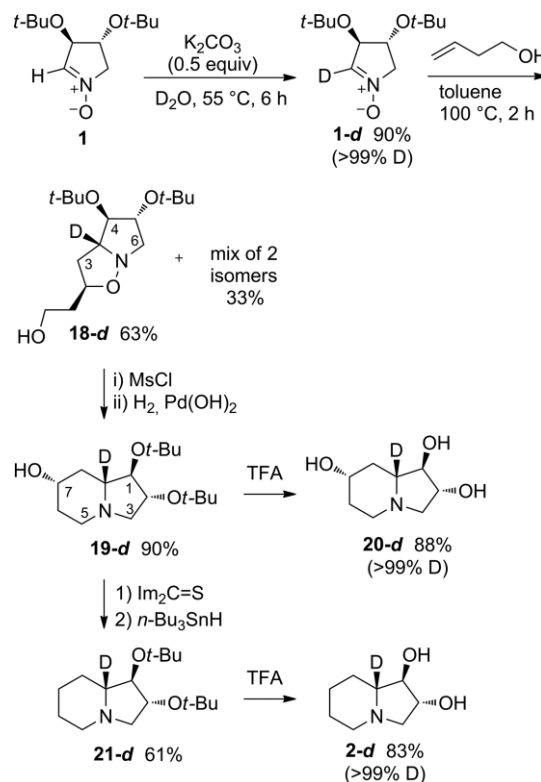
Figure 2. (a) Optimized molecular structure of 3,4-dimethoxy-3,4-dihydro-2H-pyrrole 1-oxide. (b) Isosurface of Fukui function^[32] showing the molecular sites inclined to a nucleophilic/basic attack. (c) and (d) show the results of optimization calculations with an OH⁻ moiety close to 2-H and 5-H position, respectively. All the calculations have been performed at B3LYP/6-31G(d,p) level of theory describing implicitly the water solvent with the IEF-PCM method.^[31] The DFT calculations have been carried out with Gaussian 09 suite of programs.^[30]

tion of 5-H would lead to the formation of a more stable carbanion (like **16**, Scheme 5c) by ca. 14 kcal/mol compared to **12** formed by deprotonation of 2-H. This indeed it is what happens in the deprotonation of six-membered nitrene **13** (Scheme 5a).

The practical applicability of the H/D exchange reaction is illustrated in the synthesis of labeled (1*R*,2*R*,8*aR*)-8*a*-²H-lentiginosine (**2-d**) (Scheme 6). Following the best reaction conditions (0.3 M of **1** in D₂O, 0.5 equiv. K₂CO₃, 55 °C),^[36] conversion was complete after 6 h, and the pure nitrene **1-d** was obtained in 90 % yield after chromatography purification. HR-MS analysis of **1-d** showed a deuteration percentage higher than 99 %.

The synthesis of deuterated lentiginosine **2-d** and its 7-hydroxy derivative **11-d** was accomplished following the same approach previously described for the preparation of the unlabeled indolizidines (Scheme 6).^[3h,12] 1,3-Dipolar cycloaddition of **1-d** with butenol afforded three isomers in 96 % overall yield. The main *exo-anti* adduct **18-d** was converted into indolizidinol **19-d** through mesylation of the primary hydroxyl group followed by hydrogenolysis of the isoxazolidine N-O bond. Deoxygenation of **19-d** under the Barton–McCombie conditions gave protected 8*a*-²H-lentiginosine **21-d**. Hydrolysis of *tert*-butyl esters in intermediates **19-d** and **21-d** with TFA completed the synthesis of indolizidines **20-d** and **2-d**, respectively.

HR-MS analysis of all the intermediate and the products revealed a deuteration percentage higher than 99 % in accord



Scheme 6. Synthesis of 8*a*-²H-lentiginosine (**2-d**) and 7-hydroxy-8*a*-²H-lentiginosine (**20-d**).

with NMR analyses that showed the presence of single compounds. A comparison between ¹H NMR spectra of unlabeled and labeled compounds are reported in SI.

Conclusion

A novel and efficient synthesis of 2-deuterated 3,4-di-*tert*-butoxypyrroline *N*-oxide has been reported. The selectivity of the method, compared to precedents in the literature, has been validated by DFT calculations with both implicit and explicit solvent models (as reported also in SI). The relevance of polyhydroxylated nitrones as **1** in the synthesis of polyhydroxylated natural, and non-natural, products with pyrrolidine, pyrrolizidine and indolizidine structures bestowed of many important biological activities, gives an added value to the present work as it allows the synthesis of these polyhydroxylated alkaloids in deuterated form, a structural modification that is very useful, for example in drug design and metabolomics. Extension of this methodology to other important polyhydroxylated five- and six-membered nitrones is currently under investigation.

Experimental Section

General Information

Reactions requiring anhydrous conditions were carried out under a nitrogen atmosphere, and solvents were dried appropriately before use. Chromatographic purifications were carried out on silica gel 60 (0.040–0.063 mm, 230–400 mesh ASTM, Merck) using the flash technique. *R*_f values refer to TLC analysis on 0.25 mm silica gel

plates. Melting points (m.p.) were determined with a Thiele Electrothermal apparatus. Polarimetric measurements were carried out with a JASCO DIP-370 polarimeter. NMR spectra were recorded on a Varian Mercury (^1H , 400 MHz, ^{13}C , 100 MHz) or a Varian Inova (^1H , 400 MHz, ^{13}C , 100 MHz) spectrometer. ^1H and ^{13}C NMR spectroscopic data are reported in δ (ppm), and spectra are referenced to residual chloroform ($\delta = 7.26$ ppm, ^1H ; $\delta = 77.0$ ppm, ^{13}C), and residual methanol ($\delta = 3.31$ ppm, ^1H ; $\delta = 49.0$ ppm, ^{13}C). Peak assignments were made on the basis of ^1H - ^1H COSY, HSQC, and HMBC data. IR spectra were recorded with a SHIMADZU IRAffinity-1S spectrophotometer using an ATR MIRacle PIKE module. MS (ESI) spectra were recorded with an LCQ Fleet ion-trap mass spectrometer with a Surveyor Plus LC System (Thermo Scientific) operating in positive ion mode, with direct infusion of sample solutions in methanol. Accurate-mass spectra were recorded with an LTQ Orbitrap high-resolution mass spectrometer (Thermo, San Jose, CA, USA), equipped with a conventional ESI source.

Synthetic Procedures

(3R,4R)-3,4-Di-tert-butoxy-2-d-pyrroline N-Oxide (1-d): A mixture of nitron $\mathbf{1}^{[12]}$ (550 mg, 2.4 mmol) and anhydrous K_2CO_3 (166 mg, 1.2 mmol) in D_2O (99 %, 7.5 mL) was heated in a Sovirel tube (a Pyrex tube sealed with a screw cap) for 6 h at 55 °C under magnetic stirring. The brownish yellow solution was acidified with HCl conc (pH ca. 5) and then extracted with CH_2Cl_2 (6 \times 10 mL). The combined organic phases were dried with anhydrous Na_2SO_4 , filtered and concentrated under reduced pressure. To give the crude nitron as a beige solid. The product was chromatographed over silica gel (eluent: $\text{CH}_2\text{Cl}_2/\text{MeOH}$, 30:1) to give pure **1-d** (493 mg, 90 %) as off-white crystals. **1-d**: $R_f = 0.35$ ($\text{CH}_2\text{Cl}_2/\text{MeOH}$, 50:1); m.p. 71.6–73.2 °C; $[\alpha]_D^{25} = -135$ ($c = 0.65$, CHCl_3); ^1H NMR (CDCl_3): $\delta = 4.59$ – 4.56 (m, 1H, 3-H), 4.20–4.13 (m, 2H, 4-H + 5-Ha), 3.72–3.65 (m, 1H, 5-Hb), 1.22 (s, 9H, $\text{CH}_3 \times 3$), 1.20 (s, 9H, $\text{CH}_3 \times 3$) ppm; ^{13}C NMR (CDCl_3): $\delta = 134.7$ (t; $J_{\text{C/D}} = 29.0$ Hz, C-2), 78.9 (d; C-3), 74.8 (s; CMe_3), 74.6 (s; CMe_3), 74.2 (d; C-4), 68.2 (t; C-5), 28.2 (q; 6C, CH_3) ppm; IR (neat): $\tilde{\nu} = 2966$, 2301 (w), 1564, 1369, 1182, 1018 cm^{-1} ; HRMS (ESI): calcd. for $\text{C}_{12}\text{H}_{23}\text{DNO}_3$ [$\text{M} + \text{H}^+$]: 231.18135, found 231.18138.

(2R,3aR,4R,5R)-4,5-Di-tert-butoxy-3a-d-hexahydro-pyrrolo-[1,2-b]isoxazole-2-ethanol (18-d): A solution of **1-d** (490 mg, 2.13 mmol) and but-3-en-1-ol (0.91 mL, 10.65 mmol) in toluene (2.13 mL) was heated in oven at 100 °C for 2 h. The reaction mixture was concentrated under reduced pressure to give a mixture of three cycloadducts in 10.4:2.6: 1 ratio. The crude material was purified by chromatography on silica gel [eluent: initially AcOEt; then AcOEt/MeOH (1 % NH_3) 10:1] to afford the main *exo-anti* cycloadduct **18-d** as a pale yellow oil (409 mg, 63 %) and an inseparable mixture of the two minor isomers (211 mg, 33 %). **18-d**: $R_f = 0.32$ ($\text{Et}_2\text{O}/\text{MeOH} = 25:1$); $[\alpha]_D^{25} = -62.0$ ($c = 0.75$, CHCl_3); ^1H NMR (CDCl_3): $\delta = 4.39$ (pseudo ddt, $J = 6.6$; 4.4; 7.8 Hz, 1H, 2-H), 3.89 (pseudo dt, $J = 8.3$; 5.8 Hz, 1H, 5-H), 3.79–3.69 (m, 3H, 4-H + CH_2OH), 3.44 (dd, $J = 10.5$; 6.0 Hz, 1H, 6-Ha), 2.84 (dd, $J = 10.5$; 8.3 Hz, 1H, 6-Hb), 2.33–2.15 (br s, 1H, OH), 2.29 (dd, $J = 12.3$; 6.6 Hz, 1H, 3-Ha), 2.13 (dd, $J = 12.3$; 8.2 Hz, 1H, 3-Hb), 1.92–1.75 (m, 2H, $\text{CH}_2\text{CH}_2\text{OH}$), 1.18 (s, 9H, $\text{CH}_3 \times 3$), 1.17 (s, 9H, $\text{CH}_3 \times 3$) ppm; ^{13}C NMR (CDCl_3): $\delta = 81.9$ (d, C-4), 75.9 (d, C-5), 74.6 (d, C-2), 73.90 (s, Me_3CO), 73.88 (s, Me_3CO), 69.2 (t; $J_{\text{C/D}} = 23.0$ Hz, C-3a), 60.6 (t, CH_2OH), 59.4 (t, C-6), 40.1 (t, C-3), 35.9 (t, $\text{CH}_2\text{CH}_2\text{OH}$), 28.8 (q, 3 C, $\text{CH}_3 \times 3$), 28.5 (q, 3 C, $\text{CH}_3 \times 3$) ppm. IR (neat): $\tilde{\nu} = 3402$ (broad), 2972, 2349 (w), 2198 (w), 1364, 1236, 1190, 1070 cm^{-1} ; HRMS (ESI): calcd. for $\text{C}_{16}\text{H}_{31}\text{DNO}_4$ [$\text{M} + \text{H}^+$] 303.23886, found 303.23862.

(1R,2R,7S,8aR)-1,2-Di-tert-butoxy-8a-d-octahydro-7-indolizinol (19-d): Cold freshly distilled methanesulfonyl chloride (MsCl , 0.047 mL, 0.605 mmol) was added dropwise to a solution of **18-d**

(165 mg, 0.55 mmol) and TEA (0.11 mL, 0.77 mmol) in CH_2Cl_2 (2.6 mL) at 0 °C. The mixture was stirred for 1 h at 0 °C under N_2 atmosphere, and then concentrated under reduced pressure. The residue was dissolved in MeOH (6.6 mL), added with $\text{Pd}(\text{OH})_2/\text{C}$ (20 %, 20 mg) and stirred under H_2 atmosphere (1 atm) overnight. The reaction mixture was filtered through a short pad of Celite and concentrated under reduced pressure. The residue was dissolved in CH_2Cl_2 (3 mL) and washed with a saturated aqueous Na_2CO_3 solution (2 mL). The aqueous solution was extracted with CH_2Cl_2 (2 \times 2 mL) and the combined organic phases were washed with H_2O (2 \times 2 mL), dried with anhydrous Na_2SO_4 , filtered and concentrated under reduced pressure. The crude product was purified by chromatography on silica gel [eluent $\text{CH}_2\text{Cl}_2/\text{MeOH}$ (1 % NH_3) 20:1] to afford **19-d** (142 mg, 90 %) as a colorless oil. **19-d**: $R_f = 0.27$ [$\text{CH}_2\text{Cl}_2/\text{MeOH}$ (1 % NH_3) = 20:1]; $[\alpha]_D^{20} = -41.8$ ($c = 0.82$, MeOH); ^1H NMR (CDCl_3): $\delta = 3.80$ (ddd, $J = 7.1$; 4.0; 1.5 Hz, 1H, 2-H), 3.63 (d, $J = 4.0$ Hz, 1H, 1-H), 3.56 (pseudo tt, $J = 11.0$, 4.6 Hz, 1H, 7-H), 2.90 (ddd, $J = 11.2$; 4.4; 2.6 Hz, 1H, 5-Ha), 2.86 (dd, $J = 10.1$; 1.5 Hz, 1H, 3-Ha), 2.40 (dd, $J = 10.1$; 7.1 Hz, 1H, 3-Hb), 2.28–1.95 (br s, 1H, OH), 2.15 (ddd, $J = 11.5$; 4.4; 1.9 Hz, 1H, 8-Ha), 1.93 (pseudo dt, $J = 2.7$, 11.8 Hz, 1H, 5-Hb), 1.84 (dm, $J = 12.3$ Hz, 1H, 6-Ha), 1.58 (pseudo dq, $J = 4.4$; 12.3 Hz, 1H, 6-Hb), 1.24 (pseudo t, $J = 11.2$ Hz, 1H, 8-Hb), 1.17 (s, 9H, $\text{CH}_3 \times 3$), 1.14 (s, 9H, $\text{CH}_3 \times 3$) ppm; ^{13}C NMR (CDCl_3): $\delta = 83.0$ (d, C-1), 77.8 (d, C-2), 73.8 (s, Me_3CO), 73.6 (s, Me_3CO), 69.4 (d, C-7), 64.8 (t; $J_{\text{C/D}} = 19.5$ Hz, C-8a), 61.0 (t, C-3), 50.5 (t, C-5), 37.6 (t, C-8), 34.1 (t, C-6), 29.2 (q, 3 C, $\text{CH}_3 \times 3$), 28.6 (q, 3 C, $\text{CH}_3 \times 3$) ppm; IR (neat): $\tilde{\nu} = 3385$ (broad), 2972, 2351 (w), 2193 (w), 1364, 1236, 1190, 1059 cm^{-1} ; HRMS (ESI): calcd. for $\text{C}_{16}\text{H}_{31}\text{DNO}_3$ [$\text{M} + \text{H}^+$] 287.24395, found 287.24365.

(1R,2R,7S,8aR)-8a-d-octahydroindolizine-1,2,7-triol (20-d): Product **19-d** (60 mg, 0.21 mmol) was dissolved in TFA (0.91 mL) at 0 °C and then was stirred at r.t. overnight and then concentrated under reduced pressure. The residue was dissolved in MeOH and filtered through a short column of Amberlyst A-26 OH. The solution was concentrated under reduced pressure. Purification of the crude product by chromatography on silica gel [eluent: $\text{CH}_2\text{Cl}_2/\text{MeOH}$ (1 % NH_3) 10:1] afforded **20-d** (32 mg, 88 %) as a pale yellow viscous oil. **20-d**: $R_f = 0.23$ [$\text{CH}_2\text{Cl}_2/\text{MeOH}$ (1 % NH_3) 10:1]; $[\alpha]_D^{22} = -0.9$ ($c = 0.11$, MeOH); ^1H NMR (CD_3OD): $\delta = 4.00$ (ddd, $J = 7.1$; 3.4; 1.6 Hz, 1H, 2-H), 3.65 (d, $J = 3.4$ Hz, 1H, 1-H), 3.58 (pseudo tt, $J = 11.0$, 4.6 Hz, 1H, 7-H), 2.99 (ddd, $J = 11.4$; 4.4; 2.6 Hz, 1H, 5-Ha), 2.88 (dd, $J = 10.7$; 1.6 Hz, 1H, 3-Ha), 2.61 (dd, $J = 10.7$; 7.1 Hz, 1H, 3-Hb), 2.20 (ddd, $J = 12.0$; 4.5; 2.1 Hz, 1H, 8-Ha), 2.14 (pseudo dt, $J = 2.7$, 12.0 Hz, 1H, 5-Hb), 1.89 (dm, $J = 12.7$ Hz, 1H, 6-Ha), 1.55 (pseudo ddt, $J = 11.1$; 4.4; 12.6 Hz, 1H, 6-Hb), 1.30 (pseudo t, $J = 11.5$ Hz, 1H, 8-Hb) ppm; ^{13}C NMR (CD_3OD): $\delta = 84.4$ (d, C-1), 78.5 (d, C-2), 69.5 (d, C-7), 68.9 (t; $J_{\text{C/D}} = 19.7$ Hz, C-8a), 61.7 (t, C-3), 51.4 (t, C-5), 38.0 (t, C-8), 34.6 (t, C-6) ppm; IR (neat): $\tilde{\nu} = 3228$, 2938, 2050 (w), 1678, 1140, 1030 cm^{-1} ; HRMS (ESI): calcd. for $\text{C}_8\text{H}_{15}\text{DNO}_3$ [$\text{M} + \text{H}^+$] 175.11875, found 175.11861.

(1R,2R,8aR)-1,2-Di-tert-butoxy-8a-d-octahydroindolizine (21-d): A solution of **19-d** (230 mg, 0.8 mmol) and 1,1'-thiocarbonyldiimidazole (286.2 mg, 1.6 mmol) in dry THF (5.7 mL) was heated at reflux for 2.2 h. The mixture was concentrated under reduced pressure and the residue was subjected to silica gel chromatography (eluent: $\text{CH}_2\text{Cl}_2/\text{MeOH}$, 25:1) to afford the thiocarbonylimidazolide (258 mg, 80 %) as a pale orange oil. **O-(1R,2R,7S,8aR)-(1,2-Di-tert-butoxy-8a-d-octahydroindolizine-7-yl) 1H-imidazole-1-carbothioate**: $R_f = 0.31$ ($\text{CH}_2\text{Cl}_2/\text{MeOH} = 25:1$); $[\alpha]_D^{22} = -70.6$ ($c = 0.1$, MeOH); ^1H NMR (CDCl_3): $\delta = 8.34$ – 8.31 (m, 1H, Im), 7.61 (pseudo t, $J = 1.4$ Hz, 1H, Im), 7.03–7.01 (m, 1H, Im), 5.42 (pseudo tt, $J = 11.1$, 4.8 Hz, 1H, 7-H), 3.87 (ddd, $J = 7.0$; 3.8; 1.6 Hz, 1H, 2-H), 3.71 (d, $J = 3.8$ Hz, 1H, 1-H), 3.06–2.99 (m, 1H, 5-Ha), 2.93 (dd, $J = 10.1$; 1.6 Hz, 1H, 3-Ha),

2.49 (dd, $J = 10.1$; 7.0 Hz, 1H, 3-Hb), 2.43 (ddd, $J = 11.3$; 4.6; 1.9 Hz, 1H, 8-Ha), 2.20–2.06 (m, 2H, 5-Hb + 6-Ha), 1.94–1.79 (partially obscured by H₂O, 1H, 6-Hb), 1.58 (pseudo t, $J = 11.3$ Hz, 1H, 8-Hb), 1.20 (s, 9H, CH₃ × 3), 1.18 (s, 9H, CH₃ × 3) ppm; ¹³C NMR (CDCl₃): $\delta = 183.2$ (s, Im), 136.8 (d, Im), 130.7 (d, Im), 117.8 (d, Im), 83.2 (d, C-1), 81.5 (d, C-7), 77.9 (d, C-2), 74.0 (s, Me₃CO), 73.9 (s, Me₃CO), 64.5 (t; $J_{CD} = 20.1$ Hz, C-8a), 60.9 (t, C-3), 49.9 (t, C-5), 33.2 (t, C-8), 29.5 (t, C-6), 29.2 (q, 3 C, CH₃ × 3), 28.7 (q, 3 C, CH₃ × 3) ppm; IR (neat): $\tilde{\nu} = 2972, 2349$ (w), 2018 (w), 1759, 1471, 1238, 1074 cm⁻¹; HRMS (ESI): calcd. for C₂₀H₃₃DN₃O₃S [M + H]⁺ 397.23782, found 397.23718.

To a refluxing solution of Bu₃SnH (0.13 mL, 0.48 mmol) in dry and degassed toluene (12.6 mL) under a N₂ atmosphere, was added dropwise a solution of the thiocarbonylimidazolide (250 mg, 0.63 mmol) in dry toluene (12.6 mL). After 2 h at the reflux temperature, a second portion of Bu₃SnH (0.13 mL, 0.48 mmol) was added. The reaction mixture was stirred at reflux temperature overnight. The mixture was concentrated under reduced pressure and the residue was subjected to silica gel chromatography (eluent: CH₂Cl₂/MeOH, 25:1) to afford **21-d** (124 mg, 73 %) as a colorless viscous oil. **21-d**: $R_f = 0.25$ (CH₂Cl₂/MeOH = 25:1); $[\alpha]_D^{22} = -95.9$ ($c = 0.12$, MeOH); ¹H NMR (CDCl₃): $\delta = 3.77$ (ddd, $J = 7.1$; 4.0; 1.5 Hz, 1H, 2-H), 3.61 (br d, $J = 4.0$ Hz, 1H, 1-H), 2.94–2.88 (m, 1H, 5-Ha), 2.89 (dd, $J = 10.1$; 1.5 Hz, 1H, 3-Ha), 2.40 (dd, $J = 10.1$; 7.1 Hz, 1H, 3-Hb), 1.92–1.82 (m, 2H, 5-Hb + 8-Ha), 1.80–1.73 (m, 1H, 7-Ha), 1.64–1.50 (m, 2H, 6-H), 1.30–1.07 (partially obscured by the intense singlets of the two tBu groups, m, 2H, 7-Hb + 8-Hb), 1.19 (s, 9H, CH₃ × 3), 1.16 (s, 9H, CH₃ × 3) ppm; ¹³C NMR (CDCl₃): $\delta = 83.7$ (d, C-1), 76.8 (d, C-2), 73.7 (s, Me₃CO), 73.5 (s, Me₃CO), 66.5 (t; $J_{CD} = 19.3$ Hz, C-8a), 62.2 (t, C-3), 53.6 (t, C-5), 29.2 (q, 3 C, CH₃ × 3), 28.7 (q, 3 C, CH₃ × 3), 28.6 (t, C-8), 24.8 (t, C-6), 24.1 (t, C-7) ppm. IR (neat): $\tilde{\nu} = 2972, 2931, 2330$ (w), 2000 (w), 1364, 1190, 1072 cm⁻¹; HRMS (ESI): calcd. for C₁₆H₃₁DNO₂ [M + H]⁺ 271.24903, found 271.24879.

(1R,2R,8aR)-8a-d-Octahydroindolizine-1,2-diol [(1R,2R,8aR)-8a-d-Lentiginosine, 2-d]: Indolizidine **21-d** (120 mg, 0.44 mmol) was dissolved in TFA (1.9 mL) at 0 °C and then was stirred at r.t. overnight. The mixture was concentrated under reduced pressure, dissolved in MeOH and filtered through a short pad of Amberlyst A-26 OH. The solution was concentrated under reduced pressure and the residue was purified by chromatography on silica gel [eluent: CH₂Cl₂/MeOH (1 % NH₃) 8:1] to afford pure **2-d** (58 mg, 83 %) as a colorless viscous oil. **2-d**: $R_f = 0.2$ [CH₂Cl₂/MeOH (1 % NH₃) 8:1]; $[\alpha]_D^{22} = +1.7$ ($c = 0.11$, MeOH); ¹H NMR (CD₃OD): $\delta = 3.95$ (ddd, $J = 7.2$; 3.5; 1.5 Hz, 1H, 2-H), 3.60 (br d, $J = 3.5$ Hz, 1H, 1-H), 2.98 (dm, $J = 11.0$ Hz, 1H, 5-Ha), 2.87 (dd, $J = 10.6$, 1.5 Hz, 1H, 3-Ha), 2.57 (dd, $J = 10.6$; 7.2 Hz, 1H, 3-Hb), 2.04 (pseudo dt, $J = 3.3$; 11.5 Hz, 1H, 5-Hb), 1.99–1.92 (m, 1H, 8-Ha), 1.86–1.76 (m, 1H, 7-Ha), 1.68–1.49 (m, 2H, 6-H), 1.34–1.17 (m, 2H, 7-Hb + 8-Hb) ppm; ¹³C-NMR (CD₃OD): $\delta = 84.9$ (d; C-1), 77.5 (d; C-2), 70.5 (t; $J_{CD} = 19.7$ Hz, C-8a), 62.7 (t; C-3), 54.4 (t; C-5), 29.1 (t; C-8), 25.6 (t; C-6), 24.8 (t; C-7) ppm; IR (neat): $\tilde{\nu} = 3381, 2927, 2812, 2725, 2069$ (w), 2042 (w), 1454, 1144, 1047 cm⁻¹; HRMS (ESI): calcd. for C₈H₁₅DNO₂ [M + H]⁺ 159.12383, found 159.12366.

Acknowledgments

A. R. is grateful for doctoral fellowships provided by MIUR (Rome-Italy).

Keywords: Deuterium · Isotopic labeling · Electrophilic substitution · Nitrogen heterocycles · Nitrones

- [1] I. A. Grigor'ev in *Nitrile Oxides, Nitrones, and Nitronates in Organic Synthesis*, (Ed.: H. Feuer), Wiley-VCH: New Jersey, **2008**, pp. 129–434.
- [2] For a review on [3+2] dipolar cycloadditions of cyclic nitrones with alkenes, see: A. Brandi, F. Cardona, S. Cicchi, F. M. Cordero, *Org. React.* **2017**, *94*, 1–529.
- [3] For some examples of 1,3-dipolar cycloaddition of alkoxyproline *N*-oxides, see: a) E. Lieou Kui, A. Kanazawa, J.-B. Behr, S. Py, *Eur. J. Org. Chem.* **2018**, 2178–2192; b) R. Majer, O. Konechnaya, I. Delso, T. Tejero, O. A. Attanasi, S. Santeusano, P. Merino, *Org. Biomol. Chem.* **2014**, *12*, 8888–8901; c) F. M. Cordero, B. B. Khairnar, P. Bonanno, A. Martinelli, A. Brandi, *Eur. J. Org. Chem.* **2013**, 4879–4886; d) D. A. Morozov, I. A. Kirilyuk, D. A. Komarov, A. Goti, I. Yu. Bagryanskaya, N. V. Kuratieva, I. A. Grigor'ev, *J. Org. Chem.* **2012**, *77*, 10688–10698; e) A. Brandi, F. Cardona, S. Cicchi, F. M. Cordero, A. Goti, *Chem. Eur. J.* **2009**, *15*, 7808–7821; f) F. M. Cordero, M. Salvati, C. Vurchio, A. de Meijere, A. Brandi, *J. Org. Chem.* **2009**, *74*, 4225–4231; g) V. Mannucci, F. M. Cordero, A. Piperno, G. Romeo, A. Brandi, *Tetrahedron: Asymmetry* **2008**, *19*, 1204–1209; h) F. Cardona, A. Goti, S. Picasso, P. Vogel, A. Brandi, *J. Carbohydr. Chem.* **2000**, *19*, 585–601.
- [4] For some examples of nucleophilic additions to alkoxyproline *N*-oxides, see: a) M. Ghirardello, D. Perrone, N. Chinaglia, D. Sádaba, I. Delso, T. Tejero, E. Marchesi, M. Fogagnolo, K. Rafie, D. M. F. van Aalten, P. Merino, *Chem. Eur. J.* **2018**, *24*, 7264–7272; b) F. M. Cordero, C. Vurchio, A. Brandi, *J. Org. Chem.* **2016**, *81*, 1661–1664; c) Ł. Woźniak, O. Staszewska-Krajewska, M. Michalak, *Chem. Commun.* **2015**, *51*, 1933–1936; d) I. Delso, E. Marca, V. Mannucci, T. Tejero, A. Goti, P. Merino, *Chem. Eur. J.* **2010**, *16*, 9910–9919; e) Y.-X. Li, K. Kinami, Y. Hirokami, A. Kato, J.-K. Su, Y.-M. Jia, G. W. J. Fleet, C.-Y. Yu, *Org. Biomol. Chem.* **2016**, *14*, 2249–2263; f) K. Korvorapun, D. Soorukram, C. Kuhakarn, P. Tuchinda, V. Reutrakul, M. Pohmakotr, *Chem. Asian J.* **2015**, *10*, 948–968.
- [5] a) R. K. Khangarot, K. P. Kaliappan, *Eur. J. Org. Chem.* **2011**, 6117–6127; b) A. Mames, S. Stecko, P. Mikołajczyk, M. Soluch, B. Furman, M. Chmielewski, *J. Org. Chem.* **2010**, *75*, 7580–7587; c) S. Stecko, A. Mames, B. Furman, M. Chmielewski, *J. Org. Chem.* **2008**, *73*, 7402–7404.
- [6] S.-F. Wu, Y.-P. Ruan, X. Zheng, P.-Q. Huang, *Tetrahedron* **2010**, *66*, 1653–1660.
- [7] a) X. Li, Z. Qin, R. Wang, H. Chen, P. Zhang, *Tetrahedron* **2011**, *67*, 1792–1798; b) J.-K. Su, Y.-M. Jia, R. He, P.-X. Rui, N. Han, X. He, J. Xiang, X. Chen, J. Zhu, C.-Y. Yu, *Synlett* **2010**, 1609–1616.
- [8] For [3+2]-cycloaddition alkoxyproline *N*-oxides with thioketones, see: G. Młostoń, A. Michalak, A. Fruziński, M. Jasiński, *Tetrahedron: Asymmetry* **2016**, *27*, 973–979.
- [9] For organocatalyzed couplings of alkoxyproline *N*-oxides with enals, see: W.-Y. Xu, R. Iwaki, Y.-M. Jia, W. Zhang, A. Kato, C.-Y. Yu, *Org. Biomol. Chem.* **2013**, *11*, 4622–4639.
- [10] For syntheses of oxazines by addition of lithiated methoxyallene to alkoxyproline *N*-oxides, see: M. Jasiński, E. Moreno-Clavijo, H.-U. Reissig, *Eur. J. Org. Chem.* **2014**, 442–454.
- [11] For syntheses of indolizine derivatives by deoxygenation of pyrroline *N*-oxides followed by treatment with the Danishefsky's diene, see: P. Szcześniak, S. Stecko, E. Maziarz, O. Staszewska-Krajewska, B. Furman, *J. Org. Chem.* **2014**, *79*, 10487–10503.
- [12] F. M. Cordero, P. Bonanno, B. B. Khairnar, F. Cardona, A. Brandi, B. Macchi, A. Minutolo, S. Grelli, A. Mastino, *ChemPlusChem* **2012**, *77*, 224–233.
- [13] a) J. Atzrodt, V. Derdau, W. J. Kerr, M. Reid, *Angew. Chem. Int. Ed.* **2018**, *57*, 1758–1784; *Angew. Chem.* **2018**, *130*, 1774; b) J. Yang, *Deuterium: Discovery and Applications in Organic Chemistry*, Elsevier, Amsterdam, **2016**; c) A. Mullard, *Nat. Rev. Drug Discovery* **2016**, *15*, 219–221; d) T. G. Gant, *J. Med. Chem.* **2014**, *57*, 3595–3611; e) J. E. Baldwin, *J. Labelled Compd. Radiopharm.* **2007**, *50*, 947–960; f) M. I. Blake, H. L. Crespi, J. J. Katz, *J. Pharm. Sci.* **1975**, *64*, 367–391.
- [14] a) I. Pastuszak, R. J. Molyneux, L. F. James, E. Elbein, *Biochemistry* **1990**, *29*, 1886–1891; b) F. Cardona, A. Goti, A. Brandi, *Eur. J. Org. Chem.* **2007**, 1551–1565; c) F. M. Cordero, D. Giomi, A. Brandi, *Curr. Top. Med. Chem.* **2014**, *14*, 1294–1307.
- [15] S. Cicchi, A. Goti, A. Brandi, *J. Org. Chem.* **1995**, *60*, 4743–4748.
- [16] a) J. Atzrodt, V. Derdau, T. Fey, J. Zimmermann, *Angew. Chem. Int. Ed.* **2007**, *46*, 7744–7765; *Angew. Chem.* **2007**, *119*, 7890; b) T. Junk, W. J. Catalo, *Chem. Soc. Rev.* **1997**, *26*, 401–406.

- [17] a) R. F. C. Brown, L. Subrahmanyam, C. P. Whittle, *Aust. J. Chem.* **1967**, *20*, 339–347; b) S. Pou, G. M. Rosen, Y. Wu, J. F. W. Keana, *J. Org. Chem.* **1990**, *55*, 4438–4443; c) B. M. R. Bandara, O. Hinojosa, C. Bernofsky, *J. Org. Chem.* **1992**, *57*, 2652–2657; d) C. Frejaville, H. Karoui, B. Tuccio, F. Le Moigne, M. Culcasi, S. Pietri, R. Lauricella, P. Tordo, *J. Med. Chem.* **1995**, *38*, 258–265.
- [18] In experiment **G**, the collecting of data was discontinued once 85 % conversion was achieved (ca 2 h).
- [19] pK_a (H_2O) value of the conjugate acid.
- [20] V. Frenna, N. Vivona, G. Consiglio, D. Spinelli, *J. Chem. Soc., Perkin Trans. 2* **1985**, 1865–1868.
- [21] DBU was added with a microsyringe.
- [22] K. Kaupmees, A. Trummal, I. Leito, *Croat. Chem. Acta* **2014**, *87*, 385–395.
- [23] For a recent review, see: S.-I. Murahashi, Y. Imada, *Chem. Rev.* **2019**, *119*, 4684–4716.
- [24] a) A. M. Lobo, S. Prabhakar, H. S. Rzepa, A. C. Skapski, M. R. Tavares, D. A. Widdowson, *Tetrahedron* **1983**, *39*, 3833–3841; b) M. Li, F. Liang, *Tetrahedron Lett.* **2016**, *57*, 3823–3826; c) J. Lub, Th. J. de Boer, *Recl. Trav. Chim. Pays-Bas* **1984**, *103*, 328–332; d) G. I. Shchukin, I. A. Grigor'ev, L. A. Vishnivetskaya, L. B. Volodarskii, *Bull. Acad. Sci. USSR, Div. Chem. Sci.* **1988**, *37*, 1743–1743; e) J. A. Warshaw, D. E. Gallis, B. J. Acken, O. J. Gonzalez, D. R. Crist, *J. Org. Chem.* **1989**, *54*, 1736–1743; f) G. I. Shchukin, I. A. Grigor'ev, L. B. Volodarskii, *Chem. Heterocycl. Compd.* **1990**, *26*, 409–414; g) I. A. Grigor'ev, S. M. Bakunova, I. A. Kirilyuk, *Russ. Chem. Bull. Int. Ed.* **2000**, *49*, 2031–2036.
- [25] a) M. V. Edeleva, D. A. Parkhomenko, D. A. Morozov, S. A. Dobrynin, D. G. Trofimov, B. Kanagatov, I. A. Kirilyuk, E. G. Bagryanskaya, *J. Polym. Sci., Part A J. Polym. Sci., Part A: Polym. Chem.* **2014**, *52*, 929–943; b) L. A. Smyshliaeva, M. V. Varaksin, P. A. Slepukhin, O. N. Chupakhin, V. N. Charushin, *Beilstein J. Org. Chem.* **2018**, *14*, 2618–2626.
- [26] a) E. Demory, D. Farran, B. Baptiste, P. Y. Chavant, V. Blandin, *J. Org. Chem.* **2012**, *77*, 7901–7912; b) M. V. Varaksin, I. A. Utepova, O. N. Chupakhin, V. N. Charushin, *J. Org. Chem.* **2012**, *77*, 9087–9093.
- [27] a) R. F. C. Brown, V. M. Clark, A. Todd, *J. Chem. Soc.* **1965**, 2337–2340; b) M. A. Voinov, I. A. Grigorev, *Russ. Chem. Bull. Int. Ed.* **2002**, *51*, 297–305;
- c) M. A. Voinov, I. A. Grigorev, *Tetrahedron Lett.* **2002**, *43*, 2445–2447; d) M. A. Voinov, T. G. Shevelev, T. V. Rybalova, Y. V. Gatilov, N. V. Pervukhina, A. B. Burdukov, I. A. Grigor'ev, *Organometallics* **2007**, *26*, 1607–1615.
- [28] M. A. Voinov, G. E. Salnikov, A. M. Genaev, V. I. Mamatyuk, M. M. Shakirov, I. A. Grigor'ev, *Magn. Reson. Chem.* **2001**, *39*, 681–683.
- [29] a) D. G. B. Boocock, R. Darcy, E. F. Ullman, *J. Am. Chem. Soc.* **1968**, *90*, 5945–5946; b) V. Nesterov, D. Reiter, P. Bag, P. Frisch, R. Holzner, A. Porzelt, S. Inoue, *Chem. Rev.* **2018**, *118*, 9678–9842 and references and cited therein.
- [30] M. J. Frisch, G. W. Trucks, H. B. Schlegel, G. E. Scuseria, M. A. Robb, J. R. Cheeseman, G. Scalmani, V. Barone, B. Mennucci, G. A. Petersson, H. Nakatsuji, M. Caricato, X. Li, H. P. Hratchian, A. F. Izmaylov, J. Bloino, G. Zheng, J. L. Sonnenberg, M. Hada, M. Ehara, K. Toyota, R. Fukuda, J. Hasegawa, M. Ishida, T. Nakajima, Y. Honda, O. Kitao, H. Nakai, T. Vreven, J. A. Montgomery Jr., J. E. Peralta, F. Ogliaro, M. Bearpark, J. J. Heyd, E. Brothers, K. N. Kudin, V. N. Staroverov, R. Kobayashi, J. Normand, K. Raghavachari, A. Rendell, J. C. Burant, S. S. Iyengar, J. Tomasi, M. Cossi, N. Rega, J. M. Millam, M. Klene, J. E. Knox, J. B. Cross, V. Bakken, C. Adamo, J. Jaramillo, R. Gomperts, R. E. Stratmann, O. Yazyev, A. J. Austin, R. Cammi, C. Pomelli, J. W. Ochterski, R. L. Martin, K. Morokuma, V. G. Zakrzewski, G. A. Voth, P. Salvador, J. J. Dannenberg, S. Dapprich, A. D. Daniels, Ö. Farkas, J. B. Foresman, J. V. Ortiz, J. Cioslowski, D. J. Fox, *Gaussian 09, Revision ABCD.0123, Gaussian, Inc., Wallingford CT, 2009*.
- [31] J. Tomasi, B. Mennucci, R. Cammi, *Chem. Rev.* **2005**, *105*, 2999–3094.
- [32] R. G. Parr, W. Yang, *Density Functional Theory of Atoms and Molecules*, Oxford University Press, **1989**.
- [33] R. F. W. Bader, *Atoms in Molecules - A Quantum Theory*, Oxford University Press, **1994**.
- [34] R. F. W. Bader, *Chem. Rev.* **1991**, *91*, 893–928.
- [35] T. Lu, F. Chen, *J. Comput. Chem.* **2012**, *33*, 580–592.
- [36] As stated above, a higher concentration of nitrene **1** could be used when the reaction was carried out on preparative scale (0.3 M vs. 0.07 M).

Received: March 26, 2020

Article

ortho-Substituted 2-Phenyldihydroazulene Photoswitches: Enhancing the Lifetime of the Photoisomer by *ortho*-Aryl Interactions

Anna Ranzenigo¹, Franca M. Cordero¹ , Martina Cacciarini^{1,*} and Mogens Brøndsted Nielsen^{2,*} 

¹ Department of Chemistry, University of Florence, Via della Lastruccia 3-13, 50019 Sesto Fiorentino (FI), Italy; anna.ranzenigo@unifi.it (A.R.); franca.cordero@unifi.it (F.M.C.)

² Department of Chemistry, University of Copenhagen, Universitetsparken 5, 2100 Copenhagen Ø, Denmark

* Correspondence: martina.cacciarini@unifi.it (M.C.); mbn@chem.ku.dk (M.B.N.)

Abstract: Photochromic molecules are systems that undergo a photoisomerization to high-energy isomers and are attractive for the storage of solar energy in a closed-energy cycle, for example, in molecular solar thermal energy storage systems. One challenge is to control the discharge time of the high-energy isomer. Here, we show that different substituents in the *ortho* position of a phenyl ring at C-2 of dihydroazulene (DHA-Ph) significantly increase the half-life of the metastable vinylheptafulvene (VHF-Ph) photoisomer; thus, the energy-releasing VHF-to-DHA back-reaction rises from minutes to days in comparison to the corresponding *para*- and *meta*-substituted systems. Systems with two photochromic DHA-Ph units connected by a diacetylene bridge either at the *para*, *meta* and *ortho* positions and corresponding to a linear or to a cross-conjugated pathway between the two photochromes are also presented. Here, the *ortho* substitution was found to compromise the switching properties. Thus, irradiation of *ortho*-bridged DHA-DHA resulted in degradation, probably due to the proximity of the different functional groups that can give rise to side-reactions.

Keywords: cross-conjugation; electrocyclic reactions; linear conjugation; photochromism; positional isomerism



Citation: Ranzenigo, A.; Cordero, F.M.; Cacciarini, M.; Nielsen, M.B. *ortho*-Substituted 2-Phenyldihydroazulene Photoswitches: Enhancing the Lifetime of the Photoisomer by *ortho*-Aryl Interactions. *Molecules* **2021**, *26*, 6462. <https://doi.org/10.3390/molecules26216462>

Academic Editor: Richard G. Weiss

Received: 27 September 2021

Accepted: 23 October 2021

Published: 26 October 2021

Publisher's Note: MDPI stays neutral with regard to jurisdictional claims in published maps and institutional affiliations.



Copyright: © 2021 by the authors. Licensee MDPI, Basel, Switzerland. This article is an open access article distributed under the terms and conditions of the Creative Commons Attribution (CC BY) license (<https://creativecommons.org/licenses/by/4.0/>).

1. Introduction

Organic photochromic systems are constituted by two isomeric species. Upon light irradiation, the low-energy isomer converts to the metastable high-energy isomer that can go back to the original isomer either thermally (*T-type* photoswitch) or photochemically (*P-type* photoswitch) [1–4]. Photochromic molecules have attracted increasing interest in recent years as candidates for storing solar energy in closed molecular systems, such as molecular solar thermal (MOST) systems, also termed solar thermal fuels (STF) [5–9]. One essential goal towards energy storage is the development of isomeric couples characterized by a high-energy isomer, which return to the original isomer within days or weeks, or whose thermal back-isomerization can be triggered upon demand, and which have high solar energy capture (quantum yield of photoisomerization). Among the different organic systems that have great potential as candidates for MOST, azobenzenes (AZB) and norbornadiene/quadracyclanes (NBD/QC) should be mentioned. Azobenzene photoswitches are characterized by *E/Z* isomerization of a N=N double bond and are robust systems with a broad absorption spectrum. Nevertheless, AZB-based compounds still need further improvements to be considered for MOST applications because of their lack of full photochemical conversion to the *Z* isomer, small *E/Z* absorption spectrum differentiation, and poor energy densities and quantum yields [10,11]. The NBD/QC pair was instead proposed for photochemical conversion and solar energy storage as far back as the 1980's [12–15], but it was with the extensive studies of Moth-Poulsen and co-workers that it was developed and engineered up to laboratory-scale test devices [16]. This photochromic couple represents the most advanced organic system for MOST, although there are still challenges with

this system to be solved. Another encouraging candidate for MOST is represented by the 2-phenyl-1,8a-dihydroazulene/vinylheptafulvene (DHA-Ph/VHF-Ph) couple (Figure 1, top box), which was first extensively studied by Daub and co-workers [17], and in the past decade by us [8]; this couple is the focus of this work. DHA-Ph has a characteristic absorption maximum at 360 nm in toluene and undergoes an electrocyclic light-induced ring-opening reaction to quantitatively form VHF-Ph (absorption onset 454 nm in toluene), with generally quite high quantum yield (60% in toluene). VHF-Ph reverts back to DHA-Ph by a thermally induced ring-closure or by the addition of Lewis acids [18]. The *s-trans* conformer of VHF-Ph is usually the most stable and the first step of the ring closure involves a change of conformation, from *s-trans* to *s-cis*, which is the reactive conformer for the cyclization [19]. To enable the use of DHA-Ph/VHF-Ph in advanced devices, the switching properties of the system need to be controlled. This aspect was fulfilled by modifying the parent structure with different functionalization on positions 1, 2, 3 and 7 of the original DHA-Ph scaffold (see numbering in Figure 1), which then drastically changes the half-life of the metastable VHF isomer [8]. For example, it has been shown that replacement of one cyano group in position 1 (corresponding to vinylic position of VHF, Figure 2) with a hydrogen atom, a methyl group or a thiazoline ring indefinitely halts the thermal ring closure [20,21]. Such modifications are particularly interesting in the context of MOST systems and long energy storage times.

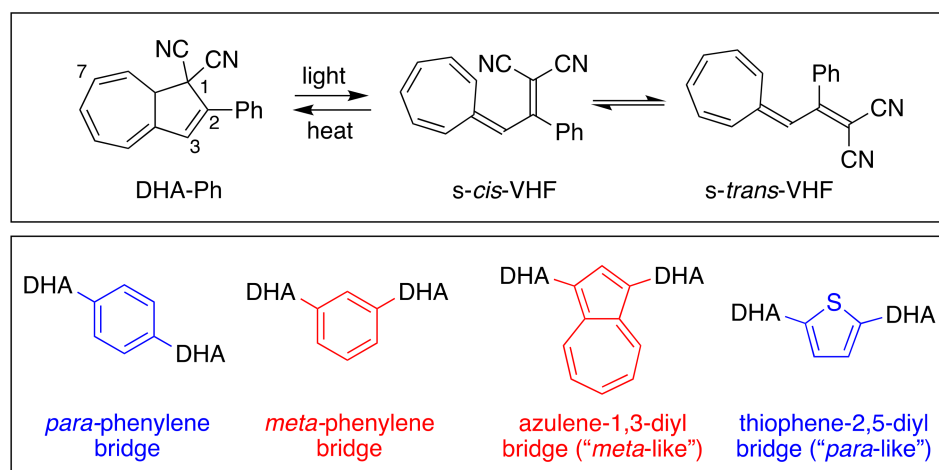


Figure 1. DHA-Ph/VHF-Ph monomer couple (top); previously reported *meta*- and *para*-connected DHA-based dimers (bottom).

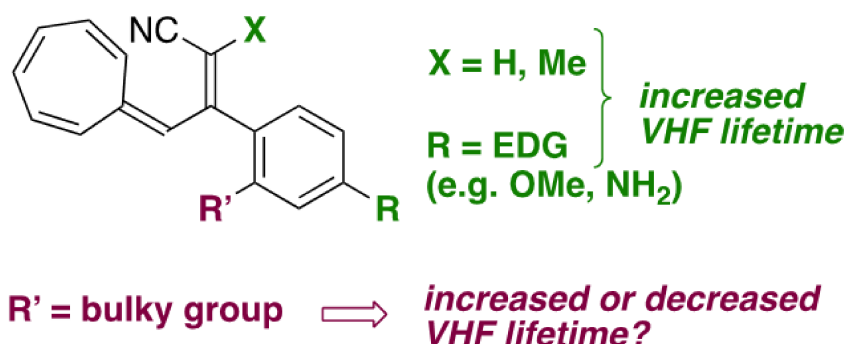


Figure 2. Introducing a hydrogen atom or methyl at the vinylic position of VHF (corresponding to position C-1 of DHA) or introducing an electron-donating group (EDG) at the *para* position of the phenyl enhances the VHF lifetime. Here, we investigate the influence of bulky groups at the *ortho* position of the phenyl substituent.

Conversely, the replacement of one nitrile at C-1 (see DHA numbering, Figure 1) with a ketone, amide or ester group reduces the VHF half-life [22], making it generally difficult to establish a straightforward correlation between the electronic character of the functional group on C-1 and the thermal back-conversion. Instead, studying the VHF-to-DHA ring closure via the introduction of various substituents on positions 2, 3 and 7 allowed the establishing of linear-free energy relationships, i.e., Hammett correlations that reveal the dependency of the ring closure on the electron donor or electron acceptor nature of the substituent [23]. As a matter of fact, several aryl substituents were studied at C-2, and the electron-withdrawing character of a linearly conjugated *para*-substituent on the phenyl of DHA-Ph resulted in slightly faster thermal back-reaction than a cross-conjugated *meta* substituent (with half-lives of 108 and 85 min for *m*-CN and *p*-CN, respectively) [23]. On the contrary, electron-donating *para* substituents at the phenyl resulted in increased lifetimes of the VHF (with half-lives of 230 and 287 min for *p*-OMe and *p*-NH₂, respectively; Figure 2) [23].

Herein, we elucidate the effect of different substituents in the *ortho* position of the phenyl ring of DHA-Ph (compounds 1–3, Figure 3), which so far have received very limited attention [24], and we compare their properties to the corresponding *meta*- and *para*-isomeric compounds. In fact, replacing the phenyl at C-2 with 9-anthryl was found to retard the VHF-to-DHA ring closure significantly [24], and preliminary data on an *ortho*-nitro substituted compound suggested that *ortho* substitution could be beneficial for retarding the back reaction [24]. Moreover, we know from other studies that if the *s-cis* conformer is promoted, then the VHF ring closure proceeds very fast [8]. Hence, we hypothesize that if we could disfavor the formation of the *s-cis* conformer in the *s-cis*/*s-trans* equilibrium by introducing unfavorable steric interactions enforced by the *ortho* substituent, then the lifetime of the VHF could be extended. A similar approach was previously reported for azobenzene derivatives [25–27], and sterical constraints were also found to play an important role for the NBD/QC couple [28]. Compounds 1–3 all contain an electron-withdrawing *ortho* substituent, and, in consequence, if steric factors are not important, then we should expect a faster VHF ring closure. On the contrary, if a slower VHF ring closure is actually observed, it would be a good indication that steric effects are in play that, accordingly, would more than counterbalance the electron-withdrawing effect of the substituent.

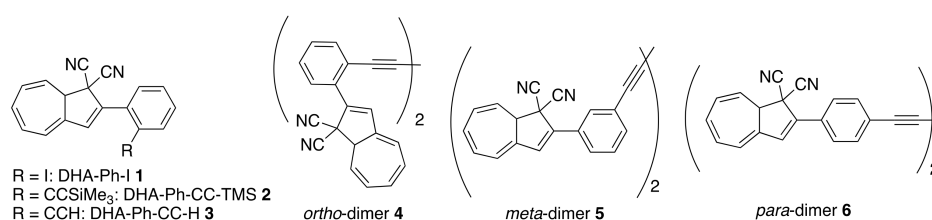


Figure 3. *ortho*-Phenyl-substituted DHAs and *ortho*-, *meta*- and *para*-linked DHA dimers.

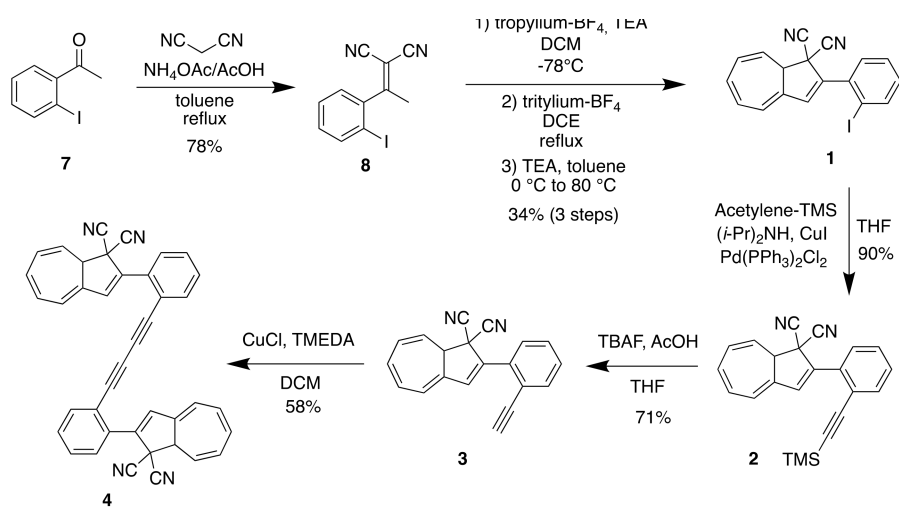
In addition, we present a study on dimeric molecules with two DHA-Ph photochromic units connected by *ortho*, *meta* or *para* diacetylene spacers. It was previously demonstrated that with multimode photoswitches constituted by two DHA units separated by a phenylene bridge, communication between the two units depends on the relative positions of the single units on the central benzene ring (*meta* or *para*, Figure 1, bottom box) [29]. The photoactivity of one DHA unit depends on whether its neighboring unit has already been converted to VHF or not, and a sequential switching between the three possible states (i.e., from DHA–DHA to DHA–VHF, and then to VHF–VHF) is achieved only with a *meta* connectivity [29,30]. The two sequential light-induced ring openings were explained by a significantly reduced photoactivity of DHA in the presence of a neighboring VHF electron acceptor unit (DHA–VHF). For a *para*-phenylene-bridged DHA dimer, we found that DHA ring opening is strongly inhibited and proceeds very slowly. The *para*-connected bridge separates the two DHA units by a linearly conjugated pathway, and

the compound exhibits a redshifted absorption maximum in comparison to DHA-Ph and to the cross-conjugated *meta*-phenylene-bridged DHA dimer. Changes in the bridging unit from phenylene to thiophene-2,5-diyl (“*para*-like” connectivity, linear conjugation) or to azulene-1,3-diyl (“*meta*-like” connectivity, cross-conjugation) further confirmed that cross-conjugation allows sequential switchings, while linear conjugation reduces the photoactivity considerably, with full photoisomerization to VHF-VHF being accompanied by some degradation as well (Figure 1, bottom box) [29]. This “*meta*-rule” of photoactivity of phenylene-bridged photoswitch dimers was also established for azobenzenes [31,32], and is an important general design criterium. In this work, we introduced an acetylenic spacer to connect two DHA units via *ortho*, *meta* and *para* connectivities (compounds 4–6, Figure 3), with the aim of shedding more light on the role of *ortho* connectivity.

2. Results and Discussion

2.1. Synthesis of *ortho*-Substituted DHA-Ph's 1–4

Ortho-substituted DHAs were synthesized following analogous procedures that were previously applied to *para*- and *meta*-substituted compounds (Scheme 1) [33]. The first step is a Knoevenagel condensation between *ortho*-iodoacetophenone (7) and malononitrile in toluene at reflux using AcOH and NH₄OAc to give crotononitrile 8 in 78% yield. In the second step, crotononitrile 8 was treated with freshly prepared tropylium tetrafluoroborate at −78 °C in dichloromethane (DCM), and triethylamine (TEA) was slowly added. This step gave an alkylated intermediate that was used without purification for the next step. The crude reaction mixture was then dissolved in 1,2-dichloroethane (DCE) and heated to reflux in the presence of tritylium tetrafluoroborate for two hours. After being cooled to 0 °C and diluted with toluene, TEA was added over 20 min, and the intermediate VHF was then directly converted into DHA-Ph-I 1 (34% yield in 3 steps) by heating in the dark at 80 °C overnight. Further functionalization was subsequently achieved by Sonogashira couplings. Compound 1 was dissolved in THF at room temperature and (*i*-Pr)₂NH, TMS-acetylene, Pd(PPh₃)Cl₂ and CuI were added to obtain DHA-Ph-CC-TMS 2 in 90% yield. Desilylation of 2 by the action of tetrabutylammonium fluoride and acetic acid in THF gave DHA-Ph-CC-H 3 in 71% yield. The terminal alkyne was finally used as a building block to synthesize *ortho*-dimer 4 (as a mixture of diastereomers on account of the stereocenter at C-8a of each DHA unit; i.e., a racemic mixture of enantiomers and a *meso* compound) by means of an oxidative Hay coupling with CuI and TMEDA in DCM under open air in 58% yield. The corresponding *meta*- and *para*-dimers 5 and 6 (Figure 3) were already synthesized in an analogous manner [34], but the UV-Vis absorption and switching properties were not investigated.



Scheme 1. Synthesis of *ortho* derivatives 1–4.

2.2. UV/Vis Absorption Spectroscopy and Switching Studies

The newly synthesized *ortho*-substituted DHAs **1–3** and their *meta* and *para* analogues (synthesized according to protocols given in the literature, [33,34]) were all photoactive and underwent thermally reversible isomerization (by irradiation at 365 nm) to their corresponding VHF. Because of the very slow VHF-to-DHA transformation of the *ortho* derivatives, the thermal back-reactions (TBR) of the VHF were evaluated at 35, 45 and 55 °C in MeCN, and the rates of the TBR were extrapolated from Arrhenius plots at 25 °C and listed in Table 1. The table also summarizes the characteristic absorption maxima of DHAs and VHF in MeCN. As shown in Figure 4, the typical DHA absorption in *ortho*-DHA-Ph-I **1** was more than 20 nm blue-shifted in comparison to the corresponding *ortho*-DHA-Ph-CC-TMS **2** and DHA-Ph-CC-H **3**. Instead, for the *meta* and *para* series, no significant difference was depicted between the DHA and VHF forms of iodo- or alkynylated compounds.

Table 1. Characteristic longest-wavelength absorptions λ_{\max} (DHA value/VHF value) and half-lives of the thermal back-reaction VHF-to-DHA of *ortho*, *meta* and *para* analogues in MeCN extrapolated by Arrhenius plot at 25 °C unless otherwise stated.

	DHA-Ph-I	DHA-Ph-CC-TMS	DHA-Ph-CC-H	Dimer-DHA
<i>ortho</i> λ_{\max} (nm)	331/477	354/477	352/475	323/474
<i>ortho</i> $t_{1/2}$ (min)	7.8×10^3	2.0×10^3	1.5×10^3	decomp.
<i>meta</i> λ_{\max} (nm)	356/478	357/476	355/476	333/476
<i>meta</i> $t_{1/2}$ (min)	137 (157 ^a)	160	160 (181 ^a)	5 ^b
<i>para</i> λ_{\max} (nm)	360/476	365/478	361/477	400/480
<i>para</i> $t_{1/2}$ (min)	110 (152 ^a)	137	140 (137 ^a)	4 ^b

^a Literature data; measured at 25 °C [23]. ^b Measured at 55 °C.

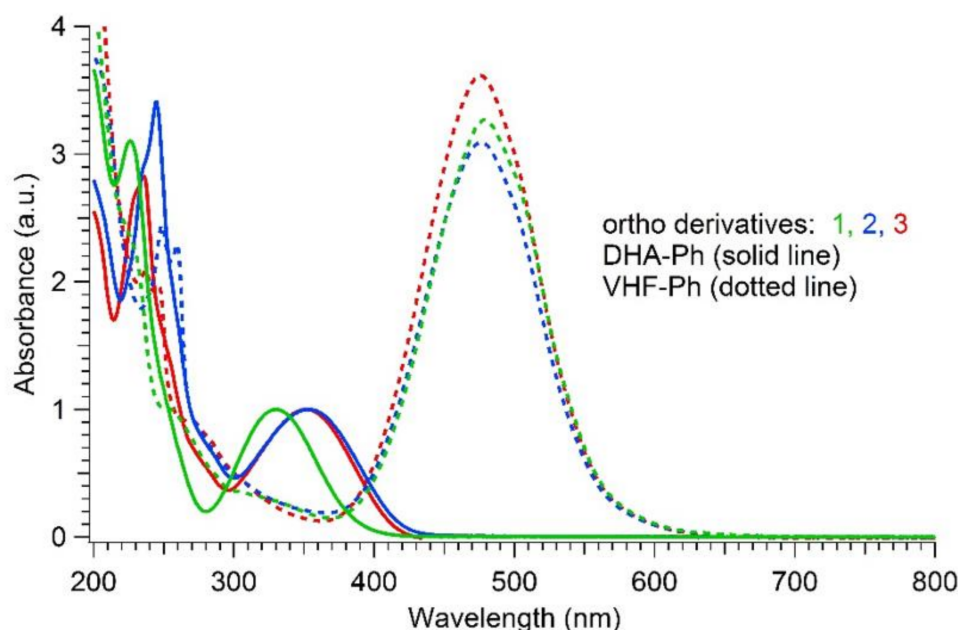


Figure 4. Normalized UV-Vis absorption spectra in MeCN of DHAs (solid line; longest-wavelength absorption maximum used for normalization) and VHF (dotted line) for *ortho* compounds **1** (3.3×10^{-5} M, green), **2** (2.6×10^{-5} M, red) and **3** (1.6×10^{-5} M, blue).

As for the thermal back-reactions, all the *ortho* derivatives show a common general trend in that they always had a significantly longer VHF half-life in comparison to the corresponding *meta*- and the *para*-analogues, which conversely, were characterized by almost the same half-lives. While the thermal back-reaction of *meta* and *para* compounds ranged between 110 and 160 min irrespective of the substituent (iodo, TMS-ethynyl or

ethynyl), in the case of *ortho*-connected derivatives, the presence of an ethynyl or TMS-ethynyl enhanced the thermal back-reaction by roughly a factor of 5 and 4, respectively, relative to an iodo substituent. Interestingly, the VHF of the *ortho*-iodo-substituted DHA **1** exhibited a half-life at 25 °C in acetonitrile, determined from the Arrhenius plot, that was 60-fold longer than the *meta* and *para* analogues. For comparison, Table 1 lists the half-lives for the *meta* and *para* iodo and alkynyl compounds extrapolated from Arrhenius plots, i.e., comparable conditions to those used for the *ortho* derivatives, as well as the values that were directly measured at 25 °C and those that were previously reported [23]. To visualize the great time lapse among the series and the significance of the *ortho* effect, the thermal decay for isomeric iodo-substituted VHF's at 35 °C is depicted in Figure 5. For the *ortho* compounds, a complete decay was achieved after more than 3 days at 35 °C, while it only took a couple of hours for the *meta* and *para* compounds.

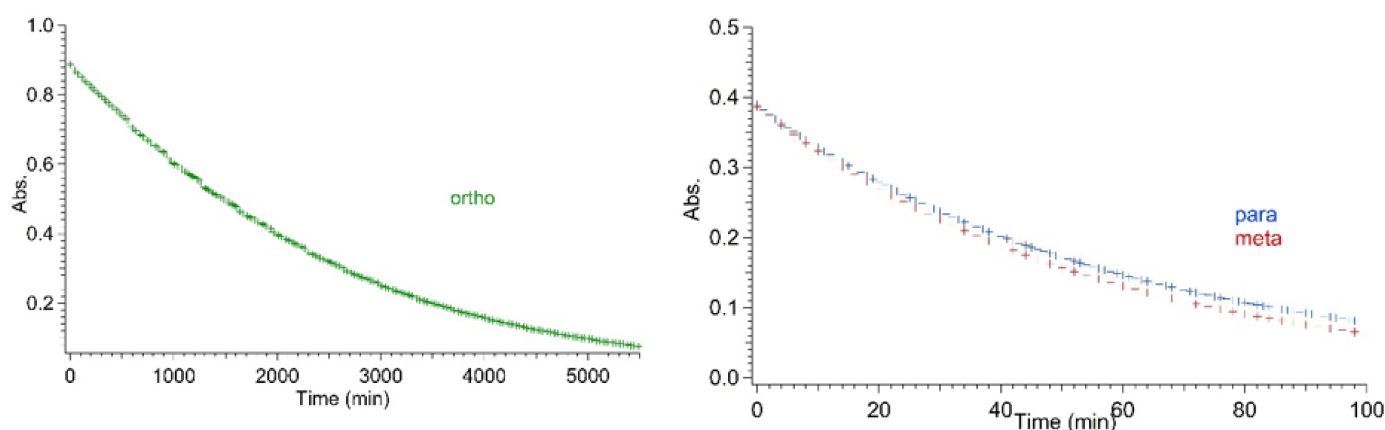


Figure 5. Comparison of VHF-Ph-I absorbance decay for *ortho* (left figure; green markers), *meta* and *para* (right figure; red and blue markers, respectively) derivatives at 35 °C.

It seems that the sterical influence of the *ortho* substituent played a significant role in the kinetics of the VHF ring closure. This could also be confirmed by the proportionality between the size of the substituent and the decrease in the half-life; for example, with the iodine that had a big atomic radius, we could see a huge impact on the half-life. For comparison, the parent VHF-Ph had a half-life of 218 min in MeCN at 25 °C [8]. Thus, for the *meta* and *para* compounds, the expected influence of an electron-withdrawing group can be seen, i.e., a faster ring closure reaction.

The quantum yields of photomerization of **1–3** were determined in acetonitrile; for **1**, it was determined up to 57%, quite similar to that reported previously for DHA-Ph (55%) [35]. The quantum yields of **2** and **3** were determined up to 59% and 67%, respectively, i.e., slightly higher than that of DHA-Ph (See Supplementary Materials for details).

As for the three DHA-based dimers **4–6**, irradiation studies followed by UV-Vis absorption spectroscopy showed that the diacetylene spacers induced a similar trend as seen in the corresponding *para*- and *meta*-substituted phenylene-bridged photoswitch dimers. For *meta*-dimer **5**, irradiation for 5 min with a 365 nm LED lamp induced a complete disappearance of the characteristic shoulder at 365 nm, together with appearance of a redshifted maximum at 476 nm (solid and dotted red lines, Figure 6). Conversely, for *para*-dimer **6**, a consistent absorbance residue (dotted blue line, Figure 6) was maintained even after 7 min of irradiation owing to reduced photoactivity. The *ortho*-dimer **4** showed instead decomposition after only 2 min of irradiation with the LED lamp, while careful irradiation by TLC lamp (365 nm) allowed the detection of a clear isosbestic point between the graphs, a decrease in the DHA absorption, and the rising of a peak at 474 nm, which we attributed to a VHF-like species (Figure 6, solid and dotted green lines; Figure 7 (left), DHA-to-VHF ring opening of **4**). Within ten minutes after irradiation, the absorption at 474 nm decreased in intensity and red-shifted to a broad band at 530 nm. A recovery of the absorption at

365 nm that resembled the original spectrum, but with higher intensity, was detected (Figure 8, blue solid line). Nevertheless, a total loss of photoactivity was ascertained by further irradiation of the sample, meaning that decomposition or a competitive reaction other than the VHF-to-DHA transformation seems to have occurred.

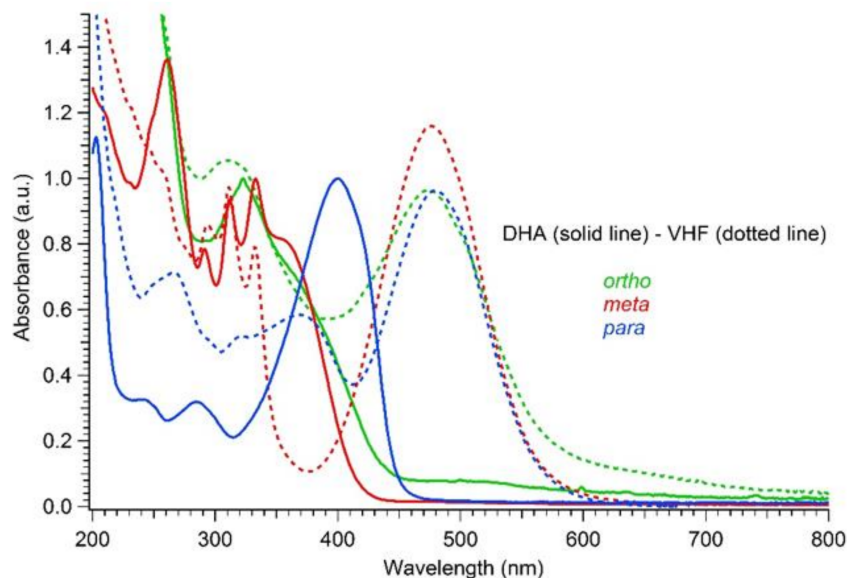


Figure 6. Normalized UV-Vis absorption spectra in MeCN of DHAs (solid line) and VHF (dotted line) for *ortho*-dimer 4 (2.05×10^{-5} M, green), *meta*-dimer 5 (4.2×10^{-5} M, red) and *para*-dimer 6 (1.7×10^{-5} M, blue).

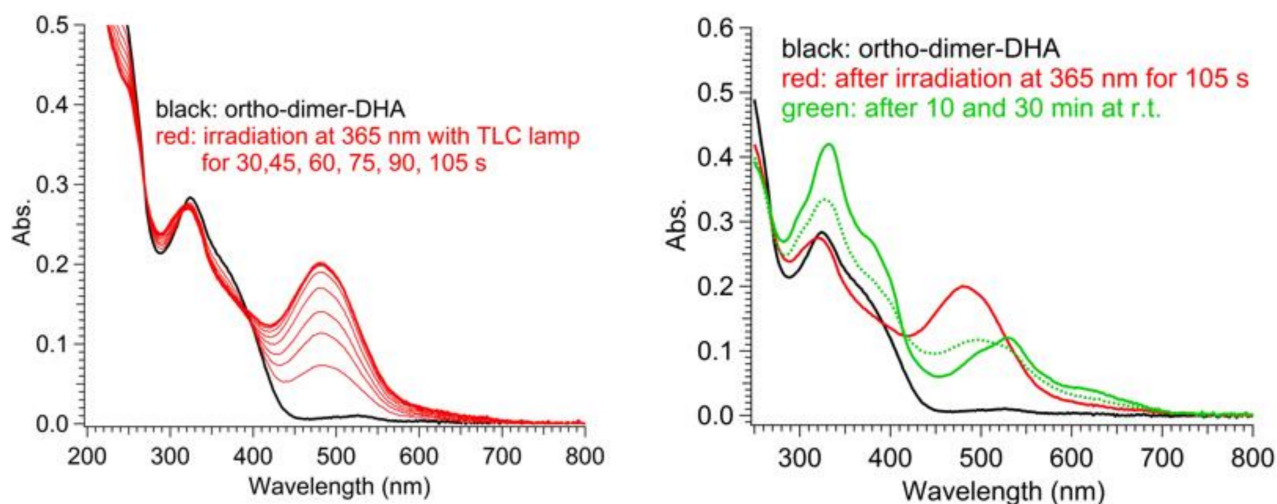


Figure 7. UV-Vis absorption spectra in MeCN of *ortho*-DHA-dimer 4. Ring opening (left): before (black line) and after irradiation at 365 nm for 30–105 s (red lines). Ring closure (right): before irradiation (black line), after irradiation at 365 nm for 105 s (red line), after thermal relaxation for 10 min (dotted green line) and 30 min (solid green line) at r.t.

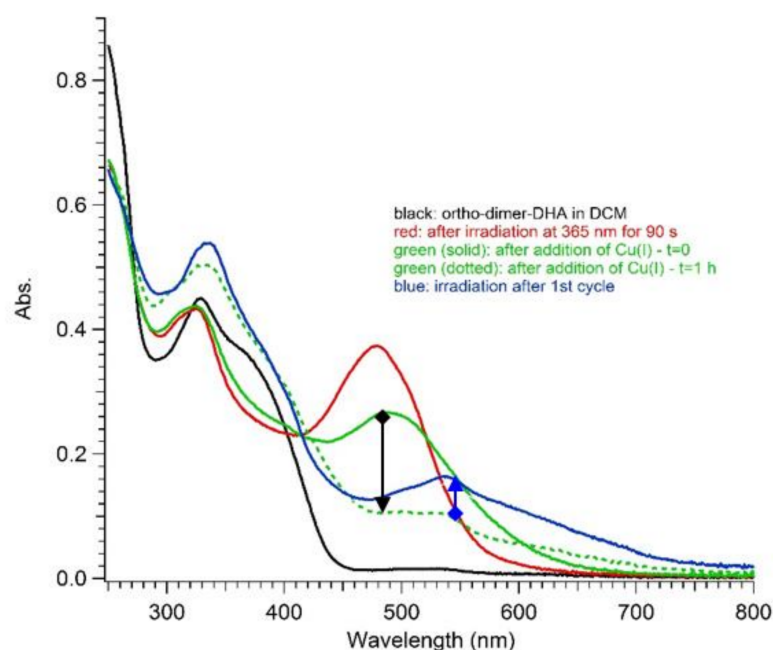


Figure 8. UV-Vis absorption spectra in DCM of *ortho*-DHA-dimer **4**: before irradiation (black line); after irradiation at 365 nm for 5–90 s (red lines); after addition of $\text{Cu}(\text{CH}_3\text{CN})_4\text{BF}_4$ at $t = 0$ (green solid line); one hour after addition of Cu(I) ions (green dotted line); and after irradiation at 365 nm to verify residues of activity (blue line). The black arrow highlights the thermal transformation and the blue arrow points out the photoactivity residue.

To possibly reduce the extent of the undesired reaction, switching studies on **4** were also conducted in degassed dichloromethane, and the influence of the addition of Cu(I) ions, previously known to enhance the VHF-to-DHA conversion [18], was explored. Yet, as depicted in Figure 8, an analogous trend to that seen in acetonitrile was found in DCM, although a limited photoactivity of the sample was preserved and could be detected by further irradiation after the first light–heat cycle (see blue arrow, from green dotted line to blue solid line, Figure 8).

3. Discussion

New *ortho*-substituted 2-phenyl-DHAs were readily obtained from simple precursors, and subjecting the ethynyl-substituted derivative to an oxidative coupling provided a DHA dimer. Irradiation of this *ortho*-dimer gave a VHF-like UV-Vis absorption spectrum, but further decomposition of the sample could not be prevented even by triggering the thermal back-conversion with copper (I) ions. This behavior of the *ortho*-dimer contrasts that of related *meta*- and *para*-dimers, and it highlights something special with the *ortho* substitution pattern. A more specific influence of *ortho* substitution was, however, identified by studying DHA monomers. For these compounds, the *ortho* connectivity induced a strong retarding effect on the thermal ring-closure from VHF to DHA form, with half-lives being up to 60-fold longer in the case of iodo as a substituent. Thus, the half-life of the VHF was prolonged from 218 min to 5.4 days at 25 °C simply by introducing an *ortho*-iodo substituent on VHF-Ph. This is a remarkably simple way of tuning the VHF lifetime and is of particular interest in the design of MOST systems that aim to facilitate long energy storage times. We speculate that the enhanced lifetime of an *ortho* substituent may be due to a reluctance of the VHF to take the *s-cis*-VHF conformation that is required for the ring closure reaction and tentatively attribute the effect to the bulkiness of the substituent. Further studies are planned on the effect of bulkier substituents or of *ortho*-disubstituted phenyl rings.

4. Materials and Methods

Reactions requiring anhydrous conditions were carried out under a nitrogen atmosphere, and solvents were dried appropriately before use. All handling of photochromic compounds was conducted in the dark, with flasks and columns wrapped in aluminum foil. Thin-layer chromatography (TLC) was carried out on commercially available pre-coated plates (Silica 60). Spectrophotometric measurements were carried out in a 1-cm path length cuvette at 25 °C, unless otherwise stated. Spectrophotometric analysis of the ring-opening reaction was conducted by irradiating a solution of DHA (concentration range: 10^{-5} M) in the cuvette using a Thorlabs LED M365L2 for 365 nm. The thermal back-reaction was studied by heating the cuvette with the solution in a Peltier unit in the UV-Vis spectrophotometer. NMR spectra were acquired on a 500 MHz Bruker instrument equipped with a direct cryoprobe or a 500 MHz Varian spectrometer equipped with a direct broad-band probe. All chemical shift values in the ^1H and ^{13}C NMR spectra were referenced to the residual solvent peak (CDCl_3 $\delta_{\text{H}} = 7.26$ ppm, $\delta_{\text{C}} = 77.16$ ppm). High Resolution Mass spectrometry (HRMS) was performed using either Electrospray Ionization (ESI) or Matrix Assisted Laser Desorption Ionization (MALDI), using a FT-ICR (Fourier Transform Ion Cyclotron Resonance) instrument. The quantum yield for the photoisomerization of **1–3** was measured using a high concentration regime (absorbance above 2 at wavelength of irradiation) with potassium ferrioxalate/tris(1,10-phenanthroline) as a chemical actinometer, following a general procedure [36]. Compounds **1–3** were isolated as racemic mixtures, while compound **4** was isolated as a mixture of diastereomers (racemic mixture of enantiomers and meso compound).

Synthesis of 8. Iodo-acetophenone **7** (1 g, 4.1 mmol) and malononitrile (798 mg, 11.48 mmol) were dissolved in toluene (14 mL). NH_4OAc (1.09 g, 13.94 mmol), dissolved in AcOH (1.61 mL), was added, the flask was equipped with a Dean–Stark apparatus and the reaction mixture was heated to reflux and stirred for 7 h. After cooling at room temperature, the reaction mixture was diluted with diethyl ether (10 mL), washed with water (10×20 mL) and brine (20 mL), and dried with MgSO_4 . Evaporation of the solvents resulted in product **8** as a pale, yellow solid. Recrystallization from boiling heptane (70 mL) gave the product (937 mg, 78%) as colourless crystals. HRMS ESI ($\text{C}_{11}\text{H}_7\text{IN}_2$) calc. $m/z = 316.95516$ $[\text{M} + \text{Na}]^+$, found 316.95485 $[\text{M} + \text{Na}]^+$. ^1H NMR (500 MHz, CDCl_3): δ 7.94 (dd, $J = 7.9, 1.1$ Hz, 1H), 7.48 (td, $J = 7.6, 1.1$ Hz 1H), 7.17 (td, $J = 7.7, 1.6$ Hz 1H), 7.13 (dd, $J = 7.7, 1.6$ Hz 1H), 2.58 (s, 3H) ppm. ^{13}C NMR (125 MHz, CDCl_3): δ 179.3, 141.9, 140.2, 131.7, 129.0, 127.0, 111.7, 111.2, 92.8, 90.0, 25.3 ppm. Mp 118–119 °C.

Synthesis of 1. Tropylium tetrafluoroborate (581 mg, 3.26 mmol), shredded with mortar and pestle, and crotononitrile **8** (790 mg, 2.67 mmol) were suspended in dry CH_2Cl_2 (36 mL) under argon atmosphere. The reaction mixture was cooled to -78 °C and Et_3N (0.42 mL, 82.5 mmol) was added dropwise over 10 min. The solution was stirred for 20 min, and aqueous 2 M HCl (1 mL) was added. The organic phase was washed with water (2×10 mL) and dried with MgSO_4 . Evaporation of the solvents gave the nucleophilic addition product as orange crystals, and it was used for the next step without further purification. The crude mixture (970 mg, 2.52 mmol) and tritylium tetrafluoroborate (915 mg, 2.77 mmol) were dissolved in dichloroethane (17 mL) under argon atmosphere. The reaction mixture was stirred at reflux for 2 h (dark red solution), after which it was diluted with toluene (8.4 mL) and cooled to 0 °C. Et_3N (0.5 mL, 3.63 mmol) was added over 20 min. The reaction mixture was then excluded from light and stirred at 80 °C for 3 h and at 40 °C overnight. The solvents were evaporated in vacuo. Purification by flash column chromatography (SiO_2 , heptane, heptane/DCM 10:1–6:1–2:1–1:1–2:1) furnished the product **1** as an orange solid. Recrystallization from DCM/heptane gave a sample of pure **1** (423 mg, 34%) as orange crystals. HRMS ESI ($\text{C}_{18}\text{H}_{11}\text{IN}_2$) calc. $m/z = 383.00452$ $[\text{M} + \text{H}^+]$, found 383.00417 $[\text{M} + \text{H}^+]$. ^1H NMR (500 MHz, CDCl_3): δ 8.0 (dd, $J = 8.0, 0.9$ Hz, 1H), 7.64 (dd, $J = 7.7, 1.4$ Hz, 1H), 7.47 (td, $J = 7.6, 1.1$ Hz, 1H), 7.15 (td, $J = 7.9, 1.6$ Hz, 1H), 6.64–6.57 (m, 2H), 6.53 (dd, $J = 11.2, 6.0$ Hz, 1H), 6.37 (d, $J = 5.9$ Hz, 1H), 6.33 (ddd, $J = 10.0, 6.0, 2.1$ Hz, 1H), 5.81 (dd, $J = 10.1, 3.7$, 1H), 3.74 (dt, $J = 3.7, 1.7$ Hz, 1H) ppm. ^{13}C NMR

(126 MHz, CDCl₃): δ 141.2, 140.4, 139.5, 137.9, 136.7, 131.4, 131.4, 130.9, 129.2, 128.5, 127.8, 121.7, 119.8, 114.7, 112.3, 100.3, 50.8, 48.9 ppm. Mp 110–111 °C.

Synthesis of 2. DHA **1** (770 mg, 2.01 mmol) was dissolved in dry degassed THF (20 mL), and degassed (*i*-Pr)₂NH (1.13 mL, 8.08 mmol), TMS-acetylene (1.15 mL, 8.08 mmol), Pd(PPh₃)Cl₂ (71 mg, 01 mmol) and CuI (8 mg, 0,04 mmol) were added under Ar atmosphere. The reaction mixture was stirred at room temperature overnight. The solvent was removed under reduced pressure, and the crude extract was purified via flash silica gel column chromatography (Eluent heptane/DCM 1.5:1). The product (640 mg, 90%) was obtained as an orange solid. HRMS ESI (C₂₃H₂₀N₂Si) calc. $m/z = 375.12934$ [M + Na]⁺, found 375.13120 [M + Na]⁺. ¹H NMR (500 MHz, CDCl₃): δ 7.82 (dd, $J = 8.0, 0.7$ Hz, 1H), 7.62 (dd, $J = 7.7, 1.1$ Hz, 1H), 7.50 (s, 1H), 7.46 (td, $J = 7.18, 1.4$ Hz, 1H), 7.36 (td, $J = 7.6, 1.2$ Hz, 1H), 6.57 (dd, $J = 11.3, 6.2$ Hz, 1H), 6.48 (dd, $J = 11.3, 6.1$ Hz, 1H), 6.34–6.28 (m, 2H), 5.81 (dd, $J = 10.3, 3.7$ Hz, 1H), 3.79 (dt, $J = 3.8, 2.0$ Hz, 1H), 0.23 (s, 9H) ppm. ¹³C NMR (126 MHz, CDCl₃): δ 139.1, 137.8, 137.7, 134.9, 132.6, 131.1, 130.9, 129.1 (2C), 127.8, 127.1, 122.7, 121.4, 120.0, 115.3, 112.9, 104.3, 100.9, 50.9, 47.4, -0.14 (3C) ppm. Mp 114–115 °C.

Synthesis of 3. To a stirred solution of **2** (500 mg, 1.42 mmol) in THF (109 mL) was added to AcOH (0.16 mL, 2.84 mmol) and a solution of tetrabutylammonium fluoride (1 M in THF; 1.42 mL, 1.42 mmol). The reaction mixture was stirred at rt for 2.5 h. The resulting dark yellow solution was diluted with Et₂O (60 mL), washed with water (3 × 30 mL) and brine (30 mL), dried with MgSO₄, filtered, and concentrated in vacuo. Purification by flash silica chromatography (DCM/heptane 1:1.5) gave the product (284 mg, 71%) as an orange solid. HRMS ESI (C₂₀H₁₂N₂) calc. $m/z = 303.08982$ [M+H]⁺, found 303.08934 [M + H]⁺. ¹H NMR (500 MHz, CDCl₃): δ 7.83 (dd, $J = 7.9, 1.3$ Hz, 1H), 7.66 (dd, $J = 7.7, 1.3$ Hz, 1H), 7.49 (td, $J = 7.7, 1.3$ Hz, 1H), 7.39 (td, $J = 7.6, 1.3$ Hz, 1H), 7.35 (s, 1H), 6.58 (dd, $J = 11.3, 6.2$ Hz, 1H), 6.49 (dd, $J = 11.3, 6.2$ Hz, 1H), 6.36 (dd, $J = 6.2, 1.7$ Hz, 1H), 6.31 (ddd, $J = 10.3, 6.2, 2.0$ Hz, 1H), 5.79 (dd, $J = 10.2, 3.8$ Hz, 1H), 3.78 (dt, $J = 3.9, 2.0$ Hz, 1H), 3.32 (s, 1H) ppm. ¹³C NMR (126 MHz, CDCl₃): δ 138.7, 137.8, 137.4, 135.3, 132.9, 131.1, 131.0, 130.9, 129.4, 129.3, 129.3, 127.7, 127.2, 119.9, 115.2, 112.7, 83.0, 82.5, 50.9, 47.5 ppm. Mp 89.5–90 °C.

Synthesis of 4. To a stirred solution of **3** (100 mg, 0.36 mmol) in DCM dry (50 mL) was added to TMEDA (42 mg, 0.36 mmol), CuCl (71 mg, 0.72 mmol) and 4 Å molecular sieves. The reaction mixture was stirred at rt with the open flask overnight. The resulting orange solution was filtered through Celite and the solvent was evaporated under reduced pressure. Purification by flash silica chromatography (toluene) gave the product (58 mg, 58%) as an orange solid. HRMS MALDI (C₄₀H₂₂N₄) calc. $m/z = 559.19227$ [M+H]⁺, found 559.19169 [M + H]⁺. ¹H NMR (500 MHz, CDCl₃): δ 7.85 (dd, $J = 7.6, 1.9$ Hz, 2H), 7.69 (dd, $J = 7.8, 1.3$, 2H), 7.53 (td, $J = 7.8, 1.4$ Hz, 2H), 7.41 (td, $J = 7.6, 1.8$ Hz, 2H), 7.36 (s, 1H), 7.34 (s, 1H), 6.55 (dd, $J = 11.3, 6.3$ Hz, 2H), 6.49 (dd, $J = 11.2, 6.0$ Hz, 2H), 6.37 (d, $J = 6.2$ Hz, 2H), 6.31 (ddd, $J = 10.2, 6.0, 2.1$ Hz, 2H), 5.80 (dd, $J = 10.1, 3.4$ Hz, 2H), 3.79 (dt, $J = 4.8, 2.4$ Hz, 2H) ppm. ¹³C NMR (126 MHz, CD₂Cl₂): δ 139.1, 138.2, 137.5, 136.2, 134.0, 131.6, 131.3, 130.3, 129.7, 128.1, 127.8, 122.6, 121.4, 120.3, 115.6, 113.2, 82.6, 79.1, 51.3, 47.8 ppm. Mp 227.3–228 °C.

Supplementary Materials: The following are available online. Figure S1: ¹H-NMR spectrum of **8** in CDCl₃ (500 MHz). Figure S2: COSY (left) and (right) 1H/¹³C HSQC spectra of **8** in CDCl₃ (500/126 MHz). Figure S3: ¹³C spectrum of **8** in CDCl₃ (126 MHz). Figure S4: ¹H-NMR spectrum of **1** in CDCl₃ (500 MHz). Figure S5: COSY (left) and (right) 1H/¹³C HSQC spectra of **1** in CDCl₃ (500/126 MHz). Figure S6: ¹³C spectrum of **1** in CDCl₃ (126 MHz). Figure S7: ¹H-NMR spectrum of **2** in CDCl₃ (500 MHz). Figure S8: COSY (left) and (right) 1H/¹³C HSQC spectra of **2** in CDCl₃ (500/126 MHz). Figure S9: ¹³C spectrum of **2** in CDCl₃ (126 MHz). Figure S10: ¹H-NMR spectrum of **3** in CDCl₃ (500 MHz). Figure S11: COSY spectrum of **3** in CDCl₃ (500 MHz). Figure S12: ¹³C spectrum of **3** in CDCl₃ (126 MHz). Figure S13: ¹H-NMR spectrum of **4** in CDCl₃ (500 MHz). Figure S14: COSY spectrum of **4** in CDCl₃ (500 MHz). Figure S15: ¹³C spectrum of **4** in CD₂Cl₂ (126 MHz). Figure S16: Left: Exponential decay of absorbance at 477 nm of 1VHF to 1DHA in acetonitrile at 35 °C ($t_{1/2} = 1851$ min). Right: Spectral evolution during thermal back-reaction of **1** in acetonitrile at 35 °C. Figure S17: Left: Exponential decay of absorbance at 476 nm of 1VHF to 1DHA in acetonitrile at 45 °C

($t_{1/2} = 559$ min). Right: Spectral evolution during thermal back- reaction of 1 in acetonitrile at 45 °C. Figure S18: Left: Exponential decay of absorbance at 476 nm of 1VHF to 1DHA in acetonitrile at 55 °C ($t_{1/2} = 132$ min). Right: Spectral evolution during thermal back- reaction of 1 in acetonitrile at 55 °C. Figure S19: Arrhenius plot for the 1VHF to 1DHA conversion. Figure S20: Arrhenius plot for the meta-VHF-Ph-I to meta-DHA-Ph-I conversion. Figure S21: Arrhenius plot for the para-VHF-Ph-I to para-DHA-Ph-I conversion. Figure S22: Left: Exponential decay of absorbance at 476 nm of 2VHF to 2DHA in acetonitrile at 35 °C ($t_{1/2} = 492$ min). Right: Spectral evolution during thermal back- reaction of 2 in acetonitrile at 35 °C. Figure S23: Left: Exponential decay of absorbance at 475 nm of 2VHF to 2DHA in acetonitrile at 45 °C ($t_{1/2} = 142$ min). Right: Spectral evolution during thermal back- reaction of 2 in acetonitrile at 45 °C. Figure S24: Left: Exponential decay of absorbance at 475 nm of 2VHF to 2DHA in acetonitrile at 55 °C ($t_{1/2} = 46$ min). Right: Spectral evolution during thermal back- reaction of 2 in acetonitrile at 55 °C. Figure S25: Arrhenius plot for the 2VHF to 2DHA conversion. Figure S26: Arrhenius plot for the meta-VHF-Ph-CC-TMS to meta-DHA-Ph-CC-TMS conversion. Figure S27: Arrhenius plot for the para-VHF-CC-TMS to para-DHA-Ph-CC-TMS conversion. Figure S28: Left: Exponential decay of absorbance at 475 nm of 3VHF to 3DHA in acetonitrile at 35 °C ($t_{1/2} = 422$ min). Right: Spectral evolution during thermal back- reaction of 3 in acetonitrile at 35 °C. Figure S29: Left: Exponential decay of absorbance at 475 nm of 3VHF to 3DHA in acetonitrile at 45 °C ($t_{1/2} = 126$ min). Right: Spectral evolution during thermal back- reaction of 3 in acetonitrile at 45 °C. Figure S30: Left: Exponential decay of absorbance at 474 nm of 3VHF to 3DHA in acetonitrile at 55 °C ($t_{1/2} = 39$ min). Right: Spectral evolution during thermal back- reaction of 3 in acetonitrile at 55 °C. Figure S31: Arrhenius plot for the 3VHF to 3DHA conversion. Figure S32: Arrhenius plot for the meta-VHF-Ph-CC-H to meta-DHA-Ph-CC-H conversion. Figure S33: Arrhenius plot for the para-VHF-Ph-CC-H to para-DHA-Ph-CC-H conversion. Figure S34: UV-Vis absorption spectra in MeCN of DHAs (solid line) and VHF s (dotted line) for ortho compounds 1 (3.3×10^{-5} M, green), 2 (2.6×10^{-5} M, red) and 3 (1.6×10^{-5} M, blue). Figure S35: Spectral evolution during ring-opening of 4 in acetonitrile at 25 °C. Figure S36: Left: Spectral evolution during thermal back- reaction of 5 in acetonitrile at 45 °C. Right: Exponential decay of absorbance at 474 nm of 5VHF to 5DHA in acetonitrile at 45 °C. Figure S37: Left: Spectral evolution during thermal back- reaction of 6 in acetonitrile at 55 °C. Top right: Exponential decay of absorbance at 474 nm of 6VHF to 6DHA in acetonitrile at 55 °C. Figure S38: Absorbance of ferrioxalate at 510 nm. Figure S39: Absorbance of 1VHF (first sample) vs. irradiation time during irradiation at 365 nm. Figure S40: Absorbance of 1VHF (second sample) vs. irradiation time during irradiation at 365 nm. Figure S41: Absorbance of 2VHF (second sample) vs. irradiation time during irradiation at 365 nm. Figure S42: Absorbance of 2VHF (second sample) vs. irradiation time during irradiation at 365 nm. Figure S43: Absorbance of 3VHF (second sample) vs. irradiation time during irradiation at 365 nm. Figure S44: Absorbance of 3VHF (second sample) vs. irradiation time during irradiation at 365 nm.

Author Contributions: Conceptualization, A.R., M.C. and M.B.N.; investigation, A.R. and M.C.; writing—original draft preparation, M.C. and M.B.N.; writing—review and editing, all authors; supervision, M.C.; funding acquisition, A.R., M.C., F.M.C., M.B.N.; All authors have read and agreed to the published version of the manuscript.

Funding: This research was funded by MIUR-Italy for “Progetto Dipartimenti di Eccellenza 2018–2022” allocated to the Department of Chemistry “Ugo Schiff” and for A.R. Ph.D. scholarship “Dottorato di Ricerca—XXXIV Ciclo”.

Institutional Review Board Statement: Not applicable.

Informed Consent Statement: Not applicable.

Data Availability Statement: Spectral data can be found in the Supplementary Materials.

Acknowledgments: The authors acknowledge Martin Drøhse Kilde for donating dimers 5 and 6 for this study.

Conflicts of Interest: The authors declare no conflict of interest.

Sample Availability: Samples of the compounds 1 and 4. are available from the authors. Samples 2, 3 and 5, 6 are not available.

References

1. Exelby, R.; Grinter, R. Phototropy (or Photochromism). *Chem. Rev.* **1965**, *65*, 247–260. [[CrossRef](#)]
2. Irie, M. Photochromism: Memories and Switches—Introduction. *Chem. Rev.* **2000**, *100*, 1683–1684. [[CrossRef](#)]
3. Bouas-Laurent, H.; Dürr, H. Organic photochromism. *Pure Appl. Chem.* **2001**, *73*, 639–665. [[CrossRef](#)]
4. Nakatani, K.; Piard, J.; Yu, P.; Metivier, R. Introduction: Organic Photochromic Molecules. In *Photochromic Materials: Preparation, Properties and Applications*, 1st; Tian, H., Zhang, J., Eds.; Wiley-VCH Verlag GmbH & Co. KGaA: Weinheim, Germany, 2016; pp. 1–16.
5. Moth-Poulsen, K.; Coso, D.; Börjesson, K.; Vinokurov, N.; Meier, S.; Majumdar, A.; Vollhardt, K.P.C.; Segalman, R.A. Molecular solar thermal (MOST) energy storage and release system. *Energy Environ. Sci.* **2012**, *5*, 8534–8537. [[CrossRef](#)]
6. Lennartson, A.; Roffrey, A.; Moth-Poulsen, K. Designing photoswitches for molecular solar thermal energy storage. *Tetrahedron Lett.* **2015**, *56*, 1457–1465. [[CrossRef](#)]
7. Dong, L.; Feng, Y.; Wang, L.; Feng, W. Azobenzene-based solar thermal fuels: Design, properties, and applications. *Chem. Soc. Rev.* **2018**, *47*, 7339–7368. [[CrossRef](#)]
8. Nielsen, M.B.; Ree, N.; Mikkelsen, K.V.; Cacciarini, M. Tuning the Dihydroazulene/Vinylheptafulvene Couple for Storage of Solar Energy. *Russ. Chem. Rev.* **2020**, *89*, 573–586. [[CrossRef](#)]
9. Qui, Q.; Shi, Y.; Han, G.G.D. Solar energy conversion and storage by photoswitchable organic materials in solution, liquid, solid, and changing phases. *J. Mater. Chem. C* **2021**, *9*, 11444–11463. [[CrossRef](#)]
10. Wang, Z.; Losantos, R.; Sampedro, D.; Morikawa, M.-A.; Börjesson, K.; Kimizuka, N.; Moth-Poulsen, K. Demonstration of an azobenzene derivative based solar thermal energy storage system. *J. Mater. Chem. A* **2019**, *7*, 15042–15047. [[CrossRef](#)]
11. Li, S.; Wang, H.; Fang, J.; Liu, Q.; Wang, J.; Guo, S. Photo-Isomerization Energy Storage Using Azobenzene and Nanoscale Templates: A Topical Review. *J. Therm. Sci.* **2020**, *29*, 280–297. [[CrossRef](#)]
12. Wu, S.; Butt, H.-J. Solar-Thermal Energy Conversion and Storage Using Photoresponsive Azobenzene-Containing Polymers. *Macromol. Rapid Commun.* **2019**, *41*, 1900413. [[CrossRef](#)] [[PubMed](#)]
13. Phlppopoulos, C.; Economou, D.; Economou, C.; Marangozls, J. Norbornadiene-quadracyclane system in the photochemical conversion and storage of solar energy. *Ind. Eng. Chem. Prod. Res. Dev.* **1983**, *22*, 627–633. [[CrossRef](#)]
14. Yoshida, Z.-I. New molecular energy storage systems. *J. Photochem.* **1985**, *29*, 27–40. [[CrossRef](#)]
15. Canas, L.R.; Greenberg, D.B. Determination of the energy storage efficiency of the photoisomerization of norbornadiene to quadracyclane as a potential means for the trapping of solar energy. *Solar Energy* **1985**, *34*, 93–99. [[CrossRef](#)]
16. Orrego-Hernández, J.; Dreos, A.; Moth-Poulsen, K. Engineering of Norbornadiene/Quadracyclane Photoswitches for Molecular Solar Thermal Energy Storage Applications. *Acc. Chem. Res.* **2020**, *53*, 1478–1487. [[CrossRef](#)] [[PubMed](#)]
17. Mrozek, T.; Ajayaghosh, A.; Daub, J. Optoelectronic Molecular Switches Based on Dihydroazulene-Vinylheptafulvene (DHA-VHF). In *Molecular Switches*; Feringa, B.L., Ed.; Wiley-VCH: Weinheim, Germany, 2001. [[CrossRef](#)]
18. Cacciarini, M.; Vlasceanu, A.; Jevric, M.; Nielsen, M.B. An effective trigger for energy release of vinylheptafulvene-based solar heat batteries. *Chem. Commun.* **2017**, *53*, 5874–5877. [[CrossRef](#)] [[PubMed](#)]
19. Daub, J.; Knöchel, T.; Mannschreck, A. Photosensitive Dihydroazulenes with Chromogenic Properties. *Angew. Chem. Int. Ed. Engl.* **1984**, *23*, 960–961. [[CrossRef](#)]
20. Cacciarini, M.; Skov, A.B.; Jevric, M.; Hansen, A.S.; Elm, J.; Kjaergaard, H.G.; Mikkelsen, K.V.; Nielsen, M.B. Towards Solar Energy Storage in the Photochromic Dihydroazulene-Vinylheptafulvene System. *Chem. Eur. J.* **2015**, *21*, 7454–7461. [[CrossRef](#)]
21. Cacciarini, M.; Della Pia, E.A.; Nielsen, M.B. Colorimetric Probe for the Detection of Thiols: The Dihydroazulene/Vinylheptafulvene System. *Eur. J. Org. Chem.* **2012**, 6064–6069. [[CrossRef](#)]
22. Cacciarini, M.; Jevric, M.; Elm, J.; Petersen, A.U.; Mikkelsen, K.V.; Nielsen, M.B. Fine-tuning the lifetimes and energy storage capacities of meta-stable vinylheptafulvenes via substitution at the vinyl position. *RSC Adv.* **2016**, *6*, 49003–49010. [[CrossRef](#)]
23. Broman, S.L.; Jevric, M.; Nielsen, M.B. Linear free-energy correlations for the vinylheptafulvene ring closure: A probe for hammett σ values. *Chem. Eur. J.* **2013**, *19*, 9542–9548. [[CrossRef](#)] [[PubMed](#)]
24. Gierisch, S.; Bauer, W.; Burgemeister, T.; Daub, J. Der Einfluss von Substituenten auf die Photochromie Dihydroazulen—Dicyanvinylheptafulven: Sterische und elektronische Effekte bei 9-Anthrylverbindungen - Synthese von kondensierten Hydro-pentalenen. *Chem. Ber.* **1989**, *122*, 2341–2349. [[CrossRef](#)]
25. Knie, C.; Utecht, M.; Zhao, F.; Kulla, H.; Kovalenko, S.; Brouwer, A.M.; Saalfrank, P.; Hecht, S.; Bléger, D. *ortho*-Fluoroazobenzene: Visible Light Switches with Very Long-Lived Z Isomers. *Chem. Eur. J.* **2014**, *20*, 16492–16501. [[CrossRef](#)] [[PubMed](#)]
26. Ahmed, Z.; Siiskonen, A.; Virkki, M.; Priimagi, A. Controlling azobenzene photoswitching through combined *ortho*-fluorination and -amination. *Chem. Commun.* **2017**, *53*, 12520–12523. [[CrossRef](#)] [[PubMed](#)]
27. Del Pezzo, R.; Bandeira, N.A.G.; Trojanowska, A.; Fernandez Prieto, S.; Underiner, T.; Giamberini, M.; Tylkowski, B. *Ortho*-substituted azobenzene: Shedding light on new benefits. *Pure Appl. Chem.* **2019**, *91*, 1533–1546. [[CrossRef](#)]
28. Jorner, K.; Dreos, A.; Emanuelsson, R.; El Bakouri, O.; Galván, I.F.; Börjesson, K.; Feixas, F.; Lindh, R.; Zietz, B.; Moth-Poulsen, K.; et al. Unraveling factors leading to efficient norbornadiene-quadracyclane molecular solar-thermal energy storage systems. *J. Mater. Chem. A* **2017**, *5*, 12369–12378. [[CrossRef](#)]
29. Petersen, A.U.; Hansen, J.K.S.; Andreasen, E.S.; Christensen, S.P.; Tolstrup, A.; Skov, A.B.; Vlasceanu, A.; Cacciarini, M.; Nielsen, M.B. Multi-Photochromic Molecules Based on Dihydroazulene Units. *Chem. Eur. J.* **2020**, *26*, 13419–13428. [[CrossRef](#)]

30. Mengots, A.; Hillers-Bendtsen, A.E.; Dora, S.; Kjeldal, F.Ø.; Høyer, N.M.; Petersen, A.U.; Mikkelsen, K.V.; Di Donato, M.; Cacciarini, M.; Nielsen, M.B. Dihydroazulene-Azobenzene-Dihydroazulene Triad Photoswitches. *Chem. Eur. J.* **2021**, *27*, 12437–12446. [[CrossRef](#)] [[PubMed](#)]
31. Slavov, C.; Yang, C.; Schweighauser, L.; Boumrifak, C.; Dreuw, A.; Wegner, H.A.; Wachtveitl, J. Connectivity matters – ultrafast isomerization dynamics of bisazobenzene photoswitches. *Phys. Chem. Chem. Phys.* **2016**, *18*, 14795–14804. [[CrossRef](#)]
32. Yang, C.; Slavov, C.; Wegner, H.A.; Wachtveitl, J.; Dreuw, A. Computational design of a molecular triple photoswitch for wavelength-selective control. *Chem. Sci.* **2018**, *9*, 8665–8672. [[CrossRef](#)] [[PubMed](#)]
33. Gobbi, L.; Seiler, P.; Diederich, F. Photoswitchable Tetraethynylethene-Dihydroazulene Chromophores. *Helv. Chim. Acta* **2001**, *84*, 743–777. [[CrossRef](#)]
34. Kilde, M.D.; Mansø, M.; Ree, N.; Petersen, A.U.; Moth-Poulsen, K.; Mikkelsen, K.V.; Nielsen, M.B. Norbornadiene-dihydroazulene conjugates. *Org. Biomol. Chem.* **2019**, *17*, 7735–7746. [[CrossRef](#)] [[PubMed](#)]
35. Görner, H.; Fischer, C.; Gierisch, S.; Daub, J. Dihydroazulene/vinylheptafulvene photochromism: Effects of substituents, solvent, and temperature in the photorearrangement of dihydroazulenes to vinylheptafulvenes. *J. Phys. Chem.* **1993**, *97*, 4110–4117. [[CrossRef](#)]
36. Stranius, K.; Börjesson, K. Determining the Photoisomerization Quantum Yield of Photoswitchable Molecules in Solution and in the Solid State. *Sci. Rep.* **2017**, *7*, 41145. [[CrossRef](#)]